UNIVERSITA' DEGLI STUDI "G. d'Annunzio"
Chieti-Pescara

SCUOLA SUPERIORE "G. d'Annunzio"

DOTTORATO DI RICERCA IN ENGINEERING, EARTH AND PLANETARY SCIENCE

CICLO XXXVII

Seismic exposure and vulnerability of masonry residential buildings in Italy: a scalable approach from regional to national assessment

Dipartimento di Ingegneria e Geologia (INGEO)

Settore Scientifico-Disciplinare ICAR/09

Dottoranda
Ylenia Di Lallo

Tutor
Prof. Giuseppe Brando
Prof. Maria Giovanna Masciotta

Anni Accademici 2021/2024

SOMMARIO

SYNOPSIS

SYNOPSIS

1. PROBLEM STATEMENT

Italy is one of the most seismically active countries in Europe, with a long history of devastating earthquakes that have highlighted the vulnerability of its built environment. This vulnerability is particularly critical in masonry buildings, which represent a significant portion of the urban fabric, especially in historical centres. Most of these structures were constructed without seismic design criteria and exhibit structural characteristics that make them highly susceptible to damage during seismic events.

In recent years, the growing awareness of the need to mitigate seismic risks has led to the development of various approaches for assessing building vulnerability. However, many of these methods are focused on local or regional scales, often falling short of addressing the complexity and diversity of Italy’s building stock. Additionally, traditional empirical methods commonly used for large-scale assessments tend to be overly simplified, sacrificing accuracy in representing structural behaviour.

In this context, this thesis aims to bridge these gaps by developing and applying an integrated approach for assessing the seismic vulnerability of masonry residential buildings on a national scale. Building upon a methodology previously developed and validated for the Abruzzo region, this research expands the scope of application to cover the entire Italian territory. The study leverages data from the national CARTIS database, which provides detailed typological and structural information on buildings, to identify representative archetypes of the country’s diverse construction practices.

A distinctive element of this thesis is the integration of kinematic and numerical analyses, enabling the simultaneous evaluation of local (out-of-plane) and global (in-plane) collapse mechanisms. This methodology provides a more accurate representation of seismic vulnerability compared to traditional empirical methods, allowing the derivation of integrated fragility curves that reflect the potential damage to buildings under various seismic scenarios. Furthermore, the research explores the comparison of different sample scales, evaluating their representativeness and offering insights for selecting the most suitable level of detail for large-scale analyses.

The structure of this thesis, divided into five chapters, reflects the logical progression of the research, from a review of the literature and methodology definition to the assessment of the national vulnerability. This approach not only addresses the complex issue of seismic vulnerability on a national scale but also proposes concrete and applicable solutions within the context of risk prevention.

2. RESEARCH GOALS

The primary objective of this thesis is to advance the understanding and evaluation of seismic vulnerability for masonry residential buildings in Italy by developing a scalable and integrated methodology. This research builds upon previous work conducted for the Abruzzo region, aiming to generalize the approach for national-scale applications. The main objectives of the study are outlined below.

The first goal is to extend and generalize the existing methodology to encompass the entire Italian territory. This involves adapting the original framework to consider the diverse construction practices, materials, and seismic hazards that characterize the various regions of Italy. By expanding the analysis from a regional to a national level, the research demonstrates how a methodology initially developed for a localized context can be applied to a broader and more complex system, providing a foundation for large-scale risk assessments.

A key aspect of this work is the identification of representative building archetypes, which serve as the basis for vulnerability assessment. Using the CARTIS database, which offers comprehensive data on the typological and structural characteristics of buildings in Italy, the research identifies archetypes that capture the most common and significant features of masonry construction. These archetypes are selected to reflect the variability in building techniques, from historical construction methods to more modern practices, ensuring that the analysis is both representative and robust.

To provide a comprehensive evaluation of seismic vulnerability, the thesis integrates kinematic and numerical approaches. Kinematic analyses are used to examine out-of-plane collapse mechanisms, which are common in masonry structures due to weak connections between walls and insufficient anchoring to floors and roofs. Numerical analyses, on the other hand, focus on in-plane mechanisms, using the Equivalent Frame Model (EFM) to simulate the global structural behaviour under seismic loads with nonlinear analysis. By combining these two approaches, the study derives integrated fragility curves that account for both local and global damage mechanisms, offering a detailed and probabilistic understanding of the potential damage scenarios.

Another important objective is to evaluate how the scale of analysis influences the results. The research analyses building samples of varying sizes and geographic coverage, from localized regional datasets to comprehensive national samples. This allows for a comparison of the accuracy and representativeness of different scales, offering insights into the trade-offs between computational feasibility and analytical precision. Based on these findings, the study provides recommendations for selecting the most appropriate scale for future national-level seismic risk assessments.

Finally, the overarching goal of this thesis is to create tools that support decision-making in seismic risk management. By offering a scalable and scientifically validated framework, the research enables policymakers and urban planners to prioritize interventions, allocate resources more effectively, and develop targeted strategies for seismic risk mitigation. This work aims to bridge the gap between scientific research and practical application, contributing to the ongoing effort to safeguard communities and preserve Italy's architectural heritage in the face of seismic hazards.

3. METHODOLOGY

The methodology adopted in this thesis combines data-driven analysis with advanced modelling techniques to assess the seismic vulnerability of masonry residential buildings across Italy. The approach is designed to address both local and global collapse mechanisms, leveraging representative building archetypes extracted from the national CARTIS database. This section provides a detailed overview of the methodological framework.

The first step in the research was the identification of representative building archetypes, which form the foundation for the seismic vulnerability analysis. The CARTIS database, a comprehensive repository of typological and structural data for buildings across Italy, was utilized to extract archetypes. The selection process was semi-automated through a procedure already present in literature and followed specific criteria to ensure that the chosen archetypes accurately reflected the variability of masonry structures throughout the country. Key parameters considered in defining the archetypes included masonry type (e.g., irregular masonry, brick masonry), number of stories, construction period, floor and roof types, and the presence or absence of structural elements such as tie rods. The methodology focused on capturing the most significant typologies based on their prevalence and seismic performance characteristics. This step resulted in three set of archetypes representative of Italy's diverse building stock, in three different size scales, providing a robust basis for subsequent analyses.

The seismic vulnerability of the identified archetypes was assessed using an integrated approach that combined kinematic and numerical analyses. This dual methodology allowed for a comprehensive evaluation of both local and global collapse mechanisms:

- Kinematic Analysis for Local Collapse Mechanisms: This analysis focused on out-of-plane failures, which are common in masonry buildings due to weak connections between walls and insufficient anchoring to horizontal structural elements. Linear and non-linear kinematic models were employed to simulate potential failure mechanisms, such as façade overturning and bending. These simulations provided insights into the displacement capacity and spectral accelerations required to trigger such mechanisms, forming the basis for deriving fragility curves.
- Numerical Analysis for Global Collapse Mechanisms: To evaluate in-plane collapse mechanisms, the Equivalent Frame Model (EFM) was used. This macroelement-based approach discretizes the masonry structure into vertical piers and horizontal spandrels, connected by rigid zones. Non-linear static analyses (pushover analyses) were conducted to simulate the building's response to horizontal seismic forces. These analyses yielded pushover capacity curves describing the relationship between base shear and top displacement, which were subsequently transformed into spectral capacity curves for comparison with seismic demands.
- Integrated Fragility Curves: The results from the kinematic and numerical analyses were combined to derive integrated fragility curves. These curves account for both out-of-plane and in-plane mechanisms, offering a holistic representation of the seismic vulnerability of each archetype. The integration process involved identifying the dominant failure mechanism under various seismic intensity levels and combining the results probabilistically.

Given the scale of the analysis, it was necessary to evaluate how the choice of sample size and geographic coverage affected the results. Three progressively larger samples were analysed:

- Regional Scale: A focused sample representing a single region, enabling a detailed understanding of local building characteristics.
- Macro-Regional Scale: A broader sample encompassing multiple regions, providing insights into regional variations while maintaining computational feasibility.
- National Scale: A comprehensive sample representing the entire Italian building stock, aimed at capturing national trends and variability.

For each sample, the methodology assessed the representativeness of the results and compared fragility curves across scales. This analysis provided critical insights into the trade-offs between detail and generalization, guiding the selection of the most suitable scale for large-scale vulnerability studies. To better understand the methodology implemented in the thesis, a flowchart has been proposed below that includes the main steps followed to achieve the expected results.

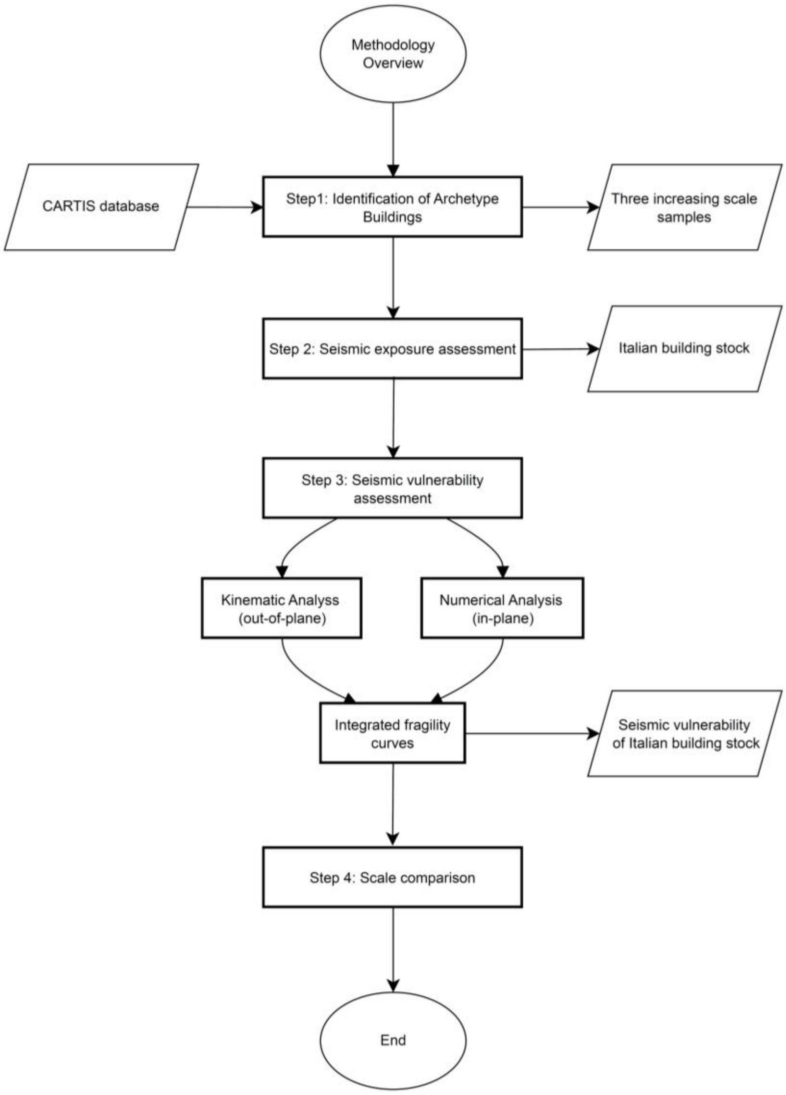

Figure 1. The implemented methodology

The methodology outlined in this thesis provides a robust framework for assessing the seismic vulnerability of masonry buildings, combining data-driven archetype selection with advanced analytical and numerical techniques. By addressing both local and global mechanisms and evaluating the impact of sample scale, the approach ensures a comprehensive and scalable solution for seismic risk assessment.

4. MAIN RESULTS

The research presented in this thesis yielded significant findings across its key chapters, highlighting both the diversity of Italy's masonry building stock and the effectiveness of the integrated vulnerability assessment methodology.

The identification of archetypes was achieved by analysing three samples of increasing geographic coverage: regional, multi-regional, and national. These archetypes were defined using the CARTIS database, focusing on parameters such as masonry type, construction period, and structural configuration. The results highlighted notable regional differences:

- Central Italy showed a prevalence of more regular brick masonry though with variations in seismic exposure due to geological and hazard differences.
- Northern regions exhibited more irregular masonry, often associated with historical centres and older construction practices.
- Southern areas reflected a mix of traditional and hybrid construction techniques, influenced by both historical practices and recent developments, especially in slabs and roofs.

This analysis underscored the importance of tailoring seismic risk assessments to regional building characteristics.

To assess the seismic vulnerability of the identified archetypes, combined kinematic analyses for out-of-plane mechanisms and numerical analyses for in-plane behaviour were used. By integrating these methods, fragility curves were developed to capture the probability of damage under various seismic intensities. The comparison of results across the three samples revealed that:

- Macro regional samples provided detailed insights suitable for localized retrofitting strategies because it captures minor damage better even in the case of low macro seismic intensity.

- National samples offered a broader perspective, ideal for large-scale risk assessments and policymaking, but it underestimates vulnerability, especially in the case of strong seismic accelerations.

This dual focus demonstrated the scalability of the methodology and its ability to address both detailed and generalized needs in seismic risk mitigation.

These results form a strong foundation for developing targeted retrofitting strategies and optimizing resource allocation for seismic risk management in Italy. The methodology's flexibility ensures its applicability across diverse contexts, bridging the gap between localized assessments and national-scale planning.

5. CONCLUSIONS, LIMITATIONS, AND FUTURE DEVELOPMENTS

This research represents a significant advancement in the field of seismic vulnerability assessment for masonry residential buildings in Italy. Its main contributions concern first of all methodological innovations in the field of structural analysis. The integration of kinematic and numerical analyses provided a comprehensive framework for evaluating both out-of-plane and in-plane collapse mechanisms. This dual approach enhances the accuracy of vulnerability assessments, particularly for large-scale applications, bridging the gap between localized empirical studies and generalized national-level models.

Furthermore, by applying the methodology to progressively larger samples (regional, multi-regional, and national), the study demonstrated its scalability and adaptability. The findings confirmed that the approach can be effectively employed to represent the diversity of Italy's building stock while maintaining analytical precision.

While this research represents a significant step forward in the assessment of seismic vulnerability for masonry residential buildings in Italy, it is not without its limitations. One of the primary constraints is the reliance on the CARTIS database, which, despite being comprehensive, may not fully reflect the complexity or recent modifications of the building stock in certain regions. This dependence on existing data introduces potential inaccuracies or omissions that could affect the representativeness of the archetypes used in the analysis.

Additionally, the fragility curves and vulnerability assessments, while robust, would benefit from further validation through experimental data or observations collected after real earthquake events. Such validation is crucial to refine the models and ensure their reliability in accurately predicting damage mechanisms. The simplifications inherent in the kinematic and numerical models used in this study, though necessary for computational feasibility, also represent a limitation. These models make assumptions about the behaviour of masonry structures under seismic loads, potentially overlooking more complex interactions or failure modes.

Looking to the future, this research opens several promising avenues for further development. One important direction is the extension of the methodology to other types of construction, such as reinforced concrete or mixed masonry structures. By broadening the scope of analysis, the approach could become a more universally applicable tool for seismic vulnerability assessment across a wider variety of building types.

Another opportunity lies in integrating socioeconomic factors into the analysis. This would allow for a more comprehensive understanding of seismic risk by considering elements such as population density, economic losses, and the costs associated with retrofitting interventions. Incorporating these factors would enhance the methodology's relevance for policymakers, enabling more informed decision-making and resource allocation.

The use of artificial intelligence and machine learning as a supplement to data already present in existing databases represents another exciting direction for future research. These technologies could be applied to automate the identification of archetypes or to process large-scale datasets more efficiently. AI-based tools could improve the precision of vulnerability modelling and streamline the analysis, making it faster and more adaptable to different contexts.

In summary, while the current study has its limitations, it provides a solid foundation for further exploration and refinement. Addressing these constraints and pursuing the suggested future directions could enhance the applicability, accuracy, and impact of the methodology, contributing significantly to seismic risk mitigation efforts in Italy and beyond.

CHAPTER I

LARGE-SCALE INTEGRATED APPROACH TO ASSESS THE SEISMIC VULNERABILITY OF MASONRY BUILDINGS AND OPTIMIZE RISK REDUCTION STRATEGIES

ABSTRACT

This study presents a comprehensive methodology for assessing the seismic exposure of residential masonry buildings in Italy using the CARTIS database, a detailed repository of typological and structural characteristics of the national building stock. This paper proposes an integrated method to assess the seismic vulnerability of masonry buildings through a reduced number of archetype models described by a few geometric and structural parameters extracted from the national CARTIS database. The approach is applied and validated through a sample of Archetype Buildings (ABs) identified by the authors as representative of the Abruzzo region (Central Italy). This set of ABs is first analysed through two separated approaches: an analytical method aimed to evaluate their out-of-plane response through linear and non-linear kinematic analyses, and a numerical method aimed to assess their in-plane behaviour by means of non-linear static analyses. The fragility curves derived from these distinct methods are then compared and combined according to specific criteria with the aim of defining integrated fragility curves – accounting for both local and global damage mechanisms – representative of the potential damage that the buildings associated with each archetype would undergo under different earthquake hazard levels. Subsequently, targeted seismic retrofitting interventions are proposed to inhibit the activation of the most probable mechanisms, allowing to verify the beneficial impact of different types of intervention and to quantify the improvement in the seismic performance of the identified archetypes. By exploiting and combining different analysis methods and reducing the number of analysed buildings to a handleable number of archetypes, the proposed approach allows to overcome the time and computational effort requested by empirical methods based on building-by-building mapping, ensuring a greater accuracy in the large-scale vulnerability assessment, and providing an efficient decision-making tool to support local and national policies in the context of seismic risk reduction.

1. INTRODUCTION

Assessing the seismic vulnerability of the built environment is the first step to undertake in order to address targeted policies for seismic risk reduction. As for historical urban centres, this aspect takes on further importance given the great amount and variety of risk-prone masonry buildings present therein. In this context, a deep knowledge of the geometric and structural characteristics of historic masonry structures is essential to understand how they respond to earthquake actions and consequently apply cost-effective mitigation measures to enhance their structural resilience during future emergency situations. Yet, the knowledge accumulation process in the case of built heritage can be very complex due to the heterogeneity of historical masonry constructions in terms of structural typologies, building techniques and materials.

There are many works in the literature that define macro-types by assigning EMS classes to specific building types [1] in order to obtain a typological description of vulnerability [2], [3] These methods require detailed information about the building, which is not always available from quick onsite surveying.

For this reason, in recent years, following the survey campaigns carried out after the last Italian earthquakes, the necessity to develop databases to collect and store information concerning the actual state of conservation of the existing built heritage progressively emerged, becoming a reality. By exploiting the considerable quantity of data therein contained, it has been possible to implement and validate simplified large-scale vulnerability models accounting for the distinctive features of the buildings located in Italian historic centres in order to predict potential damage levels under different earthquake scenarios.

Depending on the scale of the problem (regional/territorial/urban) [4], the assessment can be carried out at multiple levels, thus leading to different results in terms of accuracy. Two main methods can be used in this regard: empirical methods – i.e. methods essentially based on observations and engineering judgements – and mechanical methods – namely methods based on kinematic, or pushover analyses conducted on real buildings or prototypes. In fact, in case of earthquake shaking, masonry buildings activate either a global response, when a box-like behaviour is guaranteed and the seismic forces are resisted by the walls parallel to the direction of the action, or a local response, when the lack of connections between orthogonal walls prevents a monolithic behaviour and lead to the activation of out-of-plane mechanisms. However, when the number of buildings to analyse is significant, viable and expeditious empirical approaches based on observational methods, engineering judgment, and statistical processing of the collected data are usually preferred to perform large-scale evaluations as compared to mechanical models [5], [6], [7], [8].

Empirical methodologies introduce several simplifications aiming at reducing both the computational effort and the time needed for the analyses, thereby resulting effective for providing vulnerability screenings of large urban areas but loosing accuracy when moving to the building scale, because unable to catch the behaviour of each individual structure. Moreover, methods driven by empirical evidence become unpracticable when the vulnerability assessment is addressed to extensive territorial areas, unless the number of analysed buildings is reduced to a representative handleable number of archetypes. In fact, the results obtained for single archetypes can be easily extended to analogous buildings falling in the same category provided that the defined set of archetypes is adequately representative of the most widespread and important characteristics of the whole building stock. This way, more sophisticated analyses can be applied to each archetype [9], thus achieving a greater level of accuracy as compared to simplified large-scale empirical analyses.

The study presented in this paper is framed within the research context outlined above and takes advantage of the data gathered from an extensive survey activity carried out on the masonry residential buildings of the Abruzzo region (Central Italy) through the CARTIS form [10]. Following this activity, a semi-automated in-house procedure [11] is applied to extract from the CARTIS database a reduced number of archetype buildings upon which more elaborated analyses are performed and herein discussed. Particularly, for each archetype, both the out-of-plane and in-plane capacities against horizontal forces are investigated to estimate reliable fragility curves for the entire set of associated buildings and derive therefrom likely damage scenarios for specific intensity measures. The paper is structured as follows. Section 2 presents the main features of the Abruzzo archetype buildings and details how these structures are schematized for the purpose of the analyses. Section 3 provides an overview of the methods and tools employed to perform the study. Section 4 describes the out-of-plane analyses carried out on the identified archetypes and discusses the results obtained in terms of capacity and fragility curves. Analogously, Section 5 reports and discusses in detail the outcome of the in-plane analyses performed on the same set of archetype buildings. Subsequently, in Section 6, integrated fragility curves accounting for both in-plane and out-of-plane failures are computed. This outcome is finally used in Section 7 to drive the selection of the most appropriate retrofitting solutions aiming at reducing the seismic vulnerability of the analysed archetypes. Section 8 summarizes the main conclusions of the work and outlines possible future developments.

2. DISTINCTIVE FEATURES OF ABRUZZO RESIDENTIAL BUILDINGS

Beginning in 2014, an intensive research activity aimed at creating an inventory of structural typologies at territorial scale has been developed by the Italian Plinius Study Centre (http://plinivs.it). Among the main outcomes of this activity is the so-called CARTIS form, i.e. a form conceived to collect data about the geometrical and structural characteristics of residential buildings in urban areas by interviewing local technicians [12]. Currently used in several research tasks funded by the Italian Civil Protection Department, this form represents a valuable tool in the context of national seismic risk reduction for the identification of building features at the large scale, complementing and improving existing databases, such as the ISTAT (Italian National Institute of Statistics) census data. Given the importance of masonry structures in the history of Italian construction techniques, among the variety of surveyed structural typologies, only masonry buildings are examined in the present study. Concerning their representative features, hereinafter referred as parameters (P_i), only those regarded as the most relevant and distinctive for the structural characterization of such buildings from a seismic viewpoint are considered (Table 1). According to these criteria, a portfolio consisting of 26 archetypes (Table 2), representative of the 86% of the Abruzzo unreinforced masonry (URM) buildings, are extracted from the afore-mentioned CARTIS inventory through a semi-automated procedure [11], [13].

Table 1. Parameters considered to define the building portfolio in Abruzzo.

P_i	Parameters	Typical features in Abruzzo
P_1	Masonry type	Irregular masonry/ Bricks
P_2	Number of stories	2/3/4
P_3	Construction period	<1860 / >1945
P_4	Floor type	Rigid/ Semi-rigid / Flexible
P_5	Roof material	Heavy / Light
P_6	Tie rods	Presence / Absence
P_7	Wall thickness at ground floor	<60 cm / >60 cm
P_8	Average wall spacing	<5 m / >5 m

Table 2. Major URM building sub-typologies of the Abruzzo region based on CARTIS data.

ID	Masonry type	N° of stories	Construction period	Tie rods	Floor type	Roof material	Wall thickness	Wall spacing	Relevance [%]
1	Irregular masonry	3	< 1860	No	Flexible	Light	> 60 cm	< 5 m	9.4
2	Irregular masonry	3	< 1860	Yes	Semi-rigid	Light	> 60 cm	< 5 m	8.9
3	Irregular masonry	3	< 1860	No	Semi-rigid	Light	> 60 cm	< 5 m	7.9
4	Irregular masonry	3	< 1860	Yes	Flexible	Light	> 60 cm	< 5 m	7.9
5	Irregular masonry	4	< 1860	Yes	Semi-rigid	Light	> 60 cm	< 5 m	7.5
6	Irregular masonry	3	< 1860	No	Flexible	Heavy	> 60 cm	< 5 m	6.8
7	Irregular masonry	4	< 1860	Yes	Flexible	Light	> 60 cm	< 5 m	6.8
8	Irregular masonry	3	< 1860	No	Semi-rigid	Heavy	> 60 cm	< 5 m	3.9
9	Irregular masonry	4	< 1860	No	Flexible	Light	> 60 cm	< 5 m	2.1
10	Bricks	2	1945-1981	No	Semi-rigid	Heavy	< 60 cm	< 5 m	2.1
11	Bricks	3	1945-1981	Yes	Rigid	Heavy	< 60 cm	> 5 m	2.1
12	Irregular masonry	3	< 1860	Yes	Semi-rigid	Heavy	> 60 cm	< 5 m	1.5
13	Irregular masonry	3	< 1860	Yes	Flexible	Heavy	> 60 cm	< 5 m	1.5
14	Bricks	4	1945-1981	Yes	Rigid	Heavy	< 60 cm	> 5 m	1.5
15	Irregular masonry	4	< 1860	No	Semi-rigid	Light	> 60 cm	< 5 m	1.5
16	Bricks	2	< 1860	Yes	Flexible	Light	< 60 cm	< 5 m	1.4
17	Bricks	2	< 1860	No	Flexible	Light	< 60 cm	< 5 m	1.4
18	Bricks	3	< 1860	Yes	Flexible	Light	< 60 cm	< 5 m	1.4
19	Bricks	3	< 1860	No	Flexible	Light	< 60 cm	< 5 m	1.4
20	Bricks	4	< 1860	Yes	Flexible	Light	< 60 cm	< 5 m	1.4
21	Bricks	4	< 1860	No	Flexible	Light	< 60 cm	< 5 m	1.4
22	Irregular masonry	2	< 1860	No	Flexible	Light	> 60 cm	< 5 m	1.4
23	Bricks	3	1945-1981	No	Rigid	Heavy	< 60 cm	> 5 m	1.4
24	Irregular masonry	4	< 1860	Yes	Flexible	Heavy	> 60 cm	< 5 m	1.1
25	Irregular masonry	4	< 1860	No	Flexible	Heavy	> 60 cm	< 5 m	1.1
26	Bricks	4	1945-1981	No	Rigid	Heavy	< 60 cm	> 5 m	1.1

In what concerns the masonry type (P_1), Abruzzo URM buildings can be grouped in two main classes which reflect the geo-lithological formations of the area: irregular masonry buildings and periodic brick masonry buildings. In fact, the prevailing presence of carbonate formations in the inner part of the Abruzzo region led to a wide use of stones in this area. Conversely, the coastal area significantly differs from the interior due to the extensive presence of clays that fostered the frequent use of fire clay bricks for building. These aspects corroborate the strict connection between the building features and the specificity of the territory in which such buildings are located. The number of floors (P_2) featured by the examined buildings typically varies from 2 to 4, whereas the construction period (P_3) is either prior to 1860 or after 1945. As for the slab type (P_4), three categories are found: rigid (e.g., cement-based slabs), semi-rigid (e.g., steel beam slabs with flat brick tiles) and flexible (e.g., steel beam slabs with brick arches). Depending on the material, the roofing systems (P_5) are categorized into heavy (e.g., reinforced concrete roof) and light (e.g., wooden roof). Tie rods (P_6) are present in about 50% of the buildings. With reference to the geometric dimensions of the walls (P_7), it is noted that for irregular masonry the wall thickness varies by floor decreasing from 0.80 m (ground floor) to 0.60 m (upper floor); whereas for brick masonry, the wall thickness remains constant throughout the height with an average value of 0.60 m. The distance between walls (P_8) is generally lower than 5 m for irregular masonry and greater for brick masonry.

In order to build reliable three-dimensional models for the assessment of these Archetype Buildings (ABs), other important geometrical features are retrieved from the CARTIS data. This further refinement includes specifications about the building regularity, the average floor area and storey height, the presence of vaulted systems and the percentage of wall openings. In this regard, Abruzzo masonry residential buildings are found to be regular both in plan and in elevation (no eccentricities). The average floor area oscillates between 70 and 100 m^2. Vaults are mostly located at the ground level and are of two main types: barrel (44%) and cross (41%). The average storey height is around 2.5-3.5 m, and openings usually affect about 10% to 30% of the total area of the façade.

Based on all the afore-mentioned geometrical and mechanical information, 26 ideal models (one per archetype) representative of the entire residential masonry building stock of the Abruzzo region are built and used for the subsequent analyses (Figure.1).

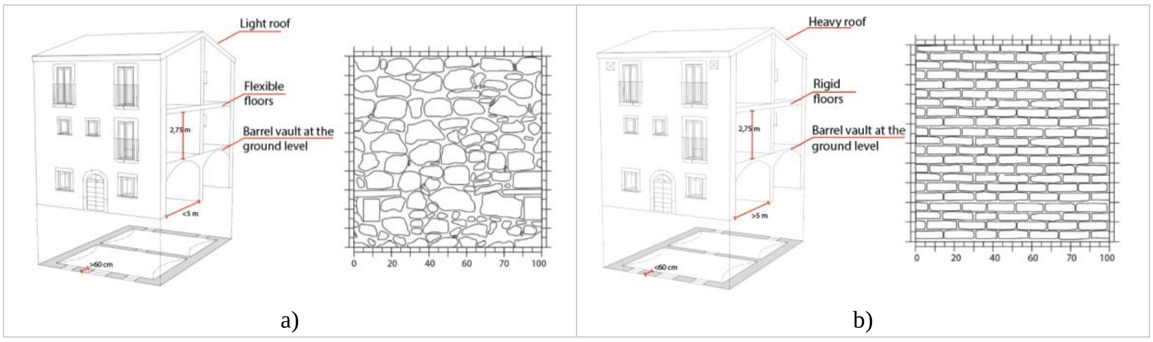

Figure.1 Ideal 3d models and masonry patterns of a) archetype building AB#1 and b) archetype building AB#11.

3. METHODS AND TOOLS

3.1 DEFINITION OF CAPACITY CURVES

The assessment of the seismic vulnerability of the identified Archetype Buildings is performed following two different analysis methods, i.e., analytical and numerical, both leading to the definition of a capacity curve describing the structural behaviour of each archetype under horizontal actions.

The analytical method, based on the implementation of linear and non-linear kinematic analyses, allows studying the out-of-plane collapse mechanisms of the macro-elements composing each representative building (local mechanisms analysis). Linear kinematic analyses are carried out with the specific aim of estimating the load multiplier α associated with the different mechanisms susceptible to activation. Each load multiplier allows identifying the spectral acceleration (Sa) referred to an equivalent Single-Degree-Of-Freedom (SDOF) system and, in turn, the peak ground acceleration (PGA) able to activate the considered kinematic mechanism in the structure. To know the displacement capacity of the system until collapse, non-linear kinematic analyses are also performed, ultimately enabling the definition of trilinear curves representing the behaviour of the structure in terms of displacement capacity.

The numerical method, based on the application of non-linear static analyses, is employed to investigate the in-plane behaviour of the identified archetypes, assuming that out-of-plane mechanisms are prevented and accounting for the structural contribution that in-plane loaded masonry walls provide to the building archetype they belong to in order to resist seismic actions (global mechanisms analysis). The numerical simulations performed within this study rely on the Equivalent Frame Model (EFM) schematization and are conducted in MIDAS-GEN environment [14], whereby pushover analyses are carried out to obtain equivalent bilinear capacity curves representing the relationship between base shear force and top displacement in each archetype.

Once trilinear and bilinear capacity curves are estimated for all archetype buildings, Damage Thresholds (DTs) are defined according to established literature criteria and then compared against a significant number of seismic demands expressed in terms of Acceleration-Displacement Response Spectrum (ADRS), with the purpose of obtaining integrated fragility curves accounting for both out-of-plane and in-plane mechanisms. Finally, based on the outcome of the vulnerability assessment of the as-built archetype configurations, the most appropriate seismic retrofitting measures are identified, and the assessment is repeated both analytically and numerically by considering the new retrofitted configurations, thus enabling a quantitative estimation of their seismic improvement. A schematic overview of the methodological pathway followed in the present study is provided in the flowchart of Figure 2.

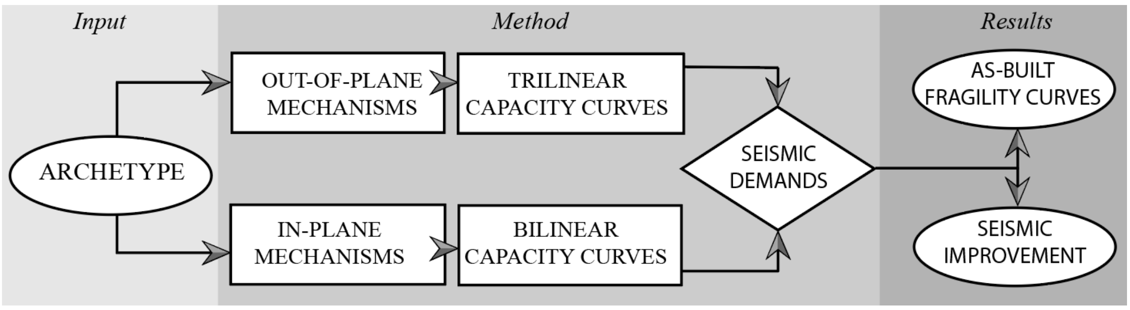

Figure 2. Methodology flowchart.

3.2 DEFINITION OF THE SEISMIC DEMAND

According to the Performance-Based Assessment (PBA) approach [15], the seismic vulnerability of ancient masonry buildings can be evaluated through fragility curves which provide the probability of exceeding a given damage state as a function of specific ground motion intensity measures. The estimation of reliable fragility function parameters is not trivial as seismic analyses involve various sources of uncertainties, including those associated with the structural capacity model and those related to the seismic input. While capacity modelling errors are epistemic in nature and can be reduced through more comprehensive knowledge, the uncertainty related to the randomness of the earthquake phenomenon, usually expressed in terms of record-to-record variability, is aleatory and irreducible [16], [17]. For this reason, in the framework of performance-based earthquake engineering, a crucial aspect is the selection of an appropriate suite of accelerograms to capture the record-to-record variability of the seismic input and, consequently, assess the structural capacity of buildings under different ground motion records.

In this work, a large set composed of 125 natural seismic records is considered to account for the uncertainties associated with the seismic demand. These records are derived from the MARS research project [18], during which a representative dataset of worldwide earthquake records was identified for large ranges of periods (up to 10 s) compatible with the maximum values of structural vibration periods relevant for engineering purposes [19]. Numerous real accelerograms consistent with the historical earthquakes occurred in Italy [20] for different return periods were also included to cover a wide range of ground motion intensity levels. This entire dataset of natural records is employed in the present study for comparing the capacity curves of the identified Archetype Buildings (Abs) and to estimate site-independent fragility curves considering both very low and very high levels of seismic hazard.

For the sake of completeness, the main features of the afore mentioned 125 accelerograms are summarized below:

- Epicentral distances: $R_{epi} < 30$ km.
- Soil type: A or B.
- Moment magnitude: $5.4 < M_w < 7.1$.
- Peak ground acceleration: 0.40 m/s^2 < PGA < 17.16 m/s^2 (X direction) and 0.40 m/s^2 < PGA < 11.58 m/s^2 (Y direction).

The accelerograms are first divided into 9 families, each one corresponding to a pre-selected range of PGA, and each family is associated to the mean PGA of the range (Table 3). Subsequently, to compare seismic capacity versus seismic demand and to assess the performance of each archetype in the considered earthquake scenarios, the selected accelerograms are transformed into Acceleration-Displacement Response Spectra (ADRS).

Table 3. Range and average PGA of the 9 families of seismic inputs.

EQ Family	Range of PGA [m/s^2]	Mean PGA [g]
1	0.4 < PGA ≤ 1.0	0.07
2	1.0 < PGA ≤ 1.5	0.13
3	1.5 < PGA ≤ 2.0	0.18
4	2.0 < PGA ≤ 3.0	0.26
5	3.0 < PGA ≤ 4.0	0.34
6	4.0 < PGA ≤ 5.0	0.46
7	5.0 < PGA ≤ 6.0	0.56
8	6.0 < PGA ≤ 7.0	0.66
9	7.0 < PGA ≤ 12.0	0.95

4. ASSESSMENT OF OUT-OF-PLANE MECHANISMS

4.1 KINEMATIC APPROACH

As well-known in the literature, out-of-plane (or I mode) collapses are the most crucial mechanisms for masonry structures under seismic actions. Different factors can influence the kinematic mechanism: *a)* lack of connections between orthogonal walls and inadequate interaction between vertical and horizontal structures (no box-behaviour); *b)* poor quality of masonry and bad organization of the facing wall; *c)* loading conditions and thrusting elements; *d)* geometric parameters.

The present work takes into consideration two types of out-of-plane failures: simple overturning (either total or partial) and bending (vertical and horizontal). To this end, for each façade of the Abs, depending on the presence or absence of constraints, the following conditions are defined:

- The masonry walls are not appropriately constrained to the remaining parts of the structure. This deficiency fosters the activation of overturning mechanisms as the walls are unrestricted at the top [21]. Therefore, the constraining condition that makes the mechanism possible is the absence of transverse connections/tie rods/ring beams. Simple overturning mechanisms are notably schematized as a rigid rotation of the wall around a cylindrical hinge. The overturning can involve different stories of the building so, assuming the absence of tie rods, the following kinematic motions are herein analysed (Figure 3a-b): global monolithic overturning of the façade [M1] and partial monolithic overturning of the façade [$M2_{B-C}$].
- The walls are constrained together by means of anti-seismic devices. Depending on their arrangement, bending mechanisms are more likely to activate [22]. Thus, assuming the presence of tie rods, other two kinematics are evaluated in the present study (Figure 3c-d), i.e., vertical bending [M3] and horizontal bending [M4]. Vertical bending usually occurs when the wall is constrained at the extremities but free in the central part. As a result, a horizontal cylindrical hinge can develop in the middle of the wall under seismic excitation. Whereas, if connections to orthogonal walls are guaranteed, but there is no effective retain at the top, the thrust transmitted by the head slab or roof can result into the formation of an oblique or vertical cylindrical hinge in the masonry wall, leading to the activation of horizontal bending mechanisms.

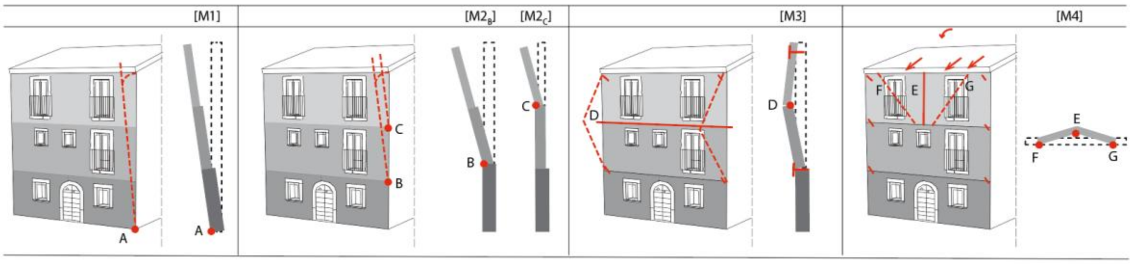

Figure 3. Possible kinematic motions for the macro-element façade.

It is worth stressing that, for all kinematics analysed herein, the façade is always assumed as monolithic. Therefore, only a specific number of kinematically admissible collapse mechanisms is evaluated. For each AB, the analyses are performed considering different constraint conditions for the walls (due to the presence/absence of possible retaining devices), the presence of thrusting elements [23], and the role played by the geometrical and typological features of the building in the activation of each possible mechanism (Table 4).

Table 4. Constraint conditions, thrusting elements and possible collapse mechanisms identified for each archetype.

Archetype	Constraint conditions	Thrusting elements	Possible kinematic mechanism
1-3-9-19-21-22	NO retaining in the interstorey	Vault	[M1], [M2]
2-4-5-8-18-20	Tie rods on top	Vault	[M1], [M2], [M3]
6-7-24-25	NO retaining in the interstorey	Vault and heavy roof	[M1], [M2]
10 -11-13-14-26	Tie rods on top	Vault and heavy roof	[M1], [M2], [M3], [M4]
12- 15	NO retaining in the interstorey	Heavy roof	[M1], [M2]
16	Tie rods on top	-	[M1], [M2], [M3]
17-23	NO retaining in the interstorey	-	[M1], [M2]

As mentioned above, the analyses of the considered out-of-plane mechanisms are conducted following both a linear and a non-linear kinematic approach. For each analysed wall and for each identified mechanism, the horizontal load multiplier α_0 that activates the kinematics is defined by applying the Principle of Virtual Works. To this end, all the internal and external forces acting on the system of rigid blocks involved in the kinematic configuration are considered, such as:

- Self-weights of the blocks, applied at their respective barycentre.
- Carried vertical loads of slabs, vaults, and roof (both dead and imposed loads) and associated thrusts.
- Seismic-induced horizontal forces proportional to the vertical loads.
- Any additional external forces, for example those transmitted by metal chains.

For each α_0, the spectral acceleration a_0* referred to an equivalent Single-Degree-Of-Freedom (SDOF) system is evaluated according to the Italian technical regulations [24], [25]. Subsequently, the acceleration leading to the activation of the mechanism – whether the position of the hinge be at the ground level or at a certain height [26], [27] – is computed. The results reveal that for all the 26 archetypes the first mechanism that activates, namely the one corresponding to the lower spectral and ground accelerations, is the complete overturning of the front façade. Particularly, the lowest load multipliers are associated with the out-of-plane collapse of the four-story buildings for both irregular (archetype #9, α_0=0,046) and brick (archetype #21, α_0=0,030) masonry.

As a second assessment criterion, non-linear kinematic analyses are performed to determine the acceleration-displacement capacity curves of the most fragile mechanisms of all archetype buildings until collapse. The capacity curves are determined according to the Italian technical regulations [25] based on four points corresponding to four distinct Performance Levels (PLs), i.e. Elastic, Damage, Near Collapse and Collapse Limit States. A typical capacity curve is shown in Figure 4, where:

- d_0* identifies the maximum lateral displacement of the equivalent SDOF system computed as given by Eq. (1). According to experimental studies on out-of-plane mechanisms [26], to obtain the actual displacement d_c*at the Collapse Limit State (CLS), d_0* must be reduced by 40% (d_c*=0,6 d_0*).

$$d_0^* = d_k \cdot \frac{\sum_{i=1}^{n+m} P_i \delta_{x,i}^2}{\delta_{x,k} \cdot \sum_{i=1}^{n+m} P_i \delta_{x,i}} \tag{1}$$

  In Eq. (1) $\delta_{x,k}$ is the virtual horizontal displacement of point k, taken as a reference for the determination of the displacement d_k, P_i is the self-weight of the block applied to its centre of gravity, n is the number of rigid blocks involved in the kinematic chain and m is the number of elements not directly involved in the mechanism but whose masses, due to the seismic action, generate horizontal forces on the elements of the kinematic chain.
- d_{NC}* is the displacement of the equivalent SDOF system corresponding to the Near Collapse Limit State (NCLS) and computed as follows:

$$d_{NC}^* = 40\%\ d_0^* \tag{2}$$

- d_D* is the displacement corresponding to the Damage Limit State (DLS) evaluated following the expression below and considering a ductility factor q = 2:

$$d_D^* = d_{NC}^*/q \tag{3}$$

- a_0* is the spectral acceleration.
- a_y* and d_y* are respectively the acceleration and the displacement corresponding to the Elastic Limit State (ELS) and they are computed considering the wall thickness (s_i), the height of the macro-element centre of masses (h_{bar}) and the fundamental period of the macro-element (T_a) as given in Eqs. 4 and 5:

$$a_y^* = \frac{s_i}{6\ h_{bar}} \tag{4}$$

$$d_y^* = a_y^* \cdot \frac{T_a^2}{4\pi^2} \tag{5}$$

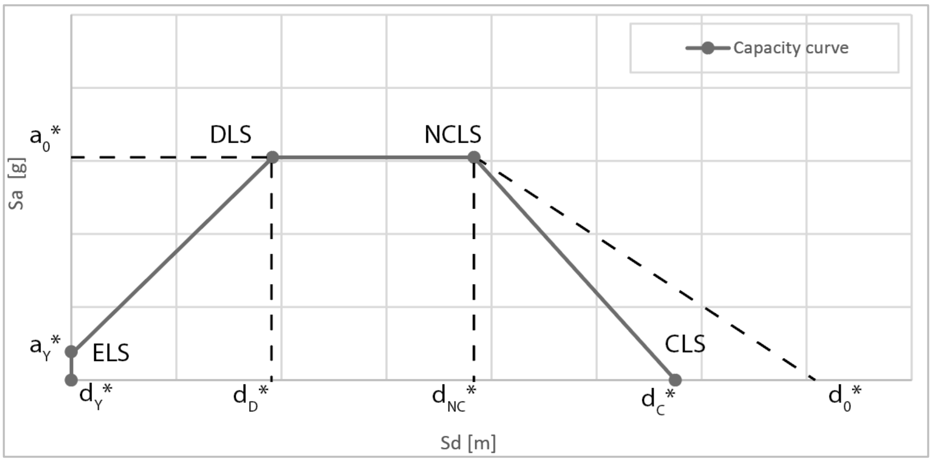

Figure 4. Typical capacity curve obtained from non-linear kinematic analyses with indication of the four Limit States.

As a general rule, 31or each AB, the capacity curve corresponding to the most brittle mechanism is selected as representative of the vulnerability of that specific archetype. Figure 5 compares the capacity curves obtained for six different ABs: three made of irregular masonry and featuring 2, 3 and 4 stories, respectively, i.e. Archetypes #22, #1, and #9; and three made of brick masonry and featuring 2, 3 and 4 stories, respectively, i.e. Archetype #17, #19, and #21. All compared buildings have flexible slabs, light roofs, and lack ties rods. It can be seen that as the number of stories decreases, the overall capacity of the building increases substantially. For brick buildings, there are also important differences in the ultimate displacements.

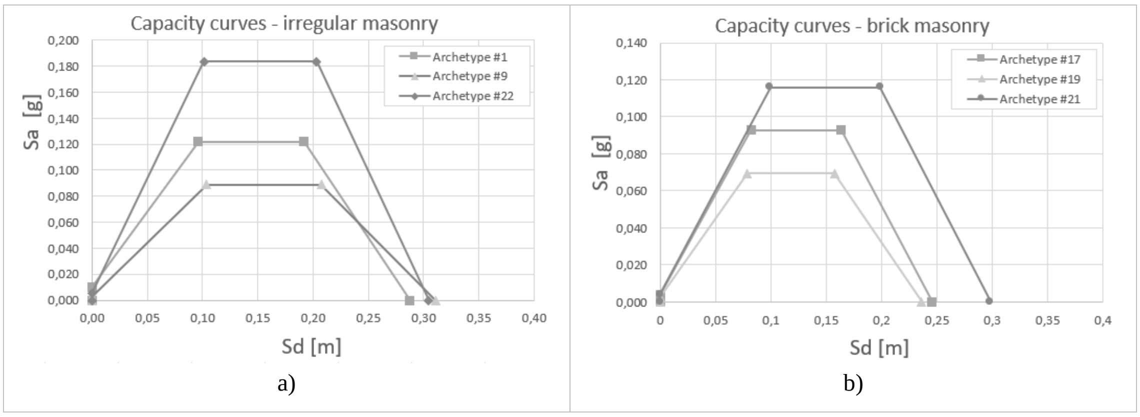

Figure 5. Trilinear capacity curves: a) irregular masonry Archetypes #1, #9, #22; b) brick masonry Archetypes #17, #19, #21.

4.2 Identification of damage thresholds

In accordance with the seismic PBA approach, which relies on the fulfilment of specific PLs in the occurrence of corresponding earthquake hazard levels, each point of the capacity curve identifies a specific damage condition of the structure. Therefore, a direct correlation between damage levels (DLs) – defined according to the EMS-98 [28] – and performance levels (PLs) can be established.

The capacity assessment procedure for each AB is carried out following literature examples having as study object a simple rigid block under horizontal actions [29]. Indeed, in this ideal case, the DLs corresponding to rocking activation and overturning, respectively associated to the Damage Limit State (DLS or D2) and Near Collapse Limit State (NCLS or D4), can be easily distinguished on the relevant capacity curve. From these points, the other damage levels, namely light damage (D1 = 0,7% D2) and total collapse damage (D5, where a = 0g) can be derived. Based on these criteria, four Damage Thresholds T(Dk) are defined in the present study for each capacity curve, as described in Table 5 [15]. From a probabilistic point of view, the attainment of a threshold corresponding to Dk means that the probability of being in a damage state greater or equal to Dk is 50%. Figure 6 illustrates the damage thresholds proposed for the different DLs in the capacity curves.

Table 5. Damage Thresholds defined for the capacity assessment of Abruzzo Abs.

T(Dk)	Damage Thresholds	Description
T(D1)	Light damage level	This threshold corresponds to 70% of T(D2);
T(D2)	Moderate damage level	Rocking activation. This threshold lies at the intersection between the rising branch and the beginning of the plastic plateau of the capacity curve.
T(D3)	Extended damage level	This threshold corresponds to the last point of the plateau, before the decreasing branch of the capacity curve.
T(D4)	Collapse	This threshold corresponds to the last point of the decreasing branch, where the acceleration becomes zero. If T(D4) is exceeded, total collapse occurs.

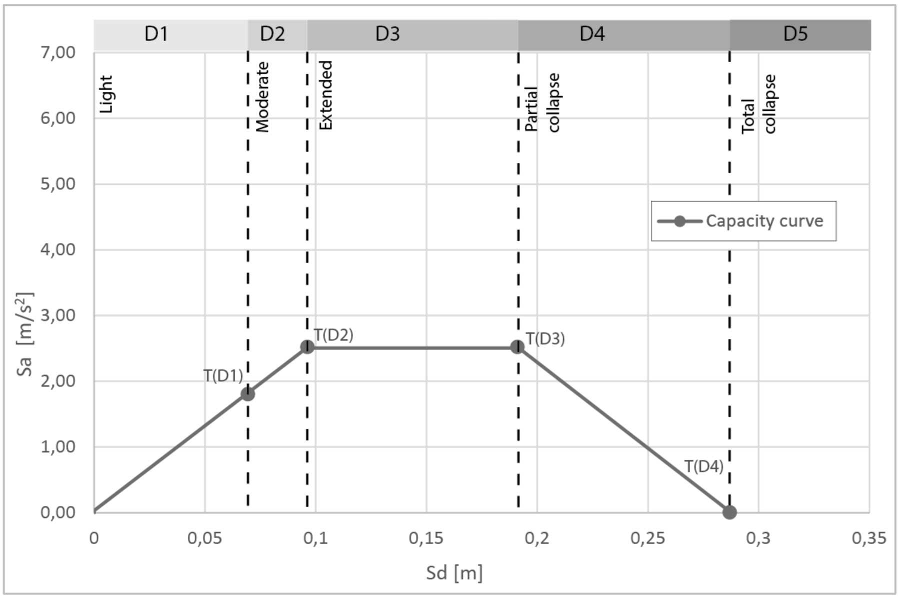

Figure 6. Generic capacity curve with indication of Damage Levels (DLs) and associated Damage Thresholds (TD_k).

4.3 Demand/Capacity comparison

Once demands in ADRS format and capacity curves are defined, the performance point (PP) of the structure under analysis can be graphically determined, thus allowing to identify the damage that the structure may suffer under the considered seismic scenario [30]. Precisely, PP is defined as the point lying at the intersection between the seismic input ADRS and the extension of the elastic branch of the system capacity curve. The procedure is exemplified in Figure 7, where the capacity curve referred to the monolithic overturning mechanism of AB #1 (dark grey line) is compared with a demand spectrum related to a seismic event with PGA of 1,65 m/s^2 (light grey line). In the represented case, the PP falls within the elastic limit state, meaning that the analysed archetype will undergo light damage in the occurrence of analogous earthquake hazard levels.

By comparing the capacity curves of the identified Abs against all the 125 demand spectra, the performance level of most Abruzzo residential buildings is assessed and the frequencies of attainment of specific Damage Limit States are derived, accounting for the record-to-record variability.

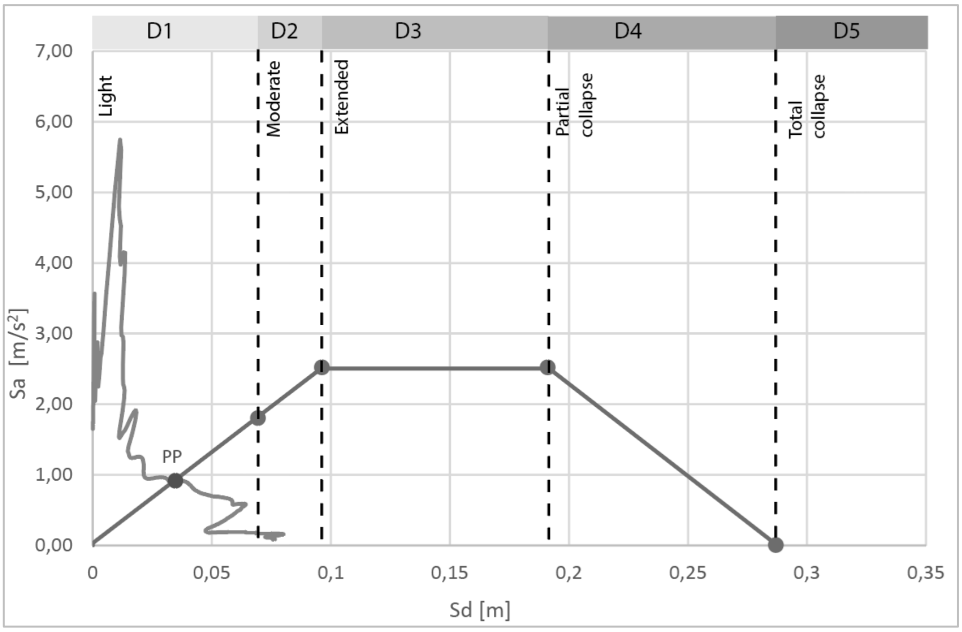

Figure 7. Definition of the PP for Archetype AB#1.

4.4 Estimation of analytical fragility curves

The obtained probabilities are first used to define the Damage Probability Matrix (DPM) and to estimate likely damage scenarios for each family of seismic inputs; subsequently, they are cumulated to create the Cumulative Damage Probability Matrix (CDPM), which defines the probability of exceeding a given Damage Limit State. The discrete values of the matrix are then plotted through lognormal functions to obtain the fragility curves associated with each archetype building. For the sake of clarity, the lognormal function is typically described by 2 parameters: the median PGA for different damage levels and the standard deviation β assumed as constant for all damage levels in order to avoid the intersection of the fragility curves within the interval of numerical integration of the risk convolution [31]. The plot in Figure 8 exemplifies the construction of fragility curves with reference to Archetype Buildings AB#1, AB #9 and AB#17. It is shown that, in the occurrence of seismic events with a PGA of 0,4 g, almost 11% of the buildings falling in the category of AB#1 will experience a damage level D5, 26% of the buildings a damage level between D4 and D5, 25% a damage level between D3 and D4, 19% a damage level between D2 and D3, and 18% a damage level between D1 and D2; while less than 1% will experience no significant damage. Analogous considerations can be made for archetypes AB #9 and AB#17.

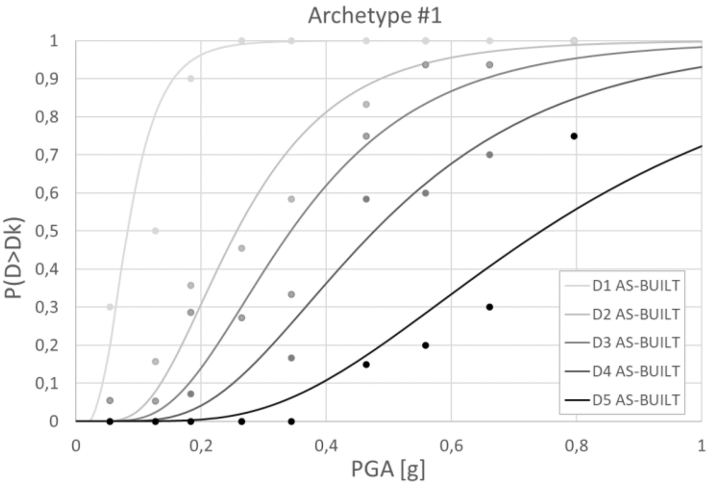

Damage	Median PGA	β
D1	0,08	
D2	0,26	
D3	0,34	0,50
D4	0,48	
D5	0,74	

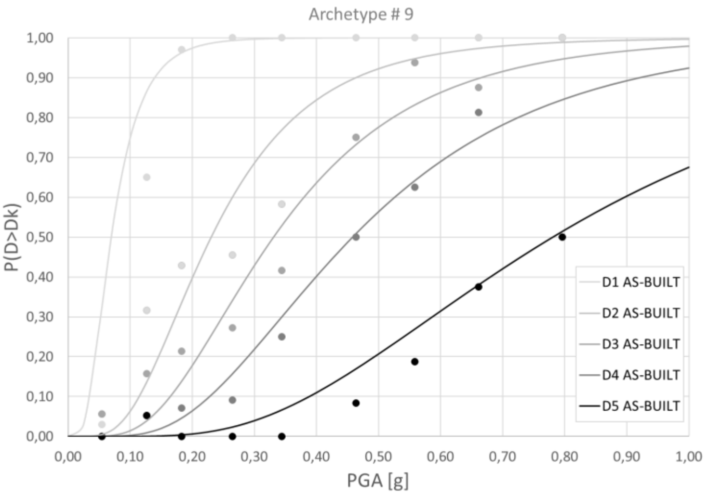

Damage	Median PGA	β
D1	0,07	
D2	0,23	
D3	0,33	0,54
D4	0,46	
D5	0,78	

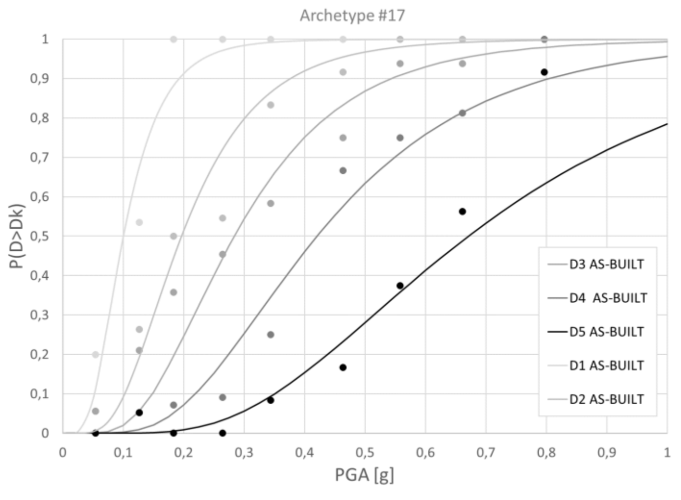

Damage	Median PGA	β
D1	0,10	
D2	0,19	
D3	0,28	0,51
D4	0,42	
D5	0,67	

Figure 8. Construction of fragility curves for AB #1, AB #9 and AB #17. Points are interpolated by a lognormal function defined by the parameters given in the right-hand side.

The afore mentioned procedure is repeated for all the 26 archetype masonry buildings identified in the Abruzzo region, allowing to derive the relevant fragility curves for each damage level and to assess the out-of-plane vulnerability of this representative set of buildings in their as-built configuration. The analytical fragility curves of the entire sample of archetypes are showed in Annex 1.

5. ASSESSMENT OF IN-PLANE MECHANISMS

5.1 NUMERICAL APPROACH

To fully assess the seismic capacity of masonry buildings, it is also crucial analysing their global behaviour by investigating all the possible in-plane (or II mode) collapse mechanisms that these structures may undergo due to horizontal forces. The technical literature is rich in numerical approaches that allow performing such type of analyses, ranging from sophisticated and detailed micro-modelling strategies [32], [33], [34] to more straightforward and expeditious macro-modelling approaches [35], [36]. Among the latter, the Equivalent Frame Modelling (EFM) approach is today the most widely used in the engineering practice.

The EFM is a macroelement-based method where the structure is ideally discretized as a frame of deformable and rigidly connected equivalent one-dimensional elements, that are piers and spandrels. In structural terms, the piers are vertical elements designed to provide support to the structure and to resist lateral forces; whereas the spandrels, on the other hand, are horizontal elements placed above the openings and extending between piers, helping to distribute and transfer the horizontal forces. Several authors have proposed different formulations to model piers and spandrels, and to connect them to each other [37], [38]. Regardless of the specific procedure, all EFM methodologies rely on simplified models and hypotheses to assess the global seismic behaviour of masonry buildings - assuming that local failure modes are prevented and require a low number of input mechanical parameters, meaning low computational burden and time/cost-saving structural analyses [39]. For these reasons, given the large number of structures to be analysed as well as the phenomena to be investigated, the EFM approach is deemed as the most suitable and efficient for the specific case being discussed.

For each of the 26 archetype buildings under investigation, an equivalent frame model is implemented in MIDAS GEN software [14] considering different assumptions based on their respective boundary conditions. Two types of elements are used: 1) elastic *beam elements* to represent both the vertical piers and the horizontal spandrels, namely the deformable parts in which seismic damage can occur; and 2) *rigid link* elements to represent the rigid zones intersecting the two deformable parts and where seismic damage does not occur. This schematization derives from the damages observed in masonry structures under past seismic events: indeed, in most cases, damage concentrated in piers and spandrels, but it did not affect the node panels, corroborating the assumption of their greater stiffness and strength with respect to the former where, conversely, wall deformations are typically concentrated. Figure 9 shows the main steps of the EFM idealization of a generic archetype building.

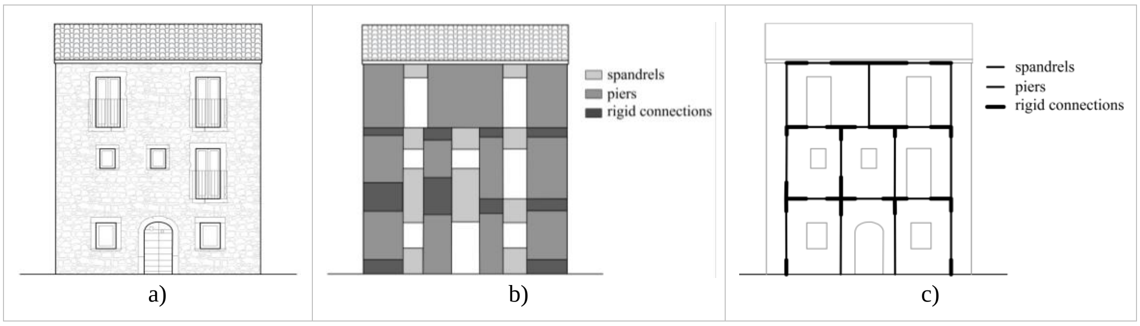

Figure 9. Identification of the equivalent frame for a generic archetype building: a) front wall of the archetype building; b) identification of spandrels, piers, and rigid connections; c) equivalent frame scheme with beam elements.

The non-linear behaviour of both piers and spandrels is numerically simulated through lumped plasticity models, defined according to the provisions of the U.S. Federal Emergency Management Agency (FEMA) [41]. Particularly, concentrated plastic hinges are assigned to critical locations of the frame, corresponding to the ends and central node of the beams in order to simulate, respectively, their bending and shear behaviour, thus accounting for both the flexural and shear failure mechanisms of the masonry panels.

The mechanical properties of the masonry material adopted for modelling each AB are chosen according to the current Italian technical code [25]. Table 6 summarizes both the elastic parameters assigned to the beams to describe the linear elastic behaviour of the masonry panels, i.e. Young's modulus (E), shear modulus (G) and weight density (γ), as well as the inelastic parameters assigned to the hinges to capture the non-linear response of the masonry, i.e. shear (τ_0) and compressive strengths (f_m). It is noted that, as regards brick masonry, different mechanical parameters are assumed depending on the age of the buildings.

Table 6. Mechanical proprieties adopted for the numerical analyses of the archetype buildings.

ID Archetype Building	**Masonry Type**	**Construction period**	**E [MPa]**	**G [MPa]**	**γ [KN/m^3]**	**τ_0 [MPa]**	**f_m [MPa]**
1-2-3-4-5-6-7-8-9-12-13-15-22-24-25	Irreg. masonry	<1860	870	290	19	0,025	1,5
16-17-18-19-20-21	Brick masonry	<1860	1200	400	18	0,05	2,6
10-11-14-23-26	Brick masonry	>1945	1500	500	18	0,09	3,45

Due to the different structural configuration of the ABs, two types of analyses are conducted:

- Global analyses in the case of archetype buildings with rigid floors, that means buildings with adequate connections between vertical and horizontal elements. To account for it, slabs are modelled as horizontal rigid diaphragms with infinite in-plane stiffness to guarantee a distribution of the seismic forces proportional to the relative stiffness of the shear walls belonging to the building.
- Analyses of single walls in the case of archetype buildings with flexible floors, namely buildings where the in-plane stiffness of the horizontal diaphragms is almost negligible. Flexible diaphragms lack the capacity to redistribute lateral forces between frames that can, indeed, translate independently. In these cases, all the walls belonging to the archetype are analysed individually and the one featuring the lowest shear strength is conservatively chosen as representative of the global in-plane response of the entire AB.

Nonlinear monotonic static analyses (NLSA) are carried out for both cases (rigid and flexible diaphragms) using a height-wise lateral force distribution proportional to masses, allowing to obtain representative pushover capacity curves for all archetypes. The pushover curve of each MDOF system, expressed in terms of base shear (F) versus top displacement of a control point (d*), is then converted into the bilinear capacity curve of an equivalent non-linear SDOF system, defined considering a modal participation factor equal to 1. This simplified curve is obtained by imposing that the linear elastic branch intersects the MDOF pushover curve at the point where the force equals 60% of the maximum ultimate force (F_u*), while the yield force (F_y), that represents the ultimate strength of the idealized SDOF system, is identified by imposing the equality of the areas subtended by the curves, considering as a maximum displacement (d_u) the point corresponding to a resistance reduction of 20%. Finally, to compare the resulting capacity curves with the seismic demand in ADRS format, all force-displacement bilinear curves are converted in spectral coordinates, leading to the so-called capacity spectra. Figure 10 exemplifies the bilinearization of the pushover curve and its conversion into a bilinear capacity spectrum.

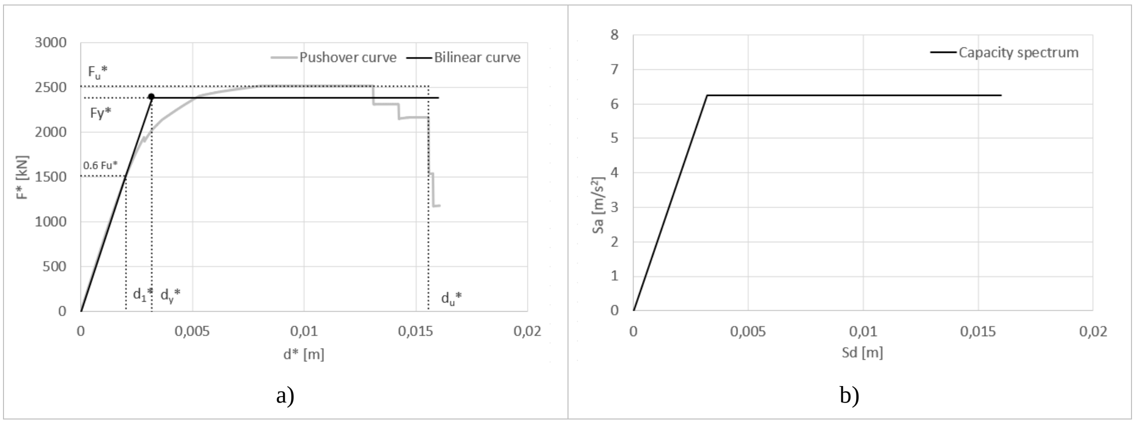

Figure 10. Generic pushover curve from NLSA: a) example of bilinearization and b) transformation into a capacity spectrum in the ADRS space.

For the sake of comparison, Figure 11 depicts the bilinear curves obtained for the same archetypes discussed in Section 4.1. As expected, the overall capacity in terms of strength of the buildings remarkably increases as the number of stories decreases, on the contrary the ductility decreases. All the pushover curves obtained from the analyses of the remaining archetypes in their as-built configuration are shown in Section 7 together with those obtained from their retrofitted configuration.

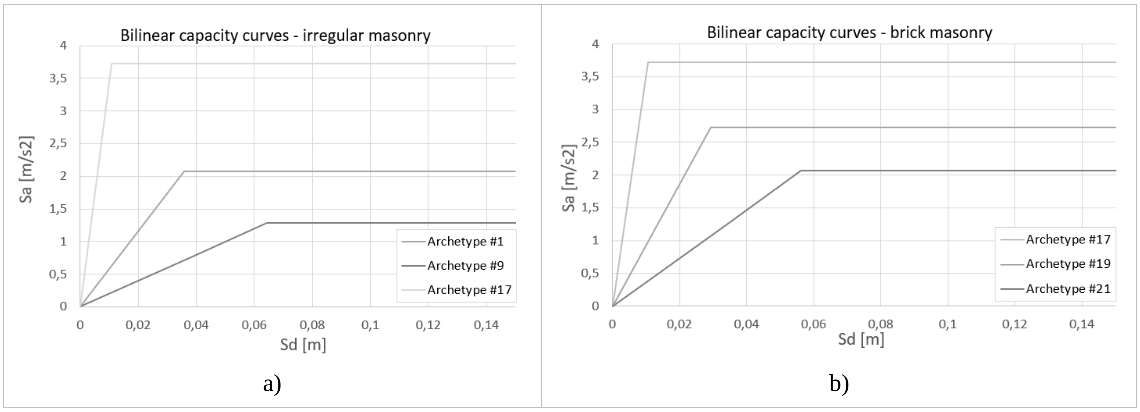

Figure 11. Bilinear capacity curves for Archetype in a) irregular masonry and b) brick masonry as the number of floors increases (from 2 to 4)

5.2 Identification of damage thresholds and comparison with seismic demand

In order to establish a correlation between DLs and PLs of the archetypes in the occurrence of different earthquake hazard levels, Damage Thresholds T(Dk) are again defined for each capacity curve [42] similarly to what done in Section 4.2 for the curves derived from the assessment of out-of-plane mechanisms. Yet, in this case, the approach employed is the one proposed by Lagomarsino and Giovinazzi in [43], where damage thresholds are defined as a function of the yielding and ultimate displacements (d_y and d_u, respectively) of the system, as follows:

- T(D1) = 0.7 d_y
- T(D2) = 1.5 d_y
- T(D3) = 0.5 (d_y + d_u)
- T(D4) = d_u

Based on these assumptions, five DLs are defined for each bilinear capacity spectrum, starting from light damage (D1 - light grey) until collapse (D5 - dark grey), as shown in the generic capacity curve reported in Figure 12, where the different damage thresholds are also highlighted. Through the comparison between the capacity curves of the equivalent SDOF systems and the seismic demands, both represented in a spectral acceleration-displacement domain, this method can allow estimating the global seismic performance of the Abruzzo masonry archetype buildings. To this end, the same set of 125 natural records used for the evaluations performed in Section 4.2, organized into families characterized by a mean reference PGA (Table 3), is employed. Analogously, the seismic input accelerograms - transformed in ADRS format - are compared with the capacity spectra of the archetypes, now derived from the non-linear static analyses.

The procedure for the identification of the Performance Point (PP) of each archetype is graphically shown in Figure 12. For comparative purposes, the capacity spectrum referred to the in-plane response of AB#1 as well as the same demand spectrum used in Section 4.3 (PGA = 1,65 m/s^2) are reported in the plot. The intersection between bilinear curve and demand spectrum provides the maximum capacity of the building as a function of a specific seismic intensity. Moreover, the location of the PP enables identifying the damage level that the structure will likely undergo under the considered seismic scenario. For the building represented in Figure 12, the PP (in red) falls within the elastic limit state, meaning that the analysed archetype will suffer light damage in the occurrence of similar earthquake hazard levels.

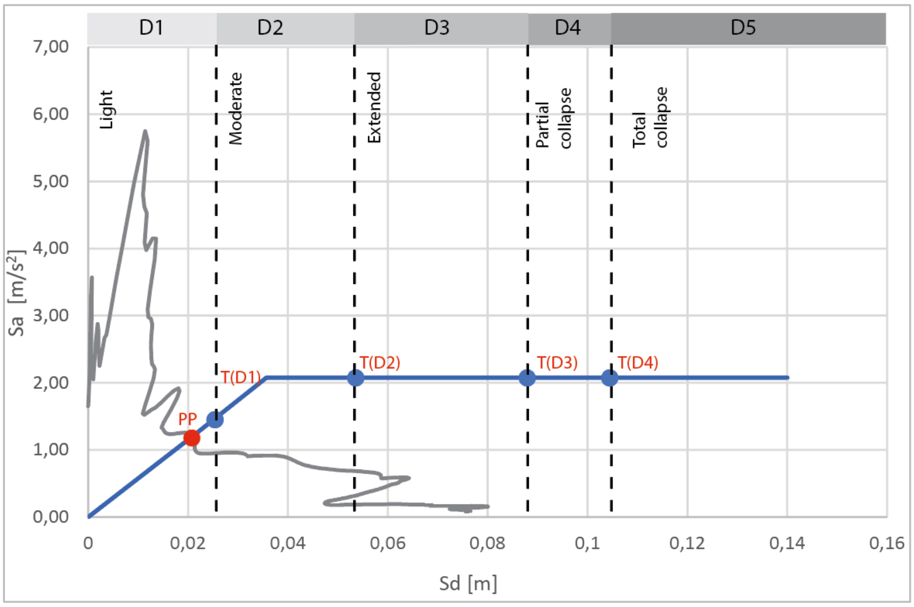

Figure 12 . Generic capacity spectrum (blue curve) with identification of Damage Levels (DLs) and Damage Thresholds (T(Dk)). The PP resulting from the comparison with the ADRS seismic demand (grey line) is also highlighted.

5.3 Estimation of numerical fragility curves

For each family of records, the frequencies of exceedance of specific Damage Limit States are assumed as probability of exceedance of a specific DL, accounting for the uncertainties associated to the record-to-record variability. These probabilities, which represent Damage Probability Matrices (DPMs), are cumulated to obtain the Cumulative Damage Probability Matrices (CDPMs), whose discrete values are used to obtain the fragility curves associated with each archetype through a lognormal distribution. A maximum likelihood estimation approach is used for fitting the data to the lognormal distribution to maximize their probability of occurrence. As already explained, a unique value of dispersion for all damage states is defined for each building typology to ensure the ordinal nature of damage [43]. Figure 13 shows the numerical fragility curves obtained for buildings AB#1, AB#9 and AB#17. The curves referring to the entire sample of archetype buildings are reported in Annex 1.

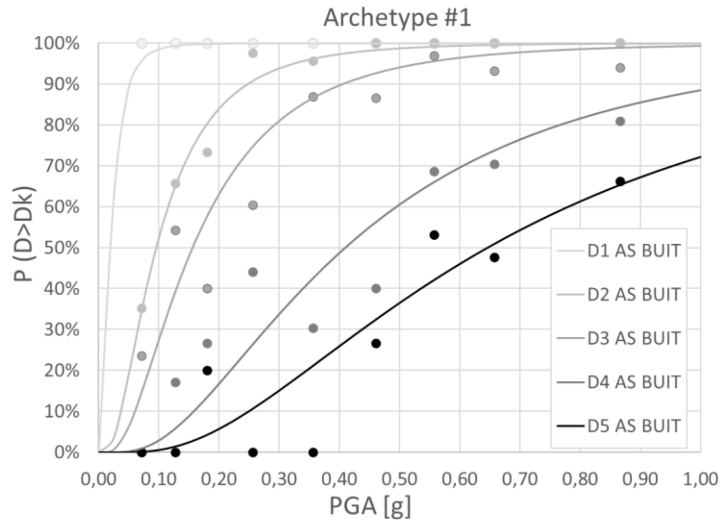

Damage	Median PGA	β
D1	0,02	
D2	0,10	
D3	0,16	0,74
D4	0,41	
D5	0,65	

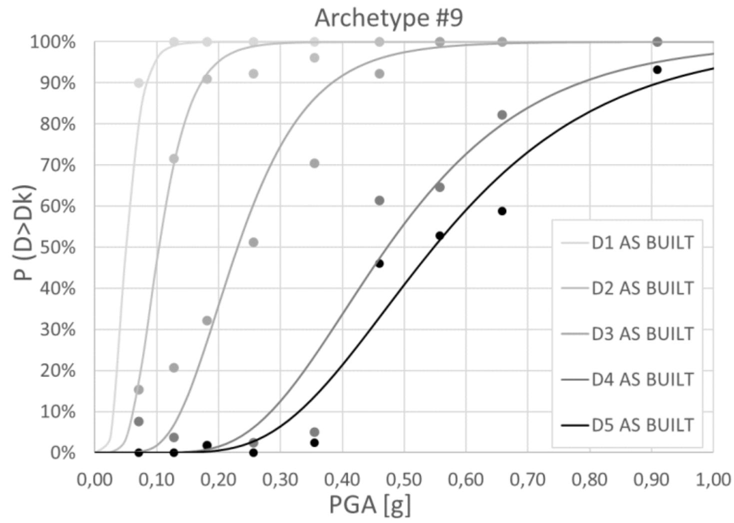

Damage	Median PGA	β
D1	0,05	
D2	0,10	
D3	0,23	0,40
D4	0,47	
D5	0,55	

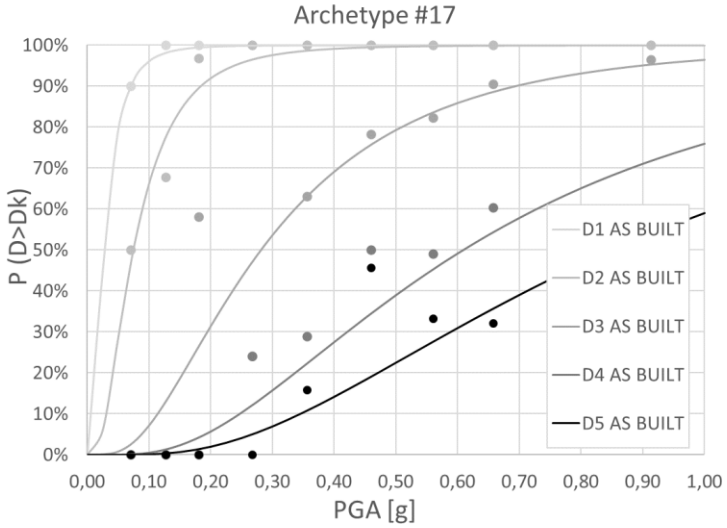

Damage	Median PGA	β
D1	0,03	
D2	0,07	
D3	0,28	0,73
D4	0,61	
D5	0,85	

Figure 13. Construction of numerical fragility curves for AB #1, AB #9 and AB #17. Points are interpolated by a lognormal function defined by the parameters given in the right-hand side.

6. INTEGRATED FRAGILITY CURVES AND COMPARISON WITH EMPIRICAL APPROACHES

The analytical and numerical approaches applied hitherto have allowed assessing the seismic vulnerability of the representative set of Abruzzo residential buildings through the computation of fragility curves respectively referred to the out-of-plane and in-plane capacities of the identified archetypes. In order to evaluate the seismic vulnerability of such buildings accounting for both local and global damage mechanisms, the fragility curves derived from the two methods are here compared and, ultimately, combined. As a general rule, between the analytical and the numerical curves of each archetype, the one associated with the highest probability of exceeding a specific damage level under progressive seismic scenarios (expressed in terms of PGA) is chosen as representative of the potential damage of that archetype. Specifically, if the fragility curves for each DL are well spaced, the most severe curve is easily discernible and selected (Figure 14a); though, when they intersect each other, the PGA value corresponding to the intersection point is identified and a new fragility curve is plotted using a lognormal function passing through the most severe points of damage resulting from both the analytical and numerical CDPMs (Figure 14b).

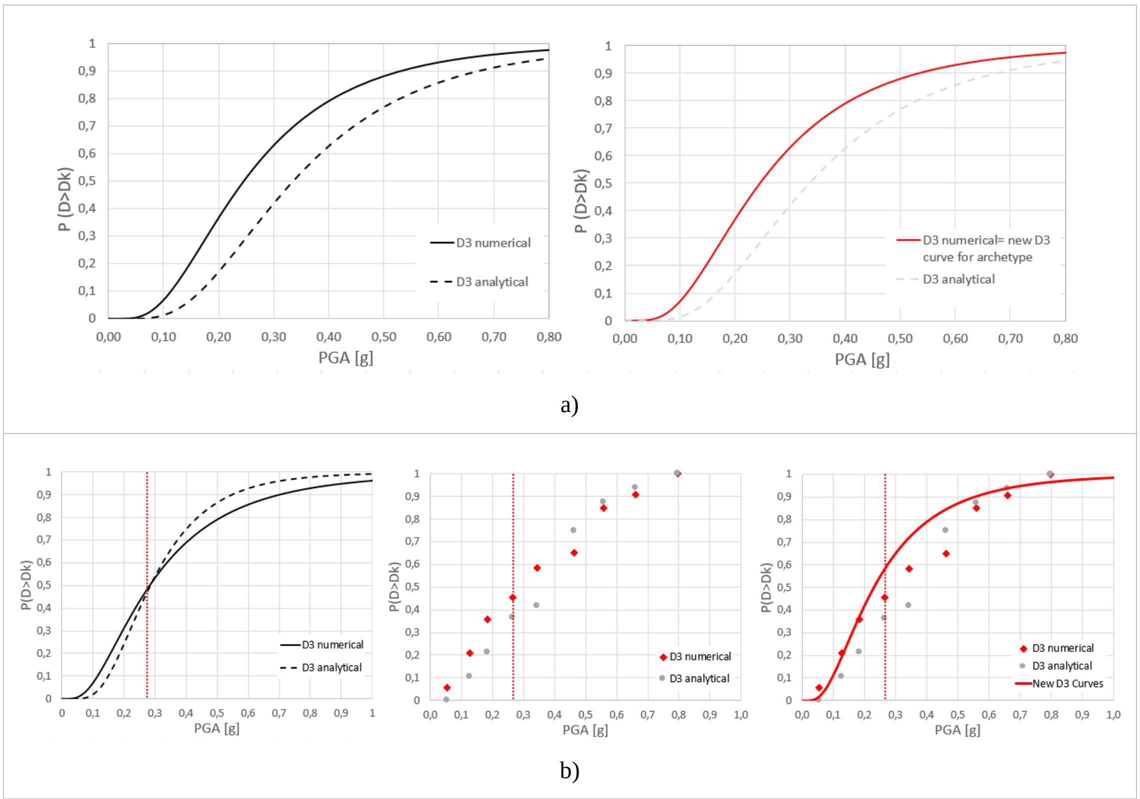

Figure 14. Definition of integrated fragility curves a) when damage curves do not intersect each other and b) when damage curves intersect each other.

Following the proposed procedure for the five damage levels and for each archetype, integrated fragility curves are derived for the entire sample of residential masonry buildings of the Abruzzo region. Figure 15 shows the final curves obtained for buildings AB#1, AB#9 and AB#17.

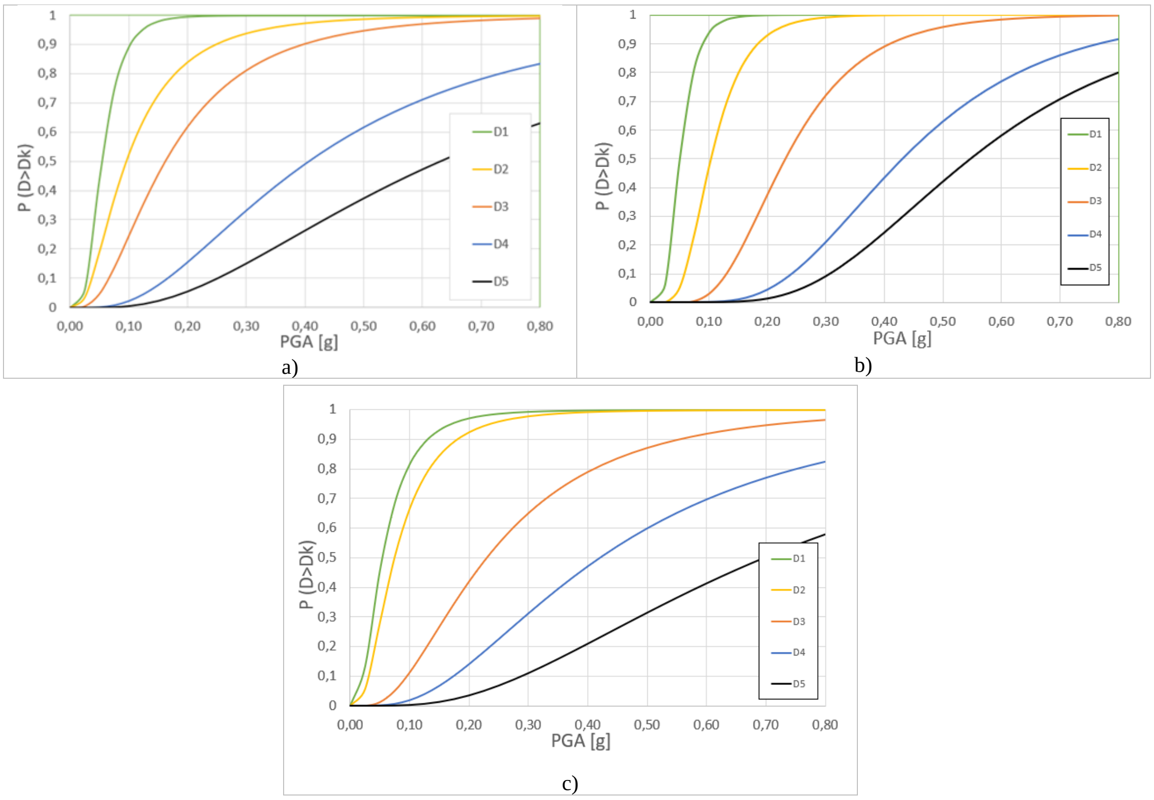

Figure 15. Final integrated fragility curves for a) Archetype #1, b) Archetype #9 and c) Archetype #17.

For completeness, the integrated fragility curves of the other archetypes are reported in Annex 1. Overall, in comparison with the analytical method, the numerical approach leads to more severe curves for light, moderate and extensive damage levels, i.e. for D1, D2 and D3, whereas for severe damage levels (D4 and D5), corresponding to the near collapse and collapse conditions, the numerical curves lead to lower expected damages.

Further interesting considerations can be drawn by comparing and cross-validating the outcome of the mechanical methodologies employed in the previous Sections with the results from a strictly empirical approach applied by the authors to residential masonry buildings of the same area and widely discussed in a past work [44]. While the former methods rely on detailed and objective analytical and numerical evaluations, the latter is based on the definition of vulnerability indexes according to observational data and engineering judgments, resulting by nature less accurate in predicting the seismic behaviour at the building scale.

The curves resulting from this comparison are plotted by damage level in Figure 16, where the continuous lines represent the mechanical fragility curves of the 26 ABs and the dashed lines represent the overall empirical fragility curves extrapolated for the residential masonry buildings of the same region. It is observed that, from the extended damage level (D3) onwards, the empirical curves average very well the mechanical curves. By contrast, for lower damage levels (D1 and D2), mechanical curves appear visibly higher than the empirical ones, meaning that the analysed buildings, for these damage levels, result much more vulnerable according to the analytical and numerical approaches than with respect to the empirical predictions. This outcome was somehow expected as empirical methodologies are more approximate and, consequently, more conservative and less able to capture lower damage levels. Moreover, it is worth stressing that the sample of residential buildings analysed with the empirical approach includes only buildings with irregular masonry without tie-rods, so it slightly differs from the sample considered to build the archetypes.

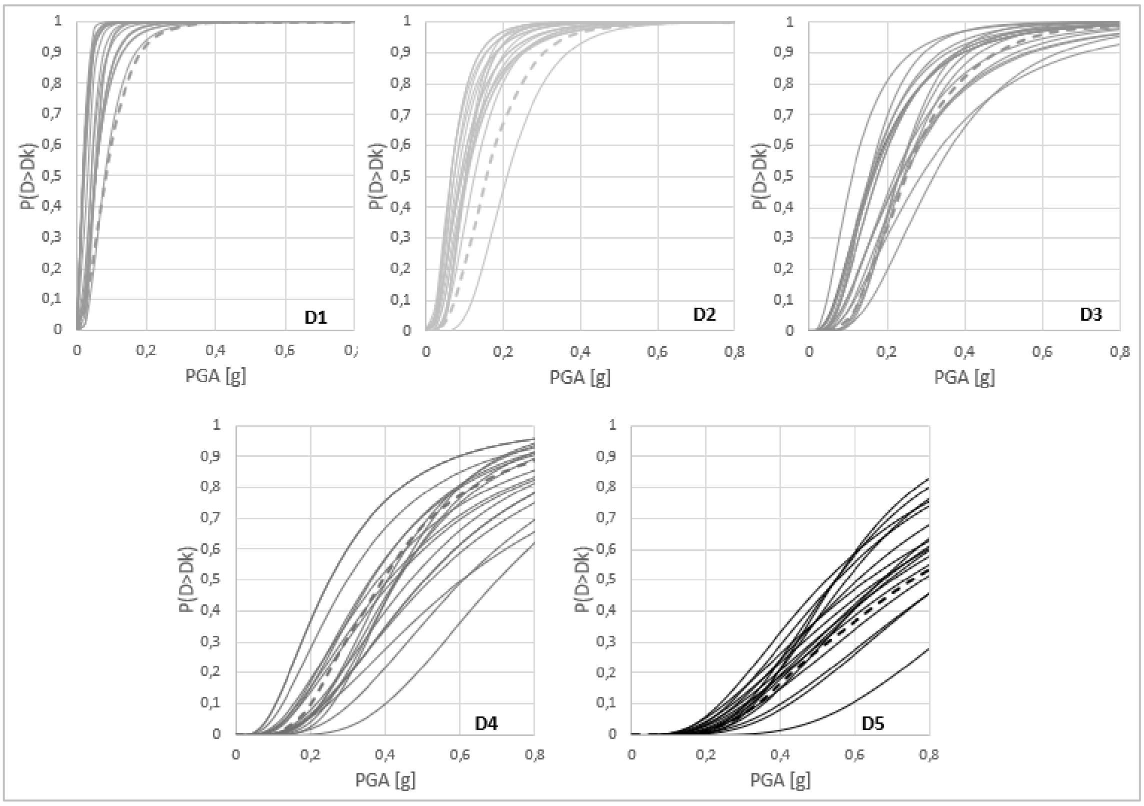

Figure 16. Comparison between mechanical curves (continuous lines) and empirical curves (dashed lines) by damage level (for the colours, the reader is referred to the online version of the article).

7. SEISMIC RETROFITTING FOR RISK REDUCTION

Rooted in the outcome of Section 6, two retrofitting solutions are proposed to reduce the potential seismic vulnerabilities of most analysed archetypes: 1) retrofitting interventions that restrain out-of-plane collapses and prevent local damage mechanisms, and 2) retrofitting interventions that improve the in-plane capacity of masonry walls favouring an enhanced global response. In either case, only solutions compatible with the reversibility concept required in case of historical constructions are considered.

Among the best and simplest devices able to inhibit out-of-plane failure mechanisms are metal tie rods applied at floor and/or roof level. During recent seismic events, the widespread use of these elements has proved effective in improving wall-to-wall, wall-to-floor and wall-to-roof connections in existing masonry buildings, fostering a box-like behaviour. Indeed, the stabilizing actions provided by the tie rods counteract the destabilizing forces originated by potential thrusting components as well as the inertia forces generated by massive elements. In what concerns the analysed archetypes, the beneficial effect of tie rods is evaluated and quantified considering different layouts: 1) single pair of tie rods inserted at the top of the building (roof level); and 2) pairs of tie rods inserted at each intermediate storey (floor level) up to a maximum of six devices, i.e. two per floor. In all configurations, the connection with the vertical masonry walls is guaranteed through steel anchor plates. The tension necessary to counteract the overturning mechanism is calculated assuming the insertion of tie rods with 28mm diameter, made of S235 steel and tightened by 20x20cm steel plates.

The effectiveness of the application of this retrofitting solution is evaluated by updating the seismic vulnerability assessment discussed in Section 4 for the as-built archetype configurations according to the new retrofitted configurations, thus leading to the definition of new fragility curves. With the aim of driving cost-efficient interventions and fostering the wise allocation of resources devoted to seismic risk mitigation strategies, the seismic improvement attained for the different tie-rods layouts is quantified by means of an “improvement factor” (*IF*). This quantity is calculated as the percentage variation of the probability of attaining a moderate damage level (D3) pre- and post-intervention (i.e. as-built vs retrofitted) under an earthquake scenario characterized by a PGA of 0,5g, see Eq. (6). In this regard, it is worth stressing that the *IF* normalization with respect to the D3 curve is applied because this DL corresponds to an intermediate damage, lying between the damage limit state (DLS) and the near collapse limit state (NCLS); whereas the PGA value assumed for the seismic hazard is selected according to the values recorded by the main quake that hit L'Aquila (Abruzzo, Italy) in 2009, which were indeed about 0.5 g [45].

$$IF_{PGA=0,5}(\%) = \frac{|P(D>D_k)_{D3-RETR} - P(D>D_k)_{D3-AS\,BUILT}|}{P(D>D_k)_{D3-AS\,BUILT}} \quad (6)$$

The improvement factors resulting from the seismic retrofitting of the analysed archetype buildings against local damage mechanisms are shown in Figure 17. It is observed that, by inserting only two tie-rods at the top of the façade, the average seismic performance level of Abruzzo archetype buildings increases by 15%; by applying four tie-rods, the average improvement is around 34 % and, by inserting tie-rods at each interstorey, the seismic performance increases up to 43%.

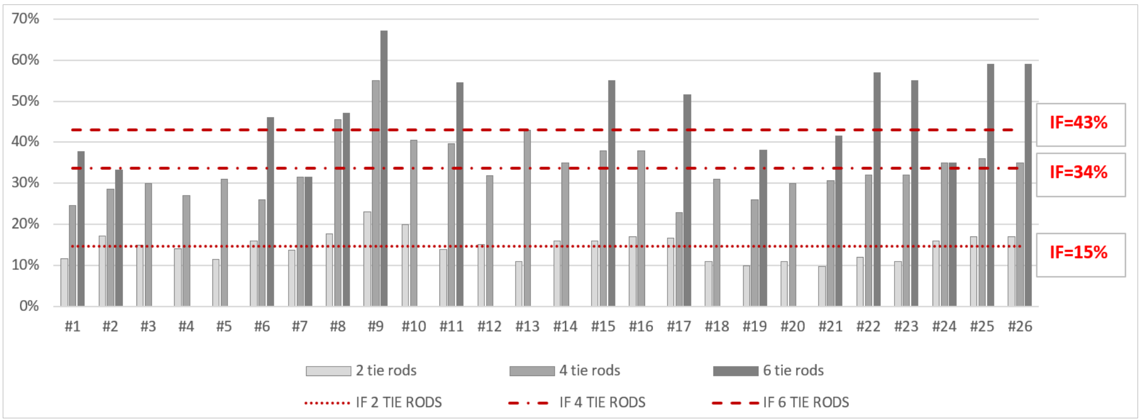

Figure 17. Improvement factors of the archetype's seismic performance against local damage mechanisms for different tie-rods configurations.

With respect to the seismic improvement of the global response of Abruzzo masonry buildings, Natural Fabric-Reinforced Cementitious Matrix (NFRCM) composites are selected as the most suitable solution to enhance the in-plane capacity of the archetypes without resorting to invasive and non-compatible techniques. Indeed, retrofit interventions based on NFRCMs allows improving the shear strength of masonry walls, similarly to FRCM-based systems, but using natural instead of synthetic fibres.

Although this type of strengthening slightly increases the thickness of the masonry wall to which it is applied, it can effectively counteract local cracking. Following the modelling assumptions proposed in the literature for this type of material, the behaviour of the NFRCM-strengthened archetype buildings is simulated considering a perfect adhesion between the composite and the masonry substrate, thus modelling the reinforced walls as a homogeneous continuum. The mechanical parameters to input in the numerical models to repeat the non-linear static analyses for the NFRCM-retrofitted configuration of the archetypes are defined according to the results from experimental shear tests performed on regular masonry specimens. Subsequently, the seismic vulnerability assessment discussed in Section 5 is updated to determine the pushover curves of the strengthened archetypes, derive the capacity spectra of the equivalent SDOF systems and compute the new fragility curves from which the improvement in the seismic performance of the buildings is estimated. Figure 18 compares the capacity curves of the archetypes before and after the application of the NFRCM retrofitting solution.

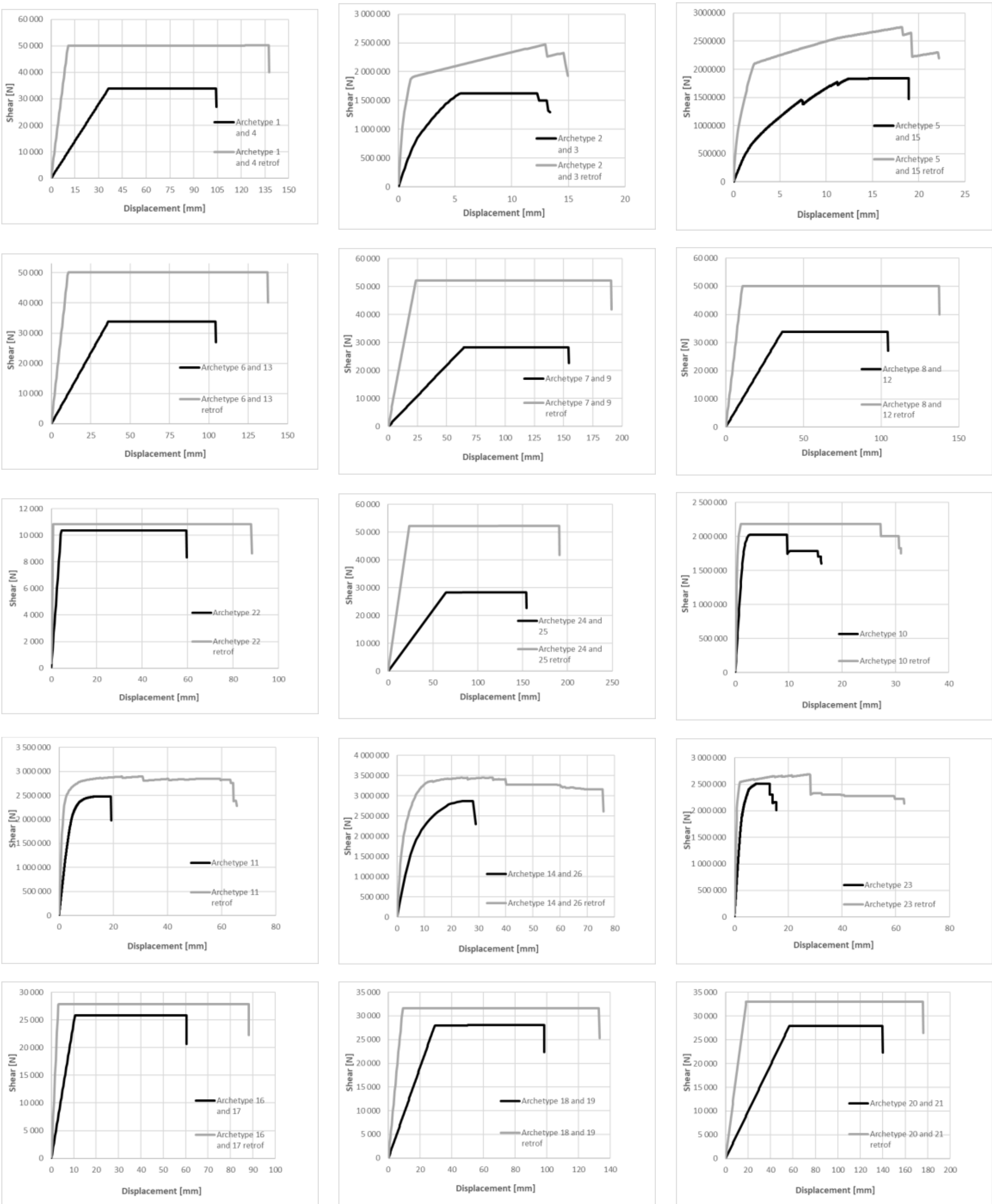

Figure 18. Pushover curves obtained from the NLSA of the archetypes in their as-built and NFRCM-retrofitted configurations.

The improvement factors resulting from the seismic retrofitting of the 26 archetype buildings against global damage mechanisms are reported in the histogram of Figure 19. It is shown that the average seismic performance of the archetypes increases by 17%. The greatest improvement is found for archetypes AB#10 and AB#23, which are brick masonry buildings with 2 and 3 stories, respectively, heavy floors and roofing, and no tie-rods.

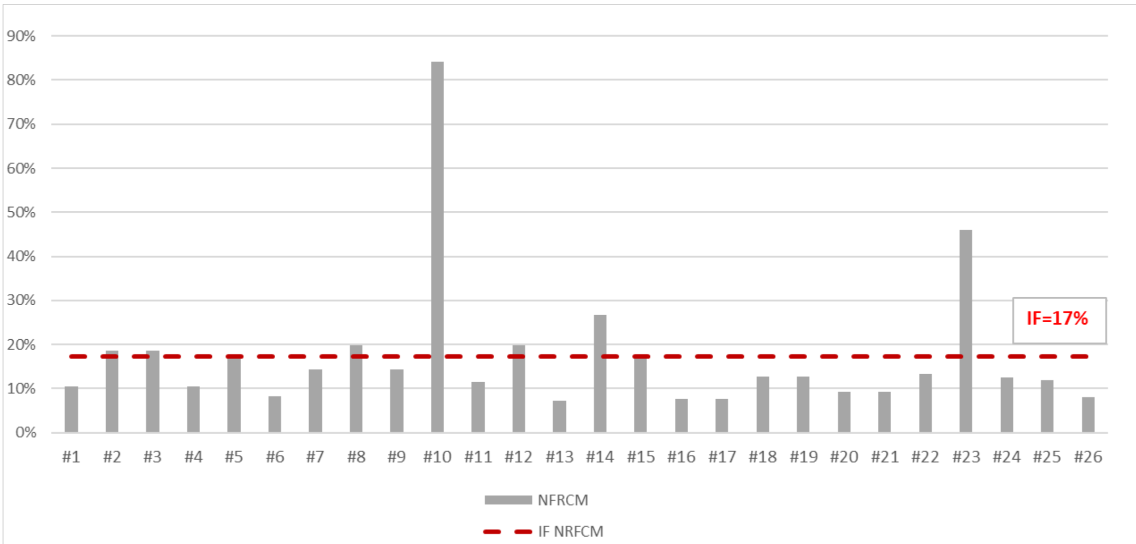

Figure 19. Improvement factors of the seismic performance against global damage mechanisms of the archetypes reinforced with NFRCM.

8. CONCLUSIONS

In this paper, an integrated approach for assessing the seismic vulnerability of residential masonry buildings at the large-scale accounting for both local and global damage mechanisms was presented. In order to overcome the limitations of conventional empirical methods, which are notoriously less accurate when applied to extensive territorial areas, the proposed approach leverages the accuracy of analytical and numerical methods - typically used for single building analyses - to study a reduced number of buildings representative of the masonry residential building stock of the Abruzzo region, referred to as archetypes, and derive therefrom reliable fragility curves and damage levels valid for the entire set of buildings associated with the identified archetypes. The approach was applied to a sample of 26 different archetypes extracted through a semi-automated procedure from the CARTIS national database. The outcome was used to drive the most appropriate seismic retrofitting solutions and to quantify the beneficial impact of targeted interventions in terms of performance level. Finally, the results were compared against those obtained from a strictly empirical approach, allowing to prove the greater accuracy of this integrated large-scale assessment at the expense of a reasonable increase in the analysis time.

The main conclusions of the study are summarized below:

- The kinematic analyses showed that for the entire set of identified ABs the first mechanism that activates is the complete overturning of the façade because of the poor connections between orthogonal walls as well as between walls and floors. The simple insertion of metal tie rods at the floor levels is proved more than effective in ensuring a better box-like behaviour of the buildings, allowing to attain a seismic improvement between 15% and 43% in the performance level of the archetypes depending on the number of ties inserted per floor.
- The numerical analyses, performed assuming an effective interlocking between orthogonal walls and the non-occurrence of out-of-plane mechanisms, allowed assessing the in-plane capacity of the archetypes in their as-built configuration showing that, regardless of the masonry type, the capacity of the archetypes increases as the number of stories decreases. The application of NFRCM reinforcements to the exterior wall surfaces of these buildings enabled improving their global behaviour of nearly 20%, particularly in the case of archetypes consisting of regular brick masonry, with rigid slabs and heavy roofs.
- The proposed improvement factor can be a valuable index to quantify the economic and structural benefits of different seismic retrofitting measures and optimize the cost-effectiveness of the interventions.
- The adoption of an integrated approach for the definition of large-scale fragility curves, encompassing both out-of-plane and in-plane mechanisms, allows identifying and selecting the most severe cumulative occurrence probabilities for each level of damage, providing an efficient decision-making tool to better prioritize investments in seismic risk mitigation strategies.

REFERENCES

[1] Saretta, Y., Sbrogiò L., Valluzzi, M. R., Assigning the macroseismic vulnerability classes to strengthened ordinary masonry buildings: An update from extensive data of the 2016 Central Italy earthquake, International Journal of Disaster Risk Reduction, Volume 62, 2021, 102318, ISSN 2212-4209, https://doi.org/10.1016/j.ijdrr.2021.102318

[2] Graziani, L., Del Mese, S., Tertulliani, A. , Arcoraci, L., Maramai, A., Rossi, A. Investigation on damage progression during the 2016–2017 seismic sequence in Central Italy using the European Macroseismic Scale (EMS-98), Bull. Earthq. Eng. 17 (2019) 5535–5558, https://doi.org/10.1007/s10518-019-00645-w

[3] Lagomarsino, S., Cattari, S. and Ottonelli, D. (2021) The heuristic vulnerability model: Fragility curves for masonry buildings. Bulletin of Earthquake Engineering 19(8): 3129–3163, https://doi.org/10.1007/s10518-021-01063-7

[4] Ferreira, T. M., Mendes, N., & Silva, R. (2019). Multiscale seismic vulnerability assessment and retrofit of existing masonry buildings. Buildings, 9(4). https://doi.org/10.3390/buildings9040091

[5] Benedetti D, Benzoni G, Parisi MA (1988) Seismic Vulnerability and Risk evaluation for old urban nuclei. Earthq Eng Struct Dyn 16:183–201.

[6] Barbat AH, Carreño ML, Pujades LG, et al (2010) Seismic vulnerability and risk evaluation methods for urban areas. A review with application to a pilot area. Struct Infrastruct Eng 6:17–38. https://doi.org/10.1080/15732470802663763

[7] Ferreira TM, Vicente R, Silva JARM, et al (2013) Seismic vulnerability assessment of historical urban centres: case study of the old city centre in Seixal, Portugal. Bull Earthq Eng 11:1753–1773

[8] Rapone D, Brando G, Spacone E, De Matteis G (2018) Seismic vulnerability assessment of historic centers: description of a predictive method and application to the case study of Scanno (Abruzzi, Italy). Int J Archit Herit 12:1171–1195. https://doi.org/10.1080/15583058.2018.1503373

[9] Morais, E. C., Vigh, L. G., & Krähling, J. (2021). Cyclic Behaviour, Dynamic Analysis and Seismic Vulnerability of Historical Building Archetypes in Hungary. International Journal of Architectural Heritage, 15(7), 1022–1042. https://doi.org/10.1080/15583058.2019.1690074

[10] Zuccaro G, Dolce M, De Gregorio D, et al. La scheda CARTIS per la caratterizzazione tipologico-strutturale dei comparti urbani costituiti da edifici ordinari. Valutazione dell'esposizione in analisi di rischio sismico. In: Proceedings of the 34th National Conference of GNGTS. Trieste. 2015.

[11] Basaglia, A., Cianchino, G., Cocco, G., Rapone, D., Terrenzi, M., Spacone, E., & Brando, G. (2021). An automatic procedure for deriving building portfolios using the Italian " CARTIS " online database. Structures, 34(June), 2974–2986. https://doi.org/10.1016/j.istruc.2021.09.054

[12] Polese, M., Gaetani. d'Aragona, M. , Prota A. "Simplified Approach for Building Inventory and Seismic Damage Assessment at the Territorial Scale: An Application for a Town in Southern Italy." Soil Dynamics and Earthquake Engineering, vol. 121, no. April 2018, Elsevier Ltd, 2019, pp. 405–20, doi:10.1016/j.soildyn.2019.03.028

[13] Cianchino G., Cocco G., Rapone D., Di Lallo Y., Masciotta M.G., Brando G., Vulnerability analytical models at the regional scale through archetype buildings: an application to the Abruzzi region, Procedia Structural Integrity, Volume 44, 2023, Pages 219-226, ISSN 2452-3216, https://doi.org/10.1016/j.prostr.2023.01.029.

[14] MIDAS Gen (2020), MIDAS Information Technology Co., http:// www. midas oft. com/ build ing/ produ cts/midas gen, http:// www. cspfea. net

[15] Lagomarsino, S., Cattari, S. PERPETUATE guidelines for seismic performance-based assessment of cultural heritage masonry structures. Bull Earthquake Eng 13, 13–47 (2015). https://doi.org/10.1007/s10518-014-9674-1.

[16] Porter, K.A. An overview of PEER's performance-based earthquake engineering methodology. Proc. Ninth International Conference on Applications of Statistics and Probability in Civil Engineering (ICASP9) July 6-9, 2003, San Francisco, CA. Civil Engineering Risk and Reliability Association (CERRA), 973-980.

[17] Takewaki, I. Beyond uncertainties in earthquake structural engineering. Frontiers in Built Environment, Vol. 1., 2015. doi: 10.3389/fbuil.2015.00001

[18] Lallemant, D., Kiremidjian, A. Accounting For Uncertainty In Earthquake Fragility Curves. In Proceedings of the 16th World Conf Earthq Eng 16WCEE, 9-13 January 2017, Santiago, Chile.

[19] A. Masi, S. Lagomarsino, M. Dolce, V. Manfredi, and D. Ottonelli, Towards the updated Italian seismic risk assessment: exposure and vulnerability modelling, vol. 19, no. 8. Springer Netherlands, 2021.

[20] V. Manfredi, A. Masi, A. G. Özcebe, R. Paolucci, and C. Smerzini, "Selection and spectral matching of recorded ground motions for seismic fragility analyses," Bull. Earthq. Eng., no. 0123456789, 2022, doi: 10.1007/s10518-022-01393-0.

[21] Casapulla C, Giresini L, Lourenço PB. Rocking and Kinematic Approaches for Rigid Block Analysis of Masonry Walls: State of the Art and Recent Developments. Buildings. 2017; 7(3):69. https://doi.org/10.3390/buildings7030069.

[22] Doherty, K., Griffith, M.C., Lam, N. and Wilson, J. Displacement-based seismic analysis for out-of-plane bending of unreinforced masonry walls. Earthquake Engng. Struct. Dyn., 2002, 31: 833-850. https://doi.org/10.1002/eqe.126.

[23] Beolchini, G. C., Milano, L., Antonacci, E. (a cura di). Repertorio dei meccanismi di danno, delle tecniche di intervento e dei relativi costi negli edifici in muratura – Definizione di modelli per l'analisi strutturale degli edifici in muratura, Volume II – Parte 1a. Convenzione di Ricerca con la Regione Marche; Consiglio Nazionale delle Ricerche – Istituto per la Tecnologia delle Costruzioni – Sede di L'Aquila; Dipartimento di Ingegneria delle Strutture, delle Acque e del Terreno (DISAT) – Università degli Studi di L'Aquila, 2005

[24] Ministero delle Infrastrutture e dei Trasporti. CIRCOLARE 21 gennaio 2019 n.7_Istruzioni per l'applicazione dell'«Aggiornamento delle "Norme tecniche per le

costruzioni"» di cui al decreto ministeriale 17 gennaio 2018. (Italian Guideline), 2019. Suppl. Ordin. alla "Gazzetta Uff n 35 del 11 febbraio 2019 - Ser Gen 337.

[25] Minister of Heritage and Cultural Activities. Circular n.26, Italian Code for protection of cultural heritage. Linee Guida per la valutazione e la riduzione del rischio Sismico del patrimonio culturale con riferimento alle norme tecniche per le costruzioni, Prot. 10953 of 2 December 2010.

[26] Doherty K, Griffith MC, Lam N, Wilson J (2002) Displacement-based seismic analysis for out-of-plane bending of unreinforced masonry walls. Earthq Eng Struct Dynam 31(4):833–850.

[27] Criber, E.; Brando, G.; de Matteis, G. The effects of L'Aquila earthquake on the St. Gemma church in Goriano Sicoli: Part I—Damage survey and kinematic analysis. Bull. Earthq. Eng., 2015, 13, 3713–3732. https://doi.org/10.1007/s10518-015-9792-4.

[28] Grünthal, G. (Ed.) European Macroseismic Scale 1998 (EMS-98) European Seismological Commission, sub commission on Engineering Seismology, Working Group Macroseismic Scales; Conseil de l'Europe, Cahiers du Centre Européen de Géodynamique et de Séismologie: Luxembourg, 1998; Volume 15.

[29] Lagomarsino, S. Seismic assessment of rocking masonry structures. Bull Earthquake Eng 13, 97–128 (2015). https://doi.org/10.1007/s10518-014-9609-x

[30] Dolce, M., Di Bucci, D. Comparing recent Italian earthquakes. Bull Earthquake Eng 15, 497–533 (2017). https://doi.org/10.1007/s10518-015-9773-7

[31] Chopra A, Goel R (1999) Capacity-Demand-Diagram Methods for Estimating Seismic Deformation of Inelastic Structures: SDF Systems. Pacific Earthq Eng Res Cent 67.

[32] Lourenço PB, Rots JG (1997) Multisurface interface model for analysis of masonry structures. J Eng Mech 123(7):660–66

[33] G. Brando, D. Rapone, E. Spacone, and M. Giovanna Masciotta, "MUDis: A low computational effort multi-unit discretization procedure for modelling masonry walls with periodic arrangement," Structures, vol. 43, pp. 1380–1406, Sep. 2022, doi: 10.1016/j.istruc.2022.07.038.

[34] Y. Di Lallo, D. Rapone, M. G. Masciotta, and G. Brando, "Non-linear analysis of URM structures through a multi-unit discretization approach," in Procedia Structural Integrity 44(2), 2023, pp. 488–495. [Online]. Available: www.sciencedirect.com

[35] D. Addessi and E. Sacco, "A multi-scale enriched model for the analysis of masonry panels," Int J Solids Struct, vol. 49, no. 6, pp. 865–880, Mar. 2012, doi: 10.1016/j.ijsol-str.2011.12.004.

[36] Dolce M (1991) Schematizzazione e modellazione degli edifici in muratura soggetti ad azioni sismiche. L'Industria delle costruzioni 25(242):44–57.

[37] Tomaževič M (1978) The computer program POR. Report ZRMK.

[38] S. Lagomarsino, A. Penna, A. Galasco, and S. Cattari, "TREMURI program: An equiv-alent frame model for the nonlinear seismic analysis of masonry buildings," Eng Struct, vol. 56, pp. 1787–1799, Nov. 2013, doi: 10.1016/j.engstruct.2013.08.002.

[39] Serena Cattari, Daniela Camilletti, Antonio Maria D'Altri, Sergio Lagomarsino, 2021. "On the use of continuum Finite Element and Equivalent Frame models for the seismic assessment of masonry walls". Journal of Building Engineering 43 (2021) 102519. doi.org/10.1016/j.jobe.2021.102519

[40] A. M. D'Altri et al., "Modeling strategies for the computational analysis of unreinforced masonry structures: review and classification," Archives of Computational Methods in Engineering, vol. 27, no. 4, pp. 1153–1185, Sep. 2020, doi: 10.1007/s11831-019-09351-x.

[41] FEMA, 1997. FEMA 273 - NEHRP Guidelines and Commentary for the Seismic Rehabilitation of Buildings. https://doi.org/10.1193/1.1586092

[42] Lestuzzi, P., Podestà, S., Luchini, C. et al. Validation and improvement of Risk-UE LM2 capacity curves for URM buildings with stiff floors and RC shear walls buildings. Bull Earthquake Eng 15, 1111–1134 (2017). https://doi.org/10.1007/s10518-016-9981-9

[43] Lagomarsino, S., Giovinazzi, S. Macroseismic and mechanical models for the vulnerability and damage assessment of current buildings. Bull Earthquake Eng 4, 415–443 (2006). https://doi.org/10.1007/s10518-

[44] Brando G, De Matteis G, Spacone E. Predictive model for the seismic vulnerability assessment of small historic centres: application to the inner Abruzzi Region in Italy. Eng Struct 2017;153:81–96. https://doi.org/10.1016/j.engstruct.2017.10.013.

[45] Masi, A., Chiauzzi, L., Braga, F. et al. Peak and integral seismic parameters of L'Aquila 2009 ground motions: observed versus code provision values. Bull Earthquake Eng 9, 139–156 (2011). https://doi.org/10.1007/s10518-010-9227-1

[46] De Carvalho Bello C. B., et al., "Numerical and theoretical models for nfrcm-strengthened masonry," Key Eng. Mater., vol. 817 KEM, pp. 44–49, 2019, doi: 10.4028/www.scientific.net/KEM.817.44.

ANNEX 1

ARCHETYPE BUILDING #1

	Typology	N. of stories	Construction period	Ring beams and tie rods	Slab type	Roof material	Wall thickness at the ground floor	Distance between walls
1	Ir. masonry	3	< 1860	Absent	Flexible	Light	> 60 cm	< 5 m

Geometrical model (frontal façade)

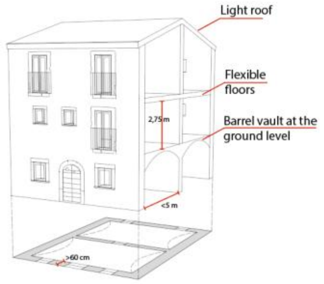

Numerical model (back façade)

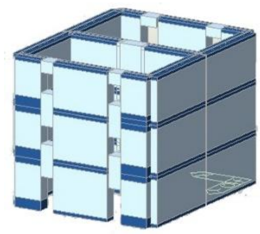

Bilinear capacity curves
ANALYTICAL METHOD

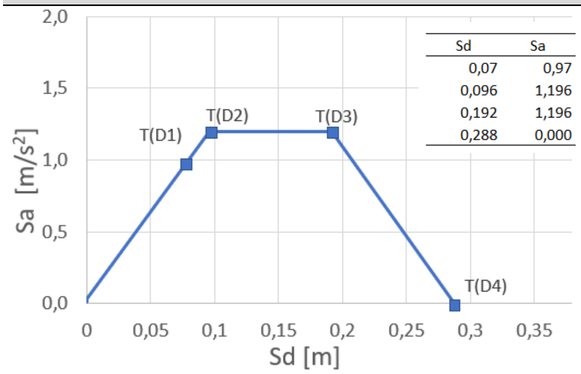

Trilinear capacity curves
NUMERICAL METHOD

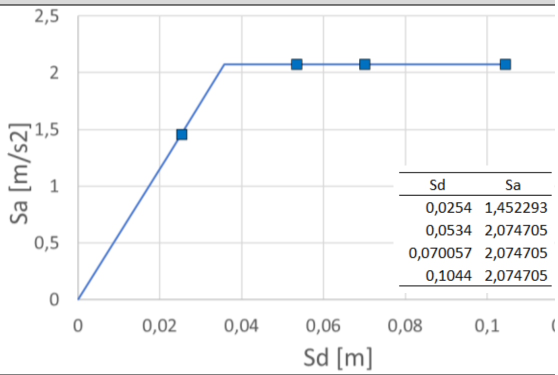

Fragility curves
(Analytical vs Numerical curves)

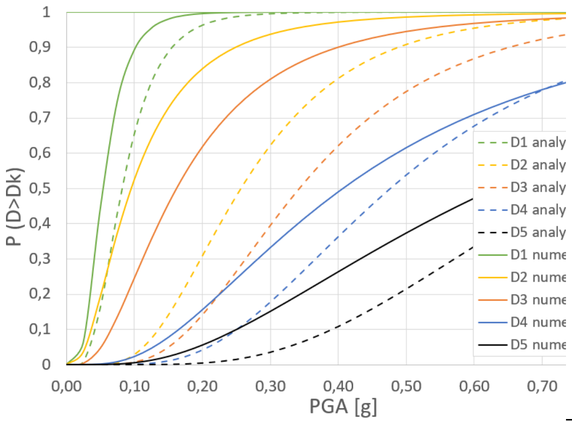

Final Fragility curves

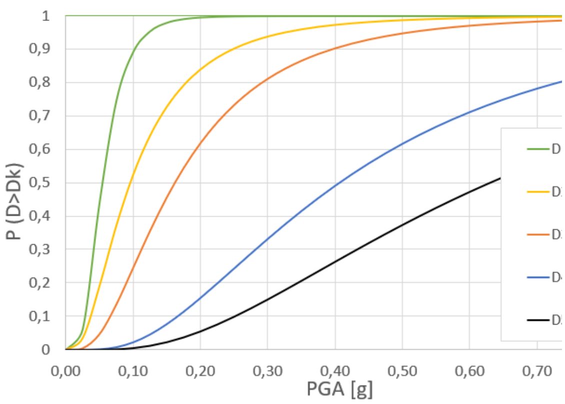

	D1	D2	D3	D4	D5
β	PGA	PGA	PGA	PGA	PGA
0,70	0,05	0,09	0,16	0,40	0,63

ARCHETYPE BUILDING #2

	Typology	N. of stories	Construction period	Ring beams and tie rods	Slab type	Roof material	Wall thickness at the ground floor	Distance between walls
2	Ir. masonry	3	< 1860	Present	Semi-rigid	Light	> 60 cm	< 5 m

Geometrical model (frontal façade)

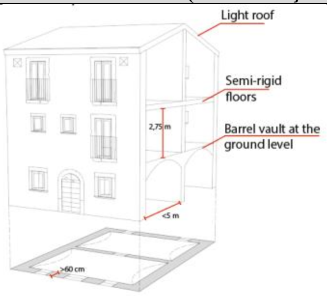

Numerical model (back façade)

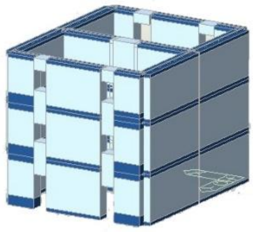

Bilinear capacity curves
ANALYTICAL METHOD

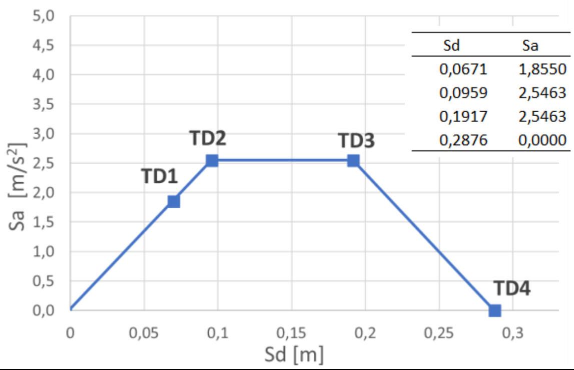

Trilinear capacity curves
NUMERICAL METHOD

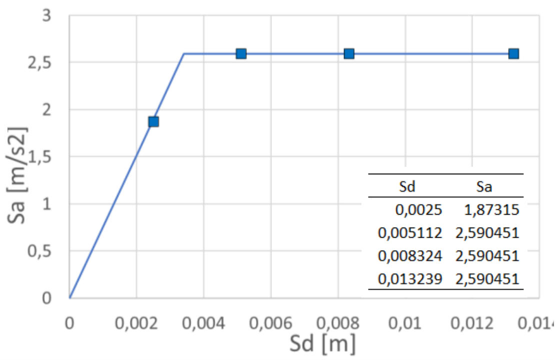

Fragility curves
(Analytical vs Numerical curves)

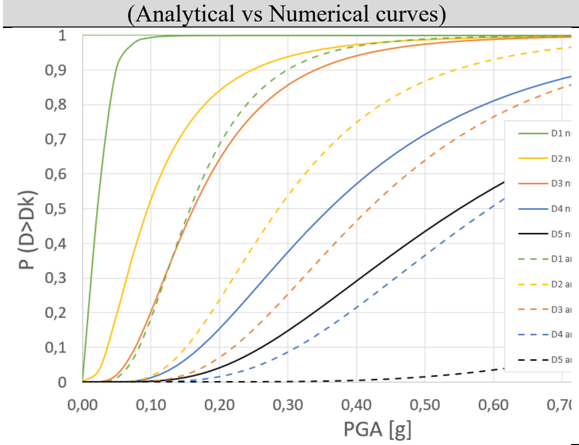

Final Fragility curves

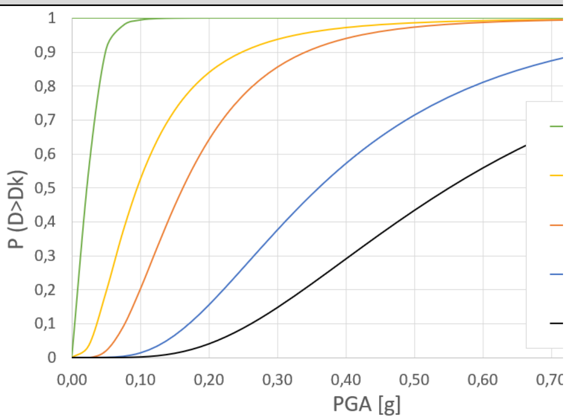

	D1	D2	D3	D4	D5
β	PGA	PGA	PGA	PGA	PGA
0,58	0,02	0,06	0,16	0,36	0,55

ARCHETYPE BUILDING #3

	Typology	N. of stories	Construction period	Ring beams and tie rods	Slab type	Roof material	Wall thickness at the ground floor	Distance between walls
3	Ir. masonry	3	< 1860	Absent	Semi-rigid	Light	> 60 cm	< 5 m

Geometrical model (frontal façade)	Numerical model (back façade)

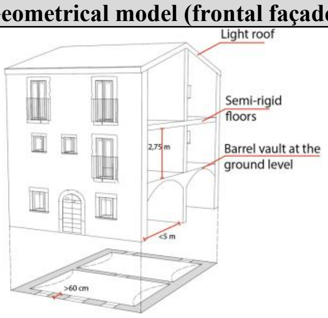

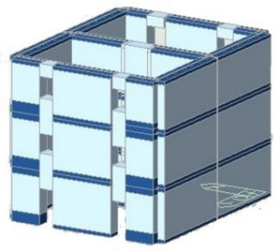

Bilinear capacity curves ANALYTICAL METHOD	Trilinear capacity curves NUMERICAL METHOD

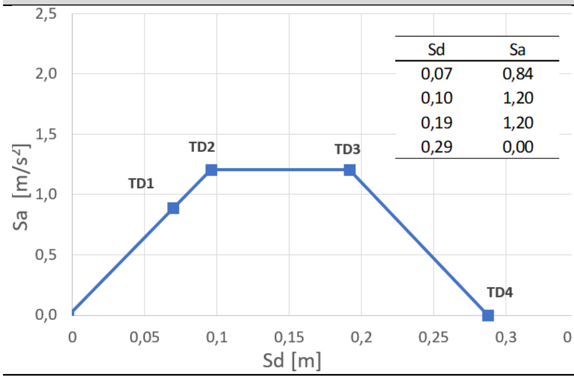

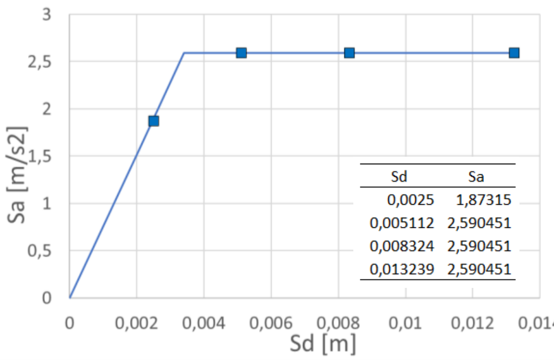

Fragility curves (Analytical vs Numerical curves)	Final Fragility curves

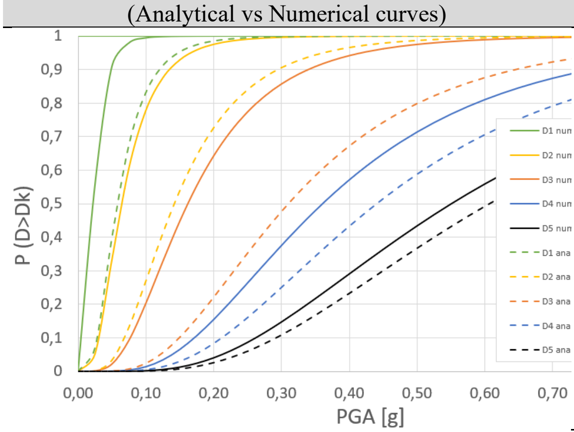

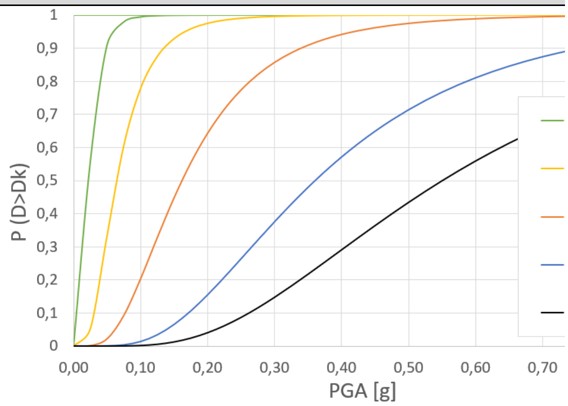

	D1	D2	D3	D4	D5
β	PGA	PGA	PGA	PGA	PGA
0,579	0,023	0,064	0,162	0,361	0,551

ARCHETYPE BUILDING #4

	Typology	N. of storie s	Construc tion period	Ring beams and tie rods	Slab type	Roof material	Wall thickness at the ground floor	Distance between walls
4	Ir. masonry	3	< 1860	Present	Flexible	Light	> 60 cm	< 5 m

Geometrical model (frontal façade)

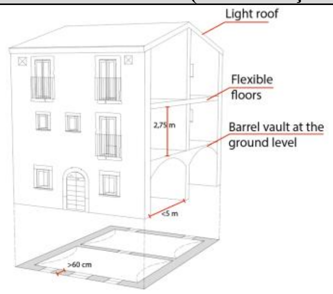

Numerical model (back façade)

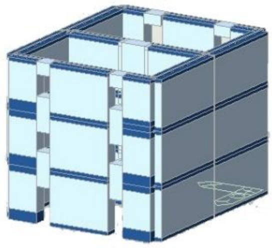

Bilinear capacity curves
ANALYTICAL METHOD

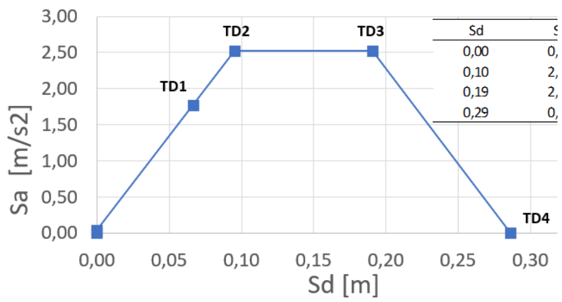

Trilinear capacity curves
NUMERICAL METHOD

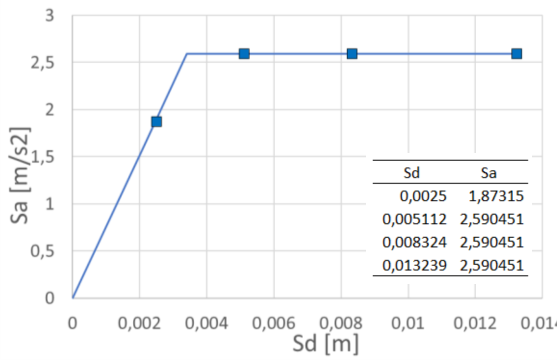

Fragility curves
(Analytical vs Numerical curves)

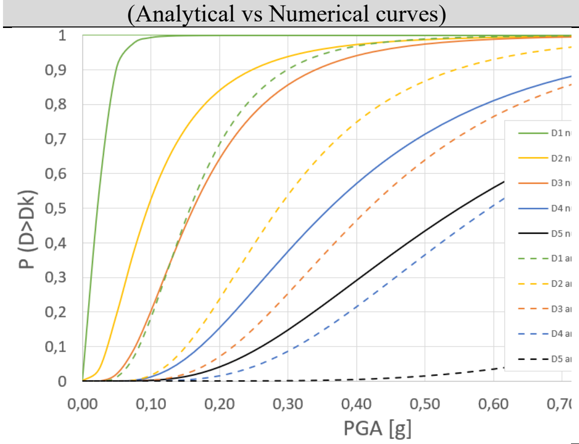

Final Fragility curves

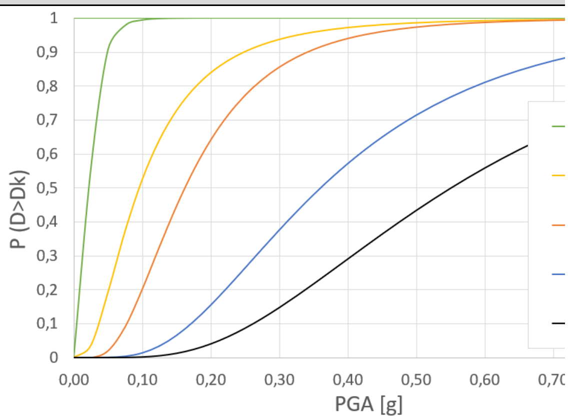

	D1	D2	D3	D4	D5
β	PGA	PGA	PGA	PGA	PGA
0,5 8	0,02	0,06	0,16	0,36	0,55

ARCHETYPE BUILDING #5

	Typology	N. of stories	Construction period	Ring beams and tie rods	Slab type	Roof material	Wall thickness at the ground floor	Distance between walls
5	Ir. masonry	4	< 1860	Present	Semi-rigid	Light	> 60 cm	< 5 m

Geometrical model (frontal façade)

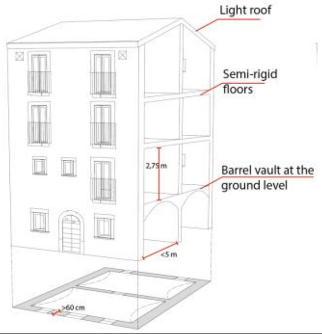

Numerical model (back façade)

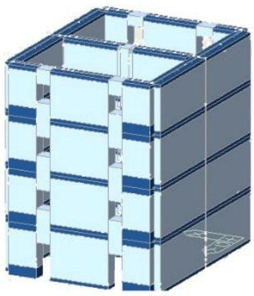

Bilinear capacity curves
ANALYTICAL METHOD

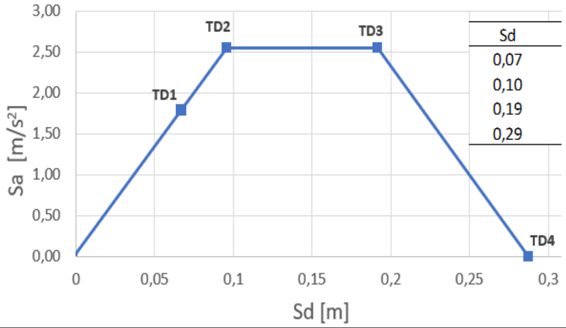

Trilinear capacity curves
NUMERICAL METHOD

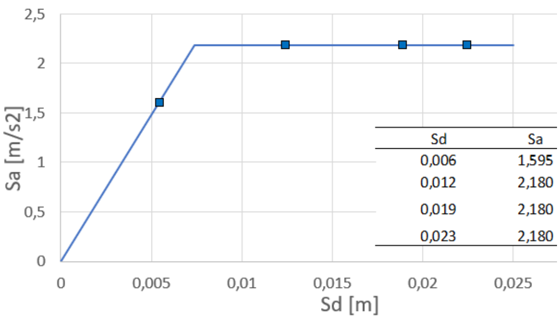

Fragility curves
(Analytical vs Numerical curves)

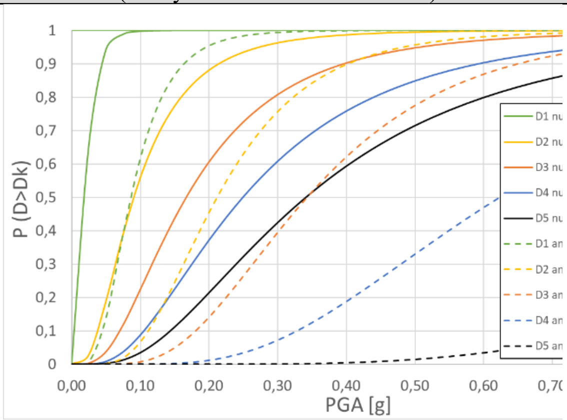

Final Fragility curves

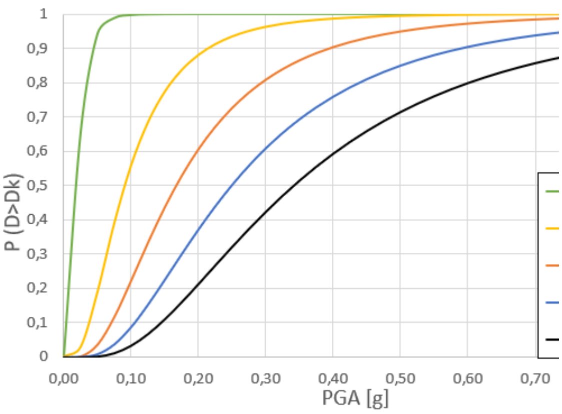

	D1	D2	D3	D4	D5
β	PGA	PGA	PGA	PGA	PGA
0,67	0,01	0,09	0,17	0,25	0,34

ARCHETYPE BUILDING #6

	Typology	N. of storie s	Construc tion period	Ring beams and tie rods	Slab type	Roof material	Wall thickness at the ground floor	Distance between walls
6	Ir. masonry	3	< 1860	Absent	Flexible	Heavy	> 60 cm	< 5 m

Geometrical model (frontal façade)	Numerical model (back façade)

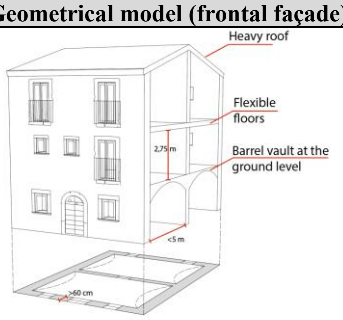

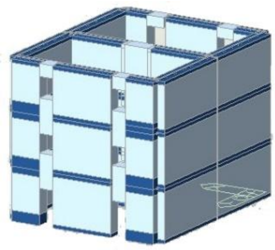

Bilinear capacity curves ANALYTICAL METHOD	Trilinear capacity curves NUMERICAL METHOD

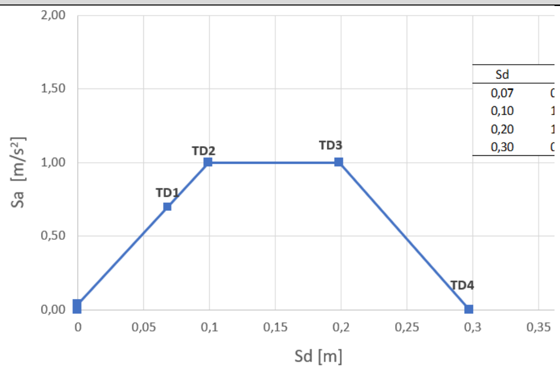

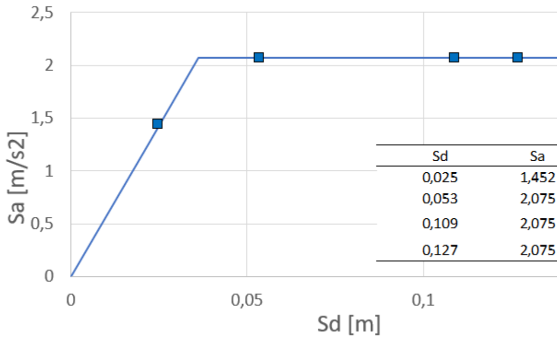

Fragility curves (Analytical vs Numerical curves)	Final Fragility curves

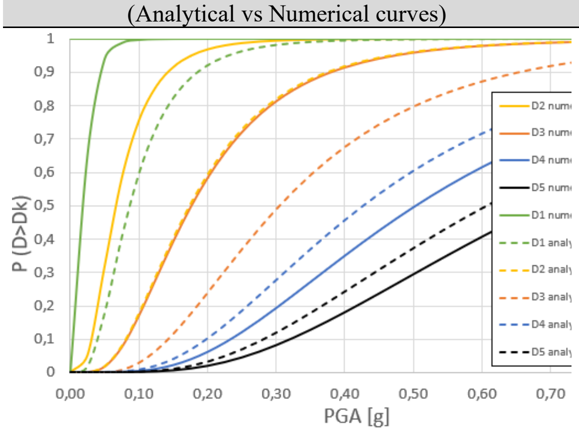

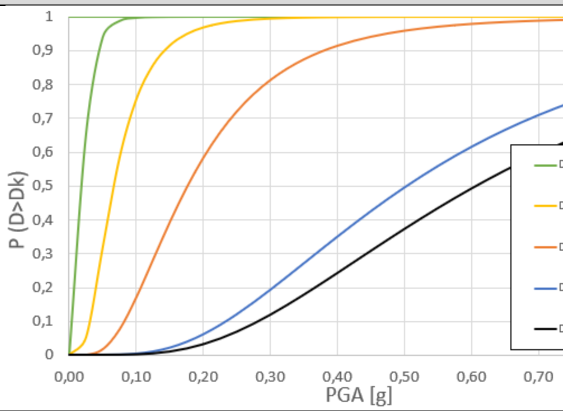

	D1	D2	D3	D4	D5
β	PGA	PGA	PGA	PGA	PGA
0,5 9	0,019	0,066	0,17	0,50	0,60

ARCHETYPE BUILDING #7

	Typology	N. of stories	Construction period	Ring beams and tie rods	Slab type	Roof material	Wall thickness at the ground floor	Distance between walls
7	Ir. masonry	4	< 1860	Present	Flexible	Light	> 60 cm	< 5 m

Geometrical model (frontal façade)	Numerical model (back façade)

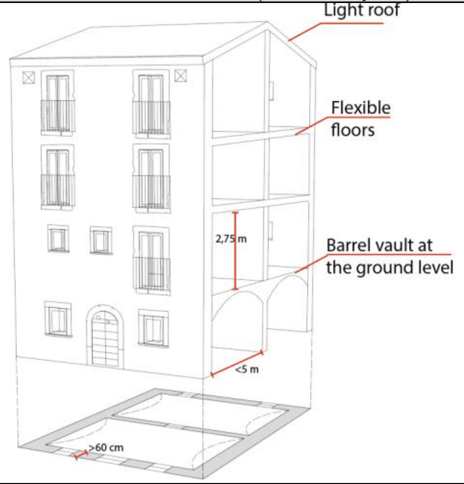

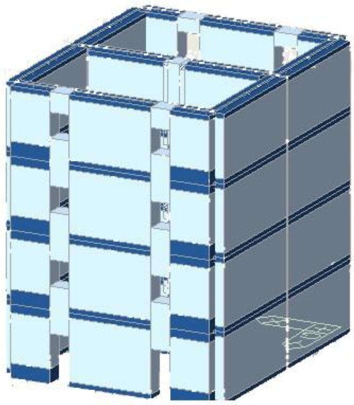

Bilinear capacity curves ANALYTICAL METHOD	Trilinear capacity curves NUMERICAL METHOD

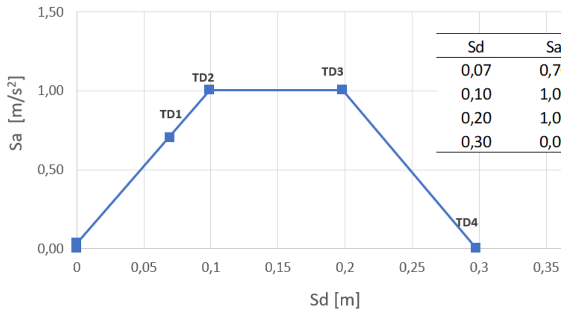

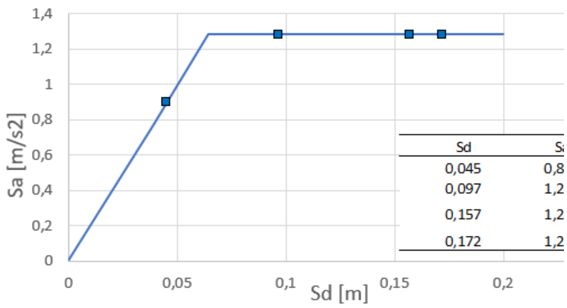

Fragility curves (Analytical vs Numerical curves)	Final Fragility curves

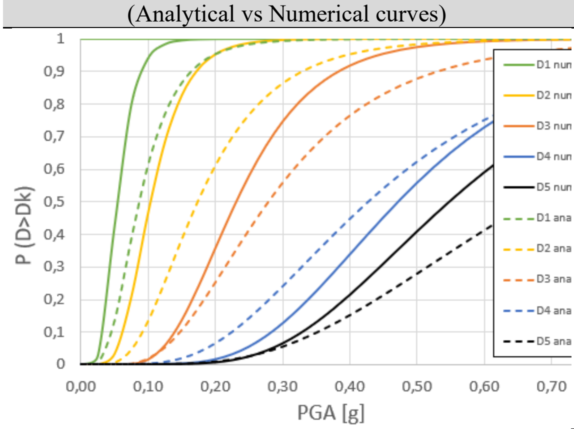

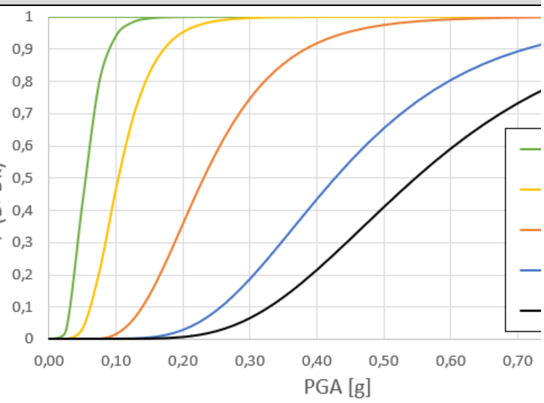

	D1	D2	D3	D4	D5
β	PGA	PGA	PGA	PGA	PGA
0,39	0,05	0,10	0,23	0,43	0,55

ARCHETYPE BUILDING #8

	Typology	N. of stories	Construction period	Ring beams and tie rods	Slab type	Roof material	Wall thickness at the ground floor	Distance between walls
8	Ir. masonry	3	< 1860	Absent	Semi-rigid	Heavy	> 60 cm	< 5 m

Geometrical model (frontal façade)

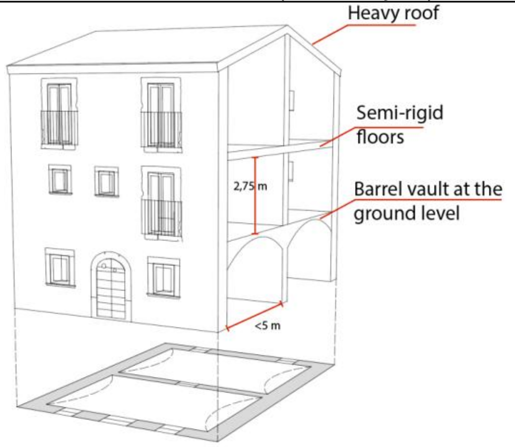

Numerical model (back façade)

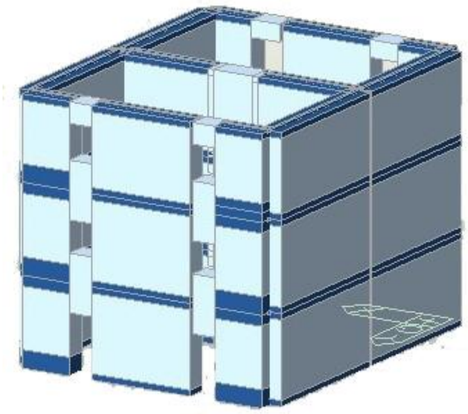

Bilinear capacity curves
ANALYTICAL METHOD

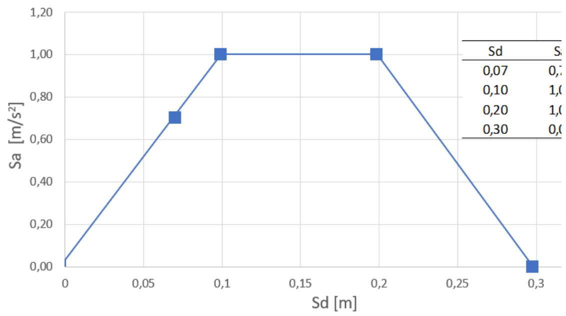

Trilinear capacity curves
NUMERICAL METHOD

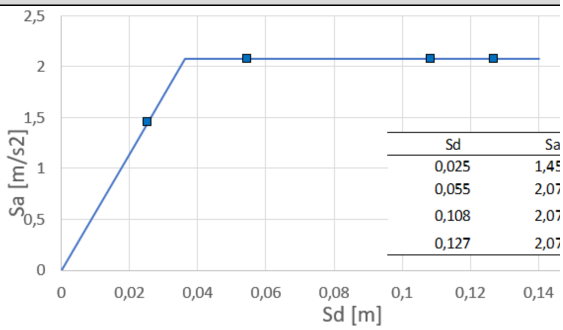

Fragility curves
(Analytical vs Numerical curves)

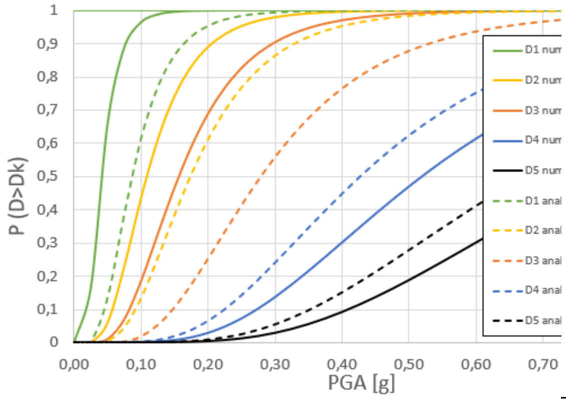

Final Fragility curves

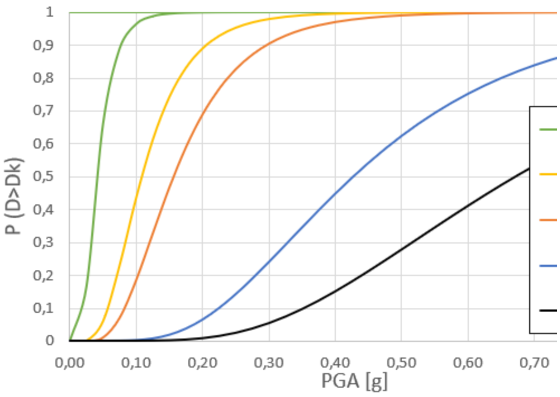

	D1	D2	D3	D4	D5
β	PGA	PGA	PGA	PGA	PGA
0,50	0,04	0,11	0,16	0,42	0,67

ARCHETYPE BUILDING #9

	Typology	N. of storie s	Construc tion period	Ring beams and tie rods	Slab type	Roof material	Wall thickness at the ground floor	Distance between walls
9	Ir. masonry	4	< 1860	Absent	Flexible	Light	> 60 cm	< 5 m

Geometrical model (frontal façade)

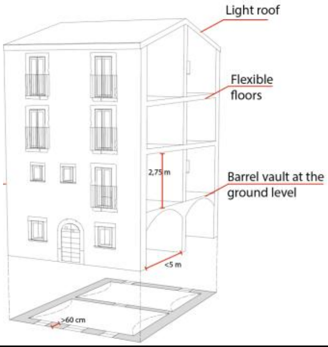

Numerical model (back façade)

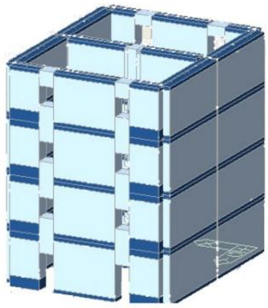

Bilinear capacity curves ANALYTICAL METHOD

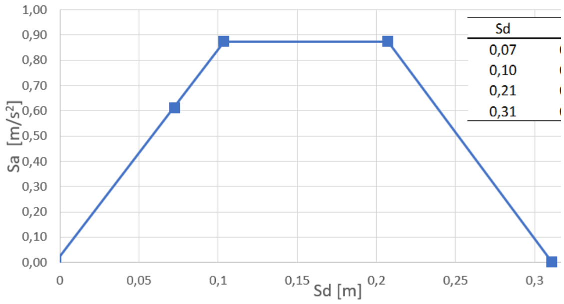

Trilinear capacity curves NUMERICAL METHOD

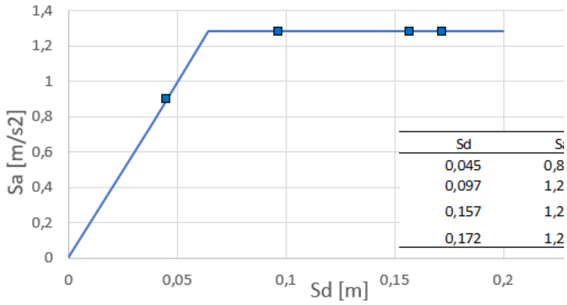

Fragility curves
(Analytical vs Numerical curves)

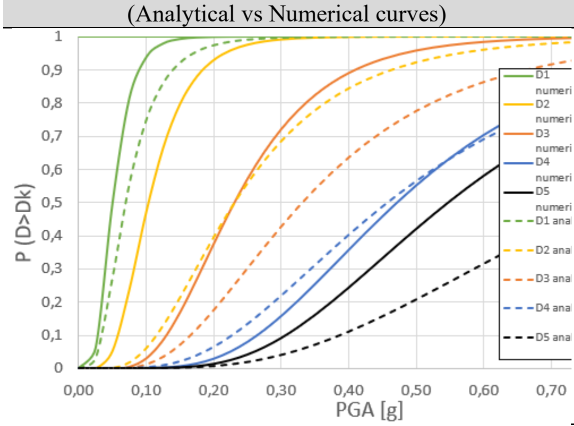

Final Fragility curves

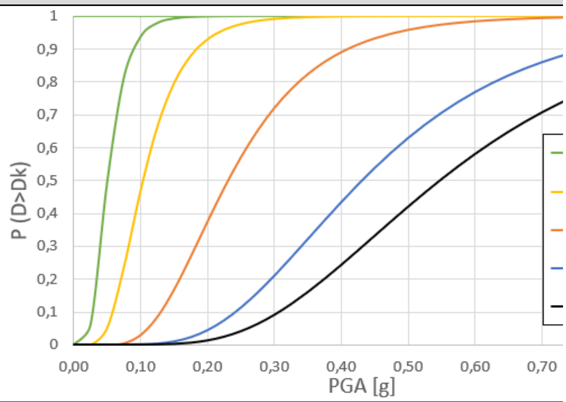

	D1	D2	D3	D4	D5
β	PGA	PGA	PGA	PGA	PGA
0,45	0,050	0,103	0,231	0,427	0,547

ARCHETYPE BUILDING #10

	Typology	N. of storie s	Construc tion period	Ring beams and tie rods	Slab type	Roof material	Wall thickness at the ground floor	Distance between walls
10	Brick	2	1945-1981	Absent	Semi-rigid	Heavy	< 60 cm	< 5 m

Geometrical model (frontal façade)	**Numerical model (back façade)**

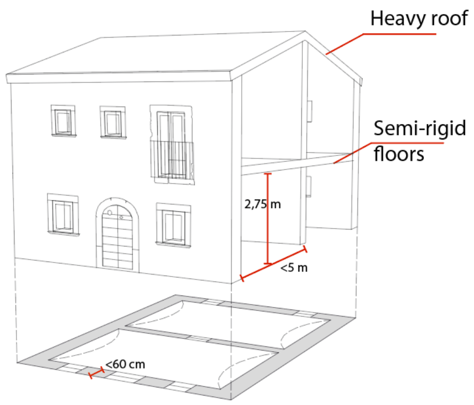

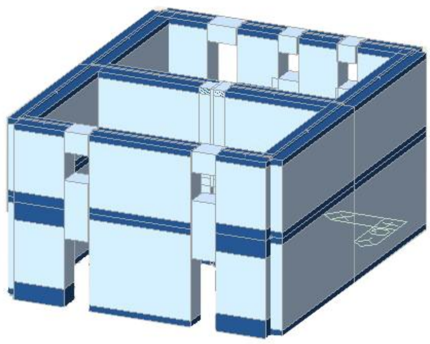

Bilinear capacity curves ANALYTICAL METHOD	**Trilinear capacity curves NUMERICAL METHOD**

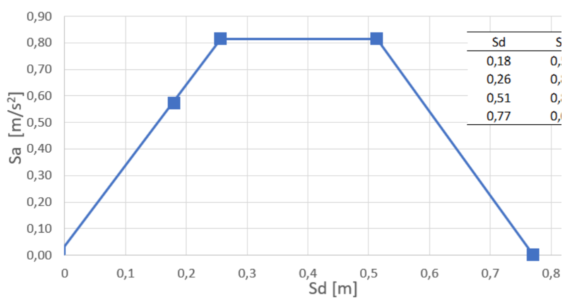

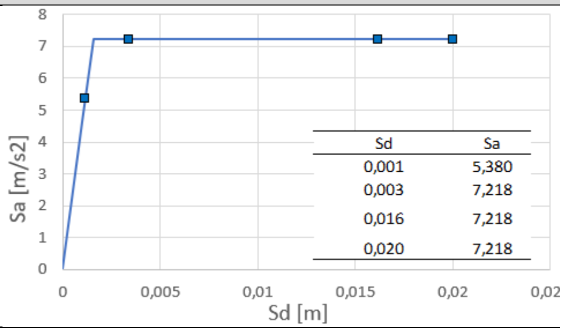

Fragility curves (Analytical vs Numerical curves)	**Final Fragility curves**

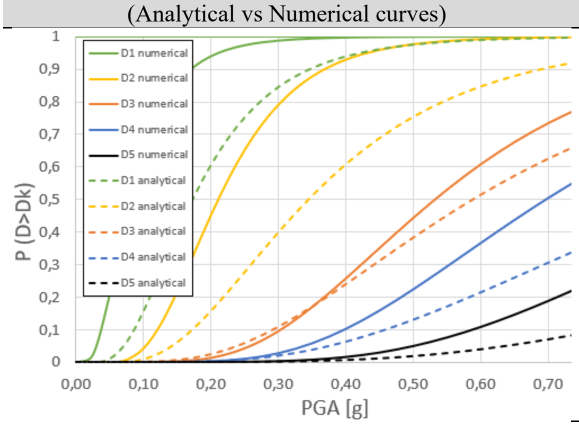

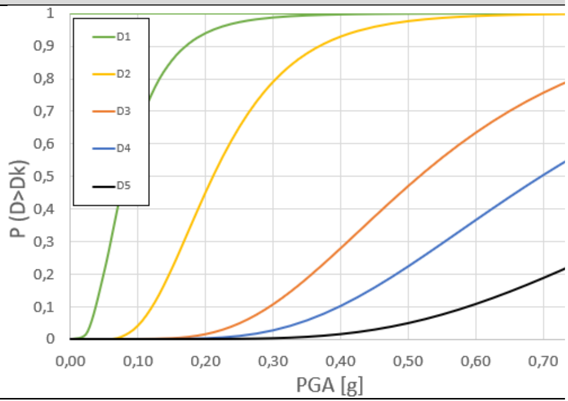

	D1	D2	D3	D4	D5
β	PGA	PGA	PGA	PGA	PGA
0,44	0,08	0,21	0,52	0,70	1,03

ARCHETYPE BUILDING #11

	Typology	N. of stories	Construction period	Ring beams and tie rods	Slab type	Roof material	Wall thickness at the ground floor	Distance between walls
11	Brick	3	1945-1981	Present	Rigid	Heavy	< 60 cm	> 5 m

Geometrical model (frontal façade)

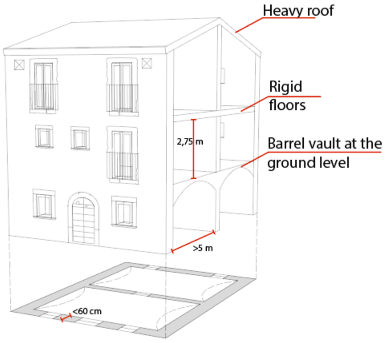

Numerical model (back façade)

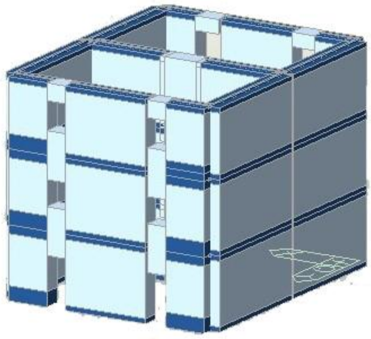

Bilinear capacity curves
ANALYTICAL METHOD

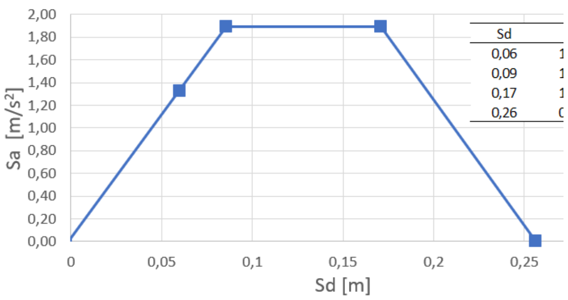

Trilinear capacity curves
NUMERICAL METHOD

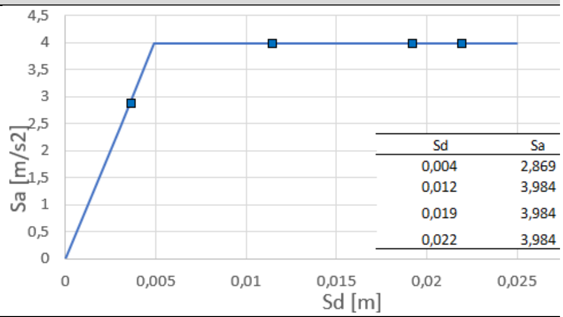

Fragility curves
(Analytical vs Numerical curves)

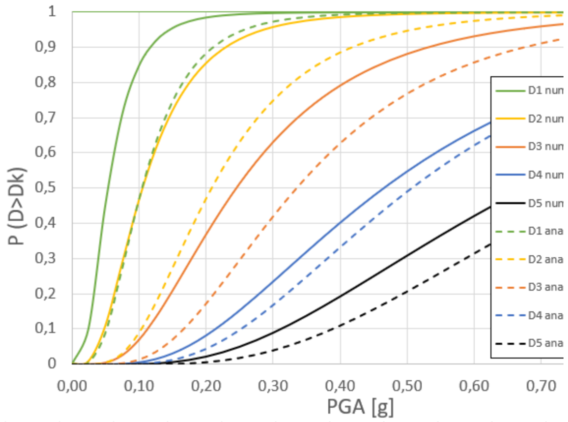

Final Fragility curves

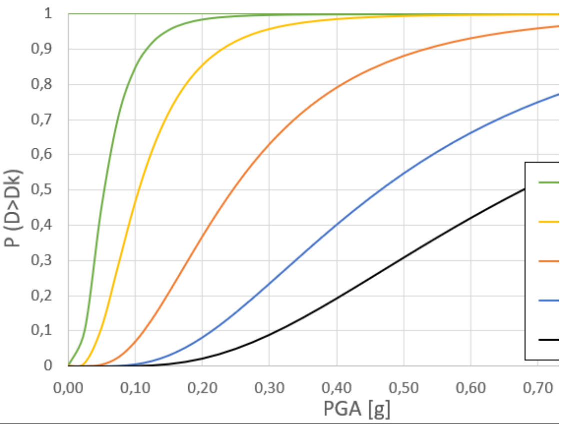

	D1	D2	D3	D4	D5
β	PGA	PGA	PGA	PGA	PGA
0,60	0,054	0,105	0,246	0,465	0,676

ARCHETYPE BUILDING #12

	Typology	N. of stories	Construction period	Ring beams and tie rods	Slab type	Roof material	Wall thickness at the ground floor	Distance between walls
12	Ir. masonry	3	< 1860	Present	Semi-rigid	Heavy	> 60 cm	< 5 m

Geometrical model (frontal façade) | **Numerical model (back façade)**

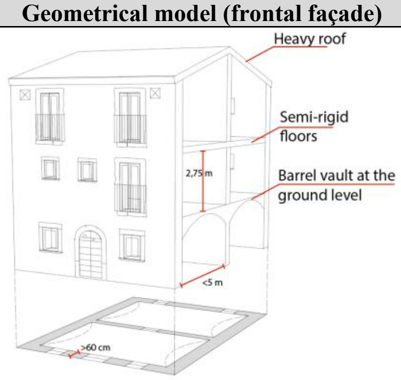

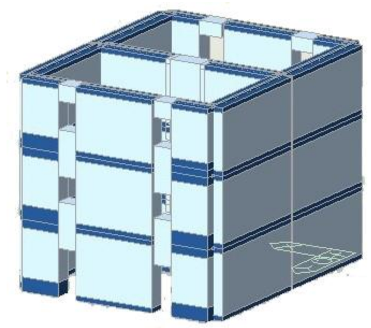

Bilinear capacity curves ANALYTICAL METHOD | **Trilinear capacity curves NUMERICAL METHOD**

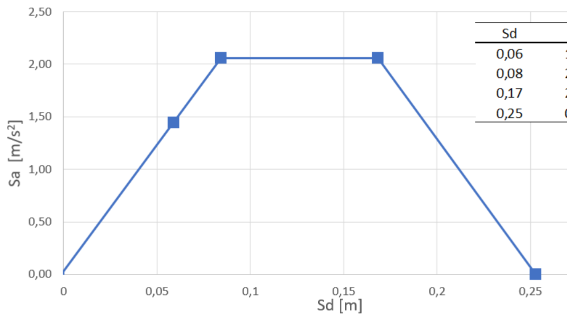

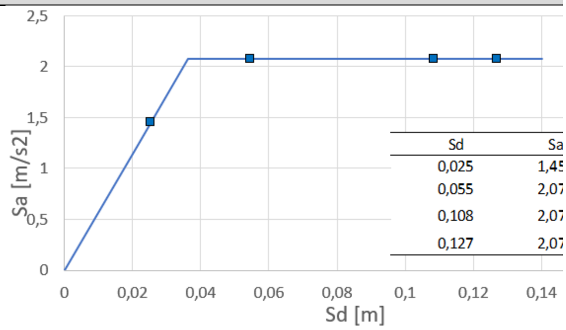

Fragility curves (Analytical vs Numerical curves) | **Final Fragility curves**

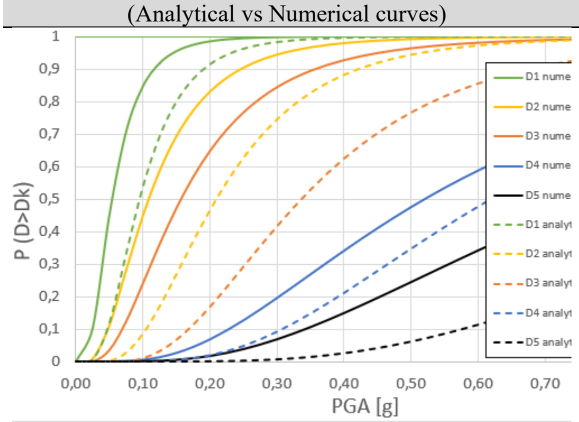

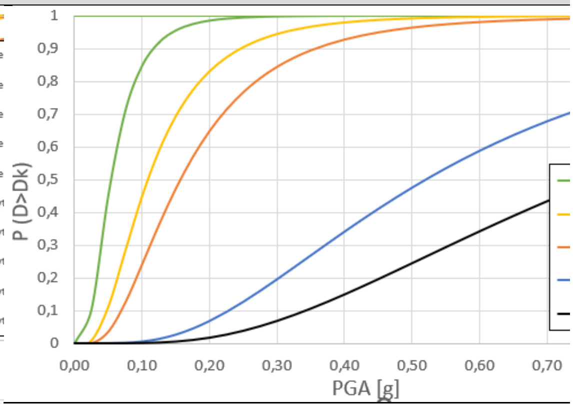

	D1	D2	D3	D4	D5
β	PGA	PGA	PGA	PGA	PGA
0,61	0,054	0,108	0,156	0,519	0,779

ARCHETYPE BUILDING #13

	Typology	N. of storie s	Construc tion period	Ring beams and tie rods	Slab type	Roof material	Wall thickness at the ground floor	Distance between walls
13	Ir. masonry	3	< 1860	Present	Flexible	Heavy	> 60 cm	< 5 m

Geometrical model (frontal façade)

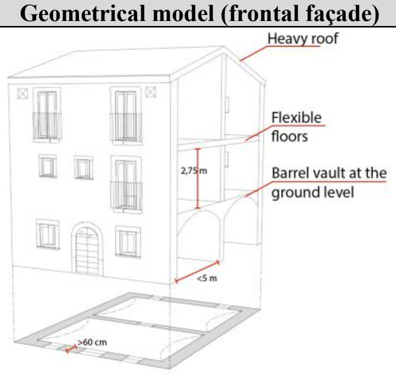

Numerical model (back façade)

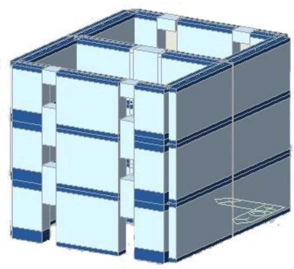

Bilinear capacity curves ANALYTICAL METHOD

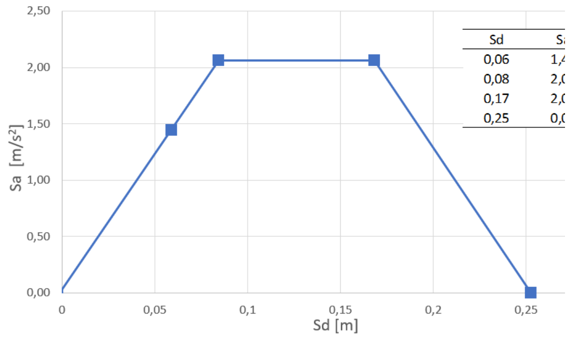

Trilinear capacity curves NUMERICAL METHOD

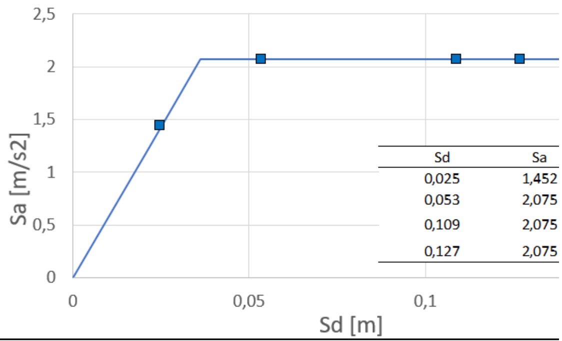

Fragility curves (Analytical vs Numerical curves)

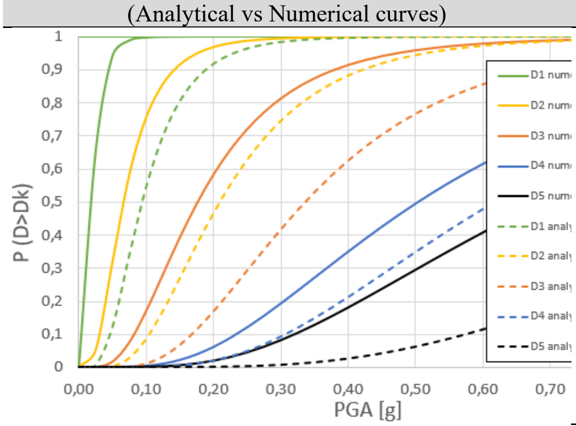

Final Fragility curves

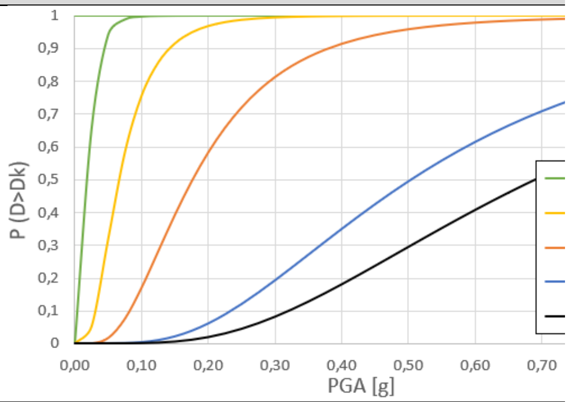

	D1	D2	D3	D4	D5
β	PGA	PGA	PGA	PGA	PGA
0,58 8	0,022	0,066	0,176	0,503	0,690

ARCHETYPE BUILDING #14

	Typology	N. of storie s	Construc tion period	Ring beams and tie rods	Slab type	Roof material	Wall thickness at the ground floor	Distance between walls
14	Brick	4	1945-1981	Present	Rigid	Heavy	< 60 cm	> 5 m

Geometrical model (frontal façade)	Numerical model (back façade)

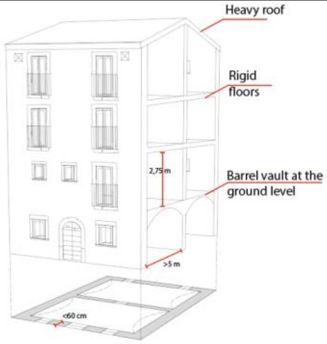

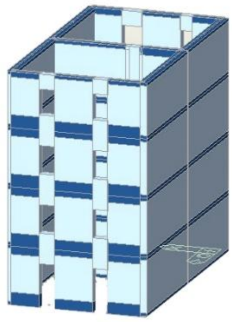

Bilinear capacity curves ANALYTICAL METHOD	Trilinear capacity curves NUMERICAL METHOD

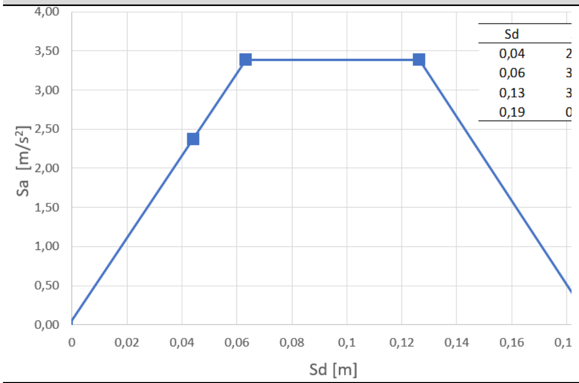

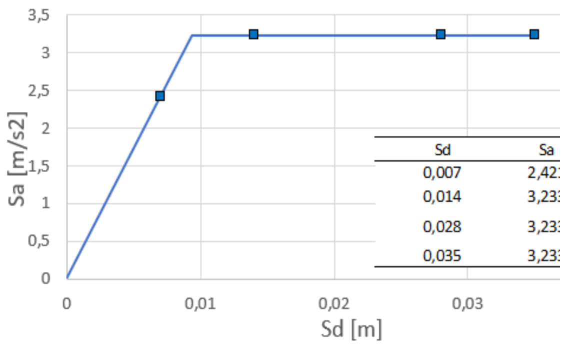

Fragility curves (Analytical vs Numerical curves)	Final Fragility curves

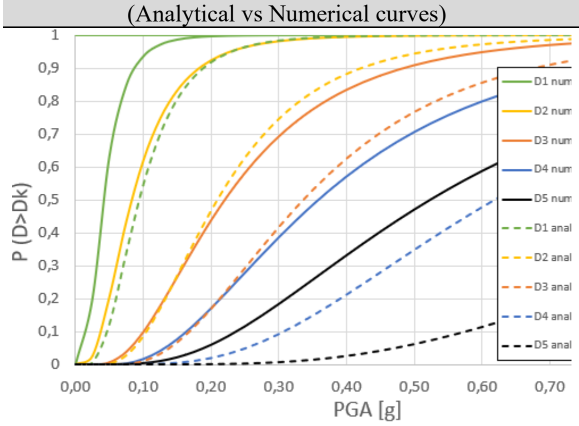

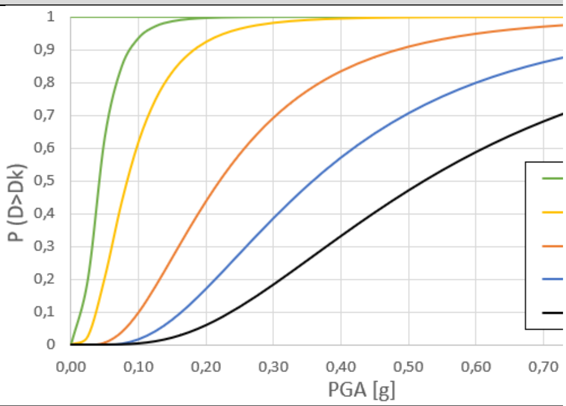

	D1	D2	D3	D4	D5
β	PGA	PGA	PGA	PGA	PGA
0,616	0,041	0,083	0,220	0,358	0,523

ARCHETYPE BUILDING #15

	Typology	N. of storie s	Construc tion period	Ring beams and tie rods	Slab type	Roof material	Wall thickness at the ground floor	Distance between walls
15	Ir. masonry	4	< 1860	Absent	Semi-rigid	Light	> 60 cm	< 5 m

Geometrical model (frontal façade)

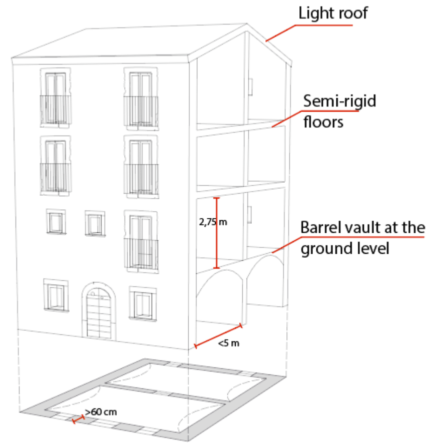

Numerical model (back façade)

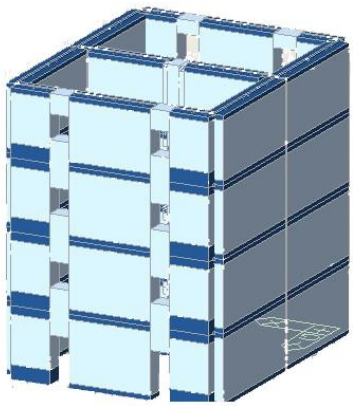

Bilinear capacity curves ANALYTICAL METHOD

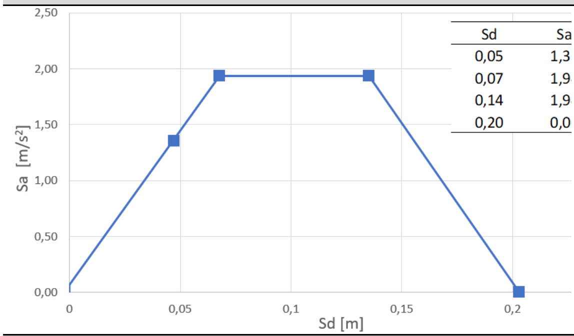

Trilinear capacity curves NUMERICAL METHOD

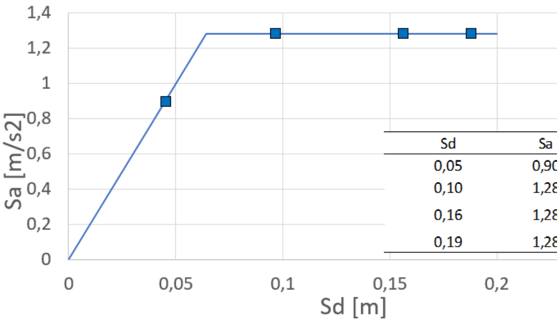

Fragility curves
(Analytical vs Numerical curves)

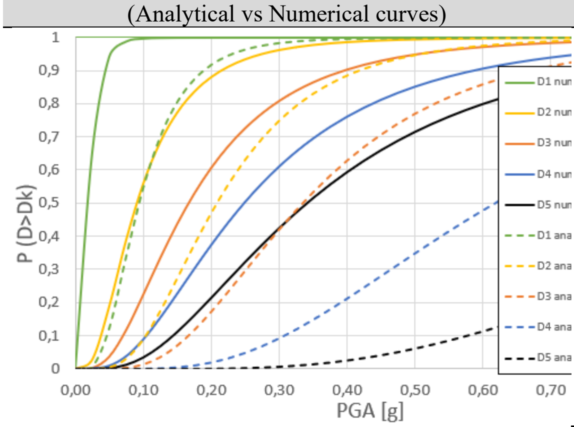

Final Fragility curves

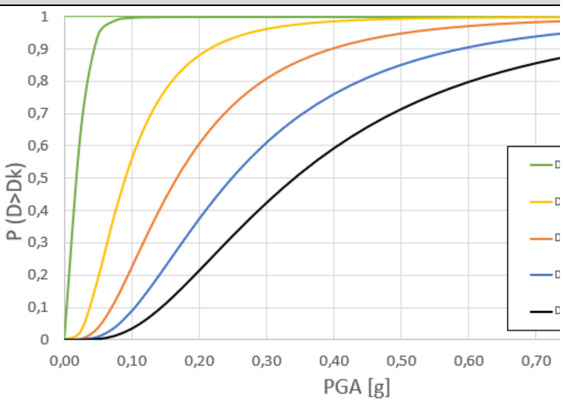

	D1	D2	D3	D4	D5
β	PGA	PGA	PGA	PGA	PGA
0,673	0,020	0,091	0,167	0,249	0,341

ARCHETYPE BUILDING #16

	Typology	N. of storie s	Construc tion period	Ring beams and tie rods	Slab type	Roof material	Wall thickness at the ground floor	Distance between walls
16	Brick	2	< 1860	Present	Flexible	Light	< 60 cm	< 5 m

Geometrical model (frontal façade)	Numerical model (back façade)

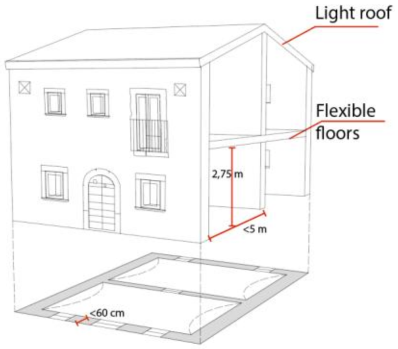

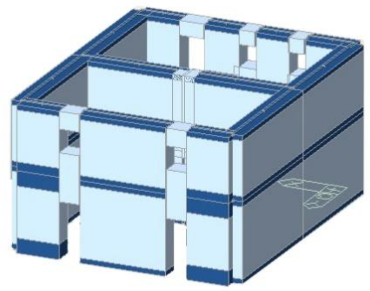

Bilinear capacity curves ANALYTICAL METHOD	Trilinear capacity curves NUMERICAL METHOD

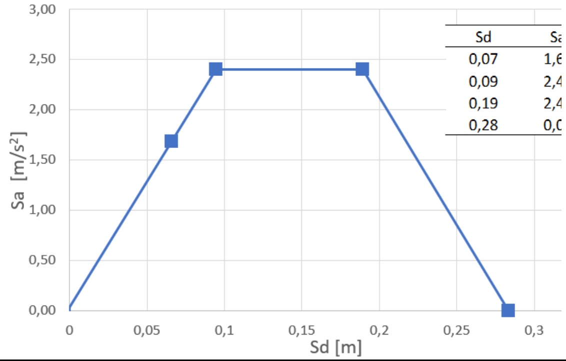

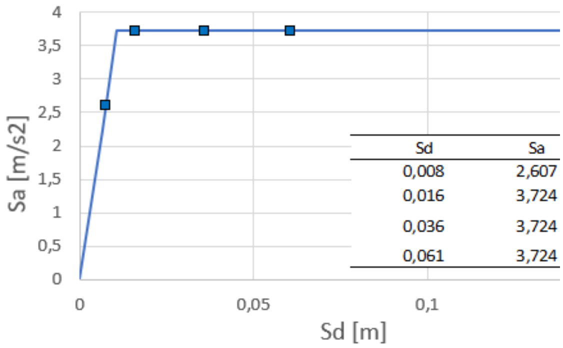

Fragility curves (Analytical vs Numerical curves)	Final Fragility curves

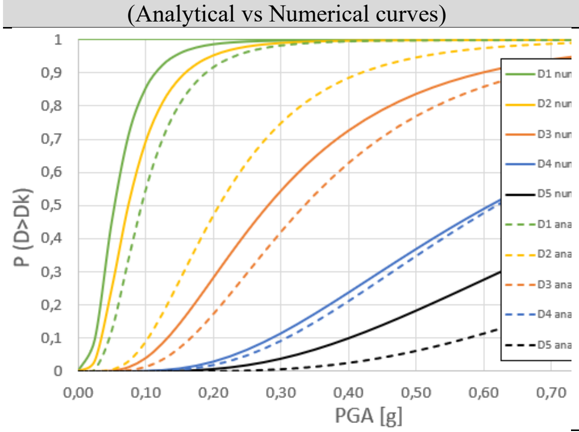

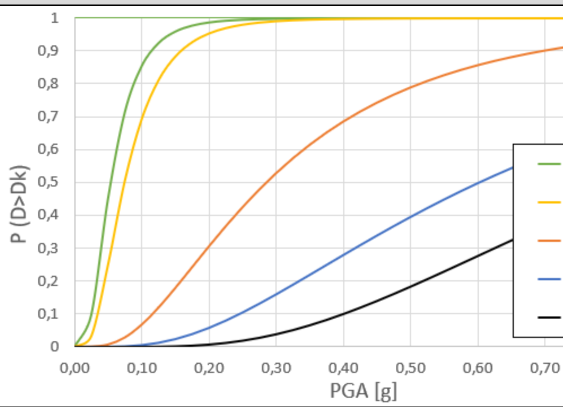

	D1	D2	D3	D4	D5
β	PGA	PGA	PGA	PGA	PGA
0,58 8	0,054	0,074	0,282	0,609	0,851

ARCHETYPE BUILDING #17

	Typology	N. of storie s	Construc tion period	Ring beams and tie rods	Slab type	Roof material	Wall thickness at the ground floor	Distance between walls
17	Brick	2	< 1860	Absent	Flexible	Light	< 60 cm	< 5 m

Geometrical model (frontal façade)	Numerical model (back façade)

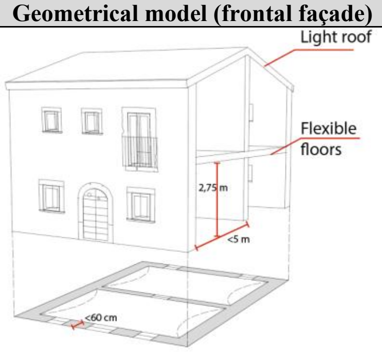

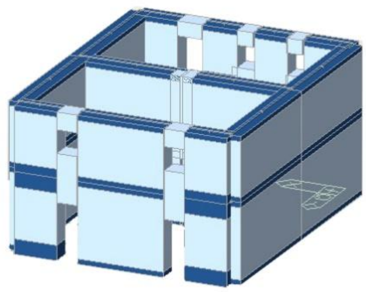

Bilinear capacity curves ANALYTICAL METHOD	Trilinear capacity curves NUMERICAL METHOD

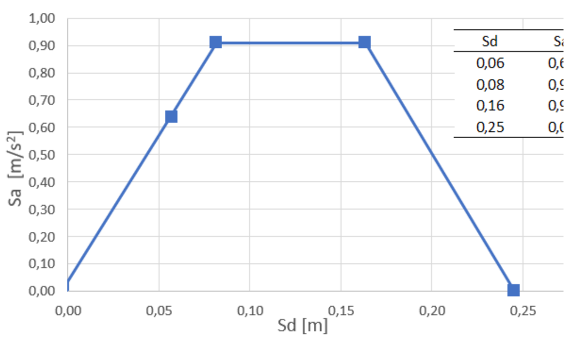

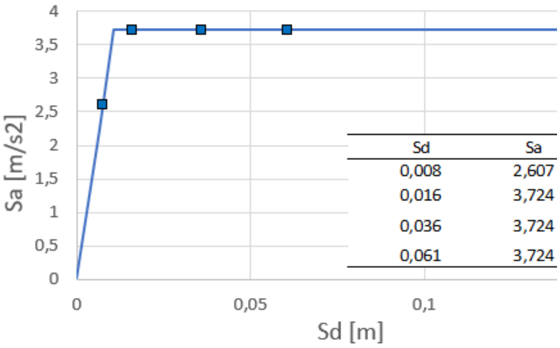

Fragility curves (Analytical vs Numerical curves)	Final Fragility curves

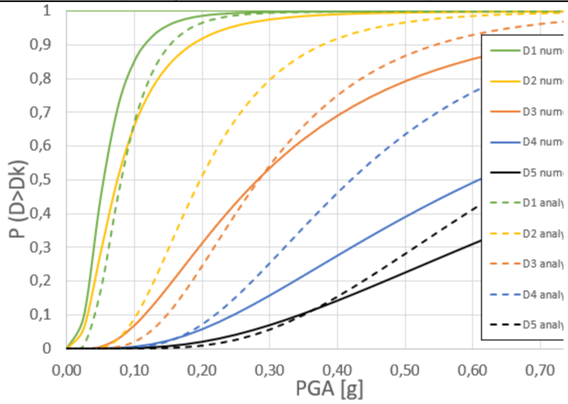

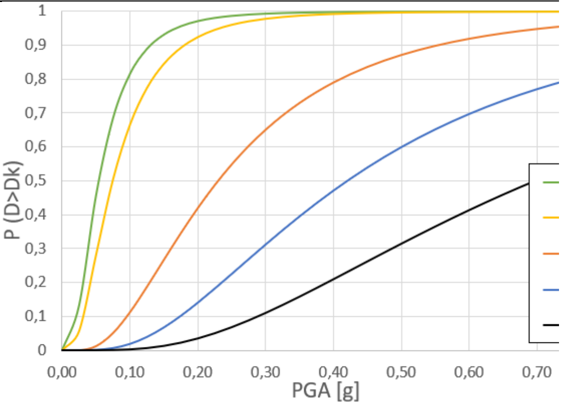

	D1	D2	D3	D4	D5
β	PGA	PGA	PGA	PGA	PGA
0,688	0,054	0,074	0,230	0,421	0,699

ARCHETYPE BUILDING #18

	Typology	N. of storie s	Construc tion period	Ring beams and tie rods	Slab type	Roof material	Wall thickness at the ground floor	Distance between walls
18	Brick	3	< 1860	Present	Flexible	Light	< 60 cm	< 5 m

Geometrical model (frontal façade) | **Numerical model (back façade)**

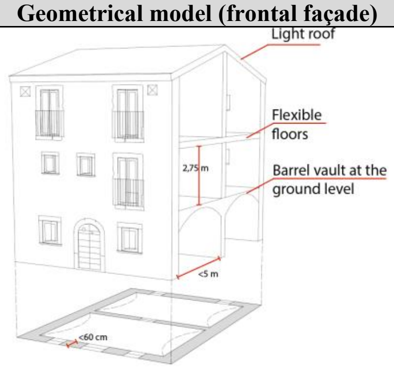

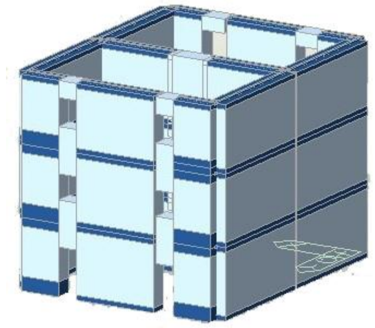

Bilinear capacity curves ANALYTICAL METHOD | **Trilinear capacity curves NUMERICAL METHOD**

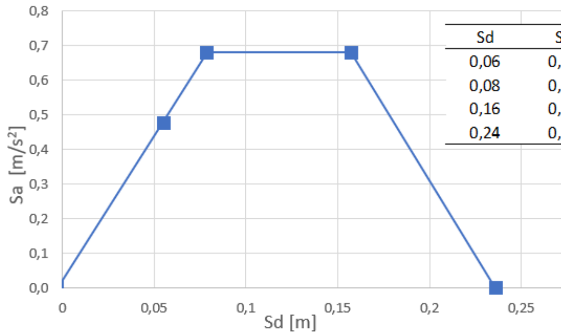

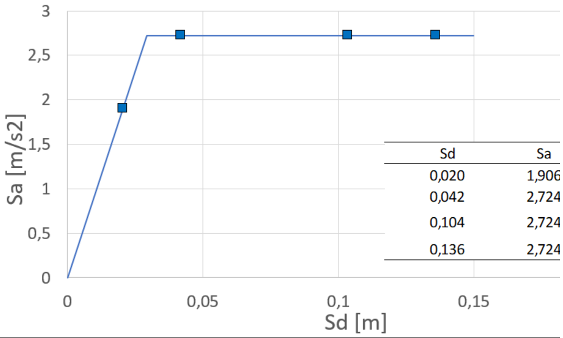

Fragility curves (Analytical vs Numerical curves) | **Final Fragility curves**

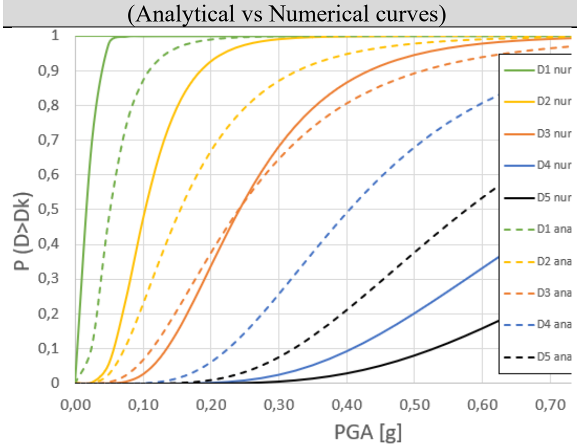

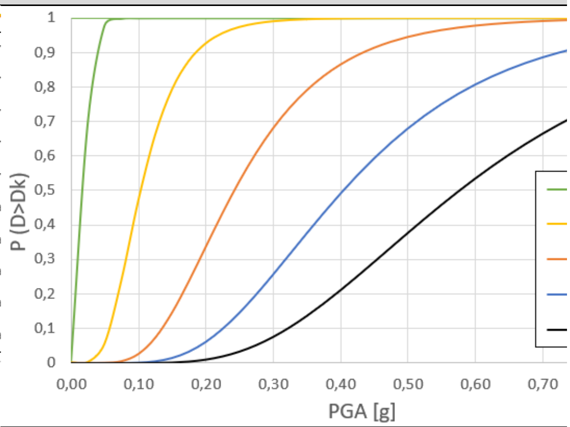

	D1	D2	D3	D4	D5
β	PGA	PGA	PGA	PGA	PGA
0,455	0,020	0,104	0,243	0,404	0,577

ARCHETYPE BUILDING #19

	Typology	N. of storie s	Construc tion period	Ring beams and tie rods	Slab type	Roof material	Wall thickness at the ground floor	Distance between walls
19	Brick	3	< 1860	Absent	Flexible	Light	< 60 cm	< 5 m

Geometrical model (frontal façade)

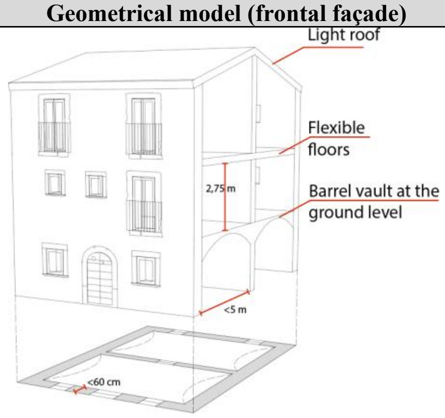

Numerical model (back façade)

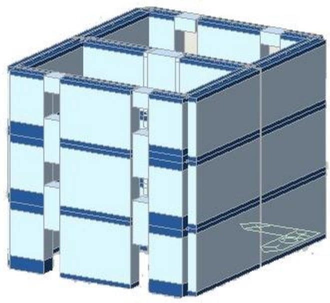

Bilinear capacity curves ANALYTICAL METHOD

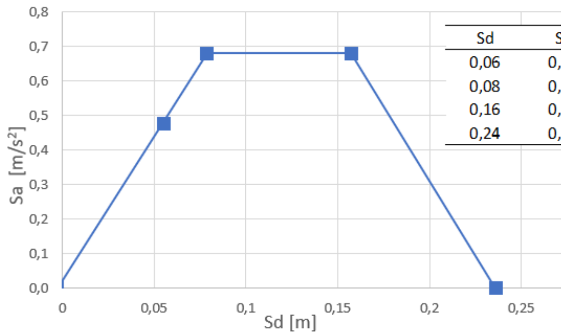

Trilinear capacity curves NUMERICAL METHOD

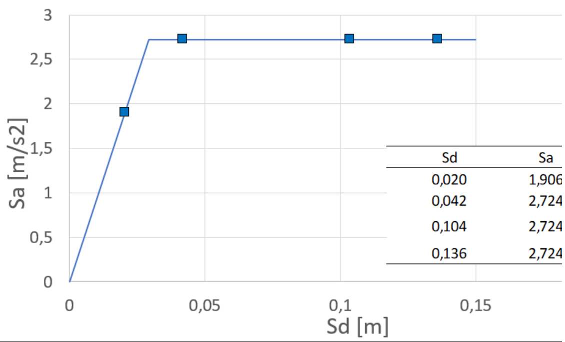

Fragility curves
(Analytical vs Numerical curves)

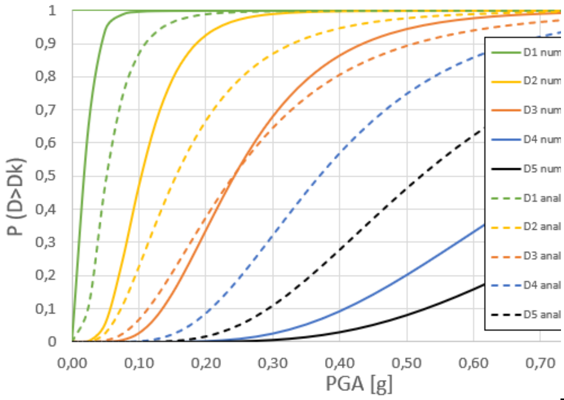

Final Fragility curves

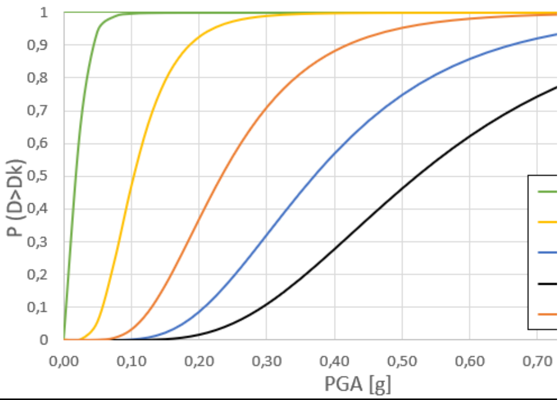

	D1	D2	D3	D4	D5
β	PGA	PGA	PGA	PGA	PGA
0,45	0,020	0,104	0,243	0,369	0,522

ARCHETYPE BUILDING #20

	Typology	N. of stories	Construction period	Ring beams and tie rods	Slab type	Roof material	Wall thickness at the ground floor	Distance between walls
20	Brick	4	< 1860	Present	Flexible	Light	< 60 cm	< 5 m

Geometrical model (frontal façade)	Numerical model (back façade)

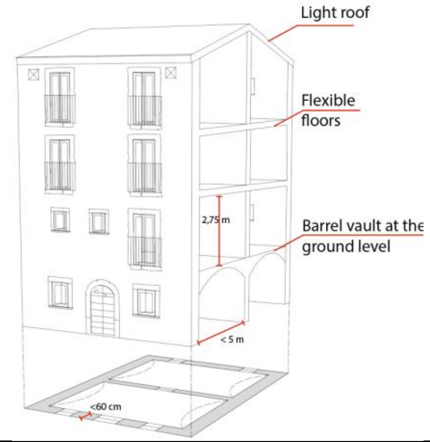

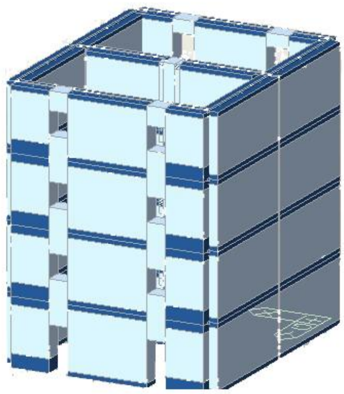

Bilinear capacity curves ANALYTICAL METHOD	Trilinear capacity curves NUMERICAL METHOD

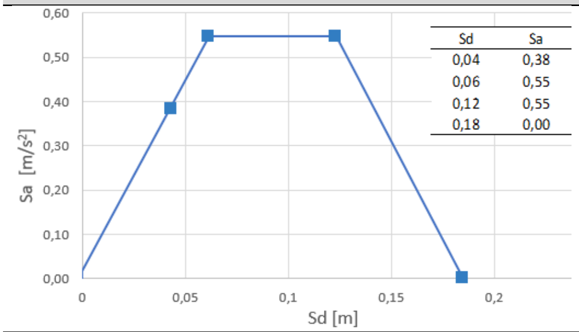

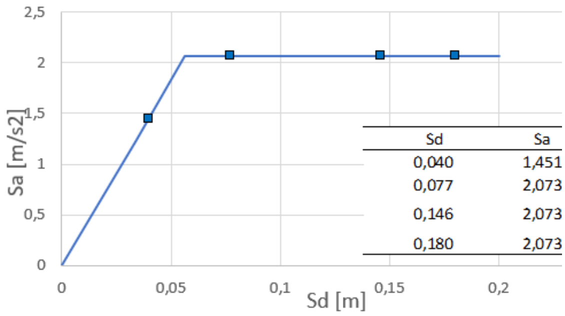

Fragility curves (Analytical vs Numerical curves)	Final Fragility curves

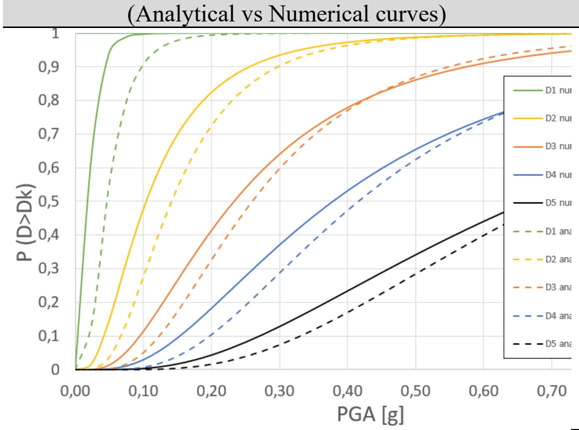

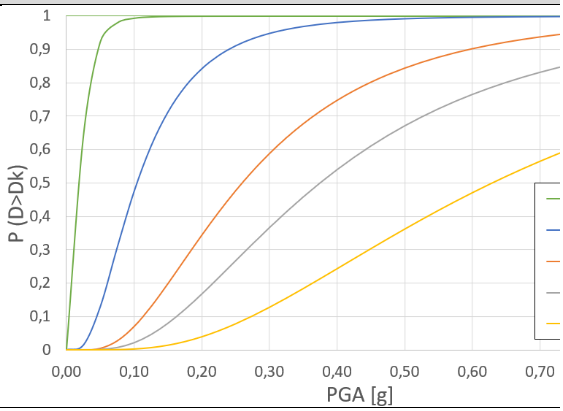

	D1	**D2**	**D3**	**D4**	**D5**
β	PGA	PGA	PGA	PGA	PGA
0,702	0,020	0,104	0,233	0,378	0,666

ARCHETYPE BUILDING #21

	Typology	N. of storie s	Construc tion period	Ring beams and tie rods	Slab type	Roof material	Wall thickness at the ground floor	Distance between walls
21	Brick	4	< 1860	Absent	Flexible	Light	< 60 cm	< 5 m

Geometrical model (frontal façade)	Numerical model (back façade)

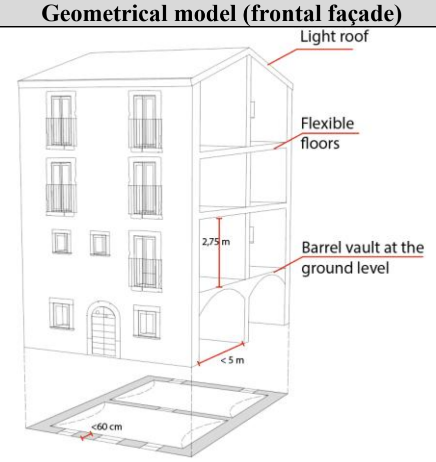

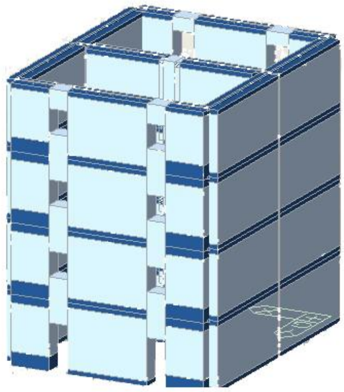

Bilinear capacity curves ANALYTICAL METHOD	Trilinear capacity curves NUMERICAL METHOD

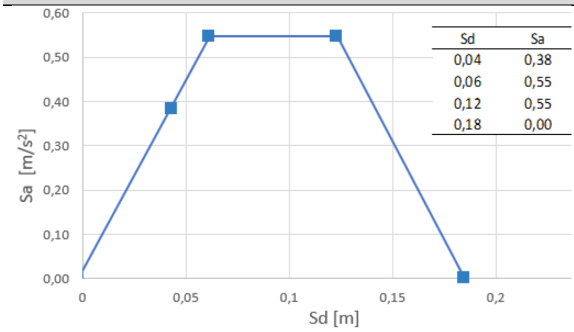

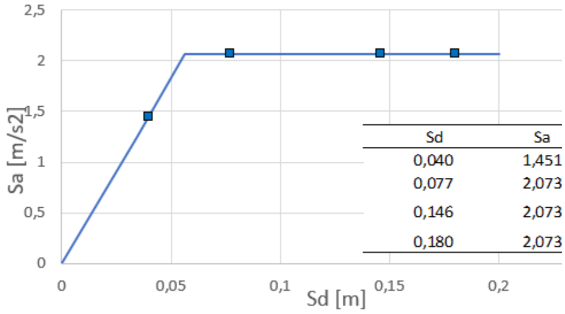

Fragility curves (Analytical vs Numerical curves)	Final Fragility curves

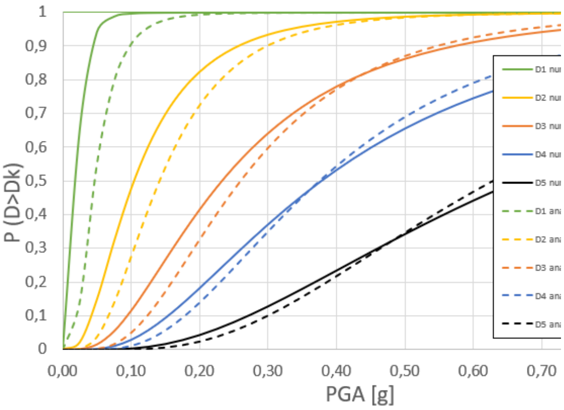

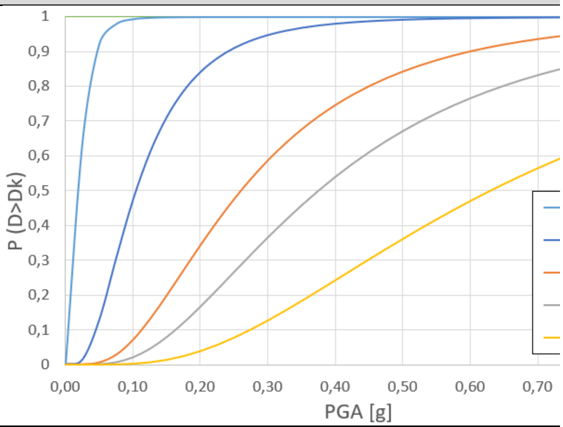

	D1	D2	D3	D4	D5
β	PGA	PGA	PGA	PGA	PGA
0,6 5	0,019	0,10	0,26	0,37	0,63

ARCHETYPE BUILDING #22

	Typology	N. of stories	Construction period	Ring beams and tie rods	Slab type	Roof material	Wall thickness at the ground floor	Distance between walls
22	Ir. masonry	2	< 1860	Absent	Flexible	Light	> 60 cm	< 5 m

Geometrical model (frontal façade)	Numerical model (back façade)

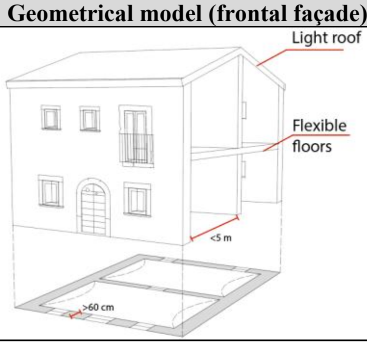

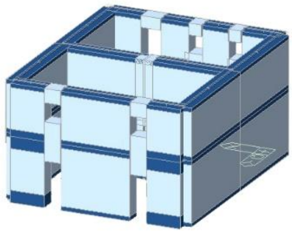

Bilinear capacity curves ANALYTICAL METHOD	Trilinear capacity curves NUMERICAL METHOD

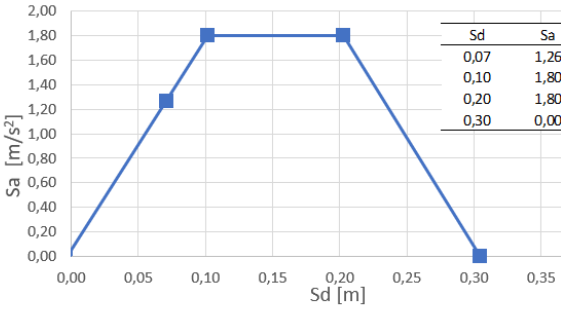

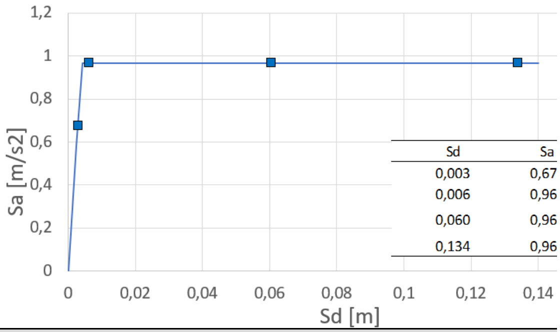

Fragility curves (Analytical vs Numerical curves)	Final Fragility curves

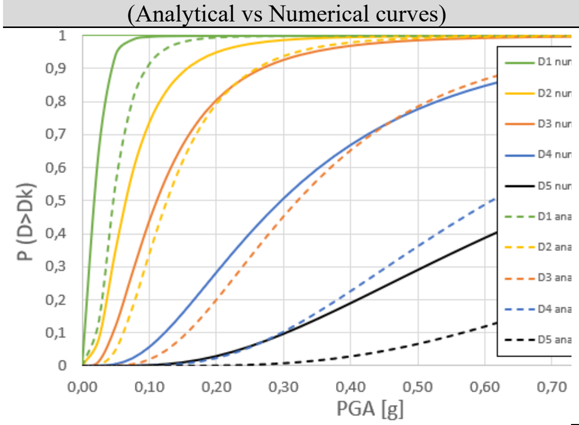

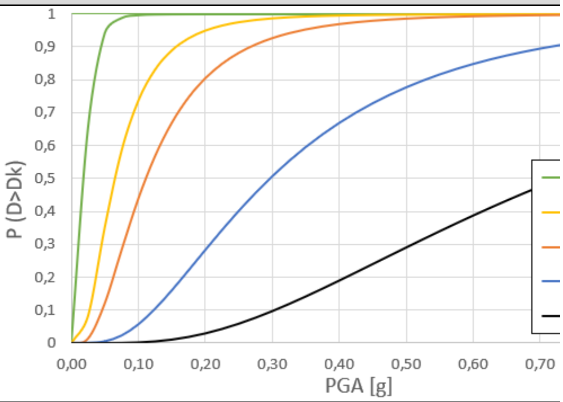

	D1	D2	D3	D4	D5
β	PGA	PGA	PGA	PGA	PGA
0,68	0,03	0,06	0,11	0,30	0,73

ARCHETYPE BUILDING #23

	Typology	N. of stories	Construction period	Ring beams and tie rods	Slab type	Roof material	Wall thickness at the ground floor	Distance between walls
23	Brick	3	1945-1981	Absent	Rigid	Heavy	< 60 cm	> 5 m

Geometrical model (frontal façade)	Numerical model (back façade)

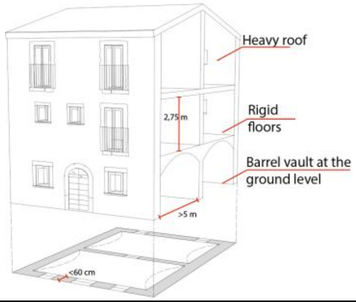

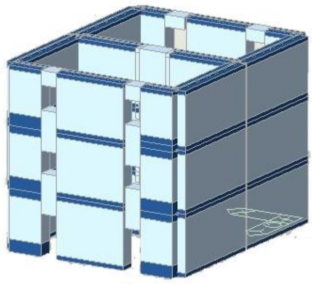

Bilinear capacity curves ANALYTICAL METHOD	Trilinear capacity curves NUMERICAL METHOD

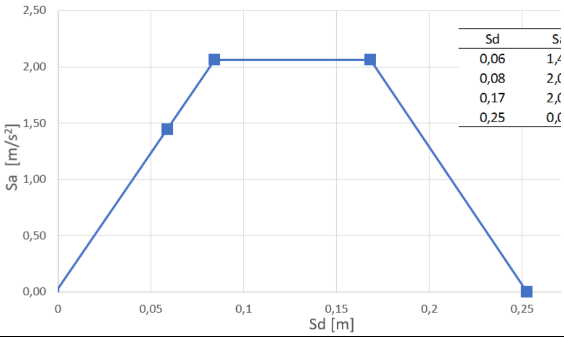

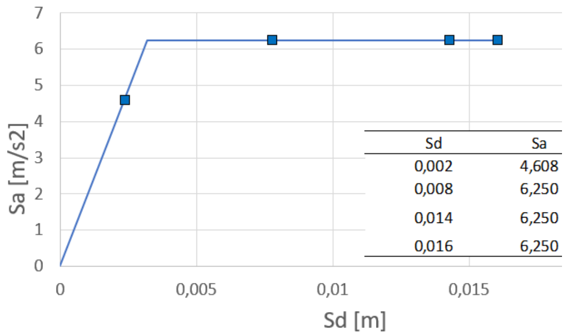

Fragility curves (Analytical vs Numerical curves)	Final Fragility curves

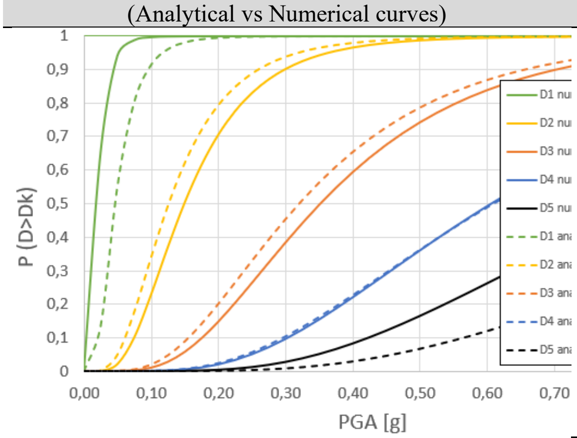

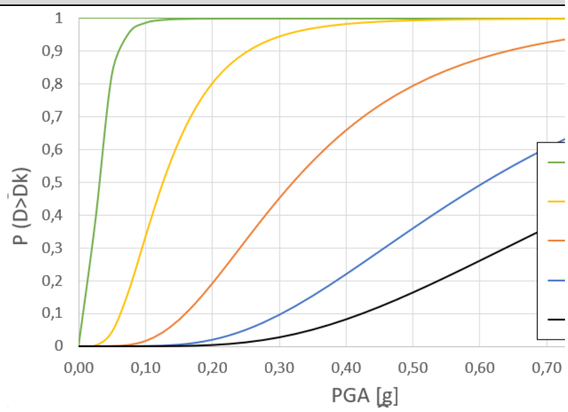

	D1	D2	D3	D4	D5
β	PGA	PGA	PGA	PGA	PGA
0,54	0,027	0,15	0,32	0,61	0,85

ARCHETYPE BUILDING #24

	Typology	N. of stories	Construction period	Ring beams and tie rods	Slab type	Roof material	Wall thickness at the ground floor	Distance between walls
24	Ir. masonry	4	< 1860	Present	Flexible	Heavy	> 60 cm	< 5 m

Geometrical model (frontal façade)

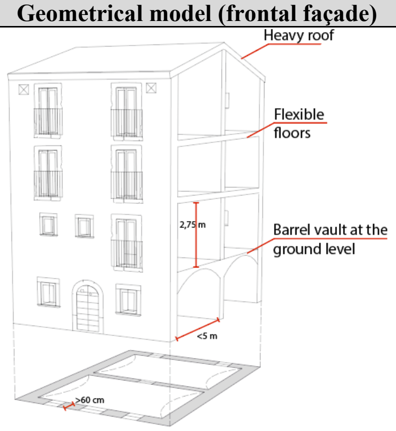

Numerical model (back façade)

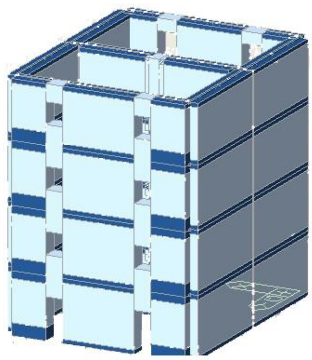

Bilinear capacity curves ANALYTICAL METHOD

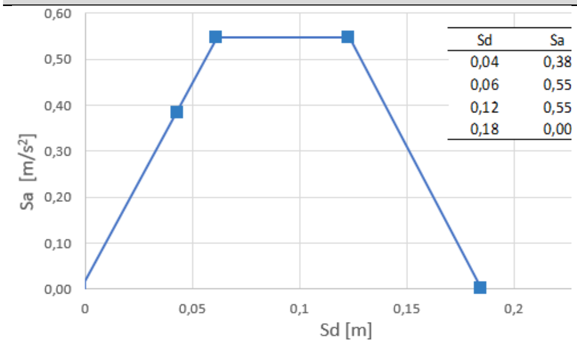

Trilinear capacity curves NUMERICAL METHOD

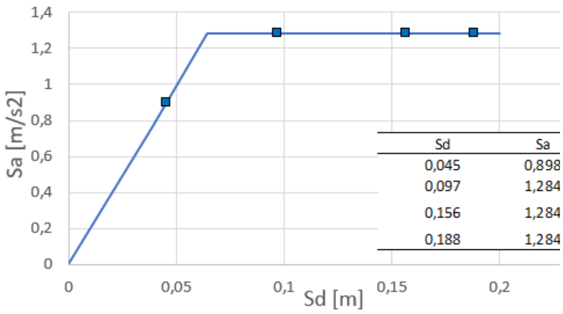

Fragility curves (Analytical vs Numerical curves)

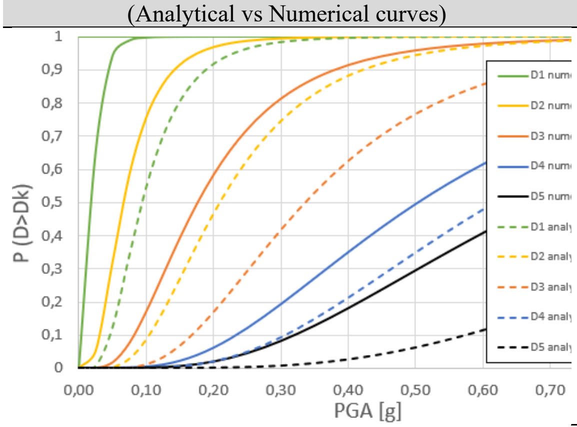

Final Fragility curves

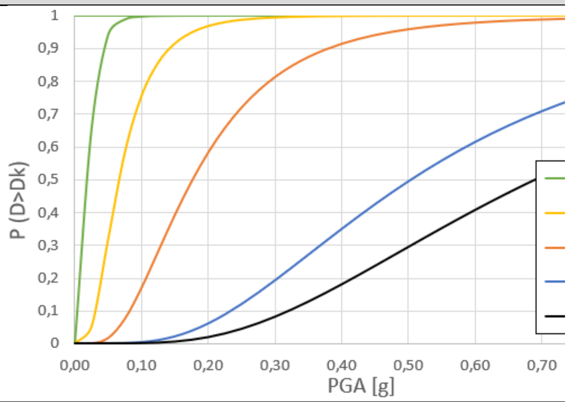

	D1	D2	D3	D4	D5
β	PGA	PGA	PGA	PGA	PGA
0,588	0,022	0,066	0,176	0,503	0,690

ARCHETYPE BUILDING #25

	Typology	N. of stories	Construction period	Ring beams and tie rods	Slab type	Roof material	Wall thickness at the ground floor	Distance between walls
25	Ir. masonry	4	< 1860	Absent	Flexible	Heavy	> 60 cm	< 5 m

Geometrical model (frontal façade)

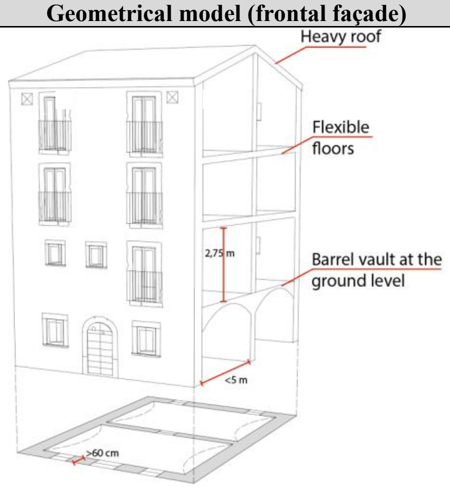

Numerical model (back façade)

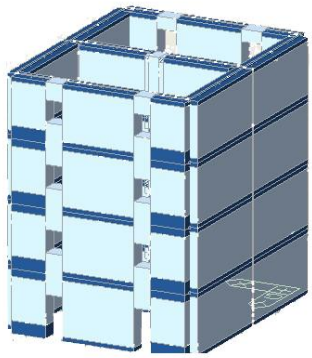

Bilinear capacity curves
ANALYTICAL METHOD

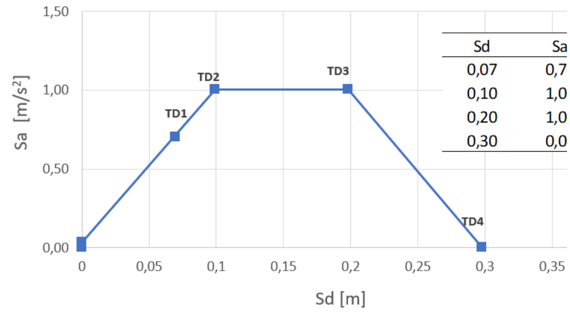

Trilinear capacity curves
NUMERICAL METHOD

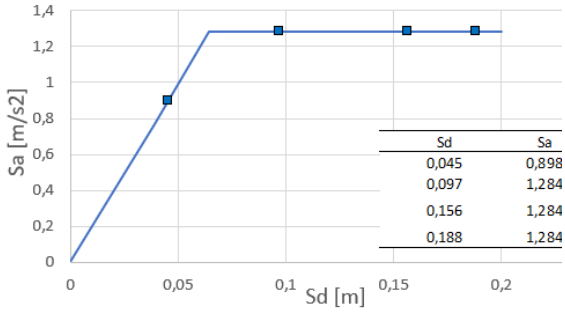

Fragility curves
(Analytical vs Numerical curves)

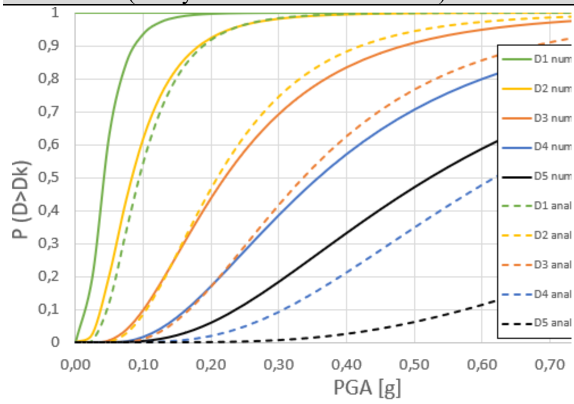

Final Fragility curves

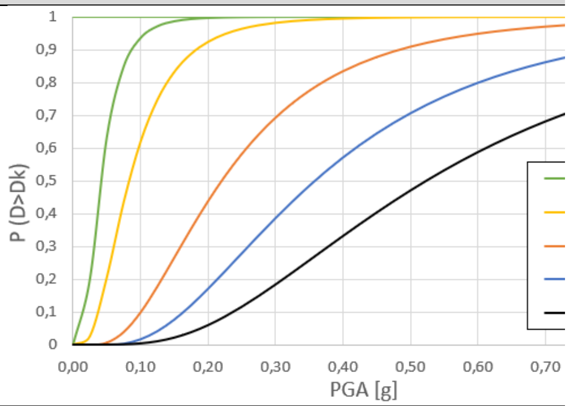

	D1	D2	D3	D4	D5
β	PGA	PGA	PGA	PGA	PGA
0,62	0,041	0,083	0,220	0,358	0,523

ARCHETYPE BUILDING #26

	Typology	N. of storie s	Construc tion period	Ring beams and tie rods	Slab type	Roof material	Wall thickness at the ground floor	Distance between walls
26	Brick	4	1945-1981	Absent	Rigid	Heavy	< 60 cm	> 5 m

Geometrical model (frontal façade)	Numerical model (back façade)

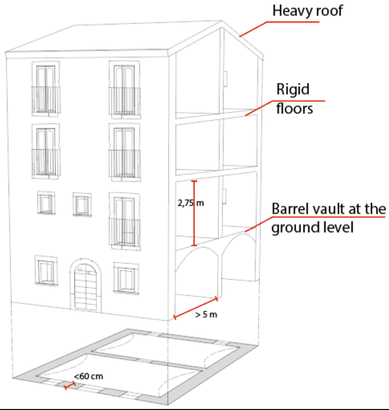

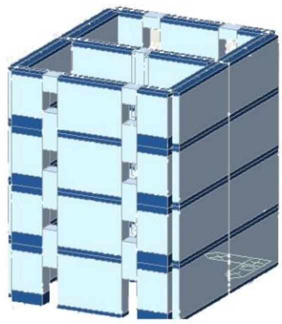

Bilinear capacity curves ANALYTICAL METHOD	Trilinear capacity curves NUMERICAL METHOD

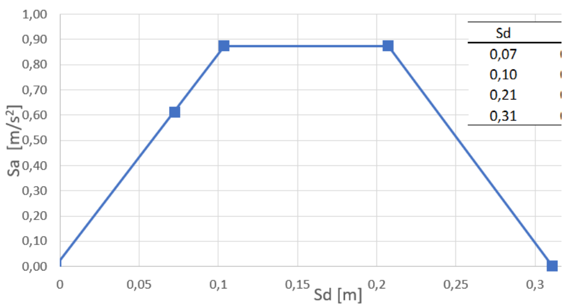

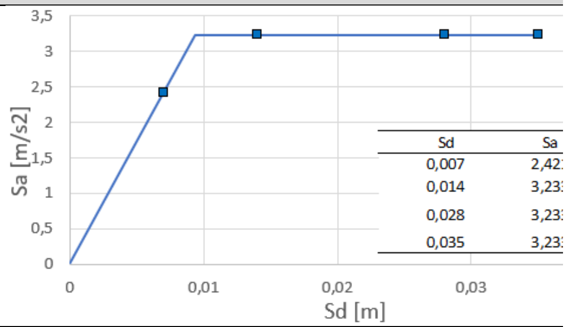

Fragility curves (Analytical vs Numerical curves)	Final Fragility curves

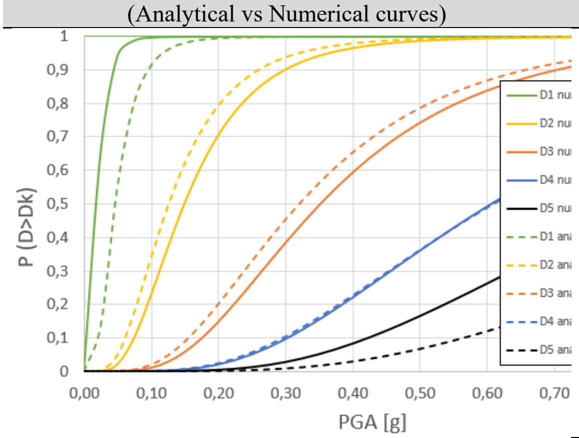

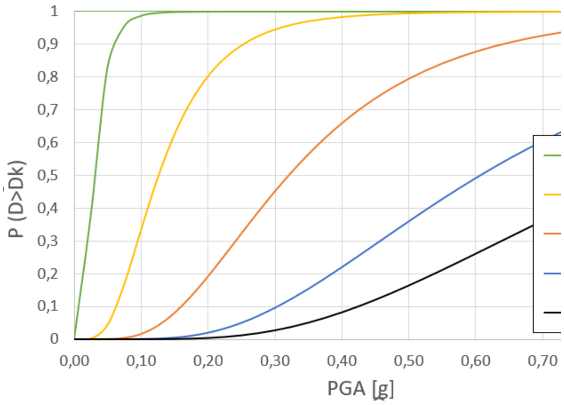

	D1	D2	D3	D4	D5
β	PGA	PGA	PGA	PGA	PGA
0,54	0,027	0,15	0,32	0,61	0,85

82

CHAPTER II

SEISMIC EXPOSURE ASSESSMENT OF EXISTING MASONRY BUILDINGS IN ITALY USING THE CARTIS DATABASE: FROM REGIONAL TO NATIONAL SCALE

ABSTRACT

This study presents a comprehensive methodology for assessing the seismic exposure of residential masonry buildings in Italy using the CARTIS database, a detailed repository of typological and structural characteristics of the national building stock. The analysis extends a previously developed regional approach to a national scale, employing archetype-based modelling to categorize buildings into representative typologies. This process involved the systematic extraction of data from the CARTIS database, followed by a multi-stage disaggregation and reaggregation procedure using a semi-automated MATLAB script. To address the complexity of Italy's seismic landscape, the study adopts a multi-scale approach, analysing seismic exposure at three geographic levels: regional, macro-regional, and national. At the regional scale, 369 archetypes were identified, capturing the diversity of building characteristics across individual regions. This detailed categorization offers high granularity, essential for localized risk assessments. At the macro-regional scale, data was aggregated into 39 representative archetypes for three broad geographic areas—Northern, Central, and Southern Italy. The national analysis synthesized the data into eight archetypes, providing a streamlined framework for large-scale risk mitigation and policy planning. The results highlight the adaptability and robustness of the proposed methodology, with consistent typological distributions observed across scales. While the regional analysis offers detailed insights into local vulnerabilities, the broader scales balance detail and computational efficiency, ensuring reliable exposure assessments for diverse decision-making needs. The study also emphasizes the importance of scale in seismic risk analysis, demonstrating how data aggregation impacts typological representativeness and the ability to generalize findings for policymaking. This work contributes to the field of seismic risk assessment by providing a scalable and validated methodology for evaluating building exposure. The findings support the development of targeted interventions and strategic policies to enhance the resilience of Italy's built environment, with implications for similar applications in other seismic-prone regions globally.

1. INTRODUCTION

The assessment of seismic risk represents a crucial aspect for understanding and addressing the consequences of earthquakes, both in terms of immediate emergency interventions and in the planning of long-term strategies for risk reduction and prevention of effects on the territory. Italy, a region characterized by high seismic activity, constantly faces the challenge of understanding and mitigating seismic risk. In fact, the presence of numerous historic centres, rich in cultural heritage and valuable masonry buildings, heightens the responsibility to preserve this heritage from seismic events.

Past experiences, such as the earthquakes in Central Italy in 2016, Emilia in 2012, L'Aquila in 2009, Molise in 2002, Umbria and Marche in 1997, Irpinia in 1980, and Reggio Calabria-Messina in 1908 [1], highlighted the high vulnerability of the civil building heritage. The economic losses, estimated at 180 billion euros over the last 50 years, in terms of emergency management, restoration, and reconstruction costs, as well as thousands of victims [2], underscore the urgency of assessing the socioeconomic impacts of earthquake-induced damages.

From this perspective, the fundamental role of "knowledge of risk scenarios" has long been recognized. Indeed, numerous predictive models was developed that incorporate information such as architectural types, structural characteristics, the number of buildings, spatial location, and socioeconomic aspects. These models allow for the estimation of damage levels, losses, and impacts on different types of buildings in the event of natural disasters. However, given the damage estimates in the face of seismic events, to reduce risk, it is necessary to implement prevention strategies aimed at reducing the vulnerability of the built heritage, the only factor that can be effectively addressed to concretely mitigate the seismic risk of an area. In fact, the primary reason for the damages sustained so far is fundamentally the high vulnerability of the building stock [3]. However, mitigating and adapting to seismic risk is not an easy task, as evaluating its components—hazard, vulnerability, and exposure—is complex [4], [5], [6]. Specifically, to assess the seismic vulnerability of buildings, numerous methods are available in the literature, differing primarily in their scale of analysis. There are methods more suitable for small-scale use (at the level of individual buildings or, at most, building aggregates) [7], [8], [9] and others better suited for large-scale assessments, ranging from entire neighbourhoods to entire regions, such as those by [10], [11], [12], [13], [14], [15] to name a few of the most common. However, these methods usually require a significant amount of data on the mechanical and geometric properties of the buildings involved to accurately characterize the seismic response. Moreover, especially when conducting large-scale analyses involving extensive areas or even entire cities, investigating these essential parameters often leads to very time-consuming and costly surveys, complicating risk assessment analyses significantly ([16], [17]). To adapt vulnerability models to local specifics, it is necessary to develop exposure models that associate building types with vulnerability classes, such as in the MARS vulnerability model [1].

Thus, the importance of having an accurate knowledge of the building stock across the entire national territory becomes evident, as it allows for the extraction of necessary data for the most suitable assessments in a given situation. “As known, exposure represents, quantitatively and qualitatively, the extent of the different anthropic elements characterizing a given geographic area (people, buildings, infrastructures, activities, and movable properties), whose conditions and/or functioning can be damaged, altered, or destroyed due to the occurrence of a seismic event" [18].

It follows that the inventory of buildings is a fundamental element in this context, as it provides essential information for understanding the heritage at risk. Only with a thorough knowledge of this inventory is it possible to evaluate vulnerability, the only factor that can be effectively addressed to concretely mitigate the seismic risk of an area, as well as to conduct exposure studies for the estimation of potential losses [19], [20].

In Italy, various approaches were adopted to develop such inventories, utilizing both data from national censuses and advanced survey techniques. These approaches reflect the complexity of the Italian seismic risk landscape, where the availability and limitations of data significantly influence the ability to assess and mitigate potential damage from earthquakes. Accurate and detailed data collection is a cornerstone of seismic risk assessment, but challenges remain in integrating disparate data sources into cohesive and comprehensive exposure models.

The Italian National Institute of Statistics (ISTAT) provides essential information on the building stock, including data on structural type, construction period, and number of floors. However, these data have limitations. They are often aggregated to protect privacy, which reduces their spatial resolution and usability for detailed seismic exposure studies. Furthermore, the dataset lacks critical structural and material parameters required to assess seismic behaviour, such as wall thickness, floor stiffness, and construction quality. While ISTAT data is a valuable starting point, its limitations necessitate the integration of additional data sources to enhance its applicability for seismic risk assessment [21], [3].

There are also other databases that collect more detailed technical information, primarily focused on post-seismic event damage assessment, such as the Da.D.O. (Database of Observed Damage) database [22]. Da.D.O. contains damage data relevant to nine of the most damaging Italian earthquakes in the 1976–2012 period, mostly referring to masonry buildings (about 78%, corresponding to about 250,000 buildings), while data on reinforced concrete (RC) buildings is lower (about 8%, corresponding to about 24,000 buildings) [23]. Other types (e.g., steel, timber, and mixed structures) or unidentified types of amount to about 12%. This database, developed by the Italian Civil Protection Department (ICPD), collects information on damage and structural features of ordinary buildings for 11 national seismic events [22]. While it provides invaluable insights into damage patterns and structural characteristics, its scope is limited to damaged buildings, making it less representative of the overall building stock [24].

It would therefore be useful to utilize a database that collects information on buildings most suitable for the various possible assessments, providing a comprehensive dataset both in terms of information and the number of buildings included. An innovative resource like the "CARTIS" form presents itself as a solution, enabling a more thorough collection of data on the structural characteristics of buildings [18], [25]. Its detailed classification has made it a preferred resource for medium-to-large scale vulnerability studies (e.g., [10], [26], [27], [28]). Recent advancements have included automated procedures for deriving building portfolios and urban compartments using CARTIS data, further enhancing its usability [29], [30]. Recognizing the limitations of existing databases, many researchers advocate for integrating multiple data sources or developing new techniques to supplement missing information. For instance, for urban-scale assessments, ISTAT census areas are often used to define urban compartments, but alternative methods, such as municipal urban plans or homogeneous structural-typological zones, have also been proposed [31], [32]. Also, approaches such as multi-level sampling [33] and probabilistic frameworks for typology classification [34] offer scalable solutions for exposure data collection. Furthermore, there are complementary GIS-Based Methods where the integration of remote sensing and GIS tools has enabled detailed exposure mapping for historical centres [35], [36]. Again, there are those who have integrated the data present in existing databases with online maps such as Google Earth and Street View in a fast and automated way [37], [38]. Lastly, multi-scale analysis has emerged as a critical aspect of exposure assessment, emphasizing the need to account for scale-dependent variations, such as [39] demonstrated how regional aggregation affects vulnerability estimates; [40] introduced hierarchical building classification frameworks to address these variations.

At the European level, significant efforts have been made to standardize seismic exposure assessment methodologies and improve data integration across countries. These initiatives aim to address the diverse construction practices, seismic hazards, and data availability that characterize the European building stock, for example with the classification proposed in [41].

Regarding the building taxonomy and standardization, the SYNER-G Project [42] established a comprehensive building taxonomy, which provides a unified framework for classifying buildings based on structural systems, materials, and construction periods. This taxonomy facilitates cross-country comparisons and harmonization of exposure data in Europe.

Regarding data collection protocols, the EMS-98 Classification System [43] remains a cornerstone for seismic vulnerability assessment in Europe. Its straightforward categorization of buildings based on vulnerability classes has been widely adopted, serving as a reference for both academic research and practical applications. Instead, more recently, projects like OpenQuake [44] have incorporated these protocols into open-access platforms, promoting the sharing of exposure and vulnerability data.

Furthermore, integrations of modern technologies have also taken place at European level: the incorporation of remote sensing and GIS technologies into European projects has significantly advanced the resolution and accuracy of exposure models. For example, [45] demonstrated how satellite imagery combined with statistical inference can refine urban-scale exposure maps. Also, the use of machine learning algorithms in seismic exposure assessments is also gaining traction. These approaches analyse large datasets, including census information and geospatial data, to identify building typologies and predict their distribution [46], [47], [48].

At least, there are probabilistic and multi-scale approaches. The Global Earthquake Model (GEM) [49], although global in scope, has been applied extensively in Europe to develop probabilistic exposure models. GEM's probabilistic frameworks account for uncertainties in building typologies and structural parameters, offering robust tools for national and regional risk assessments.

European initiatives like the EU Civil Protection Mechanism [50] and projects under the Horizon 2020 framework encourage cross-border collaboration in seismic risk assessment [51]. These efforts aim to share best practices, integrate national databases, and develop unified strategies for disaster resilience. Lastly, The RISK-UE Project [52] exemplifies this collaborative spirit, providing a comprehensive framework for urban risk assessment that integrates exposure, hazard, and vulnerability components.

In this study, the seismic exposure of Italian masonry buildings is analysed in depth using the CARTIS database, which offers a comprehensive characterization of the national building stock. The research emphasizes the distribution of typological features, through an automated archetypes-based method, their variability across different scales—

regional, macro-regional, and national—and the statistical representativeness of the archetypes identified. By focusing on these aspects, the study aims to provide valuable insights into the challenges of seismic exposure modelling, contributing to its refinement and its practical applications in risk mitigation strategies and policy development.

2. DATA AND METHODOLOGY

2.1 Data Sources: the CARTIS database

The seismic exposure of Italy's built environment necessitates a comprehensive understanding of the features that dominate the national architectural landscape.

The primary data source for this study is the CARTIS database (Typological and Structural Characterization), a comprehensive archive developed to catalogue the typological and structural characteristics of Italian buildings through the compilation of a first-level expeditious form compiled for homogeneous compartments of a municipality through the judgment of a local expert with reliable knowledge of the territory surveyed. The CARTIS form was developed in 2014 by the Plinius centre of the University "Federico II" of Nales [25] in the work-frame of the Italian research project ReLUIS (Italian Network of Academic Laboratory of Earthquake and Structural Engineering), supported by the Italian Civil Protection Department.

This database was chosen for this study because it represents a cornerstone for this effort, providing a comprehensive set of data useful for defining and categorizing the national building stock. Indeed, unlike general-purpose census data, CARTIS has been specifically designed to capture all building features relevant for seismic risk assessments. The use of this database is done through an accessible online platform [53] which can be queried by selecting the necessary data and the area for which information is needed: starting from the municipalities and extending the area to provinces, regions and national territory.

2.2 Methodological Framework

To simplify and standardize the evaluation process across a large and diversified territory, the study employs archetype-based modelling. This involves identifying representative building typologies that capture the key characteristics of the national building stock. To this aim, information on the built heritage catalogued in the CARTIS database available on the online platform pgadmin [53] were retrieved. However, the platform does not allow queries to be made that allow two or more parameters to be linked together, providing an overview of representative building typologies. Therefore, this limitation was overcome through a disaggregation-reaggregation procedure carried out with a semi-automated script in a MATLAB environment capable of returning information on the single building [30]. In the original study it was assessed on the Abruzzo region instead, here the procedure is extended to the national territory.

The archetype extraction process, summarized in Figure 1, consisted of multiple stages:

1. Selecting the analysis scale:
    - Request to the pgadmin database for data for the national territory, dividing it into three macro regions: Northern, Central, and Southern Italy.
    - Request for data for the national territory without subdivisions.
2. Data Cleaning and Disaggregation:
    - Raw data from the CARTIS database, organized by municipality, was pre-processed to remove inconsistencies, duplicates, and incomplete information.
    - The MATLAB procedure disaggregated the data by systematically combining the typological-structural variables to produce unique representations of each building.
3. Aggregation of Building Typologies:
    - Building typologies were reaggregated into representative categories using clustering algorithms based on the frequency and percentage relevance of the considered parameters.
    - The aggregation criteria prioritized typical and recurring configurations, ensuring that each archetype represented a massive portion of the building stock, each greater than 1%.
4. Output: Archetype Models:
    - At the level of macro-regions (Northern, Central, and Southern Italy), thirty-nine archetypes were identified,
    - which were subsequently reduced to eight national archetypes for a more synthetic representation.

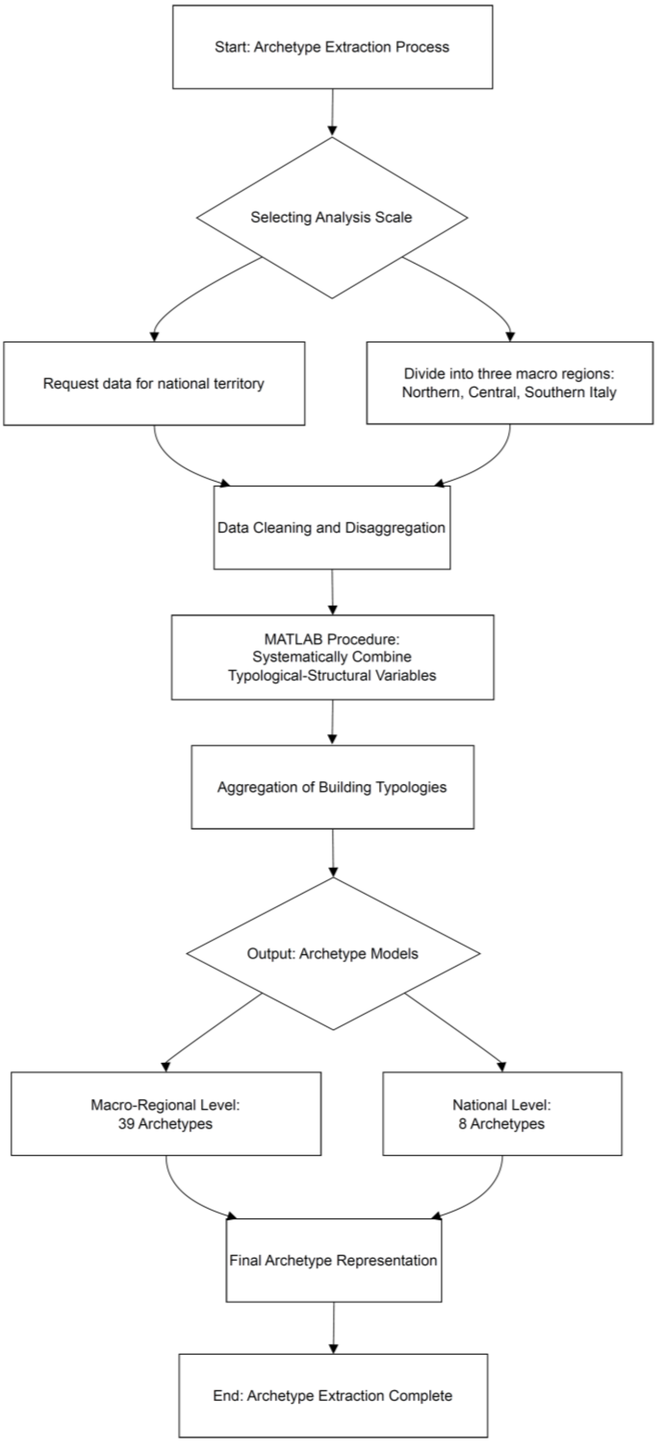

Figure 1. Flowchart of the process from the initial processing of CARTIS data to the selection of archetypes.

An important aspect, however, is to select the parameters among those available in the CARTIS form to describe the building typologies. Here, as in the original work, the building archetypes were defined based on a selection of eight parameters considered most influential on the seismic behaviour of buildings, identified through previous studies, and validated in scientific literature [54], [28].

1. Type of masonry (e.g., irregular masonry, bricks, squared stone).
2. Number of stories.
3. Construction period (e.g., pre-1860, 1861–1919, 1945–1981, post-1981).
4. Presence of tie rods.
5. Floor type (e.g., rigid, semi-rigid, flexible).
6. Roof material (e.g., heavy, light).
7. Wall thickness at the ground floor.
8. Average spacing between walls.

2.3 THE ANALYSIS SCALES

To assess exposure at a national level, in front of varied territory, the first pivot point was defining the appropriate scale of analysis. This decision is crucial, as the scale directly influences the granularity and representativeness of the results. In this study, to answer this question analysis was conducted at three progressively broader scales, each offering distinct advantages and insights (Figure 2):

- Regional Scale: This level provides a detailed examination of individual regions, capturing the specific characteristics and diversity of building typologies within each area of the Italian territory. It allows for a high-resolution understanding of local seismic exposure.
- Macro-Regional Scale: By grouping regions into three macro-areas: Northern, Central, and Southern Italy. This intermediate scale balances detail and generalization. It highlights regional patterns and trends while simplifying the analysis compared to the regional scale.
- National Scale: At this scale, data from all regions are synthesized to define archetypes representing the entire country in one shot. This approach offers a streamlined and cohesive perspective, suitable for large-scale strategic planning and policy development. Synthesizing data across all regions to identify archetypes for the entire country.

These multi-scale analyses ensure that the study accommodates the complexity of Italy's seismic risk landscape while enabling flexible application of the results to various contexts and levels of decision-making.

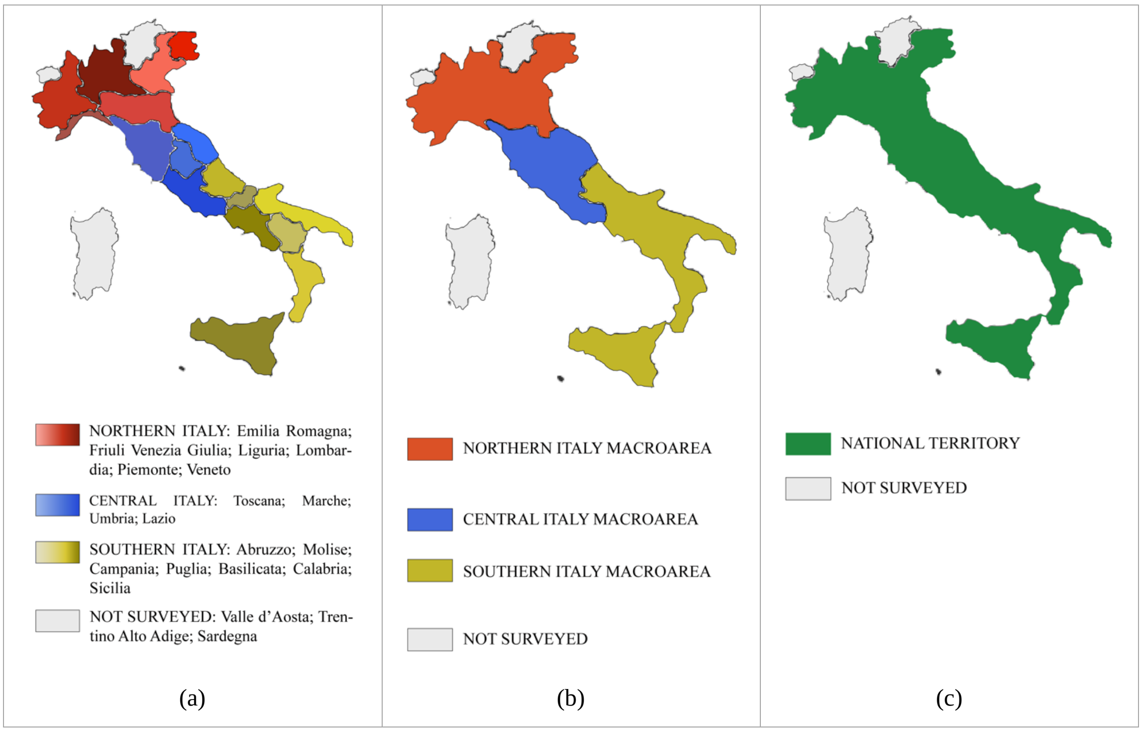

Figure 2. Variation of the areas of definition of the representative typologies: a) regional level; b) over-regional macro-areas: Northern Italy, Central Italy, Southern Italy; c) extension of the identification to the entire national territory

3. BUILDING TYPOLOGIES: THE NATIONAL PERSPECTIVE

The results of this study present the identification and distribution of building archetypes derived at three different scales of analysis: regional, macro-regional, and national. Each scale provides unique insights into the typological diversity and seismic exposure of the Italian masonry building stock.

3.1 Regional Scale

At the regional level, the CARTIS database was used to analyse the building stock individually for each of Italy's regions. This detailed analysis resulted in the identification of 369 unique archetypes, each representing specific combinations of the eight parameters selected for typological classification.

Table 1. List of archetype buildings for individual regions of Northern Italy: Emilia-Romagna, Friuli Venezia Giulia, Liguria, Veneto, Lombardia, Piemonte.

Area	ID	Masonry Type	N° of Stories	Construction Period	Tie Rods	Floor Type	Roof Material	Wall Thickness	Wall Spacing	Relevance
	1	Bricks	2	1945-1981	no	Rigid	Heavy	< 60 cm	< 5 m	25.74%
	2	Bricks	3	1945-1981	no	Rigid	Heavy	< 60 cm	< 5 m	15.80%
	3	Bricks	2	1861-1919	no	Flexible	Light	< 60 cm	< 5 m	12.90%
Emilia	4	Bricks	2	Post 1981	no	Rigid	Heavy	< 60 cm	< 5 m	8.63%
Romagna	5	Bricks	3	Post 1982	no	Rigid	Heavy	< 60 cm	< 5 m	5.78%
	6	Bricks	3	1861-1919	no	Flexible	Light	< 60 cm	< 5 m	4.60%
	7	Bricks	2	1919-1945	no	Flexible	Light	< 60 cm	< 5 m	3.55%
	8	Bricks	4	1945-1981	no	Rigid	Heavy	< 60 cm	< 5 m	2.95%

	9	Bricks	2	1945-1981	no	Rigid	Light	< 60 cm	< 5 m	2.91%
	10	Bricks	2	1861-1919	no	Rigid	Heavy	< 60 cm	< 5 m	2.54%
	11	Bricks	3	1861-1919	no	Rigid	Heavy	< 60 cm	< 5 m	2.37%
	12	Bricks	3	1945-1981	no	Rigid	Light	< 60 cm	< 5 m	1.93%
	13	Bricks	1	1945-1981	no	Rigid	Heavy	< 60 cm	< 5 m	1.83%
	14	Bricks	1	1861-1919	no	Flexible	Light	< 60 cm	< 5 m	1.57%
	15	Bricks	1	1919-1945	no	Flexible	Light	< 60 cm	< 5 m	1.57%
	16	Bricks	3	1919-1945	no	Flexible	Light	< 60 cm	< 5 m	1.30%
	17	Bricks	2	< 1860	no	Flexible	Light	< 60 cm	< 5 m	1.15%
	18	Bricks	2	1861-1919	yes	Flexible	Light	< 60 cm	< 5 m	1.02%
	19	Bricks	2	Post 1981	yes	Rigid	Heavy	< 60 cm	> 5 m	1.01%
Friuli Venezia Giulia	1	Bricks	3	1945-1981	yes	Rigid	Heavy	< 60 cm	< 5 m	16.00%
	2	Bricks	3	1945-1981	yes	Semi-rigid	Heavy	< 60 cm	< 5 m	15.50%
	3	Bricks	2	1945-1981	yes	Semi-rigid	Heavy	< 60 cm	< 5 m	11.10%
	4	Bricks	2	1945-1981	yes	Rigid	Heavy	< 60 cm	< 5 m	9.98%
	5	Bricks	4	1945-1981	yes	Rigid	Heavy	< 60 cm	< 5 m	3.42%
	6	Bricks	5	1945-1981	yes	Rigid	Heavy	< 60 cm	< 5 m	2.08%
	7	Bricks	3	1945-1981	no	Semi-rigid	Heavy	< 60 cm	< 5 m	1.84%
	8	Bricks	2	1945-1981	no	Semi-rigid	Heavy	< 60 cm	< 5 m	1.51%
	9	Bricks	4	1945-1981	no	Semi-rigid	Heavy	< 60 cm	< 5 m	1.51%
	10	Bricks	6	1945-1981	yes	Rigid	Heavy	< 60 cm	< 5 m	1.31%
	11	Bricks	1	1945-1981	no	Semi-rigid	Heavy	< 60 cm	< 5 m	1.30%
	12	Bricks	1	1945-1981	no	Rigid	Heavy	< 60 cm	< 5 m	1.01%
	13	Bricks	2	1945-1981	no	Rigid	Heavy	< 60 cm	< 5 m	1.01%
	14	Bricks	3	1945-1981	no	Rigid	Heavy	< 60 cm	< 5 m	1.01%
	15	Bricks	4	1945-1981	no	Rigid	Heavy	< 60 cm	< 5 m	1.01%
Liguria	1	Irregular masonry	2	< 1860	no	Flexible	Light	> 60 cm	< 5 m	12.20%
	2	Rough masonry	2	< 1860	no	Flexible	Light	< 60 cm	< 5 m	10.90%
	3	Rough masonry	3	< 1860	no	Flexible	Light	< 60 cm	< 5 m	7.92%
	4	Irregular masonry	3	< 1860	yes	Flexible	Light	> 60 cm	< 5 m	6.79%
	5	Bricks	2	1945-1981	yes	Rigid	Light	< 60 cm	< 5 m	5.88%
	6	Irregular masonry	3	< 1860	yes	Semi-rigid	Light	> 60 cm	< 5 m	4.59%
	7	Irregular masonry	2	< 1860	yes	Flexible	Light	> 60 cm	< 5 m	3.54%
	8	Irregular masonry	3	< 1860	no	Flexible	Light	> 60 cm	< 5 m	3.52%
	9	Rough masonry	5	< 1860	yes	Flexible	Light	> 60 cm	< 5 m	3.29%
	10	Irregular masonry	4	< 1860	yes	Flexible	Light	> 60 cm	< 5 m	3.23%
	11	Rough masonry	3	< 1860	yes	Flexible	Light	< 60 cm	< 5 m	3.18%
	12	Rough masonry	4	< 1860	yes	Flexible	Light	> 60 cm	< 5 m	2.94%
	13	Irregular masonry	4	< 1860	no	Flexible	Light	> 60 cm	< 5 m	2.87%
	14	Irregular masonry	5	< 1860	no	Flexible	Light	> 60 cm	< 5 m	2.58%
	15	Rough masonry	2	< 1860	yes	Flexible	Light	< 60 cm	< 5 m	2.14%
	16	Rough masonry	4	1919-1945	yes	Rigid	Light	> 60 cm	< 5 m	1.89%
	17	Irregular masonry	2	1861-1919	no	Flexible	Light	< 60 cm	< 5 m	1.86%
	18	Bricks	1	1945-1981	yes	Rigid	Light	< 60 cm	< 5 m	1.80%
	19	Bricks	1	1945-1981	no	Rigid	Light	< 60 cm	< 5 m	1.79%
	20	Bricks	2	1945-1981	no	Rigid	Light	< 60 cm	< 5 m	1.79%
	21	Irregular masonry	2	< 1860	no	Flexible	Light	< 60 cm	< 5 m	1.74%
	22	Irregular masonry	4	< 1860	yes	Semi-rigid	Light	> 60 cm	< 5 m	1.71%
	23	Irregular masonry	6	< 1860	no	Flexible	Light	> 60 cm	< 5 m	1.49%
	24	Irregular masonry	4	< 1860	yes	Rigid	Light	> 60 cm	< 5 m	1.29%
	25	Irregular masonry	5	< 1860	yes	Flexible	Light	> 60 cm	< 5 m	1.18%
	26	Rough masonry	5	1919-1945	yes	Rigid	Light	> 60 cm	< 5 m	1.06%
Lombardia	1	Bricks	2	< 1860	no	Rigid	Heavy	< 60 cm	< 5 m	12.60%
	2	Bricks	2	< 1860	no	Semi-rigid	Light	< 60 cm	> 5 m	7.41%
	3	Irregular masonry	2	< 1860	no	Rigid	Light	> 60 cm	> 5 m	6.33%
	4	Bricks	3	< 1860	no	Semi-rigid	Light	< 60 cm	> 5 m	5.90%
	5	Irregular masonry with courses	3	< 1860	no	Flexible	Light	> 60 cm	> 5 m	5.80%
	6	Bricks	3	< 1860	no	Flexible	Light	< 60 cm	< 5 m	5.17%
	7	Irregular masonry	2	< 1860	no	Flexible	Light	> 60 cm	> 5 m	4.73%
	8	Bricks	2	1861-1919	no	Flexible	Light	> 60 cm	> 5 m	4.14%
	9	Irregular masonry with courses	2	< 1860	no	Semi-rigid	Light	> 60 cm	> 5 m	3.98%
	10	Bricks	3	< 1860	no	Flexible	Light	> 60 cm	> 5 m	2.68%
	11	Irregular masonry with courses	3	< 1860	no	Semi-rigid	Light	> 60 cm	> 5 m	2.58%
	12	Bricks	3	1861-1919	no	Flexible	Light	< 60 cm	< 5 m	2.46%
	13	Irregular masonry	3	< 1860	no	Flexible	Light	> 60 cm	> 5 m	2.46%
	14	Irregular masonry with courses	2	< 1860	no	Flexible	Light	< 60 cm	< 5 m	2.35%
	15	Bricks	3	< 1860	no	Rigid	Heavy	> 60 cm	> 5 m	2.15%
	16	Bricks	2	< 1860	no	Flexible	Heavy	< 60 cm	< 5 m	1.91%
	17	Bricks	2	< 1860	no	Rigid	Light	< 60 cm	< 5 m	1.86%
	18	Bricks	3	1919-1945	no	Semi-rigid	Light	< 60 cm	< 5 m	1.74%
	19	Bricks	3	1861-1919	no	Semi-rigid	Light	< 60 cm	< 5 m	1.66%
	20	Bricks	2	< 1860	no	Flexible	Light	< 60 cm	< 5 m	1.52%
	21	Bricks	3	< 1860	no	Flexible	Heavy	> 60 cm	> 5 m	1.51%

	22	Irregular masonry	3	< 1860	no	Rigid	Light	> 60 cm	> 5 m	1.49%
	23	Bricks	2	< 1860	no	Flexible	Light	> 60 cm	< 5 m	1.44%
	24	Bricks	4	1919-1945	no	Semi-rigid	Light	< 60 cm	< 5 m	1.40%
	25	Irregular masonry	2	< 1860	no	Flexible	Heavy	> 60 cm	> 5 m	1.39%
	26	Irregular masonry	3	< 1860	no	Flexible	Heavy	> 60 cm	> 5 m	1.39%
	27	Irregular masonry with courses	3	< 1860	no	Flexible	Light	< 60 cm	< 5 m	1.32%
	28	Bricks	4	1861-1919	no	Semi-rigid	Light	< 60 cm	< 5 m	1.32%
	29	Bricks	3	< 1860	no	Rigid	Light	> 60 cm	> 5 m	1.23%
	30	Irregular masonry	3	< 1860	no	Flexible	Light	< 60 cm	> 5 m	1.20%
	31	Bricks	3	< 1860	yes	Flexible	Light	< 60 cm	< 5 m	1.20%
	32	Bricks	3	< 1860	yes	Flexible	Light	> 60 cm	> 5 m	1.12%
	33	Irregular masonry	2	< 1860	no	Flexible	Light	> 60 cm	< 5 m	1.10%
	34	Irregular masonry	3	< 1860	no	Flexible	Light	> 60 cm	< 5 m	1.10%
	35	Bricks	3	< 1860	no	Flexible	Heavy	< 60 cm	< 5 m	1.03%
Piemonte	1	Rough masonry	3	< 1860	no	Flexible	Light	> 60 cm	< 5 m	14.60%
	2	Squared stone	1	1919-1945	no	Rigid	Heavy	< 60 cm	< 5 m	10.10%
	3	Squared stone	2	1861-1919	no	Semi-rigid	Light	> 60 cm	< 5 m	9.85%
	4	Squared stone	2	1861-1919	no	Semi-rigid	Heavy	> 60 cm	< 5 m	7.82%
	5	Rough masonry	3	< 1860	no	Rigid	Light	> 60 cm	< 5 m	4.86%
	6	Squared stone	1	1945-1981	yes	Rigid	Heavy	< 60 cm	< 5 m	4.60%
	7	Squared stone	1	1945-1981	no	Rigid	Heavy	< 60 cm	< 5 m	4.60%
	8	Squared stone	2	1945-1981	yes	Rigid	Heavy	< 60 cm	< 5 m	4.60%
	9	Squared stone	2	1945-1981	no	Rigid	Heavy	< 60 cm	< 5 m	4.60%
	10	Squared stone	2	1861-1919	no	Rigid	Heavy	< 60 cm	< 5 m	4.34%
	11	Squared stone	1	1919-1945	yes	Rigid	Heavy	< 60 cm	< 5 m	4.34%
	12	Rough masonry	3	< 1860	no	Flexible	Heavy	> 60 cm	< 5 m	3.58%
	13	Squared stone	2	1861-1919	yes	Semi-rigid	Light	> 60 cm	< 5 m	2.39%
	14	Squared stone	2	1861-1919	yes	Rigid	Heavy	< 60 cm	< 5 m	2.15%
	15	Squared stone	2	1861-1919	yes	Semi-rigid	Heavy	> 60 cm	< 5 m	2.10%
	16	Squared stone	3	< 1860	no	Flexible	Light	> 60 cm	< 5 m	1.66%
	17	Squared stone	3	< 1860	no	Rigid	Light	> 60 cm	< 5 m	1.66%
	18	Rough masonry	3	< 1860	yes	Flexible	Light	> 60 cm	< 5 m	1.09%
	19	Squared stone	2	< 1860	no	Flexible	Light	> 60 cm	< 5 m	1.09%
	20	Squared stone	2	< 1860	no	Flexible	Heavy	> 60 cm	< 5 m	1.09%
	21	Squared stone	2	< 1860	no	Rigid	Light	> 60 cm	< 5 m	1.09%
	22	Squared stone	2	< 1860	no	Rigid	Heavy	> 60 cm	< 5 m	1.09%
	23	Squared stone	3	< 1860	no	Flexible	Heavy	> 60 cm	< 5 m	1.09%
	24	Squared stone	3	< 1860	no	Rigid	Heavy	> 60 cm	< 5 m	1.09%
	25	Squared stone	4	< 1860	no	Flexible	Light	> 60 cm	< 5 m	1.09%
	26	Squared stone	4	< 1860	no	Flexible	Heavy	> 60 cm	< 5 m	1.09%
	27	Squared stone	4	< 1860	no	Rigid	Light	> 60 cm	< 5 m	1.09%
	28	Squared stone	4	< 1860	no	Rigid	Heavy	> 60 cm	< 5 m	1.09%
Veneto	1	Bricks	3	1945-1981	yes	Rigid	Heavy	< 60 cm	< 5 m	19.10%
	2	Bricks	2	1945-1981	yes	Rigid	Heavy	< 60 cm	< 5 m	15.30%
	3	Bricks	4	1945-1981	yes	Rigid	Heavy	< 60 cm	< 5 m	14.50%
	4	Irregular masonry	2	1861-1919	yes	Rigid	Heavy	< 60 cm	< 5 m	12.80%
	5	Irregular masonry	3	1861-1919	yes	Rigid	Heavy	< 60 cm	< 5 m	12.50%
	6	Irregular masonry	3	1861-1919	yes	Flexible	Light	< 60 cm	< 5 m	5.59%
	7	Bricks	2	1945-1981	no	Rigid	Heavy	< 60 cm	< 5 m	3.48%
	8	Irregular masonry	2	1861-1919	yes	Flexible	Light	< 60 cm	< 5 m	2.52%
	9	Irregular masonry	2	1861-1919	yes	Semi-rigid	Light	< 60 cm	< 5 m	2.35%
	10	Irregular masonry	3	1861-1919	yes	Semi-rigid	Light	< 60 cm	< 5 m	2.35%
	11	Bricks	3	1945-1981	no	Rigid	Heavy	< 60 cm	< 5 m	1.97%

Table 2. List of archetype buildings for individual regions of central Italy: Lazio, Marche, Toscana, Umbria

Area	ID	Masonry Type	N° of Stories	Construction Period	Tie Rods	Floor Type	Roof Material	Wall Thickness	Wall Spacing	Relevance
Lazio	1	Irregular masonry	3	< 1860	no	Flexible	Light	> 60 cm	< 5 m	9.58%
	2	Irregular masonry	3	1861-1919	no	Flexible	Light	> 60 cm	< 5 m	8.64%
	3	Squared stone	2	1945-1981	no	Semi-rigid	Light	< 60 cm	> 5 m	5.44%
	4	Squared stone	2	Post 1981	yes	Rigid	Heavy	< 60 cm	> 5 m	4.86%
	5	Squared stone	3	Post 1981	yes	Rigid	Heavy	< 60 cm	> 5 m	4.69%
	6	Irregular masonry with courses	3	< 1860	no	Rigid	Light	> 60 cm	< 5 m	4.69%
	7	Irregular masonry with courses	2	1945-1981	yes	Semi-rigid	Light	> 60 cm	< 5 m	4.52%
	8	Irregular masonry with courses	3	1945-1981	yes	Semi-rigid	Light	> 60 cm	< 5 m	4.52%
	9	Squared stone	3	1945-1981	no	Semi-rigid	Light	< 60 cm	> 5 m	3.45%
	10	Irregular masonry	3	1861-1919	no	Rigid	Light	> 60 cm	< 5 m	3.15%
	11	Irregular masonry	2	1861-1919	no	Flexible	Light	> 60 cm	< 5 m	2.56%
	12	Irregular masonry	3	1861-1919	no	Rigid	Heavy	> 60 cm	< 5 m	1.93%
	13	Squared stone	3	1945-1981	no	Rigid	Heavy	< 60 cm	< 5 m	1.83%

	14	Squared stone	2	1945-1981	no	Rigid	Heavy	< 60 cm	< 5 m	1.79%
	15	Irregular masonry	3	< 1860	no	Rigid	Heavy	> 60 cm	< 5 m	1.69%
	16	Irregular masonry	3	1861-1919	no	Flexible	Heavy	> 60 cm	< 5 m	1.61%
	17	Irregular masonry with courses	2	1919-1945	yes	Semi-rigid	Light	> 60 cm	< 5 m	1.57%
	18	Irregular masonry with courses	3	1919-1945	yes	Semi-rigid	Light	> 60 cm	< 5 m	1.57%
	19	Irregular masonry	2	< 1860	no	Flexible	Light	> 60 cm	< 5 m	1.44%
	20	Squared stone	4	1919-1945	no	Rigid	Heavy	< 60 cm	< 5 m	1.31%
	21	Irregular masonry	3	< 1860	no	Flexible	Heavy	> 60 cm	< 5 m	1.19%
	1	Bricks	2	1861-1919	yes	Flexible	Light	> 60 cm	< 5 m	15.13%
	2	Bricks	3	1861-1919	yes	Flexible	Light	> 60 cm	< 5 m	11.57%
	3	Bricks	3	1861-1919	yes	Rigid	Light	> 60 cm	< 5 m	10.17%
	4	Bricks	3	1945-1981	no	Semi-rigid	Heavy	< 60 cm	< 5 m	9.93%
	5	Bricks	2	1861-1919	yes	Rigid	Light	> 60 cm	< 5 m	8.61%
	6	Bricks	3	1861-1919	no	Flexible	Light	> 60 cm	< 5 m	4.87%
	7	Bricks	2	1861-1919	no	Flexible	Light	> 60 cm	< 5 m	4.65%
	8	Bricks	3	1861-1919	no	Rigid	Light	> 60 cm	< 5 m	4.34%
	9	Bricks	3	1919-1945	no	Semi-rigid	Heavy	< 60 cm	< 5 m	3.16%
Marche	10	Bricks	2	1861-1919	no	Rigid	Light	> 60 cm	< 5 m	2.91%
	11	Rough masonry with courses	3	1945-1981	no	Rigid	Heavy	> 60 cm	< 5 m	2.57%
	12	Rough masonry with courses	4	1945-1981	no	Rigid	Heavy	> 60 cm	< 5 m	2.03%
	13	Bricks	3	1945-1981	yes	Rigid	Heavy	< 60 cm	> 5 m	1.83%
	14	Bricks	3	1945-1981	no	Rigid	Heavy	< 60 cm	> 5 m	1.38%
	15	Bricks	3	1861-1919	Presen t	Rigid	Heavy	> 60 cm	< 5 m	1.31%
	16	Bricks	2	1861-1919	yes	Flexible	Heavy	> 60 cm	< 5 m	1.17%
	17	Bricks	3	1861-1919	yes	Flexible	Heavy	> 60 cm	< 5 m	1.17%
	1	Irregular masonry	2	< 1860	no	Semi-rigid	Light	> 60 cm	< 5 m	12.68%
	2	Bricks	2	1945-1981	yes	Rigid	Light	< 60 cm	< 5 m	9.04%
	3	Irregular masonry	2	1919-1945	no	Semi-rigid	Light	> 60 cm	< 5 m	8.24%
	4	Irregular masonry with courses	3	< 1860	no	Flexible	Light	< 60 cm	< 5 m	6.94%
	5	Irregular masonry	2	1861-1919	no	Flexible	Light	< 60 cm	< 5 m	6.27%
	6	Irregular masonry	3	< 1860	no	Semi-rigid	Light	> 60 cm	< 5 m	5.81%
	7	Irregular masonry	3	1861-1919	no	Semi-rigid	Light	< 60 cm	< 5 m	3.37%
	8	Bricks	2	1945-1981	yes	Rigid	Light	< 60 cm	< 5 m	3.20%
	9	Bricks	3	1945-1981	no	Rigid	Heavy	< 60 cm	> 5 m	2.23%
	10	Bricks	4	1945-1981	no	Rigid	Heavy	< 60 cm	> 5 m	2.23%
	11	Irregular masonry	2	1919-1945	no	Flexible	Light	< 60 cm	< 5 m	2.21%
Toscana	12	Irregular masonry	3	< 1860	yes	Semi-rigid	Light	> 60 cm	< 5 m	1.65%
	13	Irregular masonry	2	< 1860	no	Flexible	Light	< 60 cm	< 5 m	1.56%
	14	Bricks	3	1945-1981	yes	Rigid	Heavy	< 60 cm	< 5 m	1.54%
	15	Bricks	1	1945-1981	no	Rigid	Heavy	< 60 cm	< 5 m	1.51%
	16	Bricks	2	1945-1981	no	Rigid	Heavy	< 60 cm	< 5 m	1.51%
	17	Bricks	1	1945-1981	no	Semi-rigid	Heavy	< 60 cm	< 5 m	1.49%
	18	Bricks	2	1945-1981	no	Semi-rigid	Heavy	< 60 cm	< 5 m	1.49%
	19	Irregular masonry with courses	2	< 1860	no	Flexible	Light	< 60 cm	< 5 m	1.35%
	20	Irregular masonry	3	< 1860	no	Flexible	Light	< 60 cm	< 5 m	1.18%
	21	Irregular masonry	3	1861-1919	yes	Flexible	Light	< 60 cm	< 5 m	1.12%
	22	Irregular masonry	3	< 1860	yes	Flexible	Light	< 60 cm	< 5 m	1.01%
	1	Bricks	3	1945-1981	no	Rigid	Heavy	< 60 cm	< 5 m	17.13%
	2	Irregular masonry	2	1861-1919	yes	Flexible	Light	< 60 cm	< 5 m	9.37%
	3	Bricks	4	1945-1981	no	Rigid	Heavy	< 60 cm	< 5 m	9.05%
	4	Bricks	3	Post 1981	no	Rigid	Heavy	< 60 cm	< 5 m	7.84%
	5	Bricks	2	Post 1981	no	Rigid	Heavy	< 60 cm	< 5 m	6.77%
	6	Irregular masonry	3	< 1860	yes	Flexible	Light	< 60 cm	< 5 m	5.70%
	7	Irregular masonry	3	< 1860	no	Flexible	Light	< 60 cm	< 5 m	3.44%
	8	Irregular masonry	3	1861-1919	yes	Flexible	Light	< 60 cm	< 5 m	3.21%
	9	Bricks	3	1945-1981	yes	Rigid	Heavy	< 60 cm	< 5 m	2.61%
	10	Irregular masonry	3	1861-1919	no	Flexible	Light	< 60 cm	< 5 m	2.26%
Umbria	11	Squared stone	3	1945-1981	yes	Rigid	Heavy	< 60 cm	< 5 m	1.72%
	12	Irregular masonry	3	< 1860	no	Flexible	Light	> 60 cm	< 5 m	1.56%
	13	Squared stone	3	Post 1981	yes	Rigid	Heavy	< 60 cm	< 5 m	1.54%
	14	Bricks	3	1945-1981	yes	Semi-rigid	Heavy	< 60 cm	> 5 m	1.54%
	15	Bricks	3	1945-1981	yes	Rigid	Heavy	< 60 cm	> 5 m	1.54%
	16	Irregular masonry	2	1861-1919	no	Flexible	Light	< 60 cm	< 5 m	1.44%
	17	Irregular masonry	3	< 1860	yes	Flexible	Light	> 60 cm	< 5 m	1.23%
	18	Irregular masonry	2	< 1860	no	Flexible	Light	< 60 cm	< 5 m	1.18%
	19	Irregular masonry	2	< 1860	yes	Flexible	Light	< 60 cm	< 5 m	1.12%
	20	Irregular masonry	4	< 1860	yes	Flexible	Heavy	> 60 cm	> 5 m	1.09%
	21	Irregular masonry	3	< 1860	yes	Flexible	Light	> 60 cm	> 5 m	1.07%
	22	Irregular masonry	3	< 1860	yes	Flexible	Heavy	> 60 cm	> 5 m	1.07%
	23	Irregular masonry	4	< 1860	yes	Flexible	Light	> 60 cm	> 5 m	1.04%

	24	Bricks	4	1945-1981	yes	Semi-rigid	Heavy	< 60 cm	> 5 m	1.02%
	25	Bricks	4	1945-1981	yes	Rigid	Heavy	< 60 cm	> 5 m	1.02%

Table 3. List of archetype buildings for the regions of southern Italy: Abruzzo, Molise, Puglia, Basilicata, Campania, Calabria, Sicilia

Area	ID	Masonry Type	N° of Stories	Construction Period	Tie Rods	Floor Type	Roof Material	Wall Thickness	Wall Spacing	Relevance
	1	Bricks	2	1945-1981	no	Semi-rigid	Heavy	< 60 cm	< 5 m	12.39%
	2	Irregular masonry	3	< 1860	no	Flexible	Light	> 60 cm	< 5 m	11.02%
	3	Bricks	2	< 1860	yes	Flexible	Light	< 60 cm	< 5 m	9.85%
	4	Bricks	3	1945-1981	yes	Rigid	Heavy	< 60 cm	> 5 m	5.22%
	5	Irregular masonry	3	< 1860	yes	Semi-rigid	Light	> 60 cm	< 5 m	4.85%
	6	Irregular masonry	4	< 1860	yes	Semi-rigid	Light	> 60 cm	< 5 m	3.34%
	7	Bricks	2	< 1860	no	Flexible	Light	< 60 cm	< 5 m	3.09%
	8	Irregular masonry	3	< 1860	no	Semi-rigid	Light	> 60 cm	< 5 m	3.07%
	9	Irregular masonry	3	< 1860	yes	Flexible	Light	> 60 cm	< 5 m	3.01%
	10	Bricks	3	< 1860	yes	Flexible	Light	< 60 cm	< 5 m	3.00%
	11	Bricks	4	1945-1981	yes	Rigid	Heavy	< 60 cm	> 5 m	2.34%
Abruzzo	12	Irregular masonry	3	< 1860	no	Flexible	Heavy	'> 60 cm'	< 5 m	2.34%
	13	Irregular masonry	4	< 1860	yes	Flexible	Light	> 60 cm	< 5 m	2.12%
	14	Irregular masonry	4	< 1860	no	Flexible	Light	> 60 cm	< 5 m	2.06%
	15	Irregular masonry	3	< 1860	no	Semi-rigid	Heavy	> 60 cm	< 5 m	2.05%
	16	Bricks	3	< 1860	no	Flexible	Light	< 60 cm	< 5 m	1.99%
	17	Bricks	4	< 1860	yes	Flexible	Light	< 60 cm	< 5 m	1.44%
	18	Bricks	4	< 1860	no	Flexible	Light	< 60 cm	< 5 m	1.44%
	19	Irregular masonry	3	< 1860	yes	Flexible	Heavy	> 60 cm	< 5 m	1.43%
	20	Irregular masonry	3	< 1860	yes	Semi-rigid	Heavy	> 60 cm	< 5 m	1.43%
	21	Irregular masonry	4	< 1860	no	Semi-rigid	Light	> 60 cm	< 5 m	1.36%
	22	Irregular masonry	2	< 1860	no	Flexible	Light	> 60 cm	< 5 m	1.29%
	23	Bricks	3	1945-1981	no	Rigid	Heavy	< 60 cm	> 5 m	1.18%
	24	Irregular masonry	4	< 1860	yes	Flexible	Heavy	> 60 cm	< 5 m	1.00%
	1	Irregular masonry	5	< 1860	no	Semi-rigid	Light	< 60 cm	> 5 m	9.06%
	2	Irregular masonry	5	1861-1919	no	Semi-rigid	Light	< 60 cm	> 5 m	9.06%
	3	Irregular masonry	5	< 1860	no	Semi-rigid	Heavy	< 60 cm	> 5 m	8.90%
	4	Irregular masonry	5	1861-1919	no	Semi-rigid	Heavy	< 60 cm	> 5 m	8.90%
	5	Rough masonry	3	1945-1981	yes	Semi-rigid	Light	> 60 cm	> 5 m	8.24%
	6	Irregular masonry	2	1945-1981	no	Semi-rigid	Light	< 60 cm	> 5 m	7.91%
	7	Irregular masonry	3	1945-1981	no	Semi-rigid	Light	< 60 cm	> 5 m	7.25%
	8	Bricks	3	Post 1981	yes	Rigid	Heavy	< 60 cm	> 5 m	5.44%
	9	Bricks	4	1919-1945	no	Semi-rigid	Heavy	< 60 cm	> 5 m	4.28%
Molise	10	Irregular masonry	5	< 1860	yes	Semi-rigid	Light	< 60 cm	> 5 m	3.95%
	11	Irregular masonry	5	< 1860	yes	Semi-rigid	Heavy	< 60 cm	> 5 m	3.95%
	12	Irregular masonry	5	1861-1919	yes	Semi-rigid	Light	< 60 cm	> 5 m	3.95%
	13	Irregular masonry	5	1861-1919	yes	Semi-rigid	Heavy	< 60 cm	> 5 m	3.95%
	14	Bricks	3	1945-1981	yes	Rigid	Heavy	< 60 cm	> 5 m	3.29%
	15	Bricks	4	1945-1981	no	Semi-rigid	Heavy	< 60 cm	> 5 m	1.65%
	16	Bricks	5	1919-1945	no	Semi-rigid	Heavy	< 60 cm	> 5 m	1.32%
	17	Bricks	5	1945-1981	no	Semi-rigid	Heavy	< 60 cm	> 5 m	1.32%
	18	Irregular masonry	2	1945-1981	yes	Semi-rigid	Light	< 60 cm	> 5 m	1.15%
	19	Irregular masonry	3	1945-1981	yes	Semi-rigid	Light	< 60 cm	> 5 m	1.15%
	1	Squared stone	2	1861-1919	no	Semi-rigid	Light	> 60 cm	< 5 m	12.22%
	2	Rough masonry	3	< 1860	no	Flexible	Light	> 60 cm	< 5 m	10.12%
	3	Squared stone	1	1919-1945	no	Rigid	Heavy	< 60 cm	< 5 m	7.26%
	4	Squared stone	2	1861-1919	no	Semi-rigid	Heavy	> 60 cm	< 5 m	6.72%
	5	Squared stone	3	1945-1981	no	Rigid	Heavy	> 60 cm	< 5 m	6.59%
	6	Squared stone	2	1861-1919	no	Rigid	Heavy	< 60 cm	< 5 m	5.18%
	7	Squared stone	2	1945-1981	no	Rigid	Heavy	< 60 cm	< 5 m	4.51%
	8	Squared stone	3	1945-1981	yes	Rigid	Heavy	< 60 cm	< 5 m	4.06%
	9	Squared stone	4	1945-1981	yes	Rigid	Heavy	< 60 cm	< 5 m	4.06%
	10	Squared stone	1	1945-1981	yes	Rigid	Heavy	< 60 cm	< 5 m	3.82%
	11	Squared stone	2	1945-1981	yes	Rigid	Heavy	< 60 cm	< 5 m	3.82%
Puglia	12	Squared stone	3	< 1860	no	Rigid	Heavy	< 60 cm	< 5 m	3.47%
	13	Rough masonry	3	< 1860	no	Rigid	Light	> 60 cm	< 5 m	3.13%
	14	Squared stone	1	1945-1981	no	Rigid	Heavy	< 60 cm	< 5 m	2.97%
	15	Squared stone	1	1919-1945	yes	Rigid	Heavy	< 60 cm	< 5 m	2.80%
	16	Rough masonry	3	< 1860	no	Flexible	Heavy	> 60 cm	< 5 m	2.31%
	17	Squared stone	3	1861-1919	no	Rigid	Heavy	< 60 cm	< 5 m	1.93%
	18	Squared stone	2	< 1860	no	Rigid	Heavy	< 60 cm	< 5 m	1.84%
	19	Squared stone	2	1919-1945	no	Rigid	Heavy	< 60 cm	< 5 m	1.54%
	20	Squared stone	3	1919-1945	no	Rigid	Heavy	< 60 cm	< 5 m	1.54%
	21	Squared stone	3	1945-1981	no	Rigid	Heavy	< 60 cm	< 5 m	1.54%
	22	Squared stone	3	1919-1945	no	Rigid	Heavy	> 60 cm	< 5 m	1.42%
	23	Squared stone	2	1861-1919	yes	Semi-rigid	Heavy	> 60 cm	< 5 m	1.36%
	24	Squared stone	2	1861-1919	yes	Semi-rigid	Heavy	> 60 cm	< 5 m	1.36%

	25	Squared stone	2	1861-1919	yes	Rigid	Heavy	< 60 cm	< 5 m	1.21%
Basilicata	1	Rough masonry	1	1861-1919	yes	Semi-rigid	Heavy	< 60 cm	< 5 m	10.59%
	2	Irregular masonry with courses	2	< 1860	no	Flexible	Light	> 60 cm	< 5 m	8.96%
	3	Rough masonry	1	1919-1945	yes	Semi-rigid	Heavy	< 60 cm	< 5 m	7.58%
	4	Bricks	3	1945-1981	yes	Rigid	Heavy	< 60 cm	< 5 m	6.17%
	5	Rough masonry	2	1919-1945	yes	Semi-rigid	Heavy	< 60 cm	< 5 m	6.12%
	6	Rough masonry	2	1861-1919	yes	Semi-rigid	Heavy	< 60 cm	< 5 m	5.60%
	7	Irregular masonry	2	1861-1919	no	Flexible	Light	> 60 cm	< 5 m	5.45%
	8	Bricks	2	1945-1981	yes	Rigid	Heavy	< 60 cm	< 5 m	5.30%
	9	Irregular masonry	3	< 1860	no	Flexible	Light	> 60 cm	< 5 m	2.59%
	10	Bricks	4	1945-1981	yes	Rigid	Heavy	< 60 cm	< 5 m	2.51%
	11	Rough masonry	2	1861-1919	yes	Flexible	Heavy	< 60 cm	< 5 m	2.41%
	12	Rough masonry	1	1861-1919	yes	Flexible	Heavy	< 60 cm	< 5 m	2.31%
	13	Rough masonry	1	1919-1945	yes	Flexible	Heavy	< 60 cm	< 5 m	2.31%
	14	Rough masonry	2	1919-1945	yes	Flexible	Heavy	< 60 cm	< 5 m	2.31%
	15	Bricks	2	1945-1981	yes	Rigid	Light	< 60 cm	< 5 m	2.13%
	16	Rough masonry	2	1861-1919	yes	Semi-rigid	Light	< 60 cm	< 5 m	1.91%
	17	Irregular masonry	3	1861-1919	no	Flexible	Light	> 60 cm	< 5 m	1.76%
	18	Rough masonry	2	1919-1945	yes	Semi-rigid	Light	< 60 cm	< 5 m	1.51%
	19	Rough masonry	2	1919-1945	no	Semi-rigid	Heavy	< 60 cm	< 5 m	1.51%
	20	Rough masonry	1	1861-1919	yes	Semi-rigid	Light	< 60 cm	< 5 m	1.36%
	21	Rough masonry	1	1861-1919	no	Semi-rigid	Heavy	< 60 cm	< 5 m	1.36%
	22	Rough masonry	1	1919-1945	yes	Semi-rigid	Light	< 60 cm	< 5 m	1.36%
	23	Rough masonry	1	1919-1945	no	Semi-rigid	Heavy	< 60 cm	< 5 m	1.36%
	24	Rough masonry	2	1861-1919	no	Semi-rigid	Heavy	< 60 cm	< 5 m	1.36%
	25	Irregular masonry	2	< 1860	no	Semi-rigid	Light	> 60 cm	< 5 m	1.36%
Campania	1	Squared stone	3	1945-1981	yes	Semi-rigid	Light	> 60 cm	< 5 m	12.66%
	2	Rough masonry	3	1919-1945	no	Semi-rigid	Light	> 60 cm	< 5 m	7.79%
	3	Bricks	2	1945-1981	no	Rigid	Light	> 60 cm	< 5 m	6.73%
	4	Squared stone	3	1945-1981	no	Rigid	Heavy	> 60 cm	< 5 m	4.87%
	5	Bricks	1	Post 1981	no	Rigid	Heavy	< 60 cm	> 5 m	3.89%
	6	Squared stone	4	1945-1981	yes	Semi-rigid	Light	> 60 cm	< 5 m	3.64%
	7	Squared stone	2	1945-1981	yes	Semi-rigid	Light	> 60 cm	< 5 m	3.04%
	8	Squared stone	3	1945-1981	no	Rigid	Light	> 60 cm	< 5 m	2.51%
	9	Squared stone	3	1919-1945	yes	Semi-rigid	Light	> 60 cm	< 5 m	2.36%
	10	Squared stone	2	Post 1981	no	Rigid	Heavy	< 60 cm	> 5 m	1.85%
	11	Squared stone	4	1919-1945	yes	Semi-rigid	Light	> 60 cm	< 5 m	1.83%
	12	Squared stone	2	1919-1945	yes	Semi-rigid	Light	> 60 cm	< 5 m	1.80%
Calabria	1	Irregular masonry	3	1919-1945	yes	Flexible	Light	> 60 cm	< 5 m	7.89%
	2	Irregular masonry	3	< 1860	no	Flexible	Light	< 60 cm	< 5 m	7.55%
	3	Bricks	3	1945-1981	yes	Semi-rigid	Light	> 60 cm	< 5 m	4.83%
	4	Squared stone	2	1919-1945	yes	Rigid	Light	< 60 cm	< 5 m	3.85%
	5	Irregular masonry	3	1919-1945	no	Flexible	Light	> 60 cm	< 5 m	3.45%
	6	Irregular masonry	3	< 1860	no	Semi-rigid	Light	< 60 cm	< 5 m	3.08%
	7	Squared stone	3	1919-1945	yes	Semi-rigid	Light	< 60 cm	> 5 m	2.76%
	8	Irregular masonry	3	1945-1981	no	Flexible	Light	> 60 cm	< 5 m	2.51%
	9	Irregular masonry	4	< 1860	no	Flexible	Light	< 60 cm	< 5 m	2.50%
	10	Irregular masonry	3	1861-1919	no	Flexible	Light	< 60 cm	< 5 m	2.47%
	11	Irregular masonry	3	1861-1919	no	Semi-rigid	Light	< 60 cm	< 5 m	2.47%
	12	Irregular masonry	4	< 1860	no	Semi-rigid	Light	< 60 cm	< 5 m	2.47%
	13	Irregular masonry	4	1861-1919	no	Flexible	Light	< 60 cm	< 5 m	2.47%
	14	Irregular masonry	4	1861-1919	no	Semi-rigid	Light	< 60 cm	< 5 m	2.47%
	15	Squared stone	3	1919-1945	yes	Flexible	Light	< 60 cm	> 5 m	2.29%
	16	Squared stone	3	1919-1945	no	Semi-rigid	Light	< 60 cm	> 5 m	2.29%
	17	Squared stone	3	1919-1945	no	Flexible	Light	< 60 cm	> 5 m	2.06%
	18	Squared stone	4	1919-1945	yes	Flexible	Light	< 60 cm	> 5 m	2.06%
	19	Squared stone	4	1919-1945	yes	Semi-rigid	Light	< 60 cm	> 5 m	2.06%
	20	Squared stone	4	1919-1945	no	Flexible	Light	< 60 cm	> 5 m	2.06%
	21	Squared stone	4	1919-1945	no	Semi-rigid	Light	< 60 cm	> 5 m	2.06%
Sicilia	1	Irregular masonry	2	1919-1945	no	Semi-rigid	Light	< 60 cm	< 5 m	12.28%
	2	Squared stone	3	1945-1981	no	Rigid	Heavy	< 60 cm	< 5 m	9.17%
	3	Irregular masonry	3	1861-1919	no	Flexible	Light	> 60 cm	< 5 m	8.77%
	4	Bricks	2	1945-1981	no	Rigid	Heavy	< 60 cm	< 5 m	5.85%
	5	Squared stone	2	1945-1981	no	Rigid	Heavy	< 60 cm	< 5 m	3.62%
	6	Squared stone	3	1945-1981	yes	Rigid	Heavy	< 60 cm	< 5 m	3.40%
	7	Irregular masonry	3	< 1860	no	Flexible	Light	> 60 cm	< 5 m	2.83%
	8	Irregular masonry	2	< 1860	no	Flexible	Light	> 60 cm	< 5 m	2.55%
	9	Irregular masonry	3	1861-1919	no	Flexible	Light	< 60 cm	< 5 m	2.34%
	10	Squared stone	2	1945-1981	no	Rigid	Light	< 60 cm	< 5 m	2.16%
	11	Squared stone	3	1945-1981	no	Rigid	Light	< 60 cm	< 5 m	2.15%
	12	Squared stone	4	1945-1981	yes	Rigid	Heavy	< 60 cm	< 5 m	2.14%
	13	Irregular masonry	4	1861-1919	no	Flexible	Light	> 60 cm	< 5 m	2.04%
	14	Irregular masonry	2	< 1860	no	Flexible	Heavy	> 60 cm	< 5 m	1.94%
	15	Irregular masonry	1	< 1860	no	Flexible	Heavy	> 60 cm	< 5 m	1.88%
	16	Irregular masonry	3	1919-1945	no	Flexible	Light	< 60 cm	< 5 m	1.72%
	17	Squared stone	2	Post 1981	no	Rigid	Heavy	< 60 cm	< 5 m	1.72%

18	Squared stone	3	Post 1981	no	Rigid	Heavy	< 60 cm	< 5 m	1.72%
19	Irregular masonry	4	< 1860	no	Flexible	Light	> 60 cm	< 5 m	1.40%
20	Irregular masonry	2	1861-1919	no	Flexible	Light	< 60 cm	< 5 m	1.36%
21	Irregular masonry	2	< 1860	no	Flexible	Light	< 60 cm	< 5 m	1.32%
22	Bricks	2	1945-1981	no	Rigid	Light	< 60 cm	< 5 m	1.26%
23	Irregular masonry	1	< 1860	no	Flexible	Light	> 60 cm	< 5 m	1.11%
24	Irregular masonry	2	1919-1945	no	Flexible	Light	< 60 cm	< 5 m	1.05%

The high granularity at this scale enabled the capture of local construction practices and regional architectural variations. For instance:

- In Northern Italy, regions such as Lombardy and Veneto exhibited a prevalence of brick masonry structures with rigid floors and heavier roofing materials, reflecting more modern construction techniques in urban areas.
- In Central Italy, regions like Umbria and Marche showed a significant proportion of irregular masonry buildings from pre-1860, often lacking structural reinforcements like tie rods, which increases their seismic vulnerability.
- In Southern Italy, regions such as Calabria and Sicily demonstrated a predominance of masonry buildings with flexible floor systems and a higher incidence of squared stone masonry.

This level of detail highlights the localized seismic exposure and provides crucial insights for targeted risk mitigation strategies at the regional scale.

3.2 Macro-Regional Scale

At the macro-regional scale, Italy was divided into three broad geographic areas: Northern, Central, and Southern Italy. The data from the regional scale was aggregated to identify 39 representative archetypes across these macro-regions, reducing the complexity while retaining sufficient typological diversity for broader analysis.

Table 4. List of archetype buildings for the macro-areas of northern, central, and southern Italy

Area	ID	Masonry Type	N° of Stories	Construction Period	Tie Rods	Floor Type	Roof Material	Wall Thickness	Wall Spacing	Relevance
Northern Italy	1 N	Bricks	3	1945-1981	yes	Rigid	Heavy	< 60 cm	< 5 m	15.80%
	2 N	Bricks	2	1945-1981	yes	Rigid	Heavy	< 60 cm	< 5 m	11.14%
	3 N	Bricks	2	1861-1919	no	Flexible	Light	< 60 cm	< 5 m	9.95%
	4 N	Bricks	4	1945-1981	yes	Rigid	Heavy	< 60 cm	< 5 m	9.24%
	5 N	Irregular masonry	3	1861-1919	yes	Rigid	Heavy	< 60 cm	< 5 m	7.79%
	6 N	Irregular masonry	2	1861-1919	yes	Rigid	Heavy	< 60 cm	< 5 m	7.44%
	7 N	Bricks	2	1945-1981	no	Rigid	Heavy	< 60 cm	< 5 m	7.32%
	8 N	Irregular masonry	2	1861-1919	yes	Flexible	Light	< 60 cm	< 5 m	5.17%
	9 N	Bricks	3	1945-1981	no	Rigid	Heavy	< 60 cm	< 5 m	4.73%
	10 N	Irregular masonry	3	1861-1919	yes	Flexible	Light	< 60 cm	< 5 m	2.59%
	11 N	Bricks	2	Post 1981	no	Rigid	Heavy	< 60 cm	< 5 m	2.42%
	12 N	Bricks	3	Post 1981	no	Rigid	Heavy	< 60 cm	< 5 m	1.62%
	13 N	Irregular masonry	3	1861-1919	yes	Semi-rigid	Light	< 60 cm	< 5 m	1.56%
	14 N	Irregular masonry	2	1861-1919	yes	Semi-rigid	Light	< 60 cm	< 5 m	1.43%
	15 N	Bricks	2	1945-1981	no	Rigid	Light	< 60 cm	< 5 m	1.06%
Central Italy	1 C	Bricks	2	1861-1919	yes	Flexible	Light	> 60 cm	< 5 m	9.00%
	2 C	Bricks	3	1945-1981	no	Rigid	Heavy	< 60 cm	< 5 m	7.59%
	3 C	Bricks	3	1861-1919	yes	Flexible	Light	> 60 cm	< 5 m	5.99%

	4 C	Bricks	2	1861-1919	yes	Rigid	Light	> 60 cm	< 5 m	5.95%
	5 C	Bricks	3	1861-1919	yes	Rigid	Light	> 60 cm	< 5 m	5.27%
	6 C	Bricks	3	1861-1919	no	Flexible	Light	> 60 cm	< 5 m	2.87%
	7 C	Bricks	2	1861-1919	no	Flexible	Light	> 60 cm	< 5 m	2.41%
	8 C	Bricks	2	1945-1981	yes	Rigid	Heavy	< 60 cm	< 5 m	2.38%
	9 C	Bricks	3	1945-1981	no	Semi-rigid	Heavy	< 60 cm	< 5 m	2.08%
	10 C	Bricks	3	1861-1919	no	Rigid	Light	> 60 cm	< 5 m	1.92%
	11 C	Bricks	4	1945-1981	no	Rigid	Heavy	< 60 cm	< 5 m	1.92%
	12 C	Bricks	2	1861-1919	no	Rigid	Light	> 60 cm	< 5 m	1.50%
	13 C	Bricks	3	1945-1981	no	Rigid	Heavy	< 60 cm	> 5 m	1.47%
	14 C	Bricks	3	1919-1945	no	Semi-rigid	Heavy	< 60 cm	< 5 m	1.43%
	1 S	Irregular masonry	3	< 1860	no	Flexible	Light	> 60 cm	< 5 m	9.51%
	2 S	Bricks	2	1945-1981	no	Rigid	Heavy	< 60 cm	< 5 m	8.78%
	3 S	Irregular masonry	2	1919-1945	no	Semi-rigid	Light	< 60 cm	< 5 m	8.41%
	4 S	Squared stone	2	1945-1981	no	Rigid	Heavy	< 60 cm	< 5 m	7.59%
Southern Italy	5 S	Squared stone	3	1945-1981	yes	Rigid	Heavy	< 60 cm	< 5 m	4.19%
	6 S	Irregular masonry	3	1861-1919	no	Flexible	Light	> 60 cm	< 5 m	2.62%
	7 S	Irregular masonry	2	< 1860	no	Flexible	Light	> 60 cm	< 5 m	2.05%
	8 S	Squared stone	4	1945-1981	yes	Rigid	Heavy	< 60 cm	< 5 m	1.77%
	9 S	Squared stone	3	1945-1981	no	Rigid	Heavy	< 60 cm	< 5 m	1.72%
	10 S	Irregular masonry	3	1861-1919	no	Flexible	Light	< 60 cm	< 5 m	1.39%

Key findings include:

- Northern Italy was characterized by 15 archetypes, dominated by modern brick masonry structures with rigid floors and lighter roofing materials. This reflects the higher prevalence of post-1981 constructions.
- Central Italy identified 14 archetypes, with a balanced distribution of irregular masonry and mixed masonry structures. Many buildings in this area are heritage constructions, indicating a greater seismic vulnerability.
- Southern Italy revealed 10 archetypes, which predominantly include older constructions with flexible floors and heavier roofing systems, indicative of traditional building practices.

The aggregation process at this scale effectively captured regional patterns while facilitating an intermediate level of analysis suitable for assessing broader trends in seismic exposure.

3.3 National Scale

For the national scale, the data from all regions were synthesized into 8 representative archetypes, providing a highly streamlined perspective of Italy's masonry building stock. This synthesis simplifies the evaluation of seismic exposure on a national level, making it suitable for strategic planning and large-scale policy decisions.

The national archetypes include:

- Archetypes characterized by modern construction techniques, such as brick masonry with rigid floors, prevalent in urbanized areas.

- Archetypes reflecting older, traditional structures, such as irregular masonry with flexible floor systems, common in historical centres across Italy.
- Mixed archetypes representing transitional periods of construction, combining features of both traditional and modern practices.

Table 5. List of archetype buildings identified for the entire national territory.

Area	ID	Masonry Type	N° of Stories	Construction Period	Tie Rods	Floor Type	Roof Material	Wall Thickness	Wall Spacing	Relevance
National	1	Bricks	2	1945-1981	yes	Rigid	Heavy	< 60 cm	< 5 m	12.45%
	2	Bricks	3	1945-1981	yes	Rigid	Heavy	< 60 cm	< 5 m	6.80%
	3	Irregular masonry	3	1861-1919	yes	Rigid	Heavy	< 60 cm	< 5 m	5.68%
	4	Bricks	4	1945-1981	yes	Rigid	Heavy	< 60 cm	< 5 m	4.91%
	5	Bricks	2	1945-1981	no	Rigid	Heavy	< 60 cm	< 5 m	4.67%
	6	Irregular masonry	2	1861-1919	yes	Rigid	Heavy	< 60 cm	< 5 m	4.14%
	7	Bricks	3	1945-1981	no	Rigid	Heavy	< 60 cm	< 5 m	2.89%
	8	Bricks	2	Post 1981	no	Rigid	Heavy	< 60 cm	< 5 m	1.38%

These 8 archetypes were selected based on their frequency and relevance, ensuring that each type represents a significant portion of the building stock while minimizing the loss of critical typological information.

3.4 Comparative Analysis Across Scales

The multi-scale analysis revealed key insights into the trade-offs between granularity and generalization:

- The regional scale provided the most detailed insights but required intensive computational resources and data processing.
- The macro-regional scale balanced detail and simplicity, effectively highlighting regional seismic exposure trends.
- The national scale offered a comprehensive and cohesive representation, ideal for national-level risk mitigation strategies, albeit with reduced typological specificity.

These results demonstrate the scalability and adaptability of the proposed methodology, providing a robust framework for seismic risk assessments at varying geographic levels.

4. EVALUATIONS ON THE EXPOSURE OF IDENTIFIED TYPOLOGIES

The results obtained from the analyses allow for comprehensive evaluations of seismic exposure to statistically assess the typological-structural characteristics and representativeness of buildings across different areas. These evaluations also provide insight into how the variation in analysis scale impacts the results, allowing for an assessment of the reliability of the applied methodology at increasingly broader scales.

4.1 Representativeness of Building Typologies

One key observation concerns the representativeness of the building typologies extracted from the database. Only typologies with a frequency greater than 1% were considered to ensure statistical significance. The representativeness, however, varies with the scale of analysis:

- At the regional scale, a representativeness exceeding 50% of the residential buildings catalogued in the CARTIS database is achieved with 12 to 35 typologies per region. For example, the region of Campania covers approximately 53%, whereas regions like Emilia-Romagna, Lombardia, Piemonte, and Puglia achieve nearly 100% coverage (Figure 3).
- Moving to the macro-regional scale, fewer typologies are required. In Northern Italy, 15 typologies cover 90% of the building stock, while in Central and Southern Italy, 14 and 10 typologies respectively achieve around 50% coverage (Figure 4**Errore. L'origine riferimento non è stata trovata.**).
- At the national scale, 8 representative archetypes cover 43% of the building stock. While this is a lower level of representativeness, it offers a synthetic and manageable dataset for large-scale evaluations (Figure 5**Errore. L'origine riferimento non è stata trovata.**).

The cumulative frequency of identified typologies demonstrates a consistent decrease in representativeness with increasing scale. At the regional level, 369 archetypes collectively represent over 80% of the Italian building stock, while at the macro-regional scale, 39 typologies account for 70%. The most aggregated scale, with 8 typologies, represents 43% of the buildings (Figure 6).

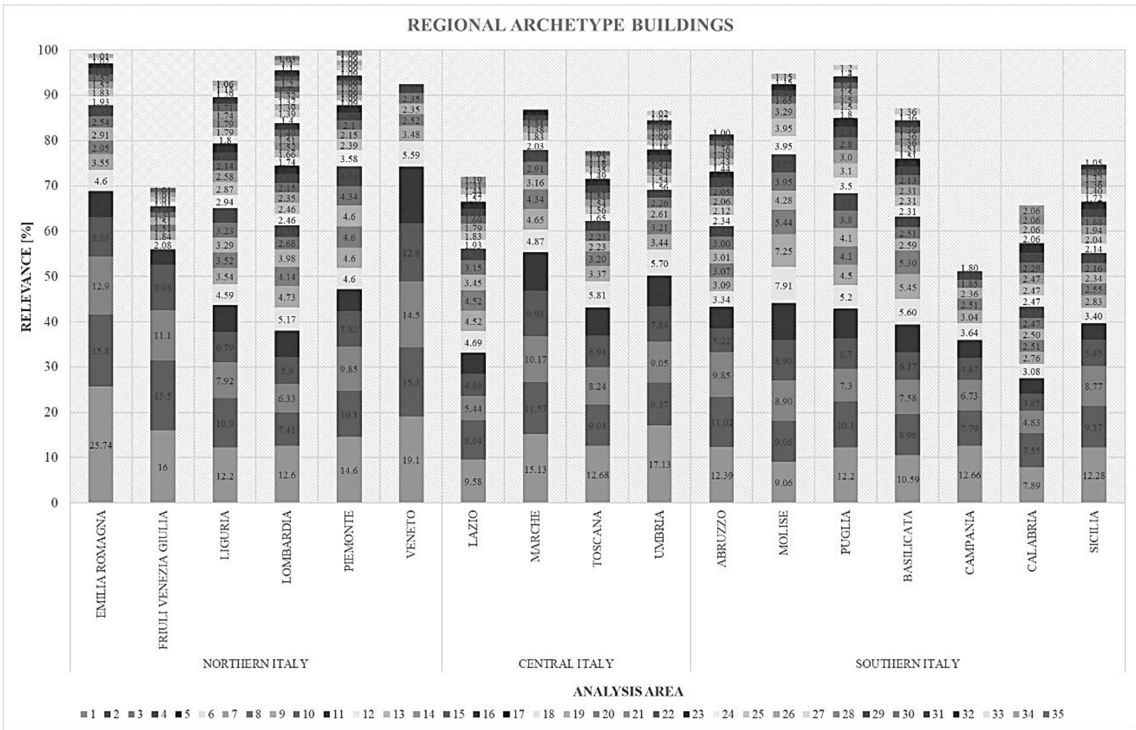

Figure 3. Representativeness of the building typologies identified by dividing the national territory into regions

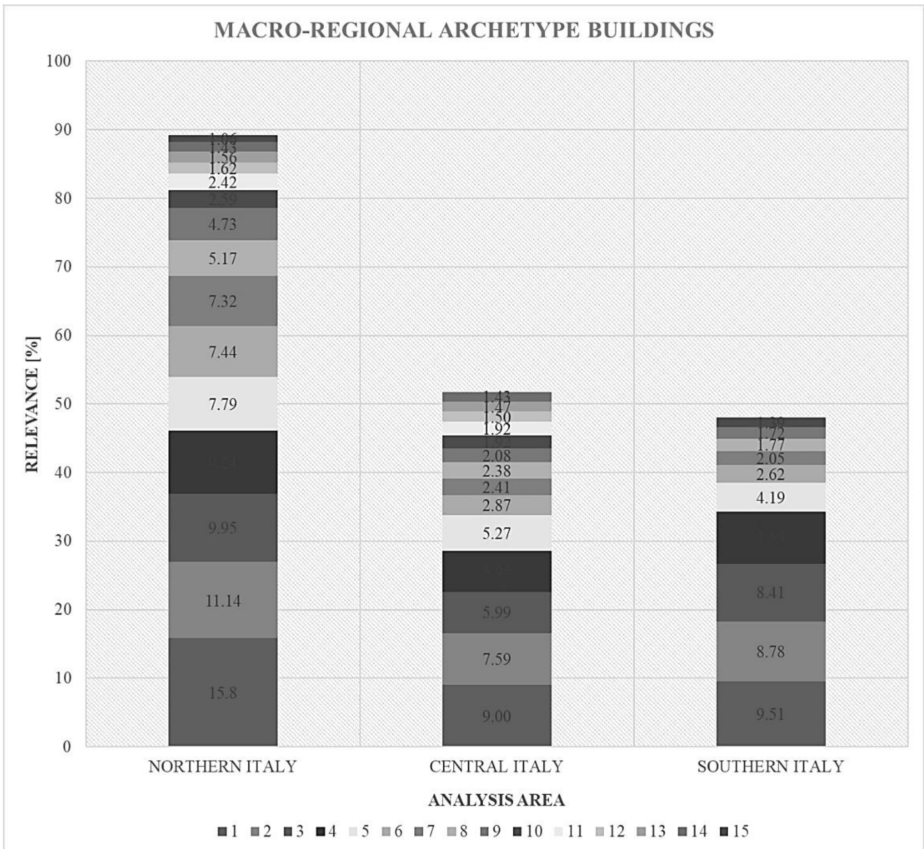

Figure 4. Representativeness of the building typologies identified by dividing the national territory into macro-areas

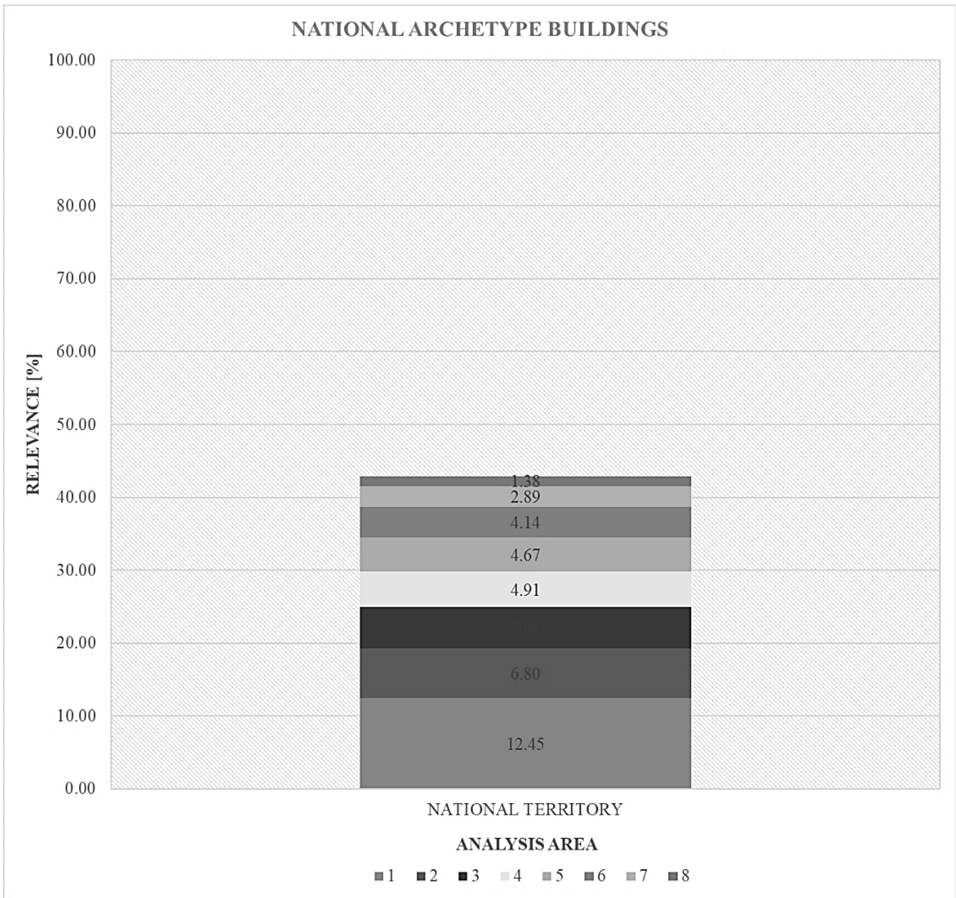

Figure 5. Representativeness of the building typologies identified for the entire national territory

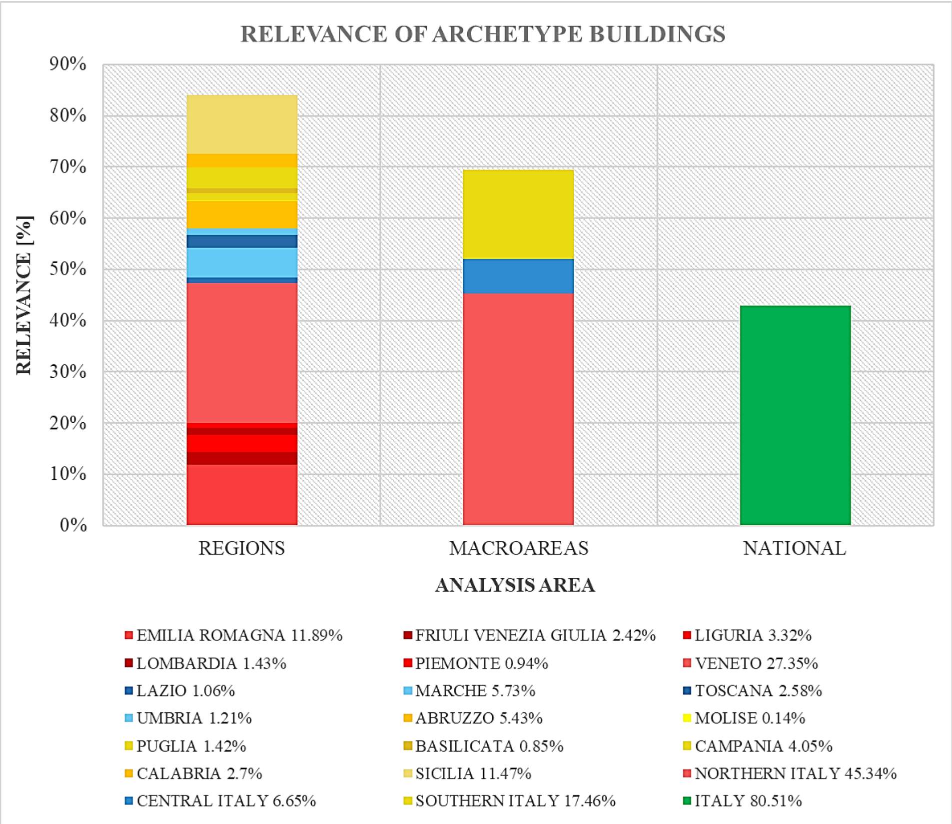

Figure 6. Comparison of building typology coverage of the national territory of the analyses at three different scales: regional, macro-areas, national

Although the representativeness of the typologies identified in the analysis on the national territory is considerably lower (43% of the buildings surveyed), the data regarding the distribution of typological and structural characteristics is perfectly consistent with the data added from the analyses at reduced scales. It can therefore be stated that, with the application of this method, reliable and accurately representative data is obtained even at the maximum scale of analysis on the national territory, considering that more detailed and less representative data emerge only by adding the data from analyses carried out at reduced scales, capable of taking into account the peculiar features of a smaller territory.

4.2 Comparison Across Scales

The comparison of typological parameters at different scales highlights the trade-off between detail and generalization:

- Northern Italy: Parameters such as masonry type and the presence of tie rods show consistent distributions across regional and macro-regional analyses. For instance, brick masonry is prevalent in both cases, representing 67% at the regional scale and 69% at the macro-regional scale. Less frequent typologies, such as squared stone masonry (1.7%), are only captured at the regional level (Figure 7).
- Central Italy: The results mirror those of the North, with coherence in typological distributions between regional and macro-regional scales. Minor differences, such as irregular masonry with courses (3.8%) or squared stone masonry (3.9%), are observed (Figure 8).
- Southern Italy: While typological distributions remain consistent, there are greater differences in frequency percentages compared to the North and Centre, reflecting more diverse data. Despite this, the results validate the methodology's ability to accurately capture representative characteristics (Figure 9).

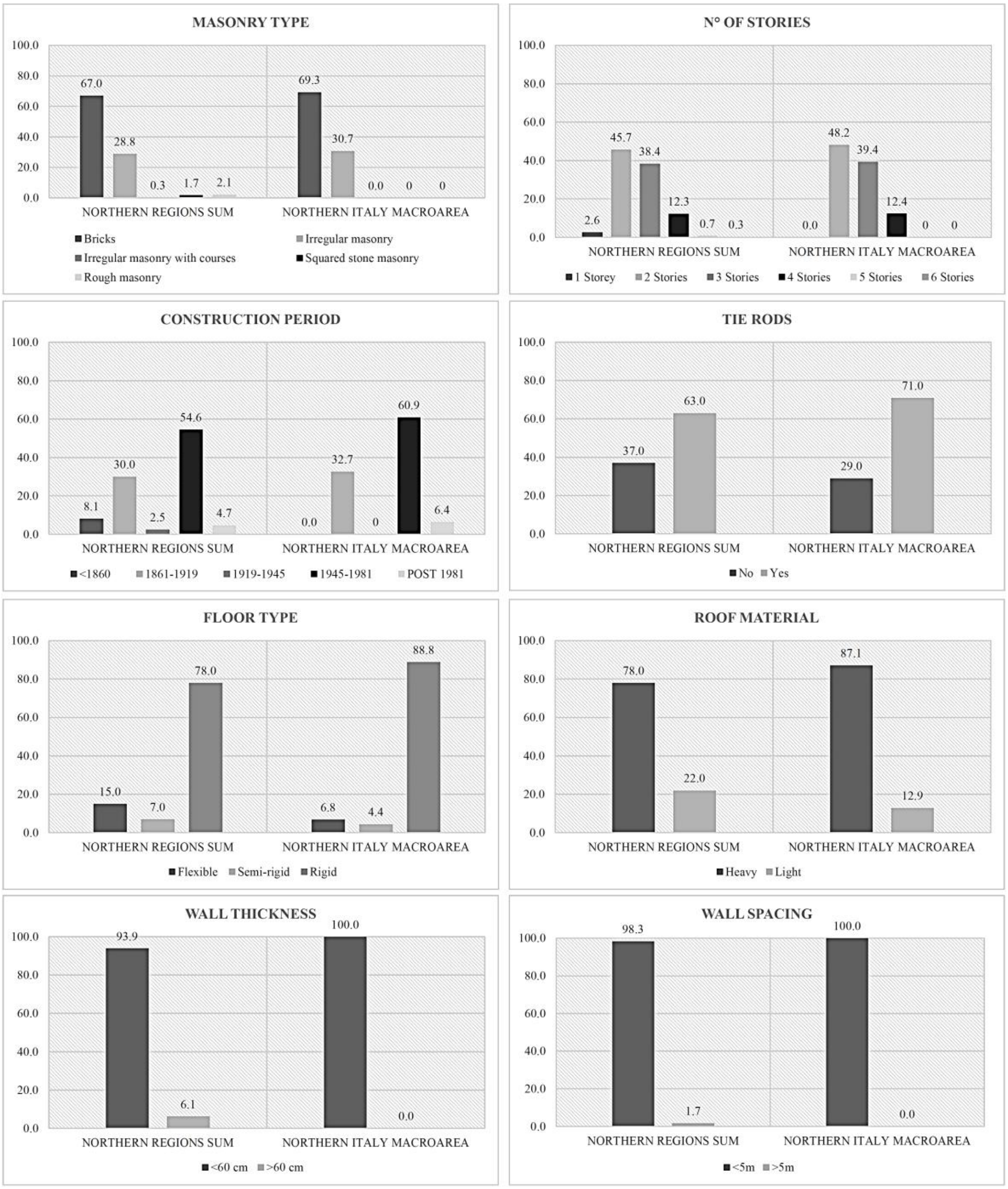

Figure 7. Percentage distributions of the eight parameters and comparison between the regions analyzed in Northern Italy and the Northen macro-area.

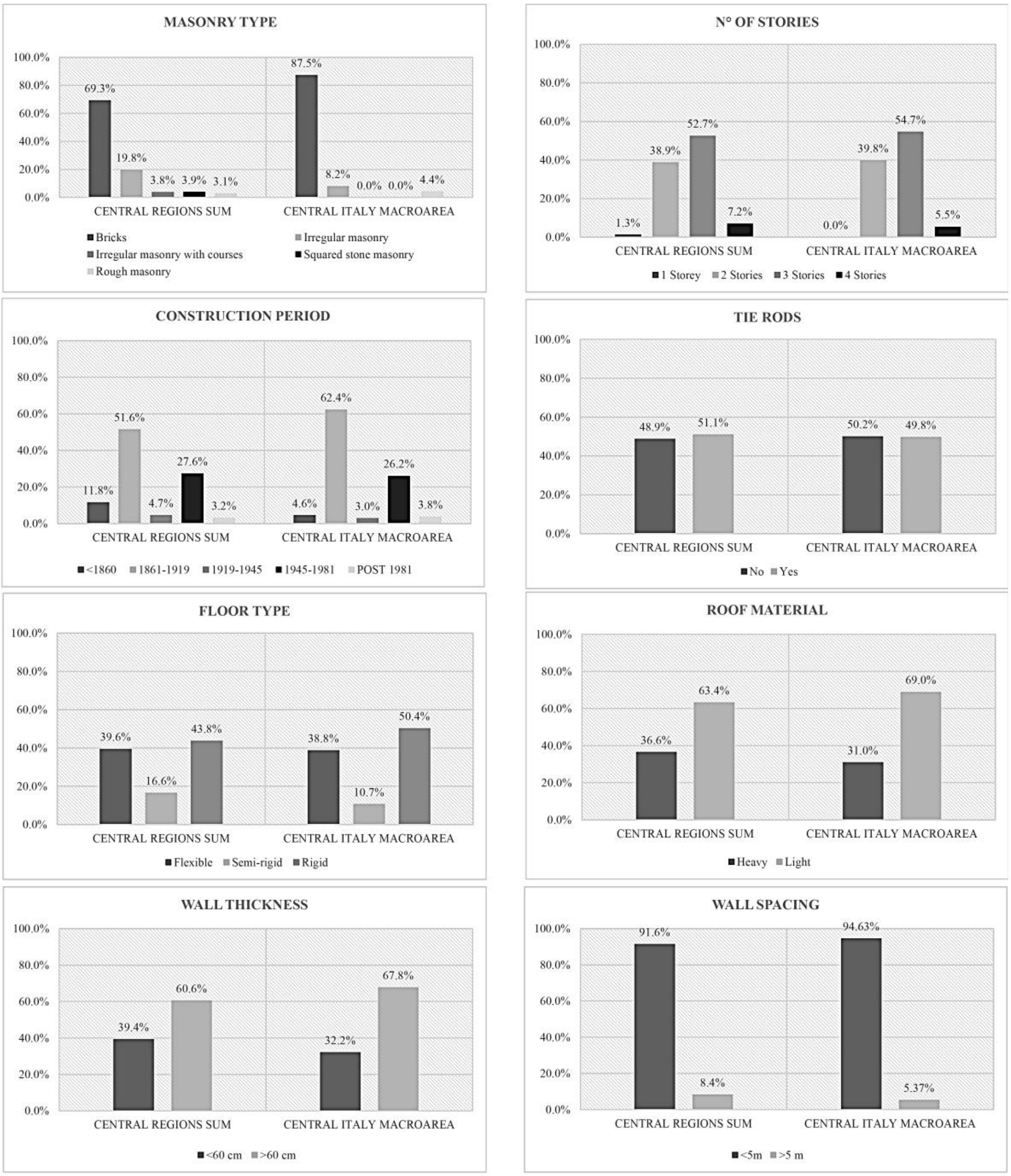

Figure 8. Percentage distributions of the eight parameters and comparison between the regions analysed in Central Italy and the Central macro-area.

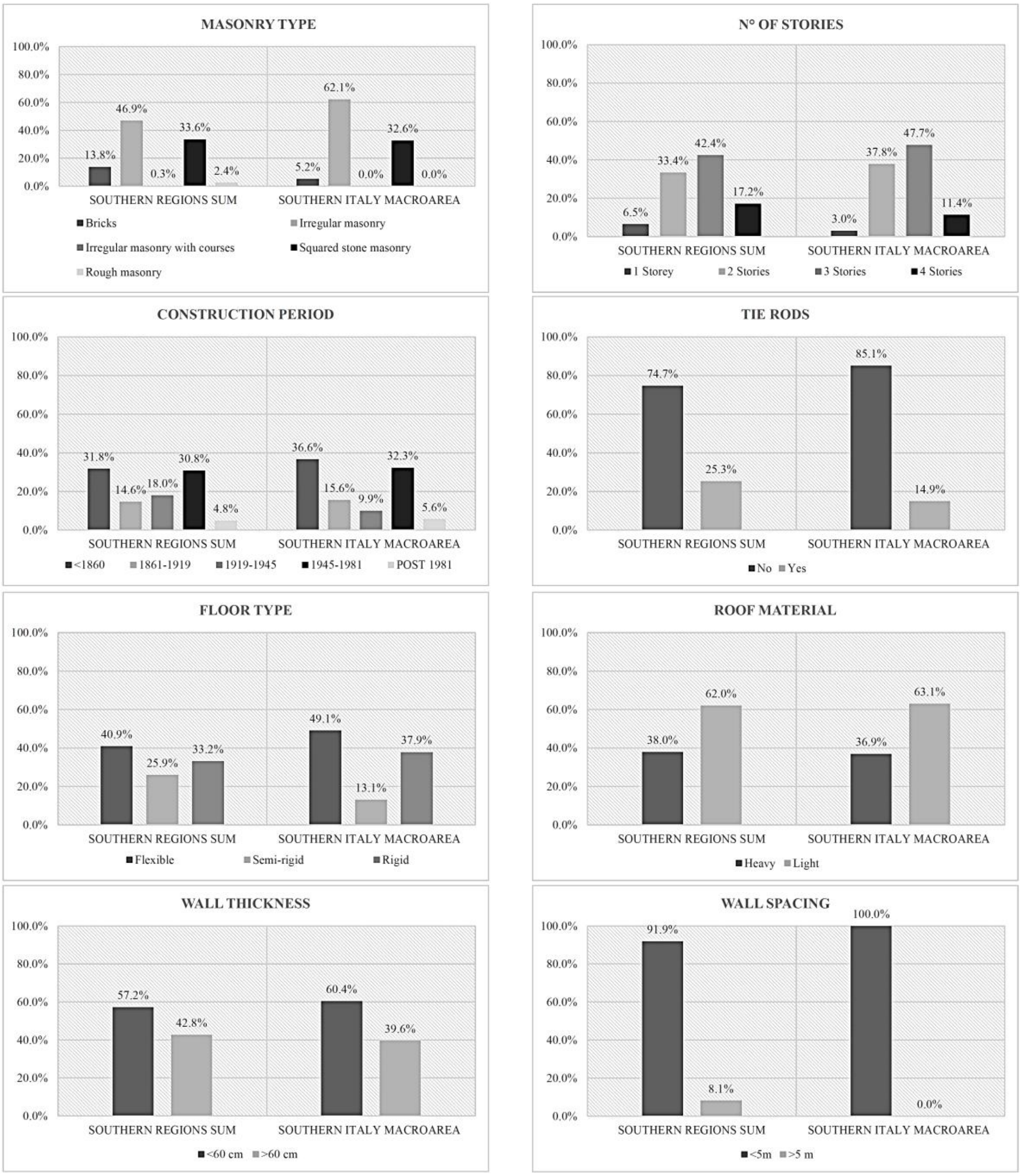

Figure 9. Percentage distributions of the eight parameters and comparison between the regions analysed in Southern Italy and the Southern macro-are.

At the national scale, the aggregation of data from all regions reveals a reliable overlap in typological distributions compared to lower scales, except for infrequent parameters such as one-story buildings (0.6%) or rough stone masonry (0.5%). These rare typologies are less significant at broader scales, ensuring the national-level analysis remains robust (Figure 10).

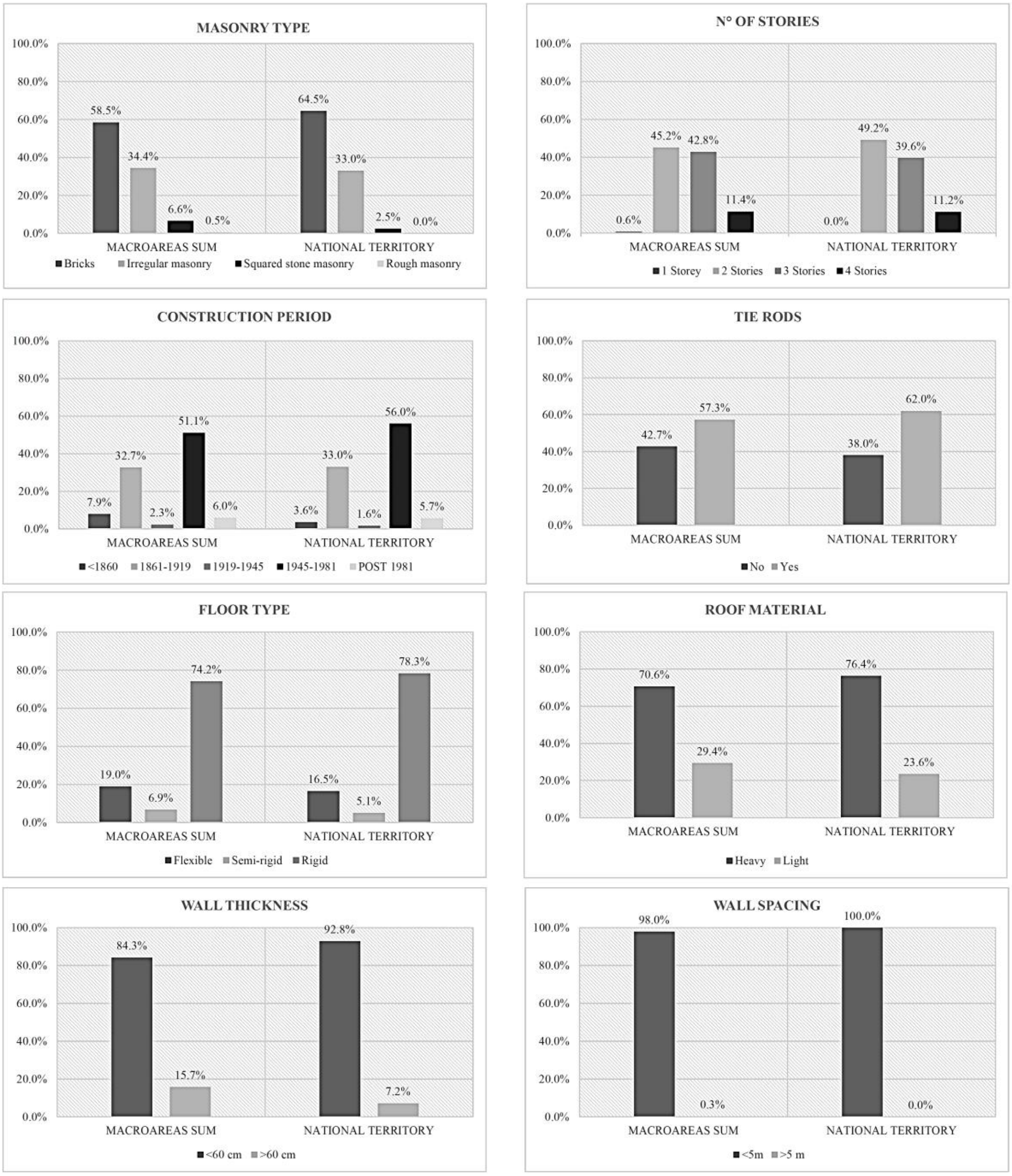

Figure 10. Percentage distributions of the eight parameters and comparison between the three macro-areas North, Centre and South and the national territory

4.3 Implications of Scale Variations

The analysis reveals that as the scale increases, the number of typologies decreases, reducing computational effort while maintaining reliable representativeness:

- Regional analyses provide detailed insights and capture localized variations but require processing a larger volume of data.
- Macro-regional analyses strike a balance between detail and efficiency, suitable for broader policymaking.

- National analyses offer a streamlined perspective, ideal for strategic decision-making but less sensitive to local nuances.

This scaling flexibility demonstrates the adaptability of the methodology, which can be tailored to different decision-making needs, from regional interventions to national-level policy planning.

5. CONCLUSIONS

The evaluation of seismic exposure across the three scales of analysis (regional, macro-regional, and national) demonstrates the robustness and adaptability of the methodology employed. The study highlights the following key conclusions:

- Granularity and Representativeness: At the regional level, the detailed categorization of 369 archetypes provides high granularity, accurately reflecting local construction practices and architectural diversity. This level of detail is crucial for precise assessments and the identification of localized vulnerabilities. As the scale broadens to macro-regional and national levels, the methodology effectively consolidates the data into representative archetypes, balancing simplicity and detail. The macro-regional analysis with 39 archetypes retains sufficient typological diversity while offering computational efficiency, whereas the national analysis synthesizes data into 8 archetypes for strategic and large-scale planning.
- Scale-Dependent Insights: The comparative analysis across scales underscores the trade-offs between granularity and computational efficiency. While regional analyses capture detailed nuances, the broader scales enable easier data management and interpretation, which are essential for policymaking and resource allocation. The methodological framework ensures that the reduction in typological diversity at higher scales does not compromise the reliability of the results.
- Validation of Methodology**:** The consistent overlap in typological distributions across the three scales validates the reliability of the CARTIS-based approach. This demonstrates the capacity of the methodology to adapt to varying scales without significant loss of critical information, ensuring robust exposure assessments that cater to diverse geographic and administrative needs.

- Implications for Risk Mitigation: The findings reinforce the importance of scalable methodologies for seismic risk assessments. The multi-scale approach enables targeted interventions at regional levels and strategic planning at national levels, addressing the unique challenges posed by Italy's complex seismic landscape.

These conclusions affirm the study's contribution to seismic exposure modelling and its relevance for disaster risk management in Italy. The insights gained can inform the development of policies and strategies to enhance the resilience of the built environment across diverse geographic contexts.

Future efforts should focus on enhancing the integration of additional datasets to refine typological classifications further and improve representativeness at broader scales. Additionally, incorporating advanced computational techniques, such as machine learning, could optimize data aggregation processes and support real-time risk assessments.

REFERENCES

[1] A. Masi, S. Lagomarsino, M. Dolce, V. Manfredi, and D. Ottonelli, “Towards the updated Italian seismic risk assessment: exposure and vulnerability modelling,” Bulletin of Earthquake Engineering, vol. 19, no. 8, pp. 3253–3286, Jun. 2021, doi: 10.1007/s10518-021-01065-5.

[2] “Presidency of the Council of Ministers Italian Civil Protection Department National risk assessment Overview of the potential major disasters in Italy: seismic, volcanic, tsunami, hydro-geological/hydraulic and extreme weather, droughts and forest fire risks.”

[3] M. Donà, P. Carpanese, V. Follador, L. Sbrogiò, and F. da Porto, “Mechanics-based fragility curves for Italian residential URM buildings,” Bulletin of Earthquake Engineering, vol. 19, no. 8, pp. 3099–3127, Jun. 2021, doi: 10.1007/s10518-020-00928-7.

[4] M. Dolce et al., “Seismic risk assessment of residential buildings in Italy,” Bulletin of Earthquake Engineering, vol. 19, no. 8, pp. 2999–3032, Jun. 2021, doi: 10.1007/s10518-020-01009-5.

[5] F. da Porto et al., “Comparative analysis of the fragility curves for Italian residential masonry and RC buildings,” Bulletin of Earthquake Engineering, vol. 19, no. 8, pp. 3209–3252, Jun. 2021, doi: 10.1007/s10518-021-01120-1.

[6] M. A. Zanini, L. Hofer, and C. Pellegrino, “A framework for assessing the seismic risk map of Italy and developing a sustainable risk reduction program,” International

Journal of Disaster Risk Reduction, vol. 33, pp. 74–93, Feb. 2019, doi: 10.1016/j.ijdrr.2018.09.012.

[7] S. Lagomarsino, S. Cattari, M. Angiolilli, S. Bracchi, M. Rota, and A. Penna, "Modelling and Seismic Response Analysis of Existing URM Structures. Part 2: Archetypes of Italian Historical Buildings," Journal of Earthquake Engineering, vol. 27, no. 7, pp. 1849–1874, 2023, doi: 10.1080/13632469.2022.2087800.

[8] A. Penna, M. Rota, S. Bracchi, M. Angiolilli, S. Cattari, and S. Lagomarsino, "Modelling and Seismic Response Analysis of Existing URM Structures. Part: Archetypes of Italian Modern Buildings," Journal of Earthquake Engineering, vol. 28, no. 4, pp. 1130–1156, 2024, doi: 10.1080/13632469.2022.2095060.

[9] A. Brunelli, F. de Silva, and S. Cattari, "Observed and simulated urban-scale seismic damage of masonry buildings in aggregate on soft soil: The case of Visso hit by the 2016/2017 Central Italy earthquake," International Journal of Disaster Risk Reduction, vol. 83, Dec. 2022, doi: 10.1016/j.ijdrr.2022.103391.

[10] G. Tocchi, M. Polese, M. Di Ludovico, and A. Prota, "Regional based exposure models to account for local building typologies," Bulletin of Earthquake Engineering, vol. 20, no. 1, pp. 193–228, Jan. 2022, doi: 10.1007/s10518-021-01242-6.

[11] F. S. Liguori, S. Fiore, F. L. Perelli, D. De Gregorio, G. Zuccaro, and A. Madeo, "A mechanical-based seismic vulnerability assessment method with an application to masonry structures in Cosenza (Italy)," Bulletin of Earthquake Engineering, vol. 21, no. 12, pp. 5655–5681, Sep. 2023, doi: 10.1007/s10518-023-01752-5.

[12] V. Buonocunto, E. Acconcia, and F. Parisi, "Seismic fragility modelling of unreinforced masonry buildings in Campania region," in Procedia Structural Integrity, Elsevier B.V., 2022, pp. 67–74. doi: 10.1016/j.prostr.2023.01.010.

[13] M. Vettore, M. Donà, P. Carpanese, V. Follador, F. da Porto, and M. R. Valluzzi, "A multilevel procedure at urban scale to assess the vulnerability and the exposure of residential masonry buildings: The case study of pordenone, northeast italy," Heritage, vol. 3, no. 4, pp. 1433–1468, Dec. 2020, doi: 10.3390/heritage3040080.

[14] P. Colajanni, C. Cucchiara, J. D'Anna, S. Pennisi, and S. Pagnotta, "Vulnerability and Seismic Exposure of Residential Building Stock in the Historic Center of Alcamo," Applied Sciences (Switzerland), vol. 13, no. 12, Jun. 2023, doi: 10.3390/app13127092.

[15] G. Tocchi, D. Ottonelli, N. Rebora, and M. Polese, "Multi-Risk Assessment in the Veneto Region: An Approach to Rank Seismic and Flood Risk," Sustainability (Switzerland), vol. 15, no. 16, Aug. 2023, doi: 10.3390/su151612458.

[16] G. P. Campostrini, S. Taffarel, G. Bettiol, M. R. Valluzzi, F. Da Porto, and C. Modena, "A Bayesian approach to rapid seismic vulnerability assessment at urban scale," International Journal of Architectural Heritage, vol. 12, no. 1, pp. 36–46, Jan. 2018, doi: 10.1080/15583058.2017.1370506.

[17] M. Vettore, M. Donà, P. Carpanese, V. Follador, F. da Porto, and M. R. Valluzzi, "A multilevel procedure at urban scale to assess the vulnerability and the exposure of residential masonry buildings: The case study of pordenone, northeast italy," Heritage, vol. 3, no. 4, pp. 1433–1468, Dec. 2020, doi: 10.3390/heritage3040080.

[18] G. Zuccaro, M. Dolce, F. L. Perelli, D. De Gregorio, and E. Speranza, "CARTIS: a method for the typological-structural characterization of Italian ordinary buildings in urban areas," Front Built Environ, vol. 9, 2023, doi: 10.3389/fbuil.2023.1129176.

[19] H. Crowley et al., "Exposure model for European seismic risk assessment," Earthquake Spectra, vol. 36, no. 1_suppl, pp. 252–273, Oct. 2020, doi: 10.1177/8755293020919429.

[20] L. D. Dávila, J. M. Cabrero, and O. Flores, "New seismic exposure modeling approach for Guatemala City," Jan. 01, 2023, Springer Science and Business Media B.V. doi: 10.1007/s10518-022-01570-1.

[21] C. Del Gaudio et al., "Empirical fragility curves for masonry buildings after the 2009 L'Aquila, Italy, earthquake," Bulletin of Earthquake Engineering, vol. 17, no. 11, pp. 6301–6330, Nov. 2019, doi: 10.1007/s10518-019-00683-4.

[22] M. Dolce et al., "Observed damage database of past italian earthquakes: The da.D.O. WebGIS," Bollettino di Geofisica Teorica ed Applicata, vol. 60, no. 2, pp. 141–164, 2019, doi: 10.4430/bgta0254.

[23] C. Del Gaudio et al., "Seismic fragility for Italian RC buildings based on damage data of the last 50 years," Bulletin of Earthquake Engineering, vol. 18, no. 5, pp. 2023–2059, Mar. 2020, doi: 10.1007/s10518-019-00762-6.

[24] G. Tondo, D. Perrone, R. Monteiro, and M. A. Aiello, "Development and rapid visual screening analysis of an Italian masonry building portfolio using post-earthquake damage observations," in Procedia Structural Integrity, Elsevier B.V., 2022, pp. 243–250. doi: 10.1016/j.prostr.2023.01.032.

[25] G. Zuccaro, M. Dolce, D. De Gregorio, E. Speranza, and C. Moroni, "La scheda CARTIS per la caratterizzazione tipologico-strutturale dei comparti urbani costituiti da edifici ordinari. Valutazione dell'esposizione in analisi di rischio sismico," 2015.

[26] G. Brando, G. Cianchino, D. Rapone, E. Spacone, and S. Biondi, "A CARTIS-based method for the rapid seismic vulnerability assessment of minor Italian historical centres," International Journal of Disaster Risk Reduction, vol. 63, Sep. 2021, doi: 10.1016/j.ijdrr.2021.102478.

[27] A. Sandoli, G. Pacella, B. Calderoni, G. Brandonisio, G. P. Lignola, and A. Prota, "Predictive hybrid fragility models for urban scale seismic assessment: a case study in Basilicata Region (Italy)," Bulletin of Earthquake Engineering, vol. 21, no. 2, pp. 1047–1077, Jan. 2023, doi: 10.1007/s10518-022-01569-8.

[28] G. Cianchino, G. Cocco, D. Rapone, Y. Di Lallo, M. G. Masciotta, and G. Brando, "Vulnerability analytical models at the regional scale through archetype buildings:

an application to the Abruzzi region," in Procedia Structural Integrity, Elsevier B.V., 2022, pp. 219–226. doi: 10.1016/j.prostr.2023.01.029.

[29] S. Ruggieri et al., "An archetype-based automated procedure to derive global-local seismic fragility of masonry building aggregates: META-FORMA-XL," International Journal of Disaster Risk Reduction, vol. 95, Sep. 2023, doi: 10.1016/j.ijdrr.2023.103903.

[30] A. Basaglia et al., "An automatic procedure for deriving building portfolios using the Italian 'CARTIS' online database," Structures, vol. 34, pp. 2974–2986, Dec. 2021, doi: 10.1016/j.istruc.2021.09.054.

[31] N. Chieffo, A. Formisano, R. Landolfo, and G. Milani, "A vulnerability index based-approach for the historical centre of the city of Latronico (Potenza, Southern Italy)," Eng Fail Anal, vol. 136, Jun. 2022, doi: 10.1016/j.engfailanal.2022.106207.

[32] C. Tosto, V. Leggieri, S. Ruggieri, and G. Uva, "Investigation of architectural typological parameters influencing seismic vulnerability of masonry buildings in historical centres: the case of Puglia," in Procedia Structural Integrity, Elsevier B.V., 2022, pp. 2036–2043. doi: 10.1016/j.prostr.2023.01.260.

[33] M. Riedel, C. Dutsch, C. Alexandrakis, I. Dini, S. Ciuffi, and S. Buske, "Seismic depth imaging of a geothermal system in Southern Tuscany," Geophys Prospect, vol. 63, no. 4, pp. 957–974, Jul. 2015, doi: 10.1111/1365-2478.12254.

[34] M. Polese, M. Di Ludovico, A. Prota, G. Tocchi, and M. Gaetani D'aragona, "XVIII CONVEGNO ANIDIS Utilizzo della scheda Cartis per aggiornamento dell'inventario ed effetto sulle stime di vulnerabilità a scala territoriale."

[35] R. Catulo, A. P. Falcão, R. Bento, and S. Ildefonso, "Simplified evaluation of seismic vulnerability of Lisbon Heritage City Centre based on a 3DGIS-based methodology," J Cult Herit, vol. 32, pp. 108–116, Jul. 2018, doi: 10.1016/j.culher.2017.11.014.

[36] W. Qi, G. Su, L. Sun, F. Yang, and Y. Wu, "'Internet+' approach to mapping exposure and seismic vulnerability of buildings in a context of rapid socioeconomic growth: a case study in Tangshan, China," Natural Hazards, vol. 86, pp. 107–139, Mar. 2017, doi: 10.1007/s11069-016-2581-9.

[37] P. Carpanese, M. Donà, and F. da Porto, "AUTOMATIC IDENTIFICATION OF BUILDING FEATURES FOR SEISMIC DAMAGE ASSESSMENT ON A LARGE SCALE," in COMPDYN Proceedings, National Technical University of Athens, 2023. doi: 10.7712/120123.10465.20406.

[38] J. Kang, M. Körner, Y. Wang, H. Taubenböck, and X. X. Zhu, "Building instance classification using street view images," ISPRS Journal of Photogrammetry and Remote Sensing, vol. 145, pp. 44–59, Nov. 2018, doi: 10.1016/j.isprsjprs.2018.02.006.

[39] R. Vicente, T. M. Ferreira, and J. A. R. Mendes da Silva, “Supporting urban regeneration and building refurbishment. Strategies for building appraisal and inspection of old building stock in city centres,” J Cult Herit, vol. 16, no. 1, pp. 1–14, Jan. 2015, doi: 10.1016/j.culher.2014.03.004.

[40] F. Cacace, G. Zuccaro, D. De Gregorio, and F. L. Perelli, “Building Inventory at National scale by evaluation of seismic vulnerability classes distribution based on Census data analysis: BINC procedure,” International Journal of Disaster Risk Reduction, vol. 28, pp. 384–393, Jun. 2018, doi: 10.1016/j.ijdrr.2018.03.016.

[41] R. Landolfo, A. Formisano, G. Di Lorenzo, and A. Di Filippo, “Classification of european building stock in technological and typological classes,” Journal of Building Engineering, vol. 45, Jan. 2022, doi: 10.1016/j.jobe.2021.103482.

[42] K. Pitilakis, P. Franchin, B. Khazai, and H. Wenzel, SYNER-G: Systemic Seismic Vulnerability and Risk Assessment of Complex Urban, Utility, Lifeline Systems and Critical Facilities, vol. 31. Dordrecht: Springer Netherlands, 2014. doi: 10.1007/978-94-017-8835-9.

[43] Gottfried. Grünthal, European macroseismic scale 1998 : EMS-98. European Seismological Commission, Subcommission on Engineering Seismology, Working Group Macroseismic scales, 1998.

[44] M. Pagani et al., “OpenQuake Engine: An Open Hazard (and Risk) Software for the Global Earthquake Model,” Seismological Research Letters, vol. 85, no. 3, pp. 692–702, May 2014, doi: 10.1785/0220130087.

[45] M. Pittore and M. Wieland, “Toward a rapid probabilistic seismic vulnerability assessment using satellite and ground-based remote sensing,” Natural Hazards, vol. 68, no. 1, pp. 115–145, Aug. 2013, doi: 10.1007/s11069-012-0475-z.

[46] C. Pietro, D. Marco, and F. da Porto, “Automatic identification of residential building features using machine learning techniques,” in Procedia Structural Integrity, Elsevier B.V., 2022, pp. 1980–1987. doi: 10.1016/j.prostr.2023.01.253.

[47] G. Tocchi, M. Polese, and A. Prota, “Improving building inventory with a machine learning approach: application in southern Italy,” in Procedia Structural Integrity, Elsevier B.V., 2022, pp. 1972–1979. doi: 10.1016/j.prostr.2023.01.252.

[48] C. Geiß and H. Taubenböck, “One step back for a leap forward: toward operational measurements of elements at risk,” Mar. 01, 2017, Springer Netherlands. doi: 10.1007/s11069-017-2742-5.

[49] H. Crowley et al., “Exposure model for European seismic risk assessment,” Earthquake Spectra, vol. 36, no. 1_suppl, pp. 252–273, Oct. 2020, doi: 10.1177/8755293020919429.

[50] European Commission, “https://ec.europa.eu/echo/,” Union Civil Protection Mechanism: Annual Work Programm.

[51] “http://www.sera-eu.org,” The Seismology and Earthquake Engineering Research Infrastructure Alliance for Europe (SERA).

[52] Z. V. Milutinovic and G. S. Trendafiloski, “An advanced approach to earthquake risk scenarios with applications to different European towns, WP4: Vulnerability of current buildings,” 2003.

[53] “https://www.pgadmin.org.”

[54] G. Brando, G. De Matteis, and E. Spacone, “Predictive model for the seismic vulnerability assessment of small historic centres: Application to the inner Abruzzi Region in Italy,” Eng Struct, vol. 153, pp. 81–96, Dec. 2017, doi: 10.1016/j.engstruct.2017.10.013.

[55] E. Criber, G. Brando, and G. De Matteis, “The effects of L’Aquila earthquake on the St. Gemma church in Goriano Sicoli: part I—damage survey and kinematic analysis,” Bulletin of Earthquake Engineering, vol. 13, no. 12, pp. 3713–3732, Dec. 2015, doi: 10.1007/s10518-015-9792-4.

[56] A. Rosti, M. Rota, and A. Penna, “Empirical fragility curves for Italian URM buildings,” Bulletin of Earthquake Engineering, vol. 19, no. 8, pp. 3057–3076, Jun. 2021, doi: 10.1007/s10518-020-00845-9.

[57] D. Benedetti, G. Benzoni, and M. A. Parisi, “Seismic vulnerability and risk evaluation for old urban nuclei,” Earthq Eng Struct Dyn, vol. 16, no. 2, pp. 183–201, Feb. 1988, doi: 10.1002/eqe.4290160203.

[58] A. H. Barbat, S. Lagomarsino, and L. G. Pujades, “Vulnerability Assessment of Dwelling Buildings,” in Assessing and Managing Earthquake Risk, Berlin/Heidelberg: Springer-Verlag, 2010, pp. 115–134. doi: 10.1007/1-4020-3608-6_6.

[59] S. Lagomarsino and S. Giovinazzi, “Macroseismic and mechanical models for the vulnerability and damage assessment of current buildings,” Bulletin of Earthquake Engineering, vol. 4, no. 4, pp. 415–443, Nov. 2006, doi: 10.1007/s10518-006-9024-z.

[60] T. M. Ferreira, R. Maio, A. A. Costa, and R. Vicente, “Seismic vulnerability assessment of stone masonry façade walls: Calibration using fragility-based results and observed damage,” Soil Dynamics and Earthquake Engineering, vol. 103, pp. 21–37, Dec. 2017, doi: 10.1016/j.soildyn.2017.09.006.

[61] S. Lagomarsino, S. Cattari, M. Angiolilli, S. Bracchi, M. Rota, and A. Penna, “Modelling and Seismic Response Analysis of Existing URM Structures. Part 2: Archetypes of Italian Historical Buildings,” Journal of Earthquake Engineering, vol. 27, no. 7, pp. 1849–1874, May 2023, doi: 10.1080/13632469.2022.2087800.

[62] G. Cianchino, “A large-scale integrated approach to assess the seismic vulnerability of masonry built Cultural Heritage in central Italy,” University “Gabriele d’Annunzio” of Chieti - Pescara, 2023.

[63] M. Dolce, “Schematizzazione e modellazione degli edifici in muratura soggetti ad azioni sismiche,” L’Industria delle costruzioni, vol. 25, no. 242, pp. 44–57, 1991.

[64] MIDAS Information Technology Co., “MIDAS Gen,” 2020.

[65] ReLUIS and Italian National Department of Civil Protection, “WP4 MARS Project – Seismic Risk Maps and Damage Scenarios. 2019-2021 ReLUIS Projec,” https://www.reluis.it/progetto-dpc-reluis-2019-2021/, vol. 2019–2021.

[66] K. A. Porter, “An Overview of PEER’s Performance-Based Earthquake Engineering Methodology,” 2003.

[67] R. Paolucci, C. Smerzini, and M. Vanini, “Bb-speedset: A validated dataset of broadband near-source earthquake ground motions from 3d physics-based numerical simulations,” Bulletin of the Seismological Society of America, vol. 111, no. 5, pp. 2527–2545, 2021, doi: 10.1785/0120210089.

[68] Ministero delle Infrastrutture e dei Trasporti, “CIRCOLARE 21 gennaio 2019 n.7_Istruzioni per l’applicazione dell’«Aggiornamento delle ‘Norme tecniche per le costruzioni’» di cui al decreto ministeriale 17 gennaio 2018. (Italian Guideline),” 2019.

[69] K. Doherty, M. C. Griffith, N. Lam, and J. Wilson, “Displacement-based seismic analysis for out-of-plane bending of unreinforced masonry walls,” Earthq Eng Struct Dyn, vol. 31, no. 4, p. 833, Apr. 2002, doi: 10.1002/eqe.126.abs.

[70] S. Lagomarsino, A. Penna, A. Galasco, and S. Cattari, “TREMURI program: An equivalent frame model for the nonlinear seismic analysis of masonry buildings,” Eng Struct, vol. 56, pp. 1787–1799, Nov. 2013, doi: 10.1016/j.engstruct.2013.08.002.

[71] S. Cattari, D. Camilletti, A. M. D’Altri, and S. Lagomarsino, “On the use of continuum Finite Element and Equivalent Frame models for the seismic assessment of masonry walls,” Journal of Building Engineering, vol. 43, p. 102519, Nov. 2021, doi: 10.1016/j.jobe.2021.102519.

[72] D. Shapiro, C. Rojahn, L. D. Reaveley, J. R. Smith, and U. Morelli, “NEHRP Guidelines and Commentary for the Seismic Rehabilitation of Buildings,” Earthquake Spectra, vol. 16, no. 1, pp. 227–239, Feb. 2000, doi: 10.1193/1.1586092.

[73] S. Lagomarsino and S. Cattari, “PERPETUATE guidelines for seismic performance-based assessment of cultural heritage masonry structures,” Bulletin of Earthquake Engineering, vol. 13, no. 1, pp. 13–47, Jan. 2015, doi: 10.1007/s10518-014-9674-1.

CHAPTER III

SEISMIC VULNERABILITY ANALYSIS OF MASONRY RESIDENTIAL BUILDINGS ON ITALIAN NATIONAL SCALE: AN INTEGRATED APPROACH WITH THE CARTIS DATABASE

ABSTRACT

This study This study presents an integrated methodology for assessing the seismic vulnerability of masonry residential buildings in Italy, leveraging the CARTIS database—a comprehensive repository of typological and structural data on the national building stock. The methodology integrates kinematic analyses for local collapse mechanisms with numerical simulations to evaluate global structural behaviour, enabling the derivation of fragility curves applicable on a national scale. Two analytical frameworks are presented: a macro-regional approach, dividing the Italian territory into Northern, Central, and Southern regions, and a national-scale model. The macro-regional approach employs 39 archetypes to capture regional variations in construction techniques, materials, and vulnerabilities, providing insights into localized seismic risks. Conversely, the national-scale model consolidates data into 8 archetypes, offering a streamlined and computationally efficient representation of the Italian building stock, ideal for large-scale seismic risk assessments. The proposed methodology emphasizes the integration of large-scale data with advanced analytical techniques, balancing precision and operational simplicity. It highlights the importance of combining local and global failure mechanism analyses to better represent the seismic performance of masonry structures. Additionally, the paper discusses the trade-offs between detail and efficiency in seismic risk evaluation and underscores the need for scalable frameworks that can adapt to varying levels of data availability and computational resources. This study aims to provide a robust framework for prioritizing seismic mitigation interventions, guiding policymakers and practitioners in developing effective strategies for risk reduction. The methodology is designed to be adaptable to different contexts, making it a valuable tool for addressing seismic risk also in other regions with similar building typologies and vulnerabilities.

1. INTRODUCTION

The assessment of seismic vulnerability of buildings is a crucial element in developing effective strategies for seismic risk mitigation, particularly in a context like Italy, characterized by significant seismic exposure [1]. Italy, with its diverse and often outdated building stock, is one of the most vulnerable countries in Europe to seismic events, as evidenced by earthquakes in recent decades [2]. In this context, masonry residential buildings, which constitute a huge portion of the built environment, are among the most at-risk categories due to their inherent structural fragility and the lack of adequate seismic reinforcement systems [3], [4].

In recent years, various approaches have been proposed for assessing the seismic vulnerability of buildings, which can be categorized into three main types: empirical, analytical, and numerical. Empirical methods, based on observations of damage from past seismic events, have been widely used for their simplicity and ability to provide rapid insights on a large scale [5], [6]. However, these approaches tend to be less accurate at the single-building level, as they do not consider the specific characteristics of individual structures.

In contrast, analytical and numerical methods, including kinematic, nonlinear static, and dynamic analyses, offer greater accuracy by providing detailed modelling of both local and global collapse mechanisms. For instance, [7] proposed a mechanical model for estimating the seismic vulnerability of masonry buildings, considering both out-of-plane and in-plane behaviour and integrating the results into fragility curves useful for probabilistic analyses. These approaches have been further enhanced by advanced computational tools and the increasing availability of detailed structural data.

Another significant development is the use of archetype building models, which reduce the number of structures analysed by representing the entire building stock with a limited set of "typical" buildings. These models enable the application of mechanical and numerical methods at regional or national levels while maintaining a balance between precision and computational effort [8]. For example, the study [9] demonstrated the effectiveness of archetypes in representing various Italian building typologies, integrating data from censuses and structural surveys.

In this context, the adoption of national databases such as CARTIS (Typological and Structural Characterization) [10], [11] has facilitated the systematization of geometric and structural data collection for existing buildings, enabling the development of representative models on a large scale. These data, combined with semi-automated methodologies for identifying archetypes, allow for overcoming the limitations of traditional approaches based on building-by-building surveys, while ensuring sufficient accuracy for large-area analyses [12], [13].

A recent study conducted for the Abruzzo region developed and validated an integrated methodology for assessing the seismic vulnerability of masonry residential buildings [13]. This approach, based on the identification of representative archetypes through a semi-automated procedure and the integration of kinematic and numerical analyses, enabled the derivation of reliable results that can be easily generalized to the entire regional building stock [14], [15]. The findings highlighted the effectiveness of this approach in combining precision and operational simplicity, providing a scalable model for application to larger areas.

The present work extends this methodology to a national scale, applying it to the entire Italian territory. The primary objective is to define representative building archetypes for different Italian regions, accounting for variations in construction typologies, materials, and local seismic vulnerability. By jointly analysing local and global collapse mechanisms, this work proposes integrated fragility curves that are valuable for planning mitigation interventions at the national level.

This analysis represents a significant step forward in the context of large-scale seismic risk management, offering a useful tool not only for prioritizing interventions but also for supporting policy decisions in the field of civil protection. The following sections describe the adopted methodology, the obtained results, and the implications for seismic risk reduction on a national scale.

2. THE SAMPLE

The seismic vulnerability analysis at the national scale was conducted using a representative sample of masonry buildings extracted from the CARTIS database (Typological and Structural Characterization) [11]. This database, developed by the Plinius Research Centre, represents a consolidated source of information on the typological and structural characteristics of the Italian building heritage, providing data such as wall typology, number of floors, construction period, and the presence of reinforcement devices like ring beams or tie rods. However, the complexity and vastness of the dataset required an effective methodology to identify representative archetypes without losing crucial information. To address this challenge, a semi-automated procedure in MATLAB already present in literature [13] was exploited for data processing and synthesis. The procedure allowed overcoming some limitations of the original database, such as the inability to perform complex queries linking multiple parameters. In the original study it was assessed on the Abruzzo region and subsequently used in seismic vulnerability studies [14], [15].

Building archetypes were defined using eight key parameters that influence seismic behaviour, identified through prior studies and validated in the scientific literature [16]. These parameters include masonry type, number of stories, construction period, presence of tie rods or string courses, floor type, roof material, wall thickness, and wall spacing.

The archetype extraction process began with selecting the analysis scale, where data from the pgAdmin database [17] was requested for three macro-regions (Northern, Central, and

Southern Italy) and for the entire national territory without subdivisions. The raw data from the CARTIS database, organized by municipality, underwent a cleaning and disaggregation process. This step removed inconsistencies, duplicates, and incomplete information. Using the MATLAB procedure [13], the data was further processed to systematically combine typological-structural variables, producing unique representations of each building type.

Subsequently, building typologies were aggregated into representative categories through clustering algorithms. These algorithms prioritized configurations that were both typical and recurring, ensuring that each archetype represented more than 1% of the building stock. The process resulted in the identification of thirty-nine archetypes at the macro-regional level, which were then consolidated into eight national archetypes to provide a more synthetic representation.

3. DESCRIPTION OF THE ITALIAN SAMPLE

3.1 THE MACRO-REGIONAL SAMPLE

The macro-regional sample was defined by dividing the Italian territory into three macro-regions: Northern, Central, and Southern Italy. A total of thirty-nine archetypes were identified, distributed as follows (Table 12):

- Northern Italy: fifteen archetypes
- Central Italy: fourteen archetypes
- Southern Italy: ten archetypes

The macro-regional sample captures the different typological and structural characteristics of buildings across Italy's three macro-regions: Northern, Central, and Southern Italy. In the North, the sample is dominated by buildings constructed with regular masonry, such as bricks, reflecting the influence of industrialization and urbanization typical of this region. By contrast, the Central region presents a more varied mix, combining irregular masonry, often found in historic town centres, with regular masonry constructions. In the South, the sample highlights a predominance of irregular masonry, typically associated with older buildings and rural environments. Structurally, the number of stories in the sampled buildings ranges from one to four. Taller buildings are more prevalent in urbanized areas, particularly in the North, while shorter structures are more typical of rural settings, particularly in the South. The periods of construction also vary significantly between the regions, with the South showing a larger proportion of pre-1900 buildings, indicative of its older building stock. The macro-regional sample also reflects adaptations to local construction traditions and geographic conditions. For instance, in the mountainous areas of the North, heavier roof materials are common. Conversely, lighter roof materials are more prevalent in the South. These regional characteristics ensure that the macro-regional archetypes effectively represent the diversity of the Italian building stock.

Table 1. Archetype buildings for the macro-areas of Northern, Central, and Southern Italy

Area	ID	Masonry Type	N° of Stories	Construction Period	Tie Rods	Floor Type	Roof Material	Wall Thickness	Wall Spacing	Relevance
Northern Italy	1 N	Bricks	3	1945-1981	yes	Rigid	Heavy	< 60 cm	< 5 m	15.80%
	2 N	Bricks	2	1945-1981	yes	Rigid	Heavy	< 60 cm	< 5 m	11.14%
	3 N	Bricks	2	1861-1919	no	Flexible	Light	< 60 cm	< 5 m	9.95%
	4 N	Bricks	4	1945-1981	yes	Rigid	Heavy	< 60 cm	< 5 m	9.24%
	5 N	Irregular masonry	3	1861-1919	yes	Rigid	Heavy	< 60 cm	< 5 m	7.79%
	6 N	Irregular masonry	2	1861-1919	yes	Rigid	Heavy	< 60 cm	< 5 m	7.44%
	7 N	Bricks	2	1945-1981	no	Rigid	Heavy	< 60 cm	< 5 m	7.32%
	8 N	Irregular masonry	2	1861-1919	yes	Flexible	Light	< 60 cm	< 5 m	5.17%
	9 N	Bricks	3	1945-1981	no	Rigid	Heavy	< 60 cm	< 5 m	4.73%
	10 N	Irregular masonry	3	1861-1919	yes	Flexible	Light	< 60 cm	< 5 m	2.59%
	11 N	Bricks	2	Post 1981	no	Rigid	Heavy	< 60 cm	< 5 m	2.42%
	12 N	Bricks	3	Post 1981	no	Rigid	Heavy	< 60 cm	< 5 m	1.62%
	13 N	Irregular masonry	3	1861-1919	yes	Semi-rigid	Light	< 60 cm	< 5 m	1.56%
	14 N	Irregular masonry	2	1861-1919	yes	Semi-rigid	Light	< 60 cm	< 5 m	1.43%
	15 N	Bricks	2	1945-1981	no	Rigid	Light	< 60 cm	< 5 m	1.06%
Central Italy	1 C	Bricks	2	1861-1919	yes	Flexible	Light	> 60 cm	< 5 m	9.00%
	2 C	Bricks	3	1945-1981	no	Rigid	Heavy	< 60 cm	< 5 m	7.59%
	3 C	Bricks	3	1861-1919	yes	Flexible	Light	> 60 cm	< 5 m	5.99%
	4 C	Bricks	2	1861-1919	yes	Rigid	Light	> 60 cm	< 5 m	5.95%
	5 C	Bricks	3	1861-1919	yes	Rigid	Light	> 60 cm	< 5 m	5.27%
	6 C	Bricks	3	1861-1919	no	Flexible	Light	> 60 cm	< 5 m	2.87%
	7 C	Bricks	2	1861-1919	no	Flexible	Light	> 60 cm	< 5 m	2.41%
	8 C	Bricks	2	1945-1981	yes	Rigid	Heavy	< 60 cm	< 5 m	2.38%
	9 C	Bricks	3	1945-1981	no	Semi-rigid	Heavy	< 60 cm	< 5 m	2.08%
	10 C	Bricks	3	1861-1919	no	Rigid	Light	> 60 cm	< 5 m	1.92%
	11 C	Bricks	4	1945-1981	no	Rigid	Heavy	< 60 cm	< 5 m	1.92%
	12 C	Bricks	2	1861-1919	no	Rigid	Light	> 60 cm	< 5 m	1.50%
	13 C	Bricks	3	1945-1981	no	Rigid	Heavy	< 60 cm	> 5 m	1.47%
	14 C	Bricks	3	1919-1945	no	Semi-rigid	Heavy	< 60 cm	< 5 m	1.43%
Southern Italy	1 S	Irregular masonry	3	< 1860	no	Flexible	Light	> 60 cm	< 5 m	9.51%
	2 S	Bricks	2	1945-1981	no	Rigid	Heavy	< 60 cm	< 5 m	8.78%
	3 S	Irregular masonry	2	1919-1945	no	Semi-rigid	Light	< 60 cm	< 5 m	8.41%
	4 S	Squared stone	2	1945-1981	no	Rigid	Heavy	< 60 cm	< 5 m	7.59%
	5 S	Squared stone	3	1945-1981	yes	Rigid	Heavy	< 60 cm	< 5 m	4.19%
	6 S	Irregular masonry	3	1861-1919	no	Flexible	Light	> 60 cm	< 5 m	2.62%
	7 S	Irregular masonry	2	< 1860	no	Flexible	Light	> 60 cm	< 5 m	2.05%
	8 S	Squared stone	4	1945-1981	yes	Rigid	Heavy	< 60 cm	< 5 m	1.77%
	9 S	Squared stone	3	1945-1981	no	Rigid	Heavy	< 60 cm	< 5 m	1.72%
	10 S	Irregular masonry	3	1861-1919	no	Flexible	Light	< 60 cm	< 5 m	1.39%

A summary of the samples is presented in Table 1, in which the features of the archetype buildings are reported in order of relevance for the three macro-areas and a three-dimensional graphic representation is instead present in Figure 1 for the macro area of Northern Italy, Figure 2 for the macro area of Central Italy and Figure 3 for Southern Italy. The building typologies extracted from the CARTIS database, through the procedure described above, were identified through eight parameters considered significant for the purposes of the seismic response. These data are not sufficient for advanced analyses there is a lack of more detailed information that allows to identify unique archetypal buildings that can be assimilated to real buildings. To translate the fifteen building typologies into archetype buildings, it was necessary to introduce other structural and geometric parameters in addition to the typological-structural data present on the CARTIS form compiled in the territory of interest. Through this integration operation, it was possible to architecturally represent the archetype buildings and carry out vulnerability analyses, even detailed ones, through both analytical and numerical methods. Specifically, were added data regarding the average floor area, the presence/absence of vaults on the ground floor, the percentage of openings on the façade, the average floor height, the presence/absence of thrusting roof slabs, the regularity in plan and elevation.

The archetypes identified by the additional data emerging from the CARTIS form are composed of a two-cell, multi-story structure with a gross floor area of approximately 70 m^2, regular in both plan and elevation. The only walls with openings are the two shorter façades identified as the "main façade" and "secondary façade" on which the vulnerability assessments of the kinematic mechanisms were carried out. The openings on these walls were differentiated based on their location, distinguishing ground-floor openings ranging from 30-50% and upper-floor openings ranging from 20-29%. Archetypes with more than two stories feature barrel-vaulted slabs on the first level, while the upper levels have flat slabs, with inter-story heights ranging between 2.50-3.50 m. The roofing system consists of two sloping surfaces with a thrusting static scheme on the walls with openings.

Northern Italy sample

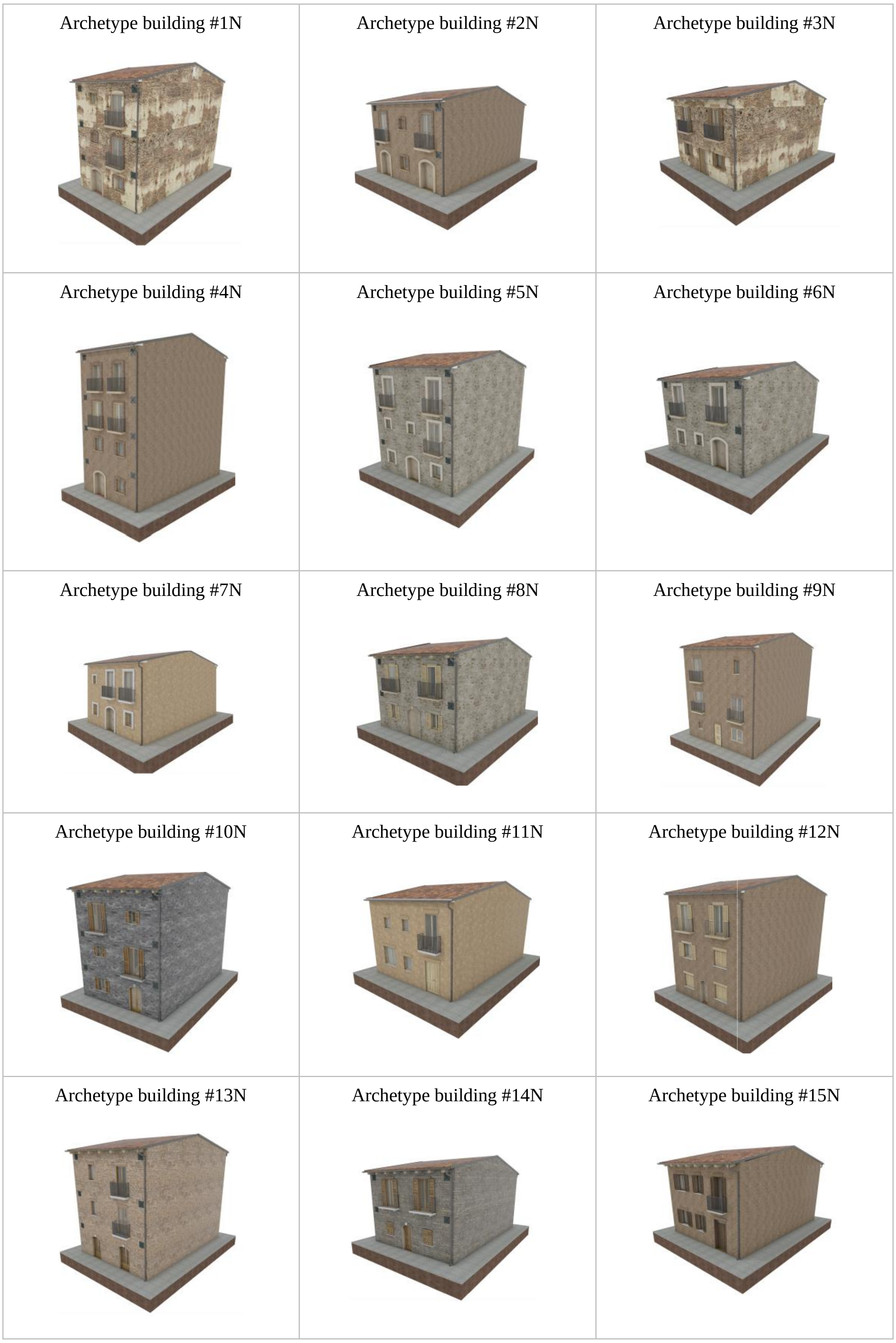

Figure 1. Graphic representation of archetype buildings for the macro-area of Northen Italy.

Central Italy sample

Figure 2. Graphic representation of archetype buildings for the macro-area of Central Italy.

Southern Italy sample

Figure 3. Graphic representation of archetype buildings for the macro-area of Southern Italy.

3.2 The National Sample

The national sample was defined by consolidating the data into eight archetypes that represent the entire Italian building stock without regional subdivisions.

The national sample was designed to simplify the representation of the Italian building stock, focusing on the most common configurations to ensure it could be effectively used for large-scale seismic vulnerability analyses. By consolidating regional data, this sample includes archetypes that capture both regular and irregular masonry constructions, striking a balance between urban and rural building types. In Table 2 summarized the features of the archetype buildings extrapolated for the national territory without subdivisions and in Figure 4 are shown in three-dimensional models.

Table 2. Archetype buildings identified for the national territory.

Area	ID	Masonry Type	N° of Stories	Construction Period	Tie Rods	Floor Type	Roof Material	Wall Thickness	Wall Spacing	Relevance
National	1	Bricks	2	1945-1981	yes	Rigid	Heavy	< 60 cm	< 5 m	12.45%
	2	Bricks	3	1945-1981	yes	Rigid	Heavy	< 60 cm	< 5 m	6.80%
	3	Irregular masonry	3	1861-1919	yes	Rigid	Heavy	< 60 cm	< 5 m	5.68%
	4	Bricks	4	1945-1981	yes	Rigid	Heavy	< 60 cm	< 5 m	4.91%
	5	Bricks	2	1945-1981	no	Rigid	Heavy	< 60 cm	< 5 m	4.67%
	6	Irregular masonry	2	1861-1919	yes	Rigid	Heavy	< 60 cm	< 5 m	4.14%
	7	Bricks	3	1945-1981	no	Rigid	Heavy	< 60 cm	< 5 m	2.89%
	8	Bricks	2	Post 1981	no	Rigid	Heavy	< 60 cm	< 5 m	1.38%

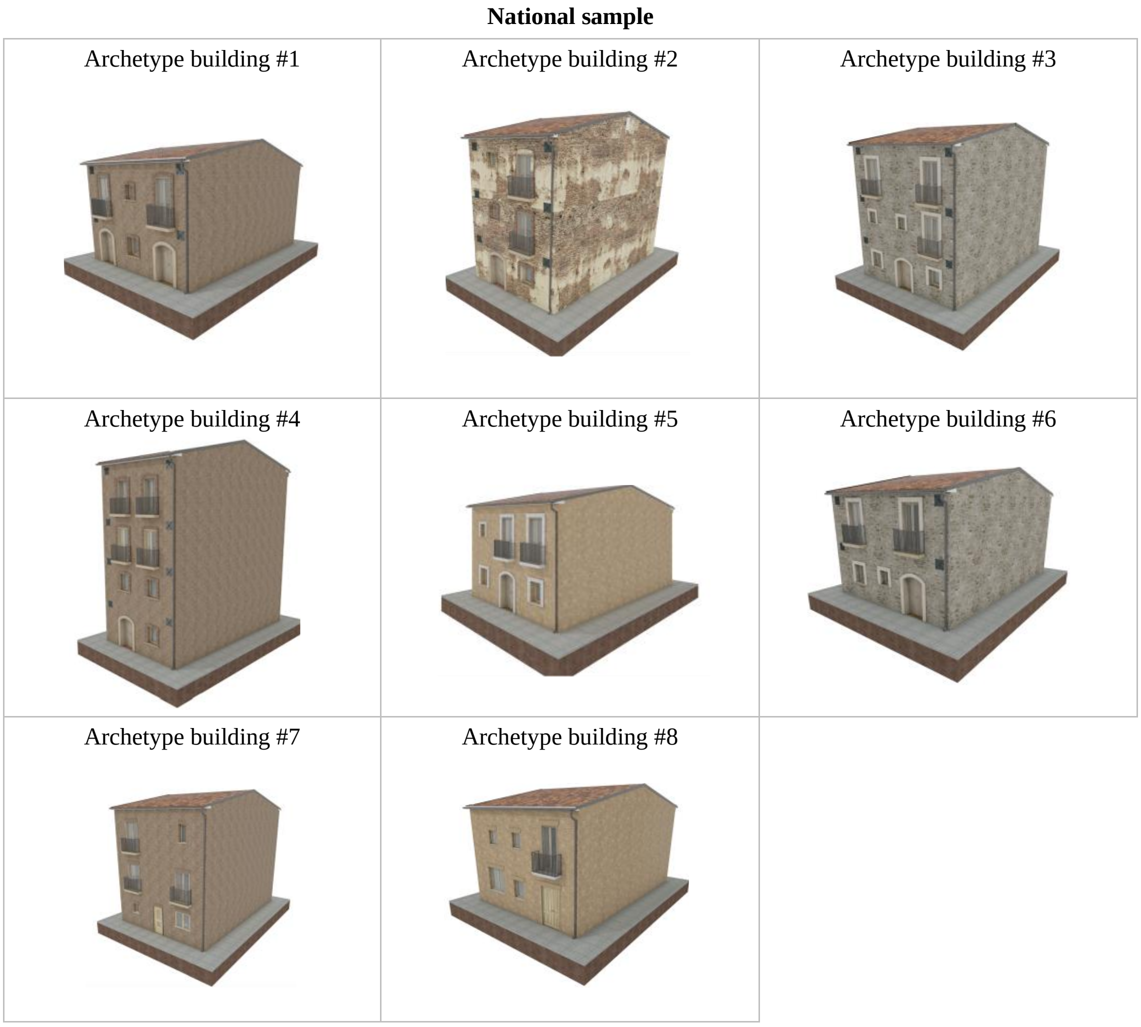

Figure 4. Graphic representation of archetype buildings for the national territory

To achieve a generalized yet representative set of archetypes, key parameters such as wall thickness, floor stiffness, and roof material were averaged across all regions. This approach ensured that the diversity of structural and typological characteristics present in the national building stock was preserved, while also streamlining the dataset for practical application. Additionally, the sample retained variability in construction periods, prioritizing categories that reflect most of the existing buildings, from pre-1900 to modern constructions. This careful balance between simplification and representativeness makes the national sample a robust tool for understanding seismic vulnerability on a broader scale.

3.3 COMPARISON OF SAMPLE FEATURES

The comparative analysis of the two samples —based on the macro-regional and national scales— reveals important insights into the representativeness and applicability of the archetype models. The macro-regional sample, with its division into Northern, Central, and Southern Italy and the inclusion of thirty-nine archetypes, provides a more detailed representation of the variability within the Italian building stock. This granularity allows for the capture of specific regional construction practices, such as the prevalence of irregular masonry in the South and the predominance of brick masonry in the North. Moreover, the macro-regional sample highlights significant differences in construction periods, structural details, and building materials, reflecting Italy's diverse architectural heritage and seismic vulnerabilities.

Conversely, the national sample, consisting of only eight archetypes, represents a more streamlined and generalized approach. By averaging parameters across regions, this sample simplifies the dataset while maintaining a level of representativeness sufficient for large-scale seismic vulnerability assessments. If, on the one hand, the reduced number of archetypes limits the ability to capture region-specific parameters, on the other hand it offers the possibility of significantly reducing the computational burden for any type of analysis one wants to do.

The choice between the two samples depends on the scope and objectives of the analysis. For policy planning and seismic risk mitigation strategies at the national level, both samples are suitable. The 8-archetype model offers a practical balance between detail and manageability in terms of computational effort. For detailed studies, the macro-regional sample provides a more nuanced understanding of regional vulnerabilities and construction practices. Obviously, the computational burden of the larger sample is slightly higher than that of the smaller sample.

In the following, both samples will be analysed and the comparison results in terms of vulnerability will be shown.

4. THE VULNERABILITY ASSESSMENT

4.1 Methods and tools for the vulnerability assessment: a combined approach

The seismic vulnerability assessment of the identified Archetype Buildings was conducted based on an integrated approach that combines kinematic analyses for out-of-plane mechanisms and numerical analyses for the global behaviour of building under horizontal actions. This approach enables a detailed representation of the seismic behaviour of the identified archetypes, with the goal of deriving reliable fragility curves applicable on a national scale.

The analytical method, based on the implementation of linear and nonlinear kinematic analyses, allows for the study of out-of-plane collapse mechanisms of the macro-elements composing each representative building (local mechanism analysis). Specifically, linear kinematic analyses are performed to estimate the load multiplier α associated with the various mechanisms susceptible to activation. This enables the identification of the spectral acceleration (S_a) related to an equivalent single-degree-of-freedom (SDOF) system and, subsequently, the peak ground acceleration (PGA) capable of activating the kinematic mechanism considered in the structure. Conversely, nonlinear kinematic analyses provide insights into the displacement capacity of the system up to collapse by identifying trilinear curves representing the structural behaviour in terms of capacity/displacement [14], defined according to the Italian technical regulations.

The numerical method, based on the application of nonlinear static analyses on numerically modeled buildings, is used to investigate the in-plane behaviour of the identified archetypes. This method assumes that out-of-plane mechanisms are prevented and considers the structural contribution of in-plane loaded masonry walls in resisting seismic actions (global mechanism analysis). The numerical simulations performed in this study rely on the structural schematization of the archetypes using the Equivalent Frame Model (EFM) [18] and are conducted within the MIDAS-GEN environment [19]. In this framework, pushover analyses are carried out to derive equivalent bilinear capacity curves representing the relationship between base shear and top displacement for each building.

Once the capacity of all archetype buildings was estimated in terms of trilinear and bilinear capacity curves, Damage Thresholds (DT) were defined according to criteria established in literature [20], [21] and compared against a significant number of seismic demands expressed in terms of an Acceleration-Displacement Response Spectrum (ADRS). This process allowed the derivation of integrated fragility curves that account for both out-of-plane and in-plane mechanisms, as will be explained in detail below.

According to the Performance-Based Assessment (PBA) approach, the seismic vulnerability of historic masonry buildings can be evaluated using fragility curves that indicate the probability of exceeding a specific damage level as a function of seismic intensity. In this study, to compare the capacity curves of buildings and estimate site-independent fragility curves across a range of seismic risk levels from low to high, a comprehensive set of 125 natural seismic recordings was used. These recordings were derived from the research activities of the WP4 MARS project (2019-21 ReLUIS Project funded by the Italian National Department of Civil Protection) [22]. These accelerograms covered a wide range of intensity levels and were specifically chosen for use in nonlinear dynamic analyses to develop site-independent fragility curves, encompassing both very low and very high seismic hazard levels. Therefore, the primary uncertainty considered in this study was related to ground motions, specifically the seismic record-to-record variability [23]. Within the framework of the ReLUIS project, unscaled recorded ground motions were chosen to approximate the uniform hazard spectra at L'Aquila for various return periods (Tr = 50, 100, 200, 475, 975, 2475, 5000, and 10000 years) and for soil category A and C, assumed as the target spectra. In total, 250 ground motions were selected, with 125 motions for soil category A and 125 for soil category C. Each record consists of two orthogonal horizontal components: H1 (North-South) and H2 (East-West). These accelerograms were employed across various building types to assess their ability to induce different damage states commonly studied in fragility analyses, particularly in multi-storey Reinforced Concrete (RC) structures typical of Italian buildings from the 1970s. Further details about the adopted seismic records can be found in [24].

4.2 Out-of-Plane Capacity Assessment of Masonry

As widely recognised in the literature, out-of-plane (or first-mode) collapses are among the most critical mechanisms for masonry structures under seismic actions. Several factors can influence the structural behaviour and facilitate the activation of kinematic mechanisms, such as the lack of connections between orthogonal walls, inadequate interaction between vertical and horizontal structures that prevents box-like behaviour, the presence of thrusting elements, and geometric and mechanical properties of the masonry.

Considering the boundary conditions and characteristics of the archetype buildings, and treating the walls as monolithic, this study considers only two types of out-of-plane collapses as admissible: simple overturning (total or partial wall failure) and vertical bending [25], [26]. For this purpose, the following two conditions are defined for each façade of the archetype buildings based on the presence or absence of constraints:

- Absence of adequate constraints for vertical walls relative to the rest of the structure: This deficiency facilitates overturning mechanisms, as walls are unrestrained at the top and free to rotate monolithically. The mechanism is triggered in the absence of transverse connections or restraints such as tie rods or summit ring beams. Simple overturning mechanisms are schematically represented as rigid rotation of the wall around a horizontal cylindrical hinge formed at the base (Figure 5a). Overturning can also involve only certain floors of the building (Figure 5b); therefore, both global monolithic overturning of the façade and partial monolithic overturning were analysed.
- Constraints for the walls through anti-seismic devices: Assuming the presence of tie rods or ring beams, depending on their placement at the wall's summit, vertical bending mechanisms are more likely to occur. This mechanism arises when the wall is constrained at its extremities but free in the middle, where a horizontal cylindrical hinge can form under seismic stress (Figure 5c-d).

Figure 5. Possible kinematic mechanisms of the walls: a) simple overturning of a monolithic wall; b) simple overturning of a portion of the wall; c-d) examples of vertical bending of a monolithic wall

The analysis of out-of-plane mechanisms was conducted using both a linear and a nonlinear kinematic approach.

For the linear analysis, the load multiplier α_0 triggering the mechanism was identified for each wall and every mechanism. This was achieved by applying the Principle of Virtual Work, taking into account all internal and external forces acting on the rigid blocks involved in the kinematic configuration, such as: self-weight of the macro-elements; vertical loads from floors, vaults, and roofs; horizontal forces induced by the earthquake; and any additional external forces, such as those transmitted by tie rods. The analytical computation of the kinematics involved calculating, for each α_0, the spectral acceleration a_0^* associated with an equivalent single-degree-of-freedom (SDOF) system, in accordance with Italian technical standards. Subsequently, the acceleration leading to the activation of the mechanism was determined.

As for the nonlinear kinematic analyses, acceleration-displacement capacity curves were determined for the most vulnerable mechanisms up to collapse. The capacity curves were derived in accordance with Italian technical standards [27], based on identifying the acceleration-displacement pairs at four points corresponding to four limit states: Elastic (ELS), Damage (DLS), Near Collapse (NCLS), and Collapse (CLS), as shown in Figure 6, where an example of capacity curve is illustrated.

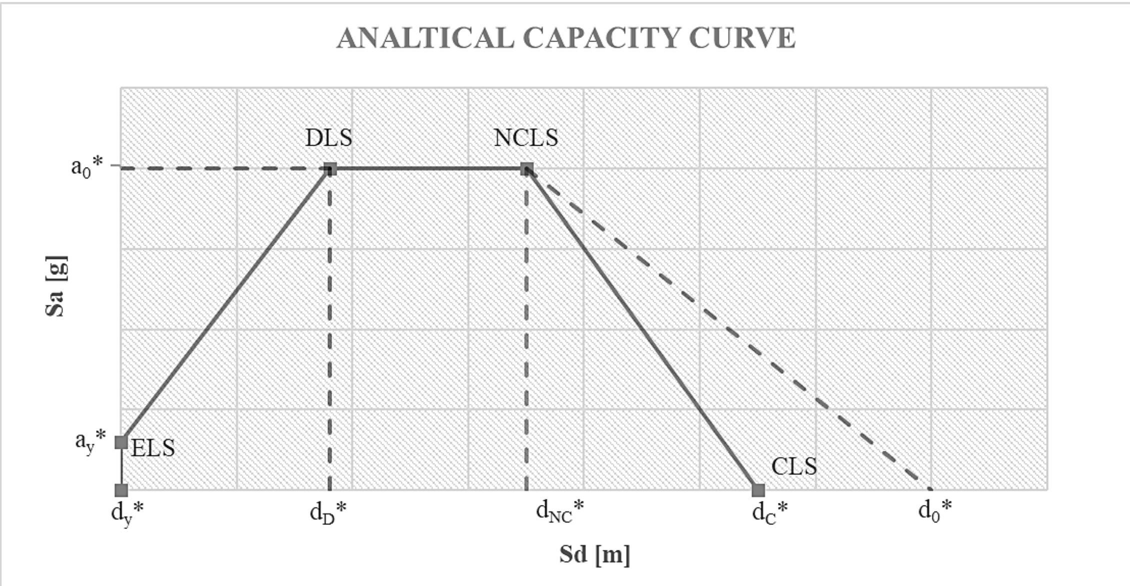

Figure 6. Typical capacity curve obtained from a nonlinear kinematic analysis with the identification of the four limit states

In this method the displacements associated with each damage level are defined according to the equations below:

- **d_c*** at the Collapse Limit State (CLS), according to experimental studies on out-of-plane mechanisms [26], is defined as 60% of the maximum lateral displacement of the equivalent SDOF system d_0*, computed as given by Eq. (1).

$$d_0^* = d_k \cdot \frac{\sum_{i=1}^{n+m} P_i \delta_{x,i}^2}{\delta_{x,k} \cdot \sum_{i=1}^{n+m} P_i \delta_{x,i}} \quad (1)$$

In Eq. (1) $\delta_{x,k}$ is the virtual horizontal displacement of point *k*, taken as a reference for the determination of the displacement d_k, P_i is the self-weight of the block applied to its centre of gravity, *n* is the number of rigid blocks involved in the kinematic chain and *m* is the number of elements not directly involved in the mechanism but whose masses, due to the seismic action, generate horizontal forces on the elements of the kinematic chain.

- **d_{NC}*** is the displacement of the equivalent SDOF system corresponding to the Near Collapse Limit State (NCLS) and computed as follows in Eq. (2):

$$d_{NC}^* = 40\%\ d_0^* \quad (2)$$

- **d_D*** is the displacement corresponding to the Damage Limit State (DLS) evaluated following the expression below (Eq. 3) and considering a ductility factor *q* = 2:

$$d_D^* = d_{NC}^*/q \quad (3)$$

- **d_y*** is the Elastic Limit State (ELS) displacement computed as a function of the wall geometry and the ELS acceleration a_y* with the Eq. (4):

$$d_y^* = a_y^* \cdot \frac{T_a^2}{4\pi^2} \quad (4)$$

Below are shown the results obtained from the kinematic analysis for all the archetypes belonging to the two samples.

4.2.1 RESULTS OF THE OUT-OF-PLANE CAPACITY ASSESSMENT

First, the assessment on the out-of-plane behaviour of the masonry walls led to the knowledge of the first in-plane mechanism activated for each archetype building, providing a first idea on the seismic behaviour of these structures. As it can be seen from the Table 3Table 3, the prevailing mechanism for the macro-areas sample is the simple overturning of a monolithic wall, briefly indicated in the table as "total façade overturning". Due to the configuration of the buildings and the construction details with which they were made—such as the lack of connections between orthogonal walls and the presence of thrusting roof systems—overturning is expected to be the first mechanism to activate. In only a few cases does the overturning appear as partial rather than total. This is observed solely in cases of four-story buildings (e.g. AB #4N, #5N, #11C, #8S), which are very tall and slender, promoting the activation of a plastic hinge before reaching the ground.

Table 3. Results of linear kinematic analyses of archetypes buildings for the macro-areas sample.

Area	ID	Kinematic mechanism	Lateral force multiplier α	Spectral acceleration a_0^* [g]
Northern Italy	1 N	Total façade overturning	0.14	0.13
	2 N	Total façade overturning	0.184	0.17
	3 N	Total façade overturning	0.053	0.05
	4 N	Partial façade overturning	0.099	0.68
	5 N	Partial façade overturning	0.047	0.08
	6 N	Total façade overturning	0.141	0.12
	7 N	Total façade overturning	0.034	0.04
	8 N	Total façade overturning	0.186	0.17
	9 N	Total façade overturning	0.012	0.01
	10 N	Total façade overturning	0.142	0.14
	11 N	Total façade overturning	0.043	0.04
	12 N	Total façade overturning	0.015	0.01
	13 N	Total façade overturning	0.165	0.16
	14 N	Total façade overturning	0.172	0.15
	15 N	Total façade overturning	0.071	0.06
Central Italy	1 C	Total façade overturning	0.353	0.32
	2 C	Total façade overturning	0.008	0.01
	3 C	Total façade overturning	0.331	0.32
	4 C	Total façade overturning	0.378	0.34
	5 C	Total façade overturning	0.347	0.33
	6 C	Total façade overturning	0.011	0.01
	7 C	Total façade overturning	0.066	0.06
	8 C	Total façade overturning	0.139	0.12
	9 C	Total façade overturning	0.006	0.01
	10 C	Total façade overturning	0.012	0.01
	11 C	Partial façade overturning	0.040	0.01
	12 C	Total façade overturning	0.066	0.06
	13 C	Total façade overturning	0.007	0.01
	14 C	Total façade overturning	0.008	0.01
Southern Italy	1 S	Total façade overturning	0.009	0.01
	2 S	Total façade overturning	0.042	0.04
	3 S	Total façade overturning	0.051	0.05
	4 S	Total façade overturning	0.041	0.04
	5 S	Total façade overturning	0.129	0.12
	6 S	Total façade overturning	0.017	0.02
	7 S	Total façade overturning	0.093	0.09
	8 S	Partial façade overturning	0.229	0.22
	9 S	Total façade overturning	0.017	0.02
	10 S	Total façade overturning	0.010	0.01

Entirely similar results are also observed for the eight-building sample from the national territory (Table 4). In this case, as with the sample from the three macro-areas, the first mechanism to activate is the simple overturning of a monolithic wall. In most cases, the mechanism involves the entire wall (total façade overturning), while in taller buildings (e.g. #3, #4), the upper portion of the wall is more vulnerable (partial façade overturning).

Table 4. Results of linear kinematic analyses of archetypes buildings for the national sample

Area	ID	Kinematic mechanism	Lateral force multiplier α	Spectral acceleration a_0^* [g]
Central Italy	1	Total façade overturning	0.184	0.17
	2	Total façade overturning	0.14	0.13
	3	Partial façade overturning	0.047	0.08
	4	Partial façade overturning	0.099	0.68
	5	Total façade overturning	0.034	0.04
	6	Total façade overturning	0.141	0.12
	7	Total façade overturning	0.012	0.01
	8	Total façade overturning	0.043	0.04

This initial result is only a preliminary approach to understanding the seismic response of the examined buildings. The result was further investigated through nonlinear kinematic analysis using the procedure described above. In accordance with the approach used for linear analyses, all possible mechanisms were evaluated for each archetype building to assess the displacement capacity of the structure up to collapse. The evolution of the load multiplier α was analysed for the various configurations of the kinematic chain, following the development of the corresponding mechanism. In Figure 7 there are the result relating to the kinematic curves obtained. Even for the non-linear analysis the most vulnerable mechanism is the total overturning of the façade. The evolution of these mechanisms is shown in Figure 7a for the Northern Italy sample; in Figure 7b for the Central Italy sample and Figure 7c for the South.

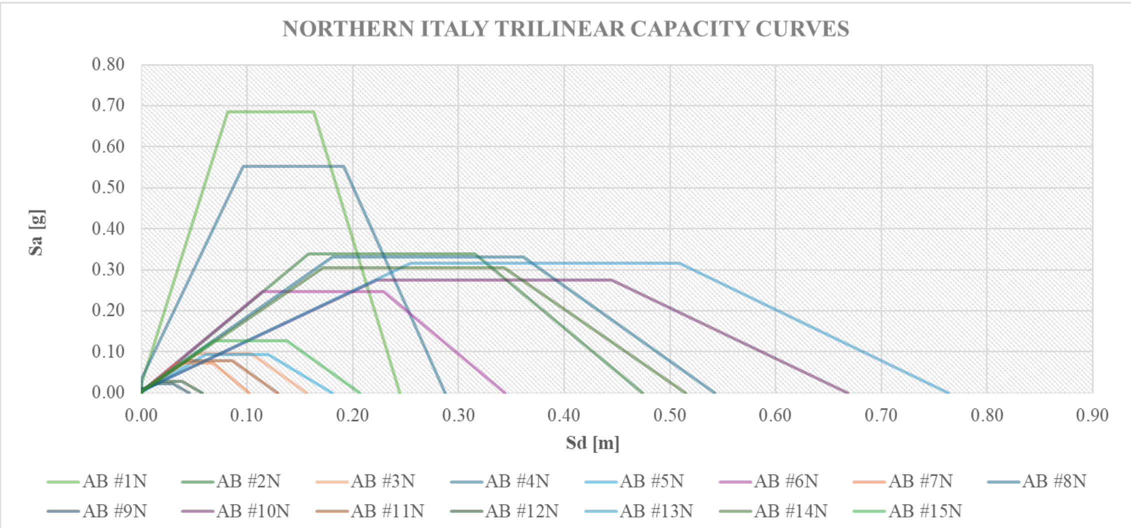

a)

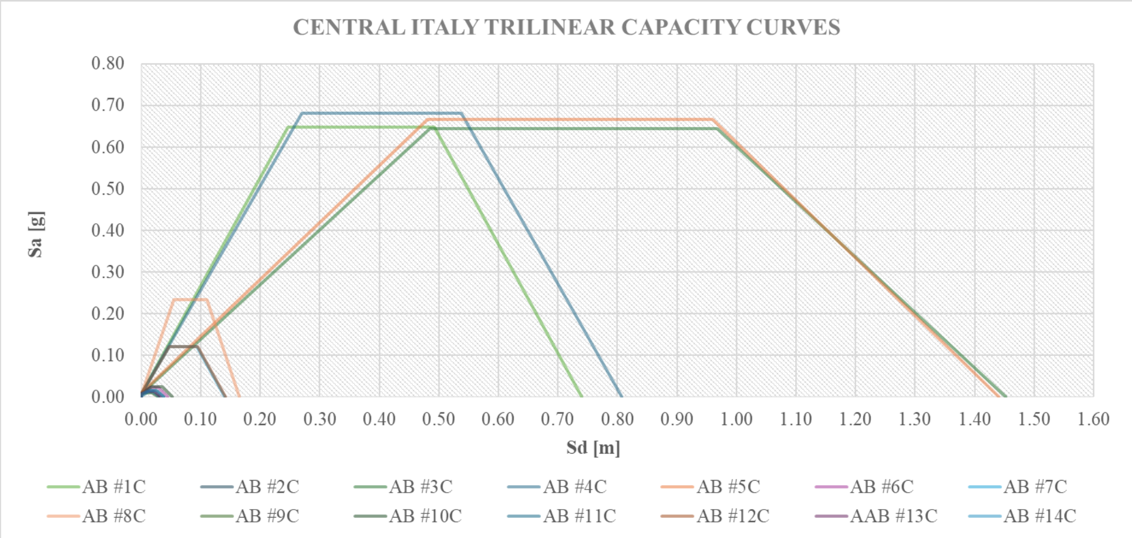

b)

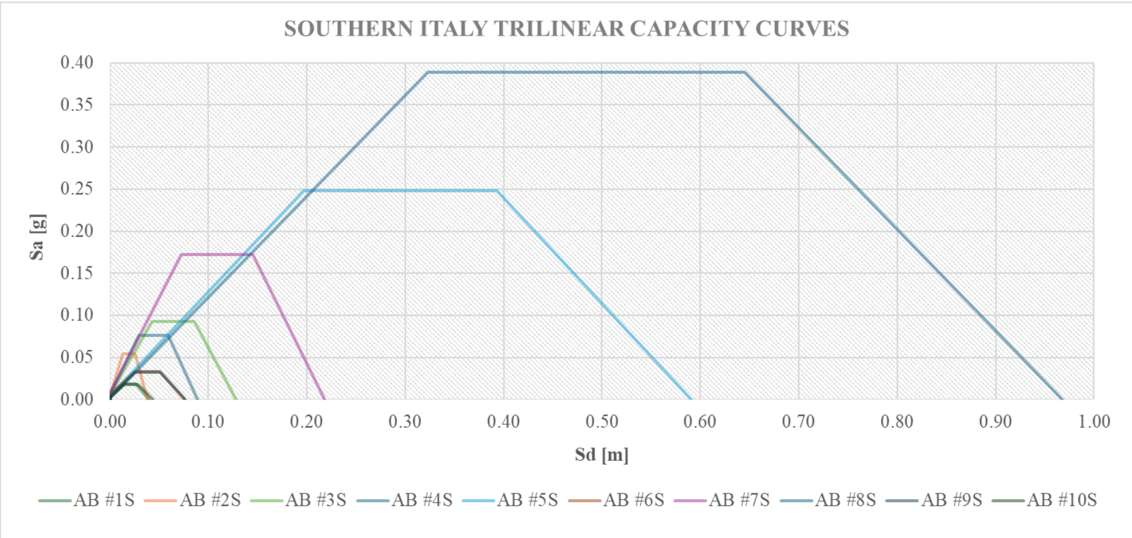

c)

Figure 7. Trilinear capacity curves obtained from nonlinear kinematic analyses for the macro-areas sample: a) Northern Italy; b) Central Italy; c) Southern Italy

Similarly, the trilinear capacity curves were also extrapolated for the national sample and are shown in Figure 8.

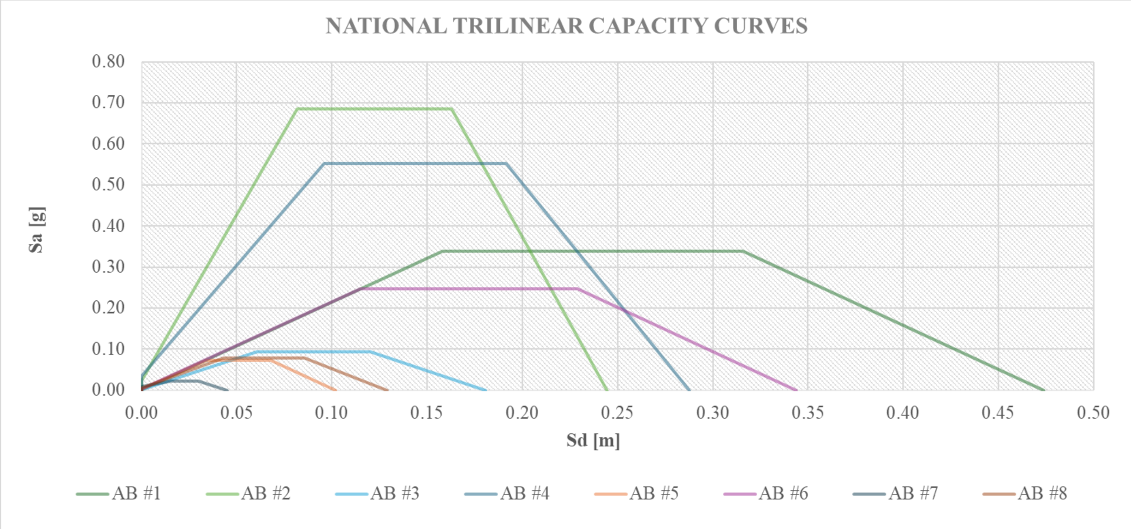

Figure 8. Trilinear capacity curves obtained from nonlinear kinematic analyses for the National sample

4.3 In-Plane Capacity Assessment of Masonry

To fully evaluate the seismic capacity of masonry buildings, it is essential to also analyse their global behaviour, examining all possible in-plane collapse mechanisms (or second-mode mechanisms) that these structures might experience under horizontal actions. In this study, the buildings were numerically modeled using the Equivalent Frame Method (EFM) [18], [28] which is currently the most widely adopted approach in engineering practice.

The EFM is a discrete-element method that idealizes and simplifies the structure as a frame composed of equivalent one-dimensional deformable elements rigidly connected by stiff zones. These elements include piers and spandrels: piers are vertical components designed to support the structure and resist lateral forces, while spandrels are horizontal elements located above openings that extend between piers, helping to distribute and transfer vertical and/or horizontal forces depending on their design. The EFM is an efficient method for rapid numerical modelling or, as in this case, for analysing a large number of buildings, as it requires a limited number of mechanical input parameters. This results in reduced computational load and significant savings in terms of time and cost for structural analyses. For these reasons, given the large number of structures to analyse and the phenomena to investigate, the EFM is considered the most suitable and efficient method for the specific case under study.

The analyses of the buildings in this study were carried out by implementing the models in the MIDAS GEN software [19]. In the EFM model, two types of elements were used to represent the different structural parts of the buildings, based on distinct assumptions related to their boundary conditions [29]. The elements employed are: 1) *elastic beams*, to represent the piers and spandrels, which are the deformable parts where seismic damage can occur; and 2) *rigid links*, which represent the stiff zones at the intersections of the deformable parts where no damage occurs.

This idealization is derived from damage observed in masonry structures following past seismic events. In many cases, damage was concentrated in the piers and lintels, while the nodal panels remained unaffected. This observation confirms the hypothesis of their higher rigidity and strength compared to the deformable parts, where wall deformations typically concentrate. Due to the differing structural configurations of the archetype buildings, two types of numerical analyses were conducted:

- Global analysis for buildings with rigid floors, i.e., structures with adequate connections between vertical and horizontal elements. In these cases, the floors were modelled as rigid horizontal diaphragms with infinite in-plane stiffness to ensure a distribution of seismic forces proportional to the relative stiffness of the building's shear walls.
- Individual wall analysis for buildings with flexible floors, i.e., structures where the in-plane stiffness of horizontal diaphragms is negligible. Flexible diaphragms cannot redistribute lateral forces among the frames, allowing them to translate independently. In such cases, all the walls of the archetype were analysed individually, and, conservatively, the wall with the lowest resistance was chosen as representative of the global in-plane response of the entire building, as it is the first to collapse.

Figure 9 and Figure 10 illustrate the EFM idealization for all the archetype buildings.

Northern Italy sample

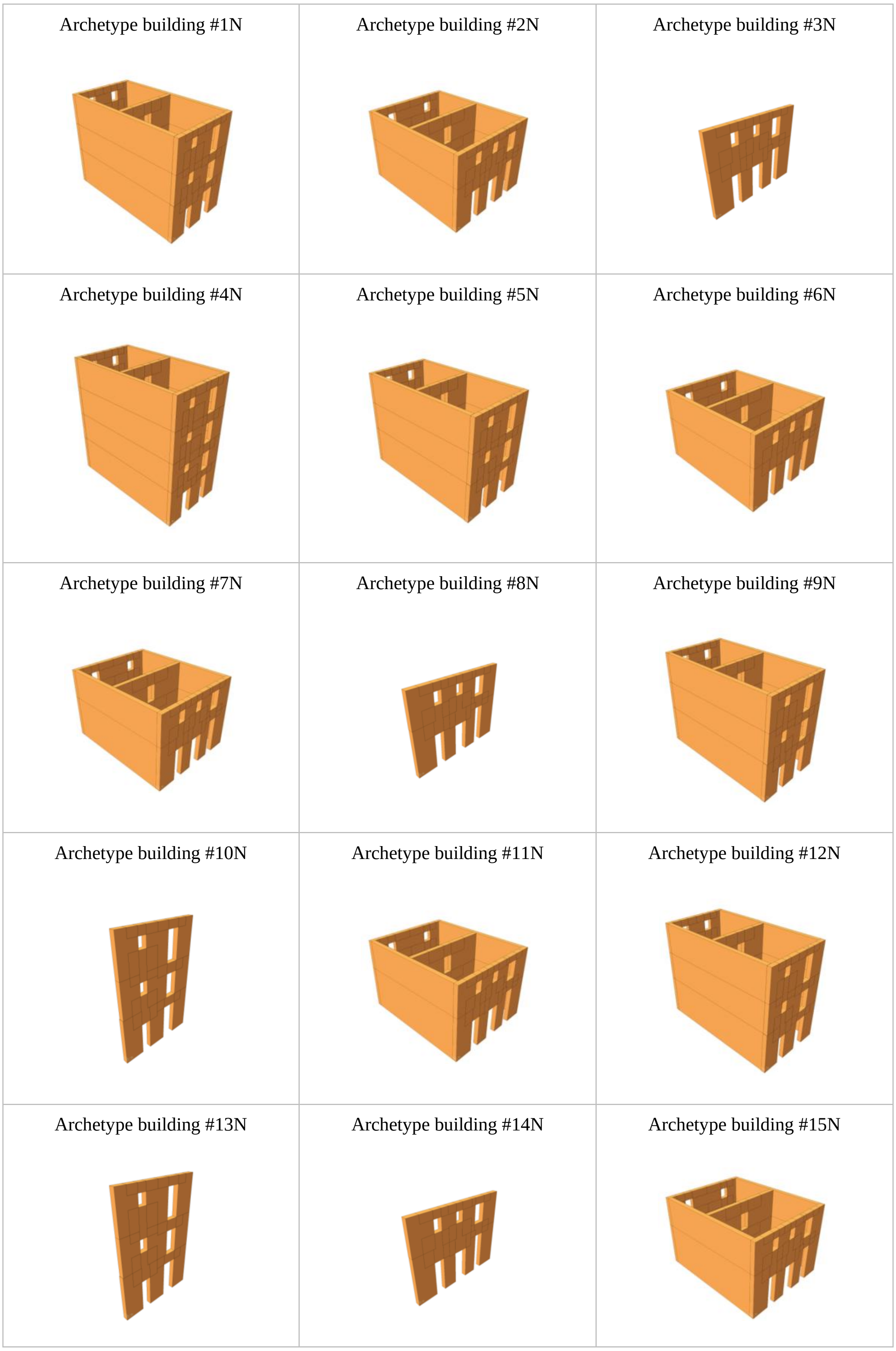

a)

Central Italy sample

Archetype building #1C 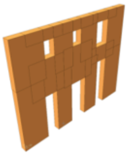	Archetype building #2C 	Archetype building #3C 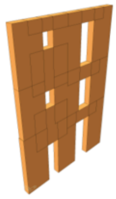
Archetype building #4C 	Archetype building #5C 	Archetype building #6C 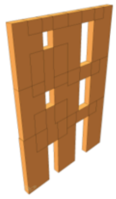
Archetype building #7C 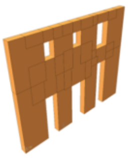	Archetype building #8C 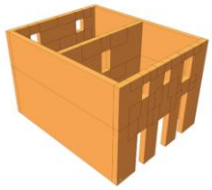	Archetype building #9C 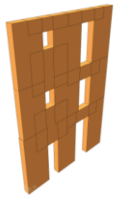
Archetype building #10C 	Archetype building #11C 	Archetype building #12C 
Archetype building #13C 	Archetype building #14C 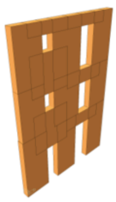	

b)

Southern Italy sample

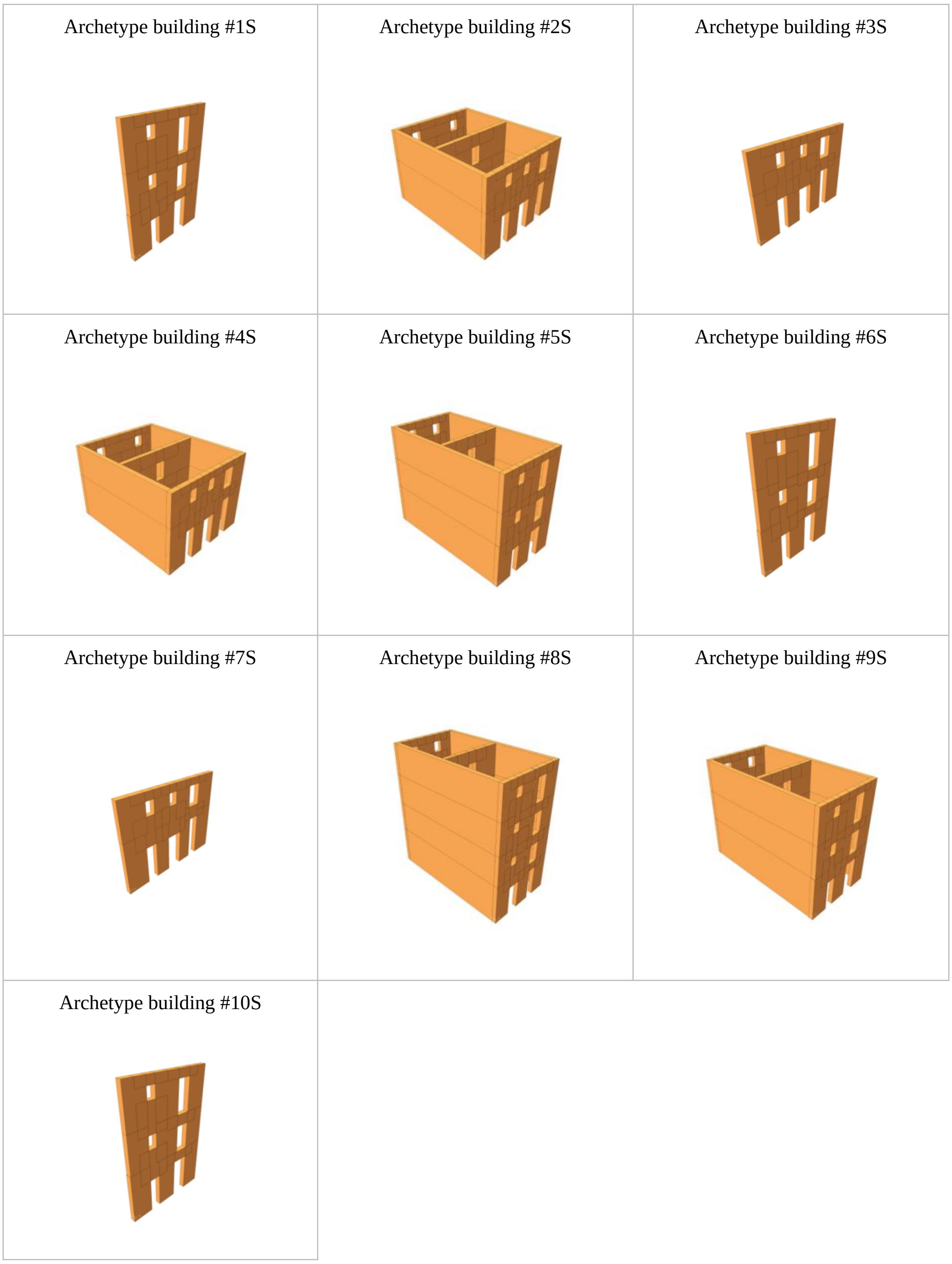

c)

Figure 9. Identification of the equivalent frame for all archetype building: a) Northern Italy sample; b) Central Italy sample; c) Southern Italy sample

National sample

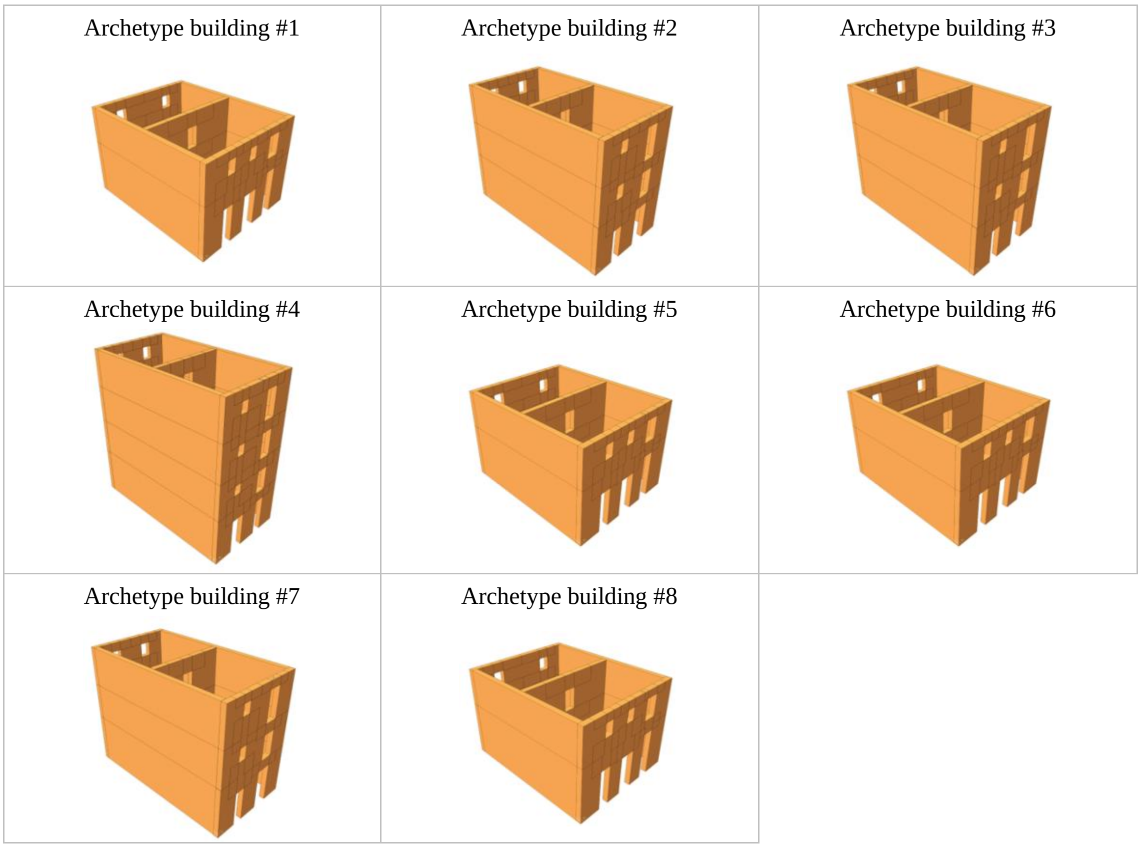

Figure 10. Identification of the equivalent frame for all archetype building of National sample

The nonlinear behaviour of piers and spandrels is numerically simulated using concentrated plasticity models, following the guidelines of the United States Federal Emergency Management Agency [30]. Specifically, concentrated plastic hinges were assigned to critical points of the frame, such as the ends and the central node of the beams, to simulate flexural and shear behaviour, respectively. The mechanical properties of the masonry material used in the modelling of each archetype building were selected in accordance with the current Italian technical code, as specified in Table C8.5.I of the Circular No. 7, dated 21 January 2019, issued by the C.S.LL.PP [27].

4.3.1 RESULTS OF THE IN-PLANE CAPACITY ASSESSMENT

For all cases, monotonic nonlinear static analyses were performed using a lateral force distribution proportional to the mass along the height of the structure. This approach allowed the derivation of representative force-displacement capacity curves for all archetypes. In Figure 11 and Figure 12 are showed the pushover curves obtained. In Figure 11a) there are the Northern Italy curves; in Figure 11b) there are the Central Italy curves and c) for Southern Italy curves. In Figure 12 there Is the National sample collection of curves.

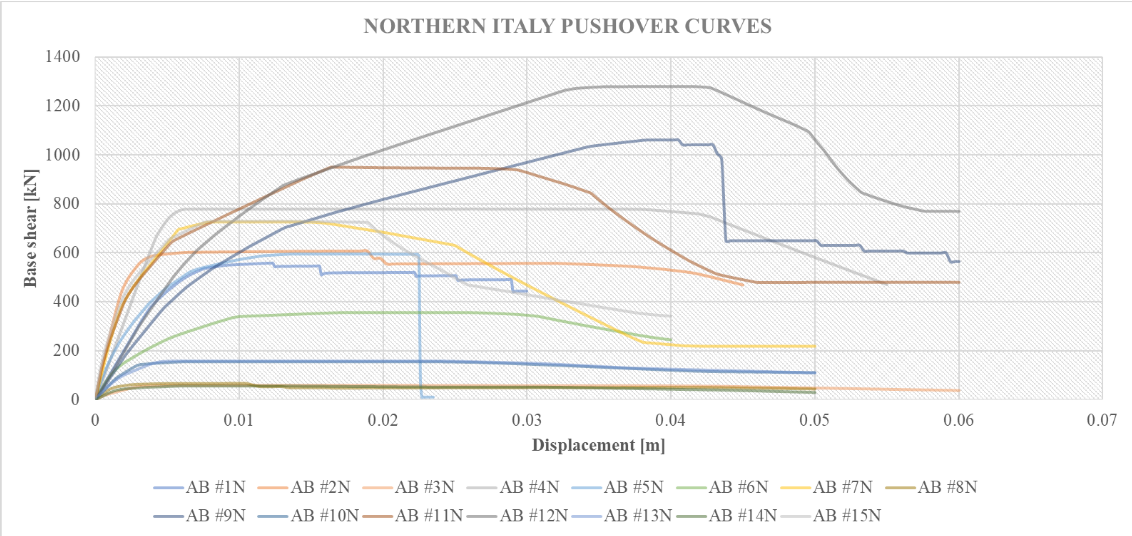

a)

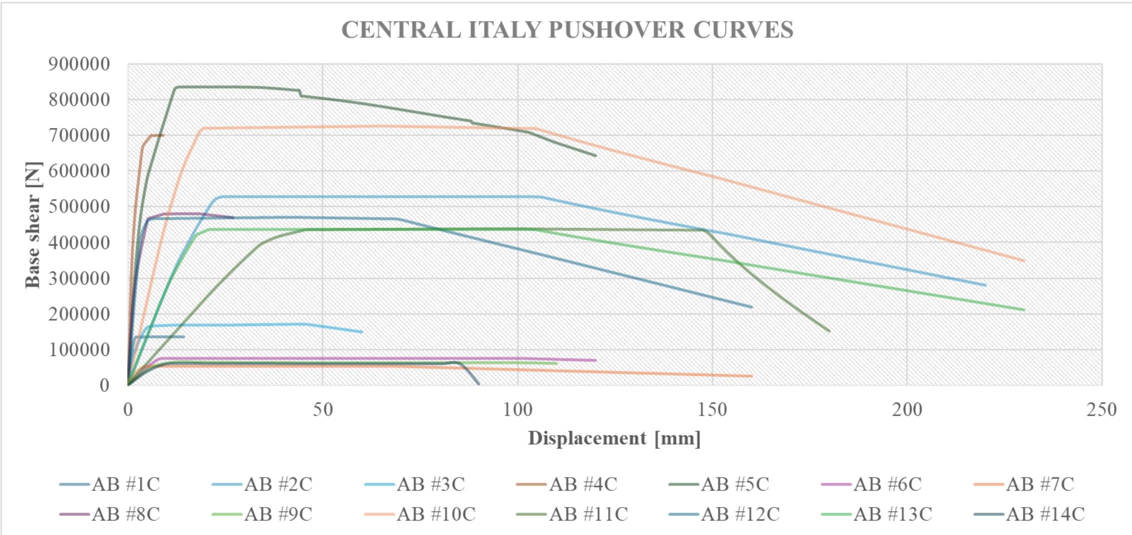

b)

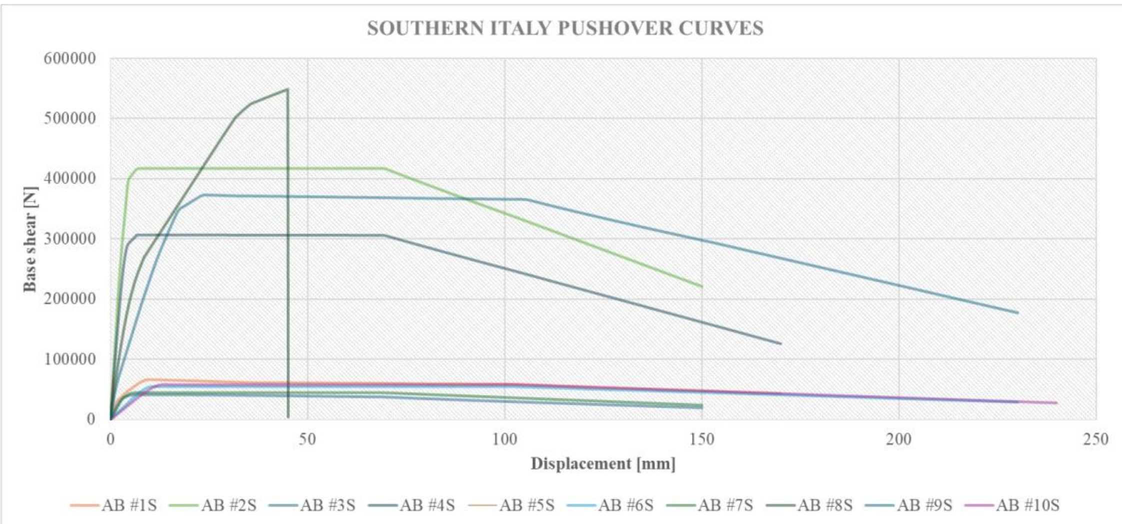

c)

Figure 11. Numerical push-over capacity curve for the macro-areas sample: a) Northern Italy sample; b) Central Italy sample; c) Southern Italy sample

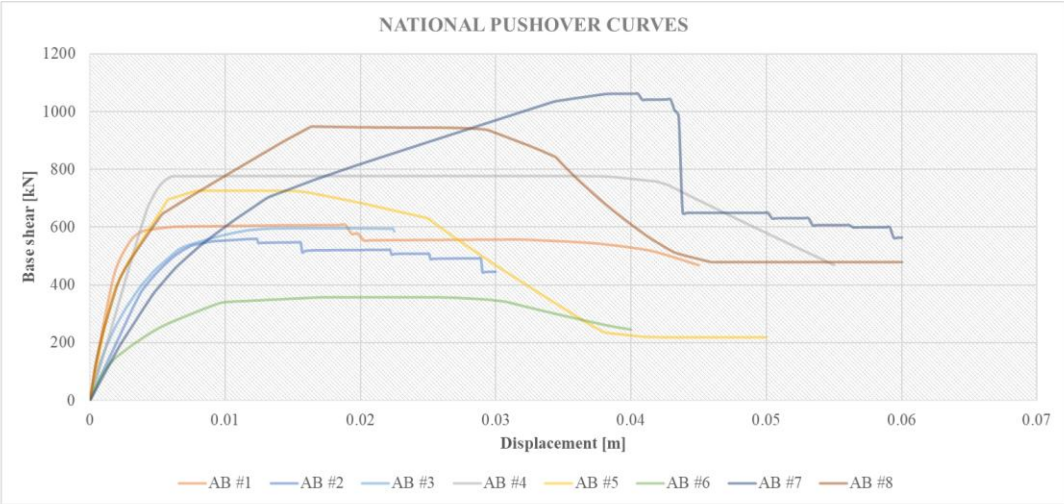

Figure 12. Numerical push-over capacity curve for the National sample

4.4 Results: Integrated fragility curves

4.4.1 Analytical and numerical damage thresholds

To evaluate the seismic performance of the archetype buildings, the comparison between capacity and demand was carried out for both out-of-plane and in-plane mechanisms, using the same methodology but with distinct definitions of damage thresholds in order to obtain fragility curves. In accordance with the Performance-Based Assessment (PBA) approach [31], each point of the capacity curve corresponds to a specific damage condition of the structure, allowing for a direct correlation between damage levels (DLs), defined according to EMS-98 [20], and performance levels (PLs). For the out-of-plane analyses, the damage thresholds $T(D_k)$ were derived following examples in the literature, treating the structure as a simple rigid block under horizontal actions. In this case, four damage thresholds were identified:

- $T(D_1)$ for light damage, corresponding to 70% of $T(D_2)$
- $T(D_2)$ for moderate damage, marking the onset of rocking activation
- $T(D_3)$ for extensive damage, corresponding to the end of the plastic plateau
- $T(D_4)$ for collapse, where acceleration reaches zero.

In order to determine the fragility curves through comparison with the seismic demand, it is necessary to transform the analytical capacity curves into capacity spectra. The following images show the identification of the damage thresholds thus defined on each of the archetypal buildings on the analytical and numerical capacity spectra. In Figure 13a are showed the damage thresholds for the archetype buildings of the Northern Italy macro area; Figure 13b the macro area Central Italy and in Figure 13c macro area Southern Italy. In Figure 14 there is the National territory collection.

Northern Italy sample

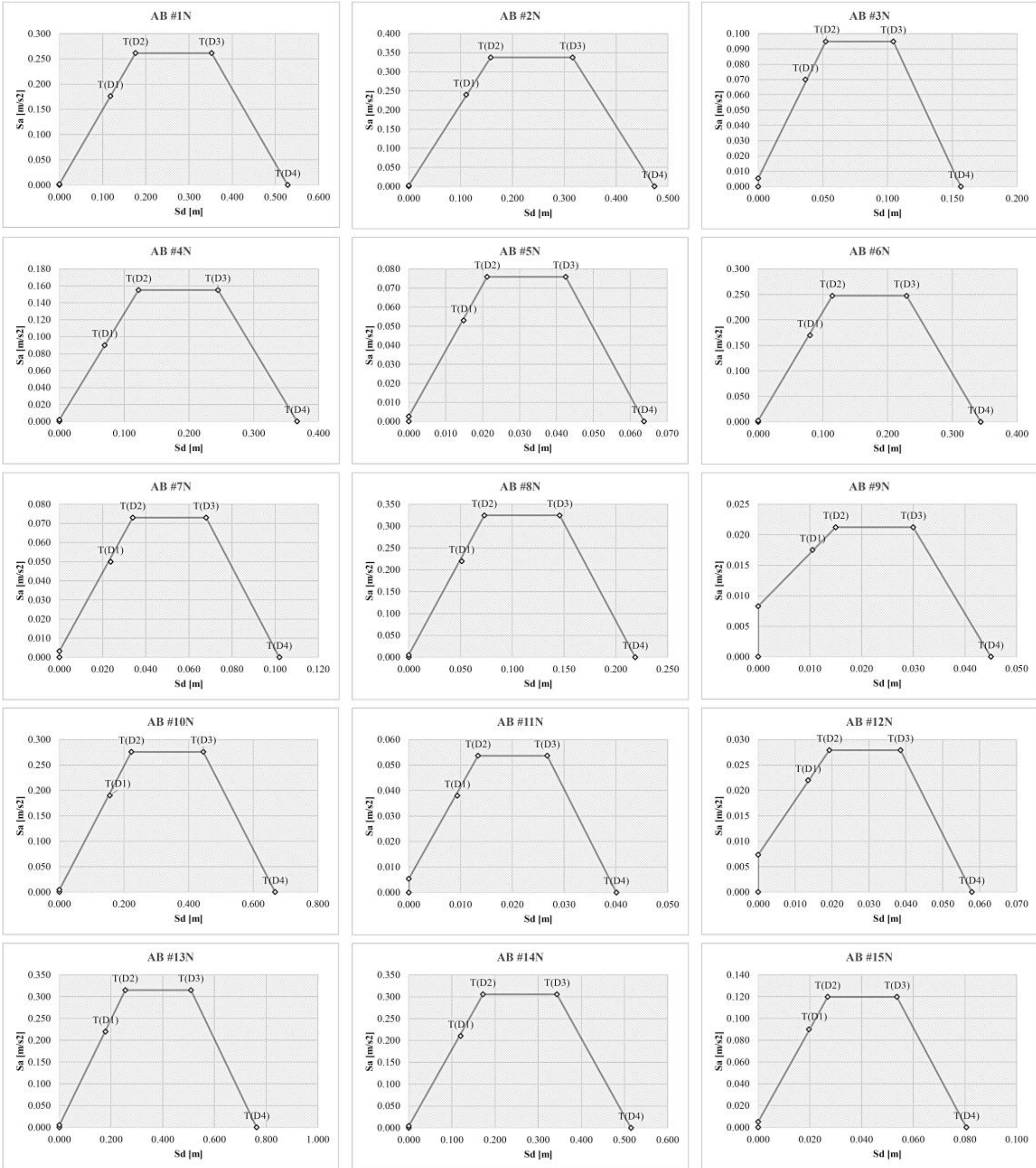

a)

Central Italy sample

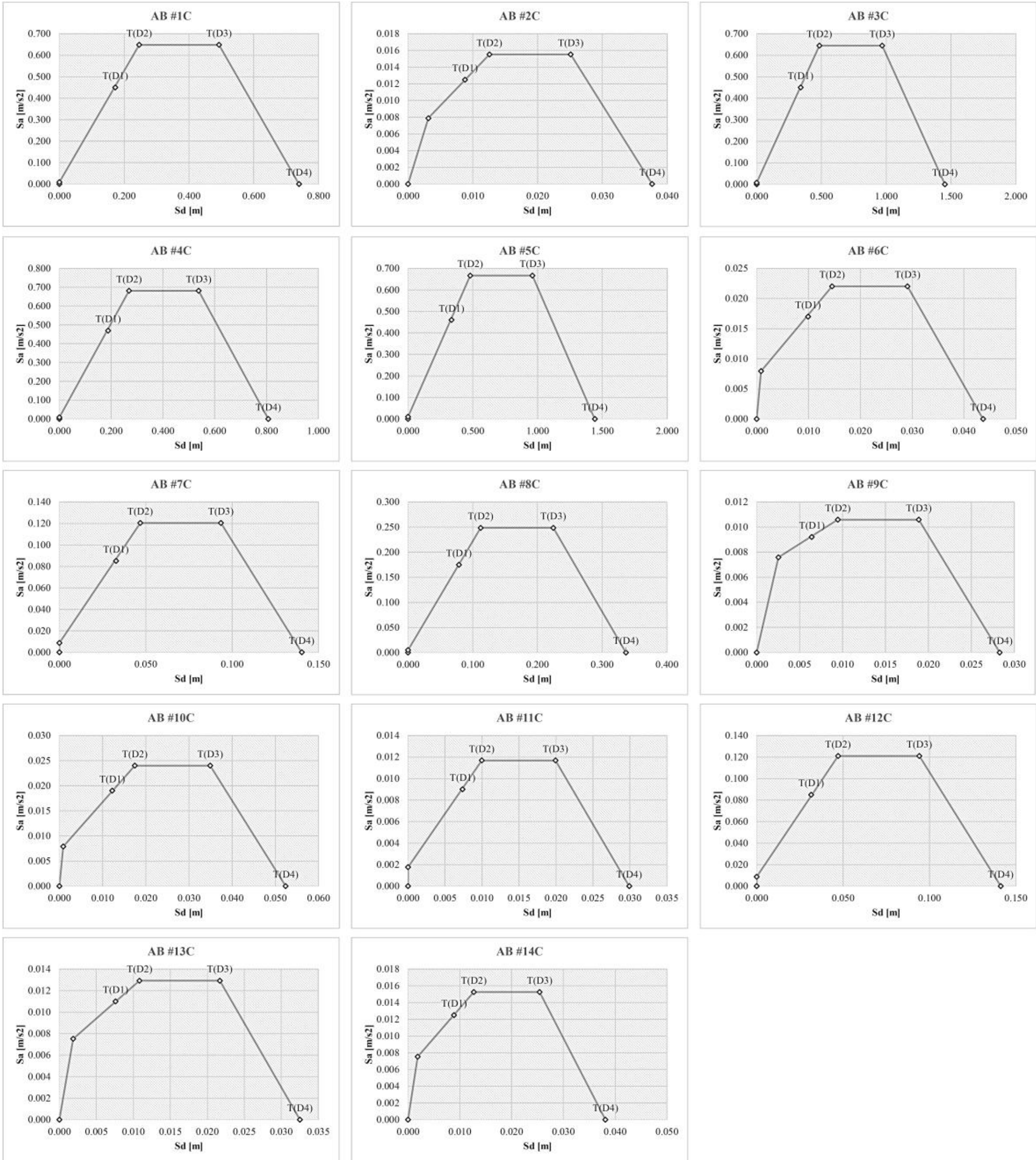

b)

Southern Italy sample

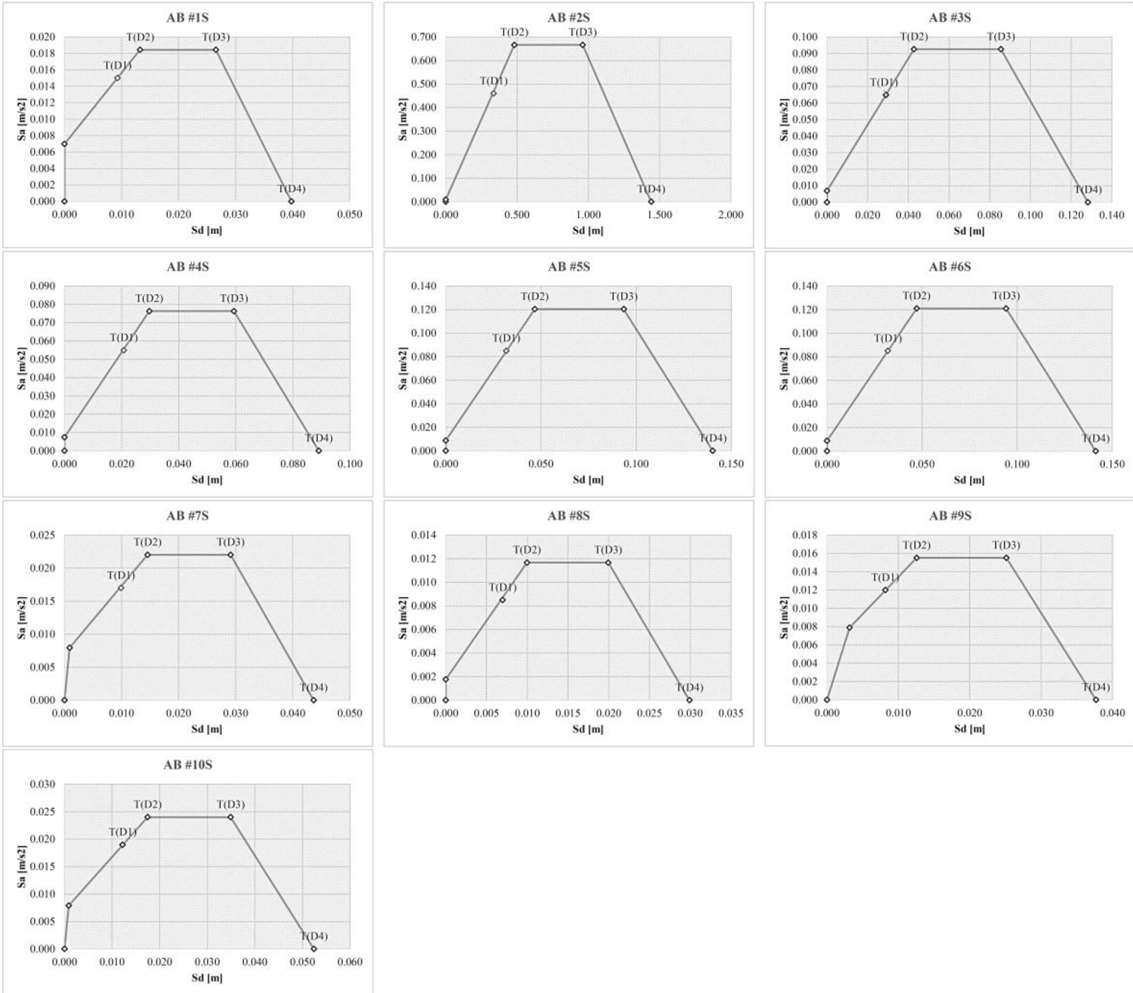

c)

Figure 13. Damage thresholds T(Di) adopted on the analytical capacity spectrum for the macro areas sample: a) Northern Italy sample; b) Central Italy sample; c) Southern Italy sample.

National sample

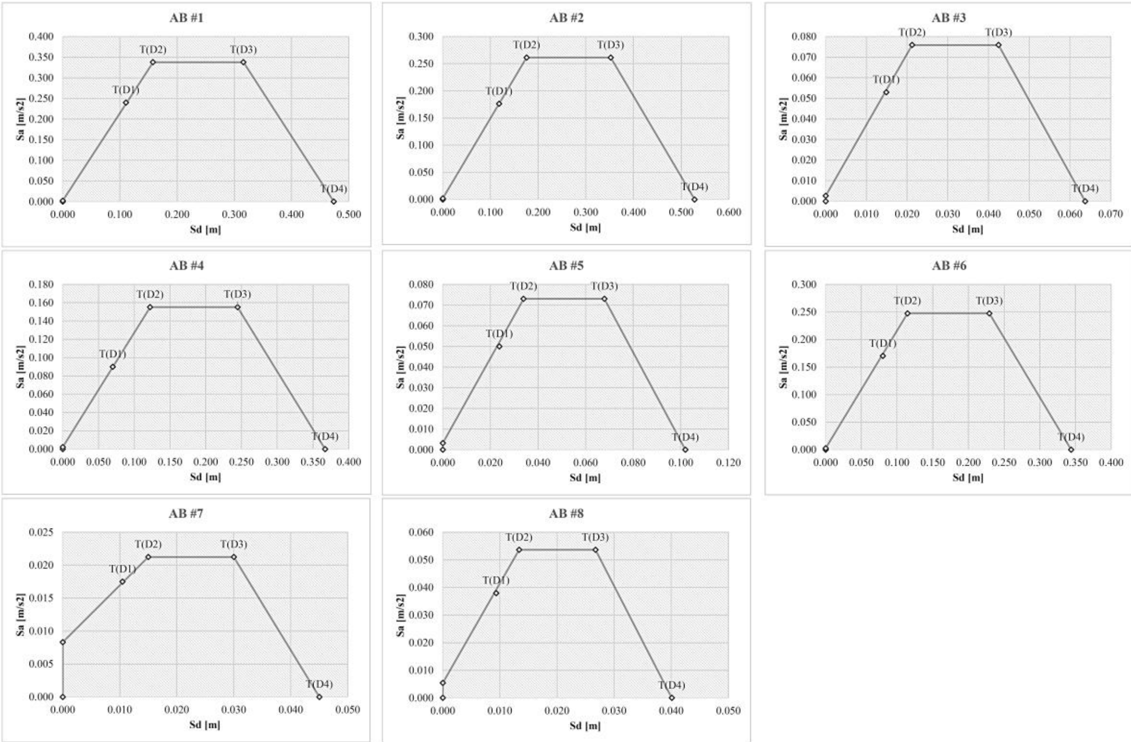

Figure 14. Damage thresholds T(Di) adopted on the analytical capacity spectrum for the National sample

Instead, for in-plane analyses, the damage thresholds were defined following the methodology proposed in [7] where, $T(D_1)$, $T(D_2)$, $T(D_3)$ and $T(D_4)$ were determined as functions of the yielding and ultimate displacements (d_y and d_u) [21], with:

- T(D1) = 0.7 d_y
- T(D2) = 1.5 d_y
- T(D3) = 0.5 (d_y + d_u)
- T(D4) = d_u

Even in the case of in-plane analysis it is necessary to transform the capacity curve into a spectrum, to compare the structural capacity with the seismic demand in ADRS format. For this reason, all bilinear curves were converted into spectral coordinates, generating the so-called capacity spectra. The pushover curve of each multi-degree-of-freedom system (MDOF), expressed in terms of base shear (F) versus the roof displacement at a control point (d*), was then converted into the bilinear capacity curve of an equivalent single-degree-of-freedom (SDOF) nonlinear system, assuming a modal participation factor equal to 1. The identification of the damage thresholds on each capacity spectrum for all the archetype buildings are shown in the following images. In Figure 15a it is possible to observe the four damage thresholds on the numerical capacity spectrum identified for the Macro area Northern Italy sample. Furthermore, in Figure 15b damage levels are shown on numerical capability spectra for the Central Italy sample and for the Southern Italy in Figure 15c. In Figure 16 the same results are showed for the National sample.

Northern Italy sample

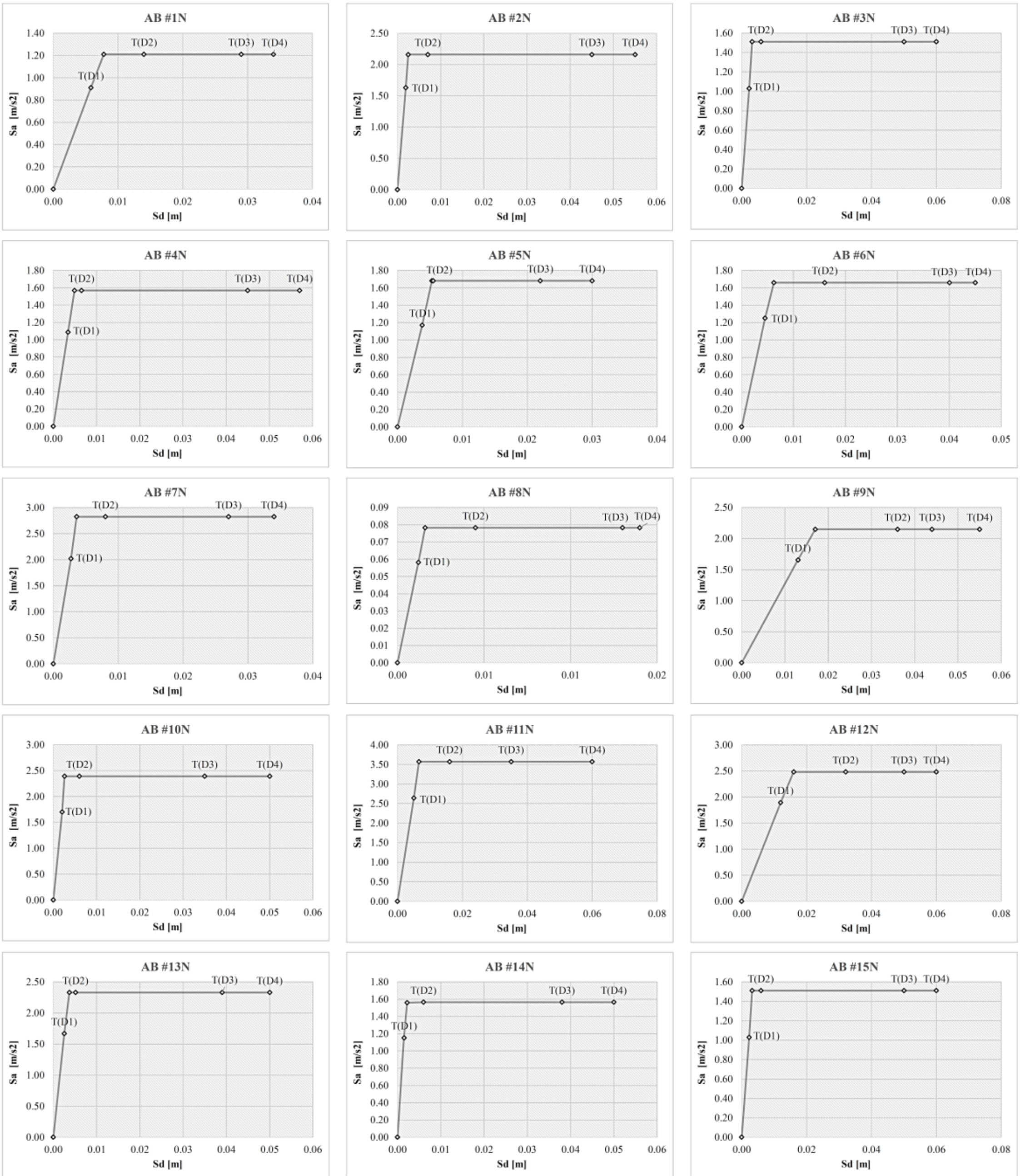

a)

Central Italy sample

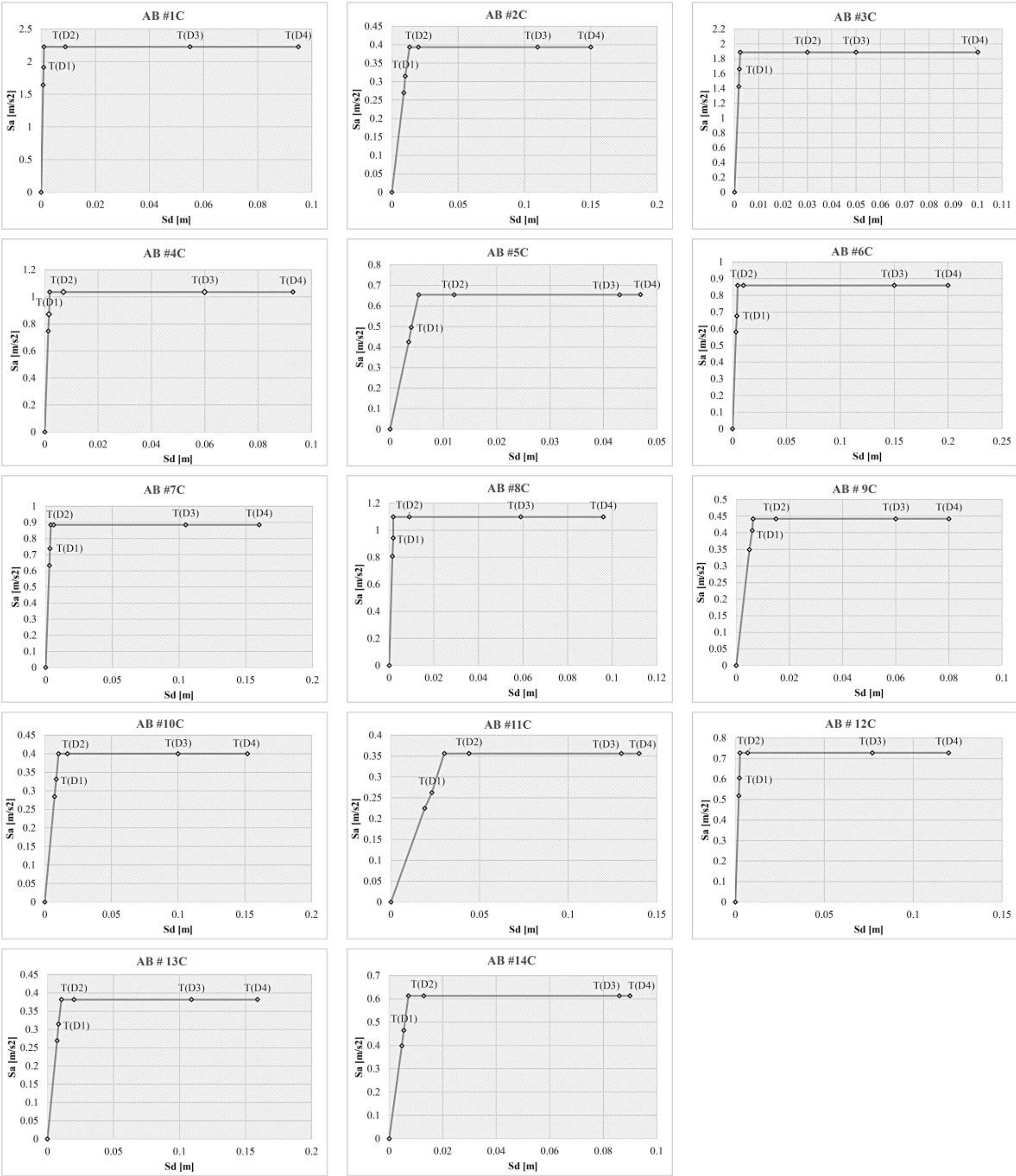

b)

Southern Italy sample

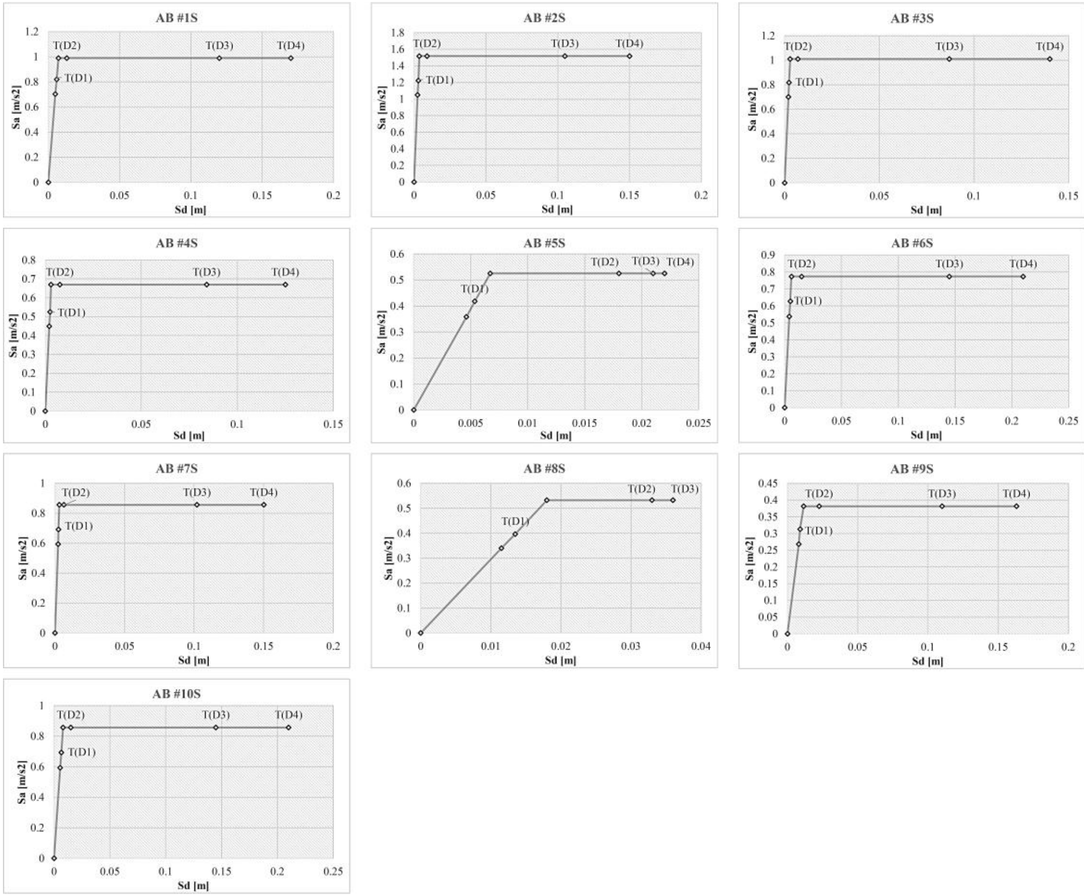

c)

Figure 15. Damage thresholds T(Di) adopted on the bilinear numerical capacity spectrum for the macro areas sample: a) Northern Italy sample; b) Central Italy sample; c) Southern Italy sample.

National sample

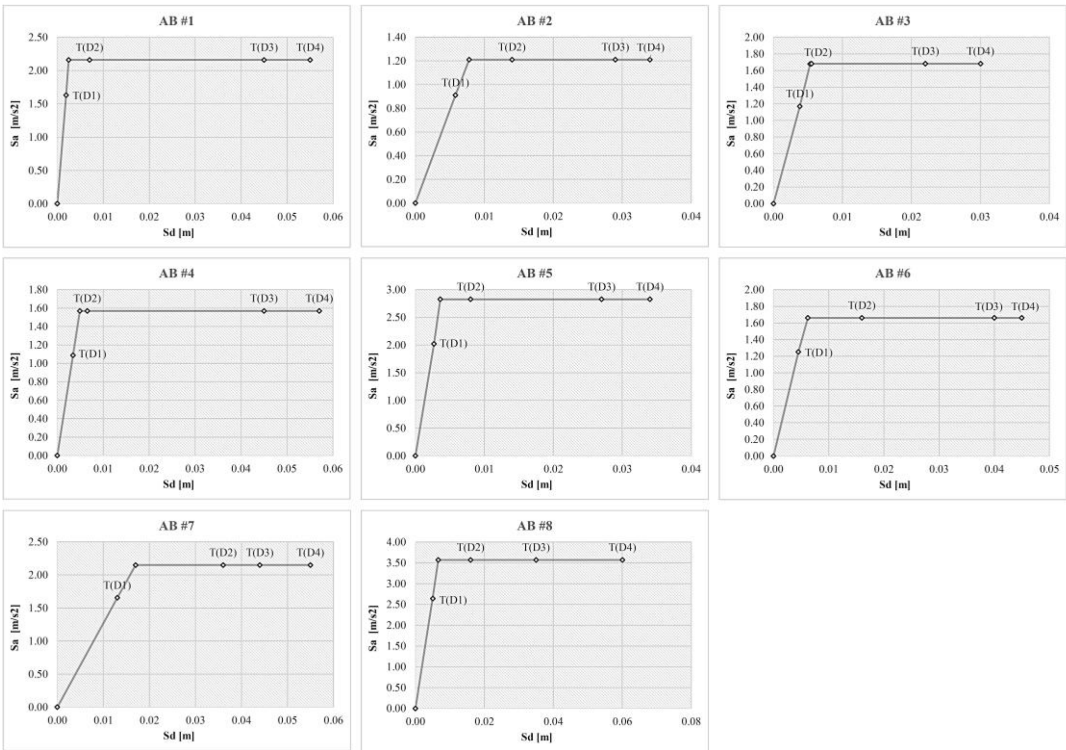

Figure 16. Damage thresholds T(Di) adopted on the bilinear numerical capacity spectrum for the National sample

Both approaches ensure that the capacity curves effectively represent the progressive deterioration of the structure under seismic actions.

4.4.2 Integrated fragility curves

Once the capacity curves and seismic demands, represented in ADRS format, were defined, the performance point (PP) of each structure was graphically identified as the intersection between the seismic demand and the extension of the capacity curve's elastic branch. This intersection enables determining the damage level the structure is likely to experience under a specific seismic scenario. By comparing the capacity spectra of the archetypes against 125 natural seismic records, organized into families characterized by mean reference PGAs, the frequencies of exceedance of specific Damage Limit States were calculated, accounting for record-to-record variability [20] [43]. These frequencies were used to construct Damage Probability Matrices (DPMs) for each archetype, which were then cumulated to create Cumulative Damage Probability Matrices (CDPMs). The CDPMs define the probability of exceeding a given DL and are expressed as discrete values that are subsequently fitted to a lognormal distribution to derive fragility curves for each archetype. In both out-of-plane and in-plane analyses, a single value of dispersion was assigned for all damage states to ensure the ordinal nature of damage levels and to prevent the intersection of fragility curves within the interval of integration for seismic risk estimation. This unified approach enabled a comprehensive assessment of the seismic performance of masonry buildings under various intensity levels and mechanisms of failure.

To comprehensively evaluate the seismic vulnerability by accounting for both local and global failure mechanisms, the fragility curves from these two approaches are compared and integrated. For each archetype, the fragility curve exhibiting the highest probability of exceeding a specific damage level under increasing seismic intensities (expressed as PGA) is selected as representative of its potential vulnerability.

Northern Italy sample

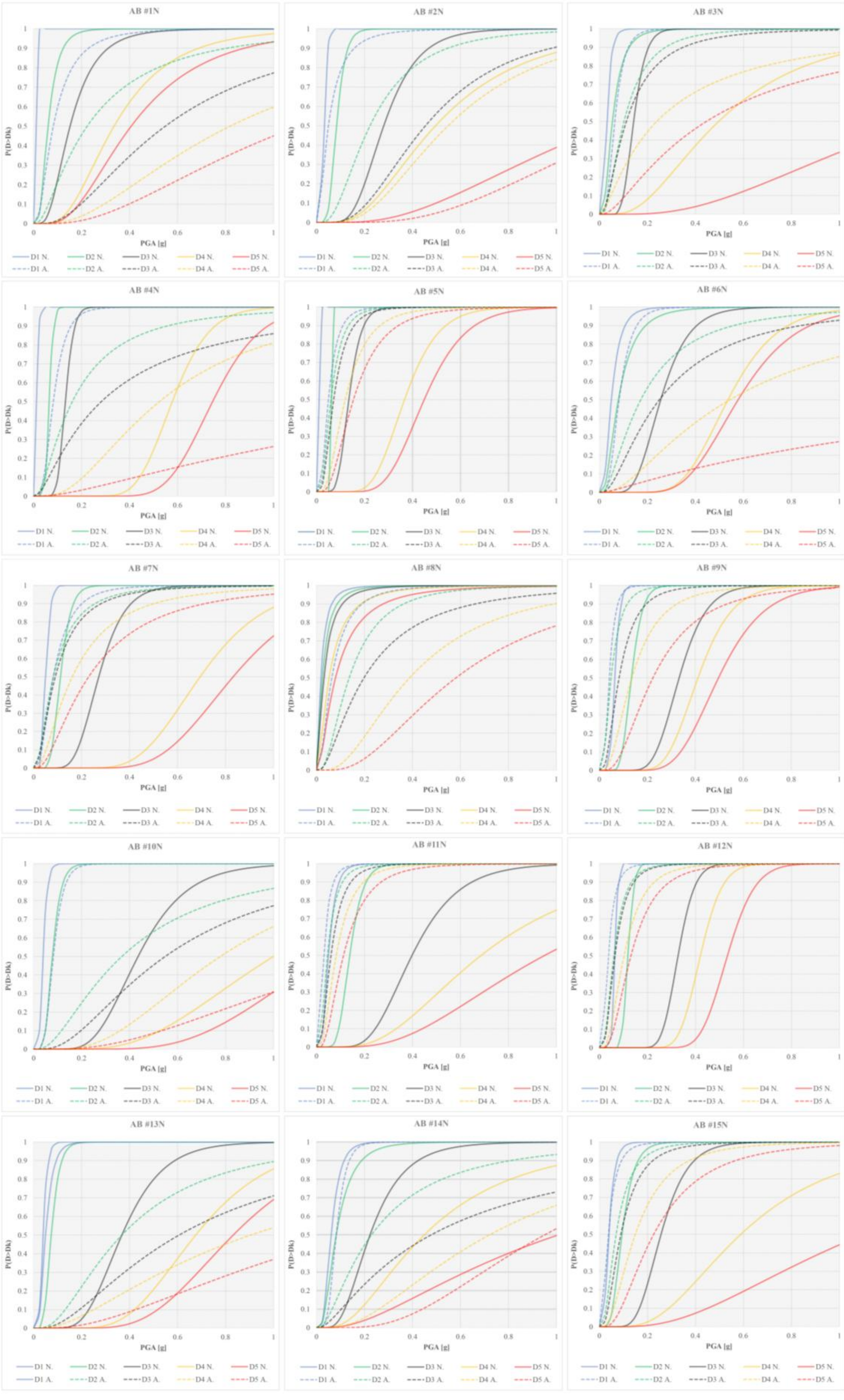

a)

Central Italy sample

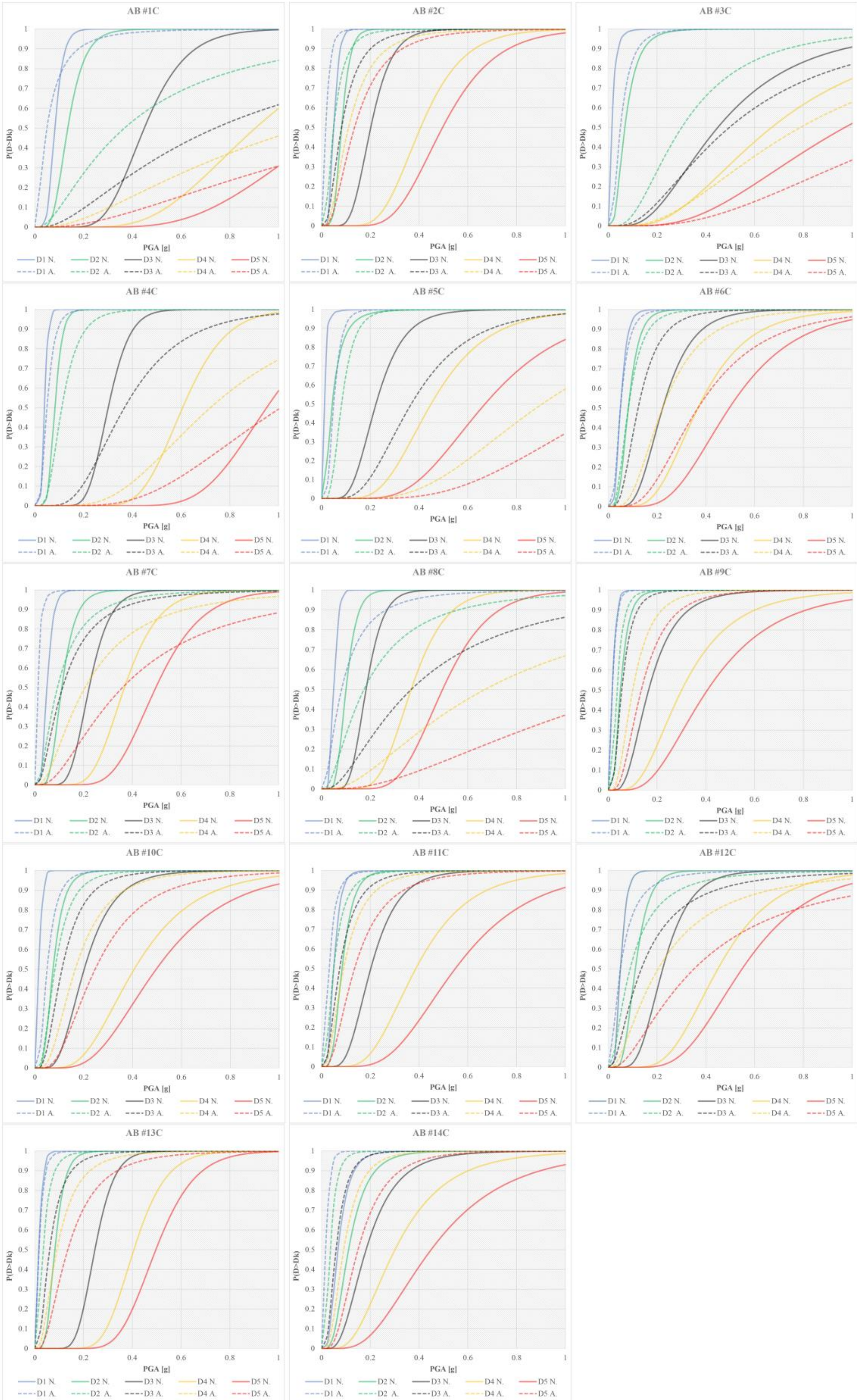

b)

Southern Italy sample

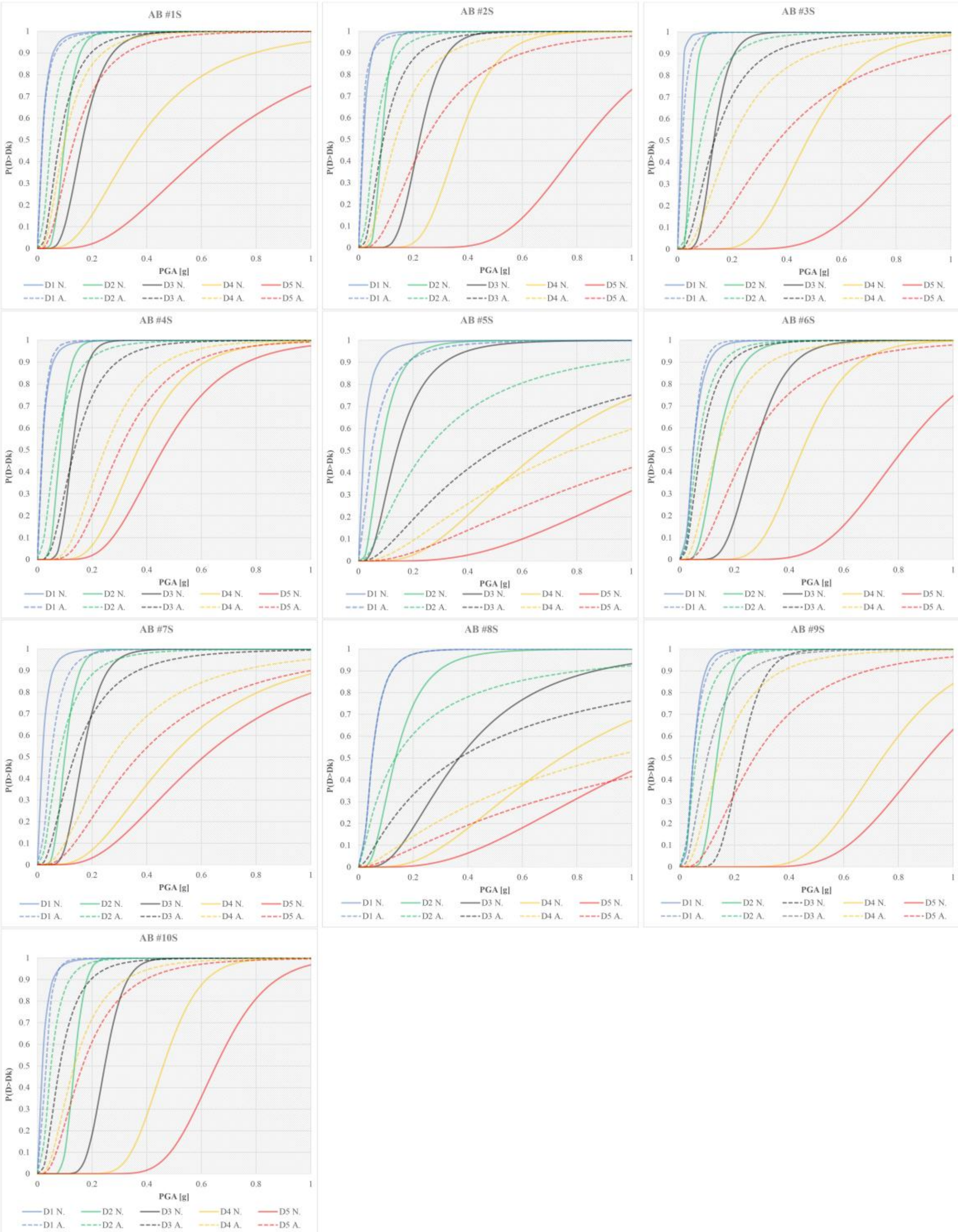

c)

Figure 17. Fragility curves for the for the macro areas sample: a) Northern Italy sample; b) Central Italy sample; c) Southern Italy sample.

National sample

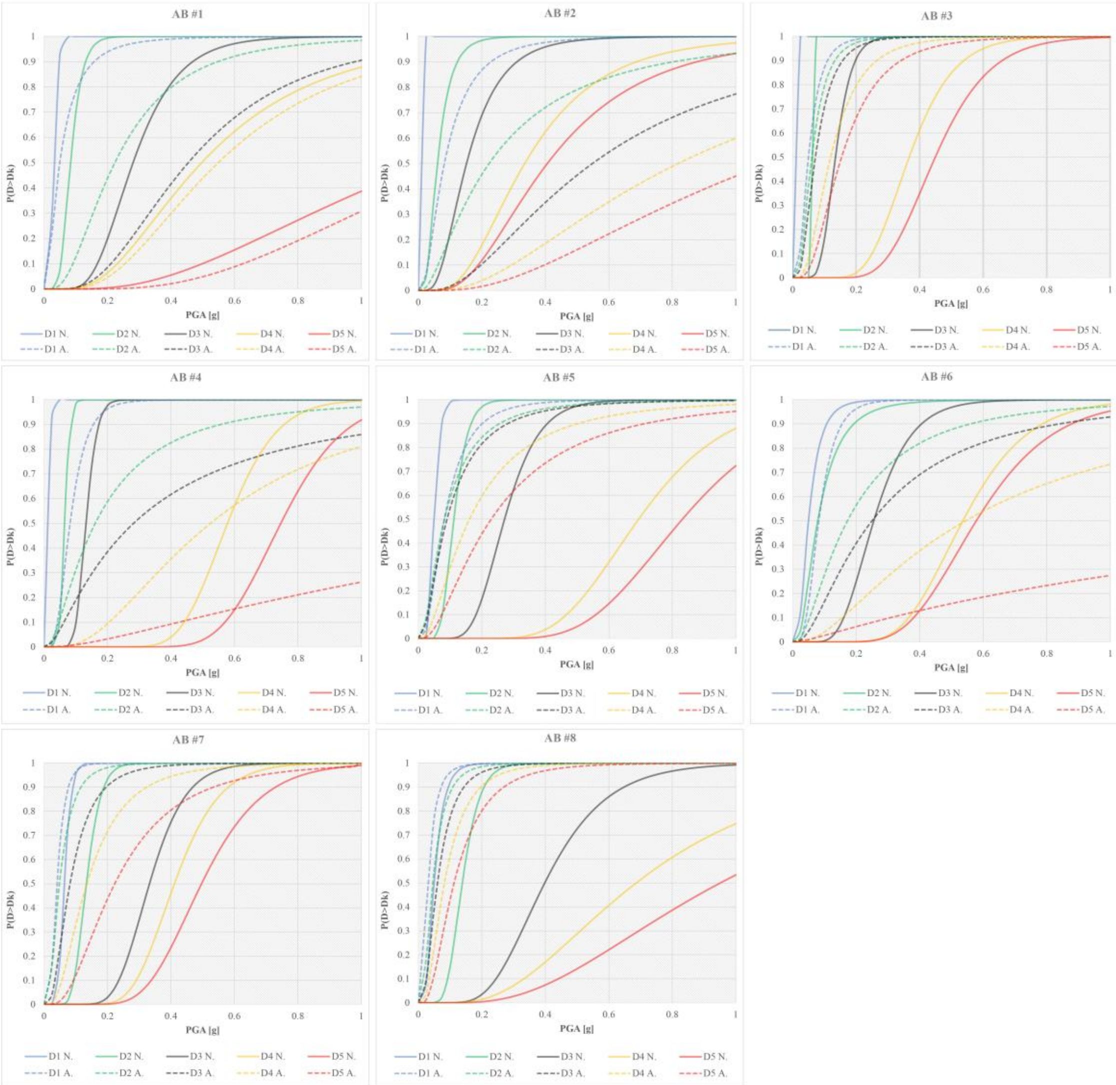

Figure 18. Fragility curves for the national sample.

The results presented highlight some important differences between the numerical and analytical methodologies used to evaluate the seismic vulnerability of buildings.

In general, the numerical methodology appears to produce more conservative estimates for lower and intermediate damage levels (D1 to D3), reflecting a heightened sensitivity to initial damages such as cracking and minor structural failures. This might reflect a more conservative approach in capturing the effects seismic events. On the other hand, the analytical methodology tends to predict higher probabilities of damage for more severe levels (D4 and D5), which represent near-collapse and collapse conditions. This divergence may arise from the different assumptions underlying each approach. The numerical method seems to better capture gradual damage progression, while the analytical approach simplifies certain behaviours, leading to more critical estimations under extreme conditions.

Looking at the macro regional samples, buildings in Northern Italy (Figure 17a) demonstrate this general trend, with the numerical method providing higher probabilities for slight and moderate damages, while the analytical method takes precedence for more extreme damage states. In Central Italy (Figure 17b), a similar pattern emerges, although the transition between the two methodologies' dominance becomes more pronounced as damage severity increases. Buildings in Southern Italy (Figure 17c), align with the overall trend but exhibit greater variability, likely reflecting the diversity in construction practices, already emerged from the analysis of the seismic exposure.

Finally, the national sample, which synthesizes these regional variations, confirms the complementarity of the two approaches (Figure 18). While numerical predictions are better suited for assessing initial damage states, the analytical method offers more critical insights for severe damages.

These results underline the importance of integrating both methodologies to achieve a comprehensive understanding of seismic vulnerability. The numerical approach is particularly valuable for evaluating early-stage damages, which are critical for planning retrofitting measures. Meanwhile, the analytical approach provides essential insights into collapse scenarios, which are vital for emergency response and long-term safety planning.

4.4.3 NATIONAL VULNERABILITY RESULTS

The total vulnerability of the Italian built heritage was assessed by putting together all the results obtained to create comprehensive fragility curves that clearly show the behaviour of the entire represented area and allows for better evaluations and comparisons.

The average fragility curves for each macro area were obtained by mathematically calculating the weighted average. This involved aggregating the fragility data from all buildings in the respective region, with weights assigned based on the relative significance of each building (number of buildings). The formula used was (eq.5):

$$P_{area}\,(PGA) = \frac{\sum_{i=1}^{n} w_i \cdot P_i(PGA)}{\sum_{i=1}^{n} w_i} \tag{5}$$

where w_i is the weight of the *i* building and $P_i\,(PGA)$ is the probability of exceedance for that building.

To what concerned the sample of the three macro areas, Figure 19 shows the average fragility curves across all damage levels (D1 to D5) for each macro area: Northern (a), Central (b), and Southern Italy (c). These curves illustrate significant regional variations in seismic vulnerability. Southern Italy shows consistently higher probabilities of exceeding damage levels across all PGA values, reflecting its greater vulnerability. Conversely, Central Italy exhibits lower probabilities, suggesting better structural resilience, while Northern Italy lies between the two, representing an intermediate level of vulnerability, especially for highest damage levels (D4 and D5).

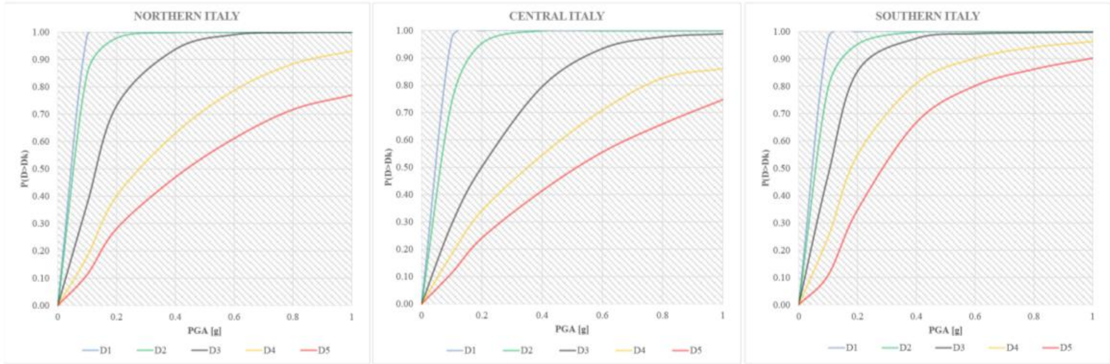

a) b) c)

Figure 19. Average Fragility Curves for Northern, Central, and Southern Italy in macro areas sample

The results for the national sample are shown in Figure 20. These curves provide a generalized representation of seismic vulnerability for the entire building stock in Italy. The results demonstrate a gradual increase in damage probability with increasing PGA, highlighting the overall vulnerability trends at a national scale.

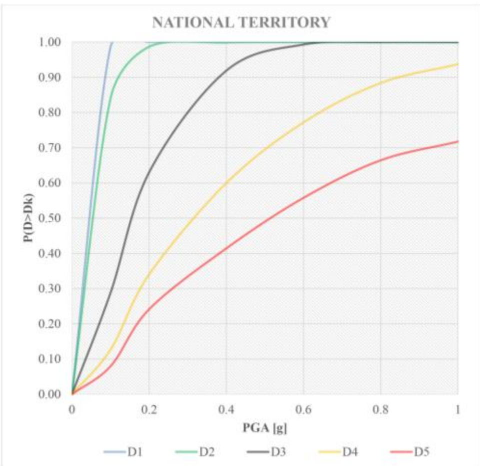

Figure 20. Average Fragility Curves for the National territory sample

Comparing the two images highlights the trade-offs between simplicity and regional specificity in seismic vulnerability analysis. The national sample provides a simplified and holistic perspective on seismic vulnerability, where the chance of exceeding damage levels is lower. However, this nationwide representation attenuates regional disparities and may overlook the distinct characteristics of Northern, Central and Southern Italy. The macro areas results show significant variability in seismic vulnerability across the nation, providing a more detailed and accurate picture, making them indispensable for targeted and location-specific interventions.

5. VULNERABILITY COMPARISON AT DIFFERENT SCALES

The selection of the reference sample is a crucial aspect in assessing the seismic vulnerability of masonry buildings. In this study, two distinct approaches have been employed: the macro-regional sample, which divides Italy into three main areas (North, Central, and South), and the national sample, which synthesizes the entire building stock into a single simplified representation. This part aims to compare the two approaches by analysing the resulting fragility curves and evaluating the implications of the observed differences.

Specifically, the analysis focuses on the ability of the two samples to accurately represent seismic vulnerability on a national scale and the operational consequences of using a more detailed or more synthetic sample.

5.1 COMPARATIVE ANALYSIS OF FRAGILITY CURVES

Fragility curves, derived from a combination of numerical and analytical analyses, describe the probability of exceeding specific damage levels (D1-D5) as a function of seismic intensity. A new graphical representation of these results is shown in Figure 21, in which the average curves of the three macro-areas and their weighted average ("Macro areas Sum" expressed in a continuous red line) representing the national territory divided into three macro-areas have been reported individually for each level of damage.

For all damage levels, the macro area weighted average effectively synthesizes the fragility curves of the three regions. This curve aligns well with the average characteristics of the regional probabilities of exceedance, although slight discrepancies emerge, particularly when comparing with the Southern region (light grey continuous line). The dashed red line, representing the national territory, shows a smoother trend and generally aligns closely with the macro area sum. However, it simplifies some regional variations, especially for higher levels of damage.

For the macro-regional sample, the curves show significant differences among the three areas analysed, according to the results showed in the previous *paragraph 4.4* too. For example, in Southern Italy, high probabilities of damage are observed, in particularly for severe damage levels (D4 and D5), even at moderate seismic intensity levels, reflecting greater vulnerability of the local building stock, characterized by irregular masonry and less resilient construction techniques. In contrast, in Central Italy (dark green continuous line), the probabilities of damage for D1 and D2 are lower, thanks to the prevalence of regular masonry and more widespread reinforcement interventions. It is the area with the lowest probability of exceeding the damage level, but it has less influence on the overall average because it is the least representative macro area due to the smaller number of buildings in this sample. In contrast, the other two macro areas, which have a larger number of buildings, carry more weight in the average. As a result, the Centre is the area that deviates the most from the average line. Northern Italy occupies an intermediate position, with probabilities falling between those of the Centre and South. This is consistent with the diverse typological characteristics of buildings in this region. However, it is the region with results closest to the average because it is the most representative region, and its outcome carries greater weight.

At least, when the curves of the macro areas sum are compared with those of the national sample ("National Territory" in red dash line), a simplification of the results emerges. For lower damage levels (D1, D2 and D3), the national curve closely matches the macro areas sum, indicating that the national sample effectively captures the average vulnerability. However, for higher damage levels (D4 and D5), the national territory curve tends to slightly underestimate vulnerability compared to the macro areas sum. This is particularly noticeable in regions with higher vulnerability, such as the South. The national sample tends to represent an average vulnerability that may mask regional specificities. For instance, the damage probabilities in the national sample are closer to those of Central Italy because it is the sample with the least vulnerability. However, this simplification might lead to an underestimation of vulnerability. These findings suggest that while the national sample provides a practical overview of seismic vulnerability, it may not fully capture regional specifics, particularly for severe damage levels. This underlines the importance of regional analysis for targeted interventions and policies in areas with higher vulnerability. Overall, the comparison highlights the complementarity of the two approaches: the national sample is useful for broad-scale evaluations, while the regional breakdown offers crucial insights for localized decision-making.

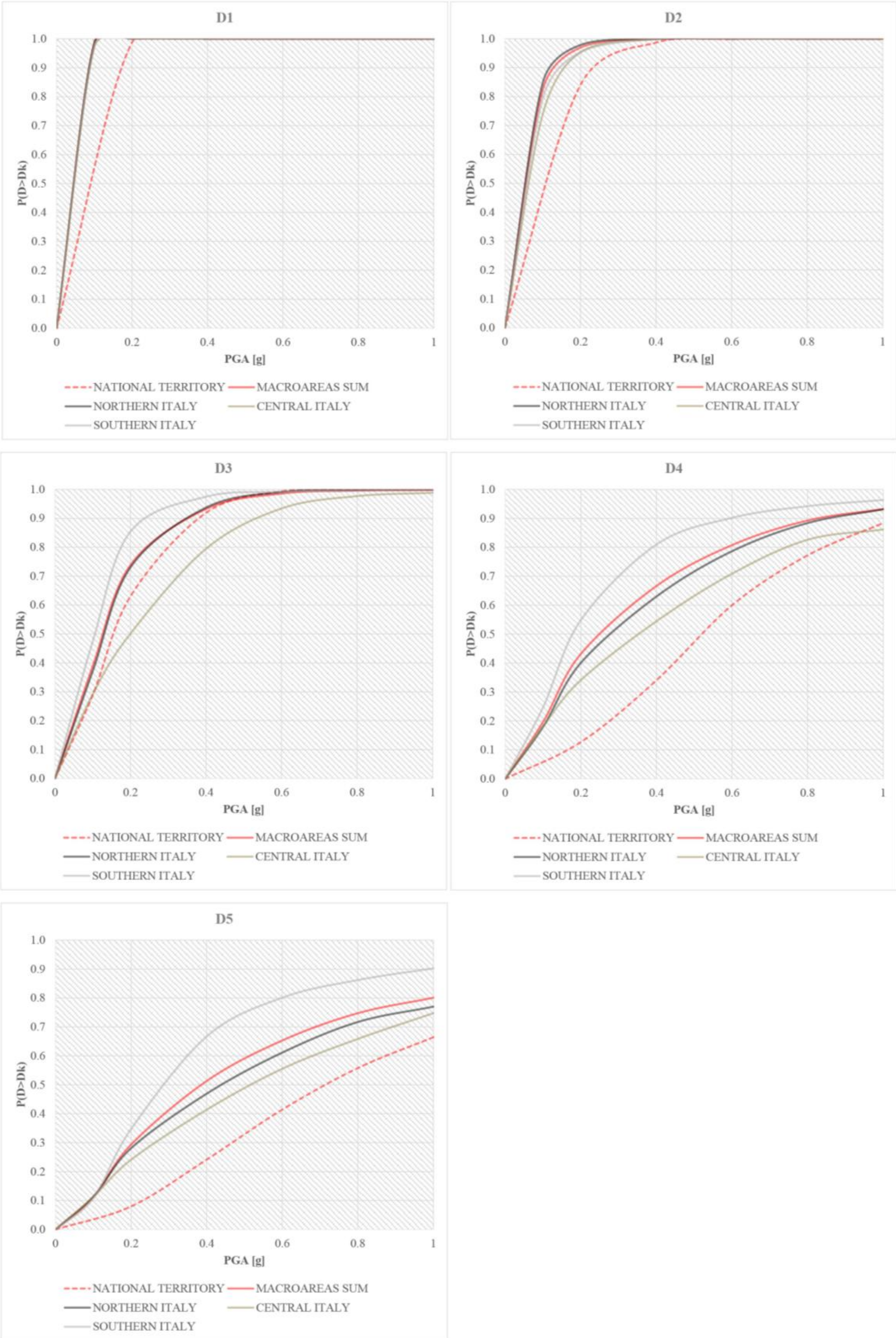

Figure 21. Comparison of Fragility Curves for Damage Levels D1 to D5 Across Macro areas and National Sample

5.2 Computational comparison between the two samples

Since the choice of the sample is also influenced by the type of analysis to be carried out and by the resources available, a further comparison between the two samples was performed in terms of computational burden.

To quantify the computational burden associated with each sample, a comparative analysis was conducted based on the number of archetypes and the corresponding computational time required for the analyses. The macro-regional sample, with its thirteen nine archetypes distributed across Northern, Central, and Southern Italy, naturally requires more time and resources compared to the more streamlined national sample, which contains only eight archetypes.

The computational requirements were assessed by considering two key factors:

- Number of analyses required per sample: Each archetype involves a set of numerical and analytical simulations, including fragility curve derivation and capacity assessments. For the macro-regional sample, this results in a significantly higher number of total analyses compared to the national sample.
- Time required for a single analysis: Although the computational cost per archetype is similar for both samples (about 7 hours for each building), the total time increases linearly with the number of archetypes.

A direct comparison of the computational effort is summarized in the following Table 5:

Table 5. Quantification of analysis time for each sample

Sample	Number of Archetypes	Total Analyses	Total Time Required [h]
Macro-regional Sample	39	156	273
National Sample	8	32	56

This comparison highlights the efficiency of the national sample for scenarios where time and computational resources are limited, in fact, the time to carry out the analyses on the smallest sample is reduced by approximately 5 times. However, the macro-regional sample provides more detailed results, making it indispensable for localized studies or when addressing regional seismic vulnerabilities.

The choice between the two samples, therefore, depends heavily on the context of the study. For large-scale analyses where synthesis and speed are priorities, the national sample is the preferred option; for detailed regional evaluations or studies involving areas with specific structural characteristics, the macro-regional sample is more appropriate despite its higher computational demand.

5.3 Conclusions and Recommendations

The analysis reveals that the choice of sample depends on the study's objectives. The national sample provides significant advantages in terms of operational simplicity. By reducing the number of archetypes from 39 in the macro-regional sample to only 8, it allows for faster and less computationally expensive analyses. This makes it a valid option for rapid, large-scale studies or to support policymaking that requires synthesized results. The national sample offers a good approximation of the average vulnerability of the building stock, but it also has limitations. The averaging of different building types and regional conditions may result in a loss of accuracy, particularly in areas with distinctive characteristics. For instance, the results of the national sample might not adequately reflect the vulnerability of historical buildings in Southern Italy or the greater resilience of buildings in the Centre. These limitations could be critical for planning targeted interventions. On the other hand, the macro-regional sample is indispensable for detailed studies that require a precise understanding of regional vulnerabilities, which are essential for localized interventions. While it demands greater computational effort, it captures the variability and specificity of different regions, making it better suited for nuanced and targeted analyses.

A good application of this method could include to combine the two approaches: use the national sample for an initial general analysis to identify broad trends and deepen the assessment of the most vulnerable areas using the macro-regional sample. This integrated approach balances precision and practicality, optimizing available resources while ensuring that critical vulnerabilities are adequately addressed.

6. CONCLUSIONS

The analytical and numerical methodologies employed thus far have facilitated the assessment of the seismic vulnerability of the national residential building stock through the derivation of fragility curves corresponding to the out-of-plane and in-plane capacities of the identified archetypes.

A key methodological contribution of this study lies in its ability to integrate large-scale data, such as the CARTIS database, with advanced modelling and analytical techniques. This has allowed for overcoming the limitations of traditional approaches based on single-building surveys or large-scale simplified analysis while maintaining a balance between precision and operational simplicity.

The analysis conducted has highlighted the importance of integrated approaches for assessing the seismic vulnerability of Italy's building heritage, particularly masonry buildings. Through the combined use of kinematic and numerical analyses, tools have been developed to effectively represent both local and global collapse mechanisms, providing fragility curves that are invaluable for planning mitigation interventions.

The results underscore the complexity of Italy's building stock, characterized by significant typological and structural heterogeneity. The division into macro-regional samples revealed local specificities, such as the greater vulnerability of irregular masonry buildings in Southern Italy compared to the higher resilience typical of Central Italy. However, the simplification offered by the national sample proved effective for large-scale analyses, providing a sufficiently accurate general representation.

The comparison between the two approaches reveals significant complementarity: the national sample provides a synthetic and rapid overview of seismic vulnerability on a national scale, while the macro-regional sample enables targeted and in-depth analyses, essential for localized intervention policies. Therefore, the choice of the analysis sample must be made by evaluating the accuracy of the result to achieve and the availability in terms of time and computational burden.

Despite the encouraging results, some limitations remain. The simplification introduced in the national sample may obscure regional specificities, risking the underestimation of local criticalities. Furthermore, the lack of more detailed data on unique structural characteristics could affect the accuracy of analyses for historic or atypical buildings.

As a possible future development, in fact, there is that of re-proposing the analyses carried out by trying to vary the choice of the sample, to understand if different subdivisions can lead to different and more accurate evaluations

The approach developed here, although focused on Italy, can be adapted to other contexts with similar characteristics, thereby contributing to the global management of seismic risk. In conclusion, this work represents a significant contribution toward a more informed and scientifically grounded management of seismic risk. The balance between precision and operational simplicity, combined with the possibility of integrating new technologies and data, makes this methodology a valuable tool for addressing the challenges posed by seismic risk in Italy and beyond.

REFERENCES

[1] E. Criber, G. Brando, and G. De Matteis, “The effects of L’Aquila earthquake on the St. Gemma church in Goriano Sicoli: part I—damage survey and kinematic analysis,” Bulletin of Earthquake Engineering, vol. 13, no. 12, pp. 3713–3732, Dec. 2015, doi: 10.1007/s10518-015-9792-4.

[2] G. Brando, G. De Matteis, and E. Spacone, “Predictive model for the seismic vulnerability assessment of small historic centres: Application to the inner Abruzzi Region in Italy,” Eng Struct, vol. 153, pp. 81–96, Dec. 2017, doi: 10.1016/j.engstruct.2017.10.013.

[3] A. Rosti, M. Rota, and A. Penna, “Empirical fragility curves for Italian URM buildings,” Bulletin of Earthquake Engineering, vol. 19, no. 8, pp. 3057–3076, Jun. 2021, doi: 10.1007/s10518-020-00845-9.

[4] M. Dolce et al., “Observed damage database of past italian earthquakes: The da.D.O. WebGIS,” Bollettino di Geofisica Teorica ed Applicata, vol. 60, no. 2, pp. 141–164, 2019, doi: 10.4430/bgta0254.

[5] D. Benedetti, G. Benzoni, and M. A. Parisi, “Seismic vulnerability and risk evaluation for old urban nuclei,” Earthq Eng Struct Dyn, vol. 16, no. 2, pp. 183–201, Feb. 1988, doi: 10.1002/eqe.4290160203.

[6] A. H. Barbat, S. Lagomarsino, and L. G. Pujades, “Vulnerability Assessment of Dwelling Buildings,” in Assessing and Managing Earthquake Risk, Berlin/Heidelberg: Springer-Verlag, 2010, pp. 115–134. doi: 10.1007/1-4020-3608-6_6

[7] S. Lagomarsino and S. Giovinazzi, “Macroseismic and mechanical models for the vulnerability and damage assessment of current buildings,” Bulletin of Earthquake Engineering, vol. 4, no. 4, pp. 415–443, Nov. 2006, doi: 10.1007/s10518-006-9024-z.

[8] T. M. Ferreira, R. Maio, A. A. Costa, and R. Vicente, “Seismic vulnerability assessment of stone masonry façade walls: Calibration using fragility-based results and observed damage,” Soil Dynamics and Earthquake Engineering, vol. 103, pp. 21–37, Dec. 2017, doi: 10.1016/j.soildyn.2017.09.006.

[9] S. Lagomarsino, S. Cattari, M. Angiolilli, S. Bracchi, M. Rota, and A. Penna, “Modelling and Seismic Response Analysis of Existing URM Structures. Part 2: Archetypes of Italian Historical Buildings,” Journal of Earthquake Engineering, vol. 27, no. 7, pp. 1849–1874, May 2023, doi: 10.1080/13632469.2022.2087800

[10] G. Zuccaro, M. Dolce, D. De Gregorio, E. Speranza, and C. Moroni, "La scheda CARTIS per la caratterizzazione tipologico-strutturale dei comparti urbani costituiti da edifici ordinari. Valutazione dell'esposizione in analisi di rischio sismico," 2015.

[11] G. Zuccaro, M. Dolce, F. L. Perelli, D. De Gregorio, and E. Speranza, "CARTIS: a method for the typological-structural characterization of Italian ordinary buildings in urban areas," Front Built Environ, vol. 9, 2023, doi: 10.3389/fbuil.2023.1129176.

[12] S. Ruggieri et al., "An archetype-based automated procedure to derive global-local seismic fragility of masonry building aggregates: META-FORMA-XL," International Journal of Disaster Risk Reduction, vol. 95, Sep. 2023, doi: 10.1016/j.ijdrr.2023.103903.

[13] A. Basaglia et al., "An automatic procedure for deriving building portfolios using the Italian 'CARTIS' online database," Structures, vol. 34, pp. 2974–2986, Dec. 2021, doi: 10.1016/j.istruc.2021.09.054.

[14] G. Cianchino, G. Cocco, D. Rapone, Y. Di Lallo, M. G. Masciotta, and G. Brando, "Vulnerability analytical models at the regional scale through archetype buildings: an application to the Abruzzi region," in Procedia Structural Integrity, Elsevier B.V., 2022, pp. 219–226. doi: 10.1016/j.prostr.2023.01.029.

[15] G. Cianchino, "A large-scale integrated approach to assess the seismic vulnerability of masonry built Cultural Heritage in central Italy," University "Gabriele d'Annunzio" of Chieti - Pescara, 2023.

[16] G. Brando, G. Cianchino, D. Rapone, E. Spacone, and S. Biondi, "A CARTIS-based method for the rapid seismic vulnerability assessment of minor Italian historical centres," International Journal of Disaster Risk Reduction, vol. 63, Sep. 2021, doi: 10.1016/j.ijdrr.2021.102478.

[17] https://www.pgadmin.org.

[18] M. Dolce, "Schematizzazione e modellazione degli edifici in muratura soggetti ad azioni sismiche," L'Industria delle costruzioni, vol. 25, no. 242, pp. 44–57, 1991.

[19] MIDAS Information Technology Co., "MIDAS Gen ," 2020.

[20] Gottfried. Grünthal, European macroseismic scale 1998 : EMS-98. European Seismological Commission, Subcommission on Engineering Seismology, Working Group Macroseismic scales, 1998.

[21] V. Buonocunto, E. Acconcia, and F. Parisi, "Seismic fragility modelling of unreinforced masonry buildings in Campania region," in Procedia Structural Integrity, Elsevier B.V., 2022, pp. 67–74. doi: 10.1016/j.prostr.2023.01.010.

[22] ReLUIS and Italian National Department of Civil Protection, "WP4 MARS Project – Seismic Risk Maps and Damage Scenarios. 2019-2021 ReLUIS Projec," https://www.reluis.it/progetto-dpc-reluis-2019-2021/, vol. 2019–2021.

[23] K. A. Porter, "An Overview of PEER's Performance-Based Earthquake Engineering Methodology," 2003.

[24] R. Paolucci, C. Smerzini, and M. Vanini, "Bb-speedset: A validated dataset of broadband near-source earthquake ground motions from 3d physics-based numerical simulations," Bulletin of the Seismological Society of America, vol. 111, no. 5, pp. 2527–2545, 2021, doi: 10.1785/0120210089.

[25] Casapulla C, Giresini L, Lourenço PB. Rocking and Kinematic Approaches for Rigid Block Analysis of Masonry Walls: State of the Art and Recent Developments. Buildings. 2017; 7(3):69. https://doi.org/10.3390/buildings7030069.

[26] K. Doherty, M. C. Griffith, N. Lam, and J. Wilson, "Displacement-based seismic analysis for out-of-plane bending of unreinforced masonry walls," Earthq Eng Struct Dyn, vol. 31, no. 4, p. 833, Apr. 2002, doi: 10.1002/eqe.126.abs.

[27] Ministero delle Infrastrutture e dei Trasporti, "CIRCOLARE 21 gennaio 2019 n.7_Istruzioni per l'applicazione dell'«Aggiornamento delle 'Norme tecniche per le costruzioni'» di cui al decreto ministeriale 17 gennaio 2018. (Italian Guideline)," 2019.

[28] S. Lagomarsino, A. Penna, A. Galasco, and S. Cattari, "TREMURI program: An equivalent frame model for the nonlinear seismic analysis of masonry buildings," Eng Struct, vol. 56, pp. 1787–1799, Nov. 2013, doi: 10.1016/j.engstruct.2013.08.002.

[29] S. Cattari, D. Camilletti, A. M. D'Altri, and S. Lagomarsino, "On the use of continuum Finite Element and Equivalent Frame models for the seismic assessment of masonry walls," Journal of Building Engineering, vol. 43, p. 102519, Nov. 2021, doi: 10.1016/j.jobe.2021.102519.

[30] D. Shapiro, C. Rojahn, L. D. Reaveley, J. R. Smith, and U. Morelli, "NEHRP Guidelines and Commentary for the Seismic Rehabilitation of Buildings," Earthquake Spectra, vol. 16, no. 1, pp. 227–239, Feb. 2000, doi: 10.1193/1.1586092.

[31] S. Lagomarsino and S. Cattari, "PERPETUATE guidelines for seismic performance-based assessment of cultural heritage masonry structures," Bulletin of Earthquake Engineering, vol. 13, no. 1, pp. 13–47, Jan. 2015, doi: 10.1007/s10518-014-9674-1.

FINAL REMARKS AND FUTURE DEVELOPMENTS

FINAL REMARKS AND FUTURE DEVELOPMENTS

1. INTRODUCTION

This chapter summarizes the main contributions and findings of this thesis, reflecting on its innovations and significance in advancing the understanding of seismic vulnerability at the national scale for masonry residential buildings in Italy. Additionally, it identifies the limitations of the work and proposes future research directions to expand and refine the current approach.

2. SUMMARY OF METHODOLOGY AND INNOVATIONS

The methodology presented in this thesis builds upon prior research conducted for the Italian Abruzzo region (Chapter 1) and extends it to the entire Italian territory. The innovations introduced include:

- The application of the CARTIS database, which offers detailed typological and structural characteristics of the national building stock, enabling a data-driven definition of archetype models.
- An integrated vulnerability assessment approach that combines kinematic and numerical analyses. This dual methodology provides a comprehensive evaluation of both out-of-plane and in-plane mechanisms, offering more accurate fragility curves compared to empirical methods.
- The adoption of a multi-scale sampling strategy, progressively increasing the spatial coverage to represent the national masonry building stock while maintaining computational efficiency.

3. MAIN RESULTS

The findings of this research provide detailed insights into the seismic vulnerability of masonry residential buildings across Italy, offering both regional specificity and national-level applicability. These results can be categorized into two main areas: seismic exposure and vulnerability assessment.

3.1 Exposure Analysis

The exposure analysis conducted in Chapter 2 highlights the diversity and complexity of the Italian building stock, focusing on masonry structures. Key findings include:

- Identification of Archetypes: Using the CARTIS database, a representative set of masonry building archetypes was identified, capturing the most critical structural and typological characteristics at the national scale. These include parameters such as masonry type, floor type, construction period, number of stories, and roof materials.
- Progressive Sampling Strategy: Sample 1 focused on a regional scale, allowing a detailed characterization of structural variations within a confined area; Sample 2 expanded the area to include multiple regions, providing broader geographic coverage while maintaining computational feasibility; Sample 3 extended the analysis to the entire national territory, representing a comprehensive depiction of Italy's masonry building stock.
- Regional Variability: The analysis revealed significant heterogeneity in building typologies across Italy, reflecting the influence of local historical construction practices and geological conditions. For instance, in the central regions, irregular masonry is prevalent, often associated with historical centres; in northern and coastal areas, brick masonry is more common, with notable differences in construction periods and structural regularity and, in the south, there is a wider variability of the sample due to more heterogeneous building typologies.

These results are crucial for tailoring seismic risk assessments to the specific needs of different regions.

3.2 Seismic Vulnerability Analysis

The seismic vulnerability assessment presented in Chapter 3 builds upon the exposure analysis to develop fragility curves for the identified archetypes. This section synthesizes the methodology and key outcomes:

- Integrated analytical and numerical approaches: Kinematic analyses focused on out-of-plane collapse mechanisms, identifying common vulnerabilities such as poor connections between orthogonal walls and between walls and floors. This analysis demonstrated that façade overturning is often the first failure mechanism in unreinforced masonry buildings, especially those with flexible floors and heavy roofs. Instead, numerical analyses: Addressed in-plane mechanisms using the Equivalent Frame Model (EFM). This approach revealed how global structural responses vary with the number of stories and masonry type. Notably, brick masonry buildings showed higher in-plane capacities compared to irregular masonry structures, but also reduced ductility.

- Comparison of Samples: Results for the smaller macro regional sample were highly accurate but required much more analysis due to the larger sample size. On the contrary, the national-scale sample introduced broader applicability with little effort but required careful calibration to maintain accuracy because a smaller sample must not lose representativeness. Indeed, by ccomparing fragility curves derived from these samples it has emerged that larger samples better capture national trends but may underestimate local peculiarities.
- Fragility Curve Insights: Integrated fragility curves, combining in-plane and out-of-plane mechanisms, provided a comprehensive understanding of damage probabilities under varying seismic intensities. For moderate seismic events, buildings with flexible floors and without tie rods demonstrated a significantly higher probability of moderate and severe damage. For stronger seismic events, differences between regions and archetypes became more pronounced, emphasizing the importance of tailored retrofitting strategies.

4. PRACTICAL IMPLICATIONS

The results of this thesis offer significant implications for seismic risk management in Italy, with practical applications ranging from the development of national policies to urban planning. One of the primary contributions of this work is its ability to provide scientific support for seismic prevention policies, enhancing the effectiveness of interventions and optimizing resource allocation. The proposed methodology allows for the precise identification of key vulnerabilities in masonry buildings at the national scale, creating a solid foundation for prioritizing mitigation actions.

From an urban planning perspective, the findings of this research can guide local governments in managing areas at seismic risk. Detailed knowledge of the distribution of building types and their specific vulnerabilities provides tools to plan targeted interventions and promote resilient urban development. In particular, the ability to map building fragilities on a territorial scale represents an opportunity to integrate seismic risk assessments into urban planning and the revitalization of historical centres.

Another crucial aspect is the contribution of the thesis to the design of seismic retrofitting strategies. Thanks to the integrated approach adopted, it is possible not only to identify the most vulnerable building types but also to quantitatively evaluate the effectiveness of various structural strengthening measures.

Finally, this work represents a step forward in providing decision-making tools for government and local authorities. The ability to use integrated fragility curves and exposure models to simulate seismic risk scenarios allows for more effective planning of mitigation strategies. In a context like Italy, where the density of historical building stock and the frequency of seismic events present ongoing challenges, adopting advanced methodologies like the one proposed in this thesis can significantly improve risk management capabilities, safeguarding human lives and reducing the economic impact of earthquakes.

5. LIMITATIONS OF THE STUDY

While the findings are promising, certain limitations should be acknowledged:

- Data Gaps: Although CARTIS is a comprehensive database, it may lack granularity for some regions, potentially affecting the representativeness of certain archetypes. furthermore, it is a constantly evolving database, so this result is only a temporary snapshot of the buildings surveyed with this approach.
- Simplifications in Modelling: The use of archetype models and integrated analysis approaches involves inherent assumptions that may not fully capture the complexity of individual buildings. Different assumptions could be made regarding other situations of the building to be analysed or the analysis techniques to be used.

6. FUTURE RESEARCH DIRECTIONS

Building on this work, several avenues for future research are proposed:

- Expanding Typologies: Incorporating other construction types, such as reinforced concrete or hybrid masonry structures, to generalize the findings to a broader spectrum of buildings.
- Advanced Modelling Techniques: Leveraging machine learning and artificial intelligence to refine archetype selection and vulnerability modelling, using larger and more diverse datasets.

- Dynamic Seismic Risk Assessment: Integrating socio-economic and environmental factors to develop a more holistic approach to seismic risk, accounting for human vulnerability and resilience.
- Field Validation: Conducting post-earthquake surveys to validate and enhance the developed fragility models.
- Integration with Climate Risks: Exploring the intersection of seismic vulnerability with climate change impacts, such as increased soil instability due to extreme weather events.

7. CONCLUSION

This thesis represents a step forward in seismic vulnerability analysis at the national scale, combining methodological rigor with practical applications. By addressing both local and global damage mechanisms, the research provides tools and insights to support seismic risk mitigation strategies in Italy. The proposed future developments aim to further enhance the utility and applicability of this work, ensuring its continued relevance in addressing seismic challenges in Italy and beyond.